BRIDGING MEMBRANE BIOPHYSICS TO MICROBIOLOGY: INNOVATING TOWARDS NEW PEPTIDE AND PEPTIDE-BASED ANTIMICROBIALS

EDITED BY: Miguel A. R. B. Castanho, Lorenzo Stella, Sattar Taheri-Araghi and Sergey A. Akimov

PUBLISHED IN: Frontiers in Medical Technology

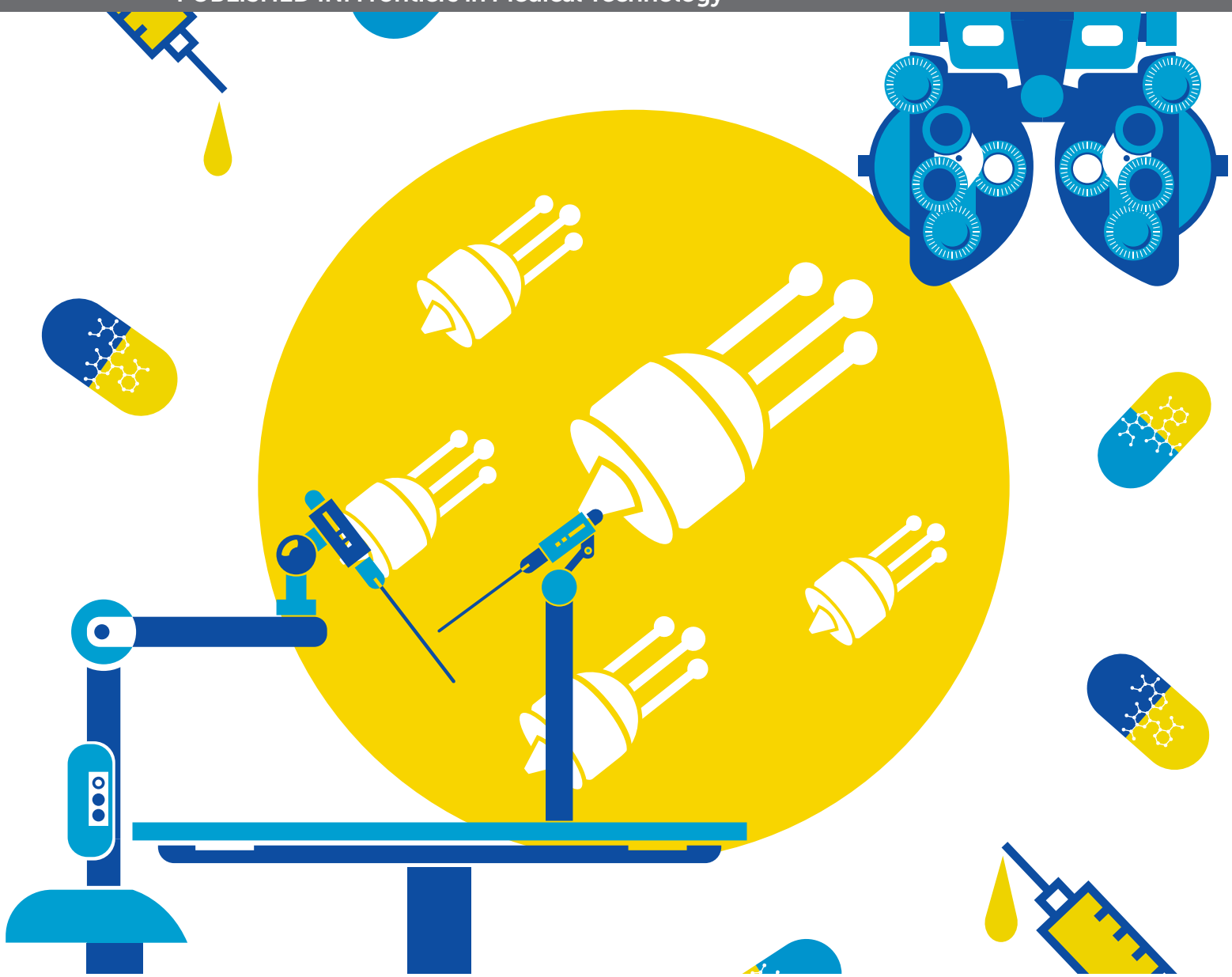

frontiers Research Topics

frontiers

ISSN 1664-8714
ISBN 978-2-88971-352-3
DOI 10.3389/978-2-88971-352-3

About Frontiers

Frontiers is more than just an open-access publisher of scholarly articles: it is a pioneering approach to the world of academia, radically improving the way scholarly research is managed. The grand vision of Frontiers is a world where all people have an equal opportunity to seek, share and generate knowledge. Frontiers provides immediate and permanent online open access to all its publications, but this alone is not enough to realize our grand goals.

Frontiers Journal Series

The Frontiers Journal Series is a multi-tier and interdisciplinary set of open-access, online journals, promising a paradigm shift from the current review, selection and dissemination processes in academic publishing. All Frontiers journals are driven by researchers for researchers; therefore, they constitute a service to the scholarly community. At the same time, the Frontiers Journal Series operates on a revolutionary invention, the tiered publishing system, initially addressing specific communities of scholars, and gradually climbing up to broader public understanding, thus serving the interests of the lay society, too.

Dedication to Quality

Each Frontiers article is a landmark of the highest quality, thanks to genuinely collaborative interactions between authors and review editors, who include some of the world's best academicians. Research must be certified by peers before entering a stream of knowledge that may eventually reach the public - and shape society; therefore, Frontiers only applies the most rigorous and unbiased reviews.
Frontiers revolutionizes research publishing by freely delivering the most outstanding research, evaluated with no bias from both the academic and social point of view. By applying the most advanced information technologies, Frontiers is catapulting scholarly publishing into a new generation.

What are Frontiers Research Topics?

Frontiers Research Topics are very popular trademarks of the Frontiers Journals Series: they are collections of at least ten articles, all centered on a particular subject. With their unique mix of varied contributions from Original Research to Review Articles, Frontiers Research Topics unify the most influential researchers, the latest key findings and historical advances in a hot research area! Find out more on how to host your own Frontiers Research Topic or contribute to one as an author by contacting the Frontiers Editorial Office: frontiersin.org/about/contact

BRIDGING MEMBRANE BIOPHYSICS TO MICROBIOLOGY: INNOVATING TOWARDS NEW PEPTIDE AND PEPTIDE-BASED ANTIMICROBIALS

Topic Editors:
Miguel A. R. B. Castanho, University of Lisbon, Portugal
Lorenzo Stella, University of Rome Tor Vergata, Italy
Sattar Taheri-Araghi, California State University, United States
Sergey A. Akimov, Frumkin Institute of Physical Chemistry and Electrochemistry (RAS), Russia

Citation: Castanho, M. A. R. B., Stella, L., Taheri-Araghi, S., Akimov, S. A., eds. (2022). Bridging Membrane Biophysics to Microbiology: Innovating Towards New Peptide and Peptide-based Antimicrobials. Lausanne: Frontiers Media SA. doi: 10.3389/978-2-88971-352-3

Table of Contents

frontiers in Medical Technology

EDITORIAL
published: 19 July 2021
doi: 10.3389/fmedt.2021.699154

Editorial: Bridging Membrane Biophysics to Microbiology: Innovating Towards New Peptide and Peptide-Based Antimicrobials

Lorenzo Stella[1], *Sergey A. Akimov*[2], *Sattar Taheri-Araghi*[3] *and Miguel A. R. B. Castanho*[4]*

[1] Department of Chemical Science and Technologies, University of Rome Tor Vergata, Rome, Italy, [2] Laboratory of Bioelectrochemistry, Frumkin Institute of Physical Chemistry and Electrochemistry (RAS), Moscow, Russia, [3] Department of Physics and Astronomy, California State University, Northridge, CA, United States, [4] School of Medicine, Instituto de Medicina Molecular, University of Lisbon, Lisbon, Portugal

Keywords: lipid, peptide, drug, translation, bacteria

Editorial on the Research Topic

Bridging Membrane Biophysics to Microbiology: Innovating Towards New Peptide and Peptide-Based Antimicrobials

OPEN ACCESS

Edited by:
Laura Orian,
University of Padua, Italy

Reviewed by:
Giovanni Ribaudo,
University of Brescia, Italy

***Correspondence:**
Miguel A. R. B. Castanho
macastanho@medicina.ulisboa.pt

Specialty section:
This article was submitted to Pharmaceutical Innovation, a section of the journal Frontiers in Medical Technology

Received: *23 April 2021*
Accepted: *21 June 2021*
Published: *19 July 2021*

Citation:
Stella L, Akimov SA, Taheri-Araghi S and Castanho MARB (2021) Editorial: Bridging Membrane Biophysics to Microbiology: Innovating Towards New Peptide and Peptide-Based Antimicrobials. Front. Med. Technol. 3:699154. doi: 10.3389/fmedt.2021.699154

Molecular biophysicists and microbiologists working on antimicrobial peptides (AMPs) are traditionally worlds apart. While biophysicists prefer detailed structural and functional approaches in systems they have total control of, such as lipid vesicles, microbiologists trade the details of molecular interactions for the "biorealism" of working with live bacteria. These two types of studies seemed impossible to reconciliate, until now. In recent years, biophysical techniques started to be applied in the quantitative investigation of the interaction of AMPs with target and host cells, providing several novel insights in the mechanism of action of these molecules. The articles of this Research Topic provide a comprehensive overview of the current state-of the-art in this area.

Top researchers devoted to AMPs, translating molecular biophysical approaches to bacterial microbiology, have gathered in this Research Topic publication to (i) review how imaging and spectroscopy techniques can be used to unveil AMP action directly in live bacteria, and (ii) present the fundamentals of the mechanism of action of AMP obtained with such techniques, including the influence of intracellular factors, synergy, and cell density. Structure-function relationships and a vision for future applications of antimicrobial surfaces are also present.

Gelmi et al. present a general overview of the experimental approaches that provide information on peptide-cell interaction, including fluorescence and calorimetry to quantify peptide-cell association, circular dichroism, and NMR to investigate the secondary structure of cell-bound peptides, infrared and NMR spectroscopies to study peptide effects on membrane structure and dynamics, zeta potential experiments to clarify the electrostatic aspects of the interaction, microscopies, and cytofluorimetry to study peptide localization and effects on bacterial growth and perturbation of cell membranes, scattering techniques to study peptide effects on cell shape and photocrosslinking coupled with mass spectroscopy to identify potential protein targets.

Clayton reviews the applications of fluorescence microscopic techniques to follow in real time the main events involved in bacterial killing. These studies are starting to illustrate the complexities of peptide-cell interaction: for instance, they showed that the timescale of AMP effects on bacteria is orders of magnitude slower than that required for the perturbation of artificial membranes, identified preferred sites of attack in cell membranes and demonstrated that peptide sequestration by dead cells can protect the rest of the bacterial population from the action of AMPs.

Booth focuses on deuterium solid state NMR studies of intact bacteria treated with AMPs. This approach provides information on peptide-induced perturbation of cell-membranes. For instance, it showed that some AMPs can cause disruption of the lipid bilayer at peptide:lipid ratios lower than those needed for killing, suggesting that membrane disruption may not be the only mechanism by which they harm cells.

Separovic et al. address in-cell solid-state NMR studies of AMPs, too, providing an overview of the different molecules that can be investigated with this technique, including peptidoglycans, lipopolysaccharides, phospholipids, DNA and AMPs themselves. The power of this non-invasive technique is exemplified by a recent study, which revealed a peptide-induced disruption of the molecular packing of both bacterial membranes and DNA.

Benfield and Henriques focus on the experimental approaches that can determine the mechanism of action of AMPs, and particularly differentiate peptides perturbing cellular membranes from those that interact with intracellular targets. Disruption of membranes can be observed in cells, using fluorophores that detect membrane depolarization or accessibility of the intracellular space. By comparing membrane perturbation and cell viability, membranes can be confirmed or excluded as the main target of AMPs. Peptide uptake into bacterial cells can be investigated using flow cytometry and fluorescence microscopy. Finally, intracellular protein targets of AMPs can be identified using bacterial proteome microarrays.

Bechinger et al. analyze the crucial property of synergy in AMPs: often, two (or more) peptides together have a higher activity than the single components. The molecular mechanisms of this effect are still heatedly debated. For the synergism between magainin 2 and PGLa, different hypotheses have been put forward, involving direct interaction of the peptides or changes in peptide orientation, but experiments performed with lipid mixtures correctly mimicking bacterial membranes support lipid mediated effects that favor peptide/membrane binding for the AMP mixture. The authors also show that a major effect of a synergistic combination is to increase the steepness of bacterial killing as a function of peptide concentration. This finding is consistent with a previous study on other AMPs (1) and provides a novel perspective on AMP synergism.

Duong et al. also address synergism, both among different AMPs and between AMPs and other classes of antibacterials, including histones, which co-localize with AMPs in innate immunity components. Such synergies might arise if one antimicrobial agent favors pore formation by the other, or if it acts on intracellular targets that can be reached more easily after pore formation.

Marx et al. present original research that bridges the antimicrobial activity of two lactoferricin derivatives (LF11-215 and LF11-324) in *E. coli* and lipid vesicles. In particular, they determined both an upper limit on the number of surface-adsorbed peptides and total number of peptides partitioned into the bacteria These data indicate that 95–99% of LF11-215 and LF11-324 molecules accumulate inside cells, suggesting that these AMPs might act on intracellular targets.

Schefter et al., in their original work, discuss several parameters that influence AMP activity and selectivity: density of target and host cells, competitive peptide association to the two cell populations, and peptide sequestration by association to intracellular targets. The authors propose a biophysical model, based on chemical equilibria, leading to a prediction of the cell-density dependence of peptide activity and selectivity, and allowing the correct design and interpretation of selectivity measurements.

Strandberg et al. review the specific class of artificial AMPs constituted by sequences of alternating cationic and hydrophobic residues, such as $[KL]_n$, or $[RW]_n$. When bound to membranes, these peptides attain a beta-like structure. Longer peptides can also form beta-aggregates in solution. Medium length peptides of 8–10 amino acids appear to be the optimum compromise for a high activity and low toxicity.

Mullen et al. present their perspective on the use of peptides and other molecules to design antimicrobial surfaces. This is a view into the future of peptide-based products and technologies to fight bacterial threats, mainly biofilms, which are probably the next big challenge ahead for AMP developers.

After bridging molecular biophysics to microbiology, it is important to bridge these fields to bacterial biofilm biomedicine. AMPs are up to the challenge. Are we, too?

AUTHOR CONTRIBUTIONS

Manuscript content was discussed and decided by all authors. MC and LS drafted the manuscript. All authors revised the manuscript.

REFERENCES

1. Yu G, Baeder DY, Regoes RR, Rolff J. Combination effects of antimicrobial peptides. *Antimicrob Agents Chemother*. (2016) 60:1717–24. doi: 10.1128/AAC.02434-15

Conflict of Interest: The authors declare that the research was conducted in the absence of any commercial or financial relationships that could be construed as a potential conflict of interest.

frontiers in Medical Technology

MINI REVIEW
published: 11 December 2020
doi: 10.3389/fmedt.2020.610997

Mode-of-Action of Antimicrobial Peptides: Membrane Disruption vs. Intracellular Mechanisms

*Aurélie H. Benfield and Sónia Troeira Henriques**

School of Biomedical Sciences, Institute of Health & Biomedical Innovation, and Translational Research Institute, Australian Research Council Centre of Excellence for Innovations in Peptide and Protein Science, Queensland University of Technology, Brisbane, QLD, Australia

Antimicrobial peptides are an attractive alternative to traditional antibiotics, due to their physicochemical properties, activity toward a broad spectrum of bacteria, and mode-of-actions distinct from those used by current antibiotics. In general, antimicrobial peptides kill bacteria by either disrupting their membrane, or by entering inside bacterial cells to interact with intracellular components. Characterization of their mode-of-action is essential to improve their activity, avoid resistance in bacterial pathogens, and accelerate their use as therapeutics. Here we review experimental biophysical tools that can be employed with model membranes and bacterial cells to characterize the mode-of-action of antimicrobial peptides.

Keywords: peptide-lipid interactions, bacterial membrane, cellular uptake, biophysical methodologies, peptide therapeutics

OPEN ACCESS

Edited by:
Lorenzo Stella,
University of Rome Tor Vergata, Italy

Reviewed by:
Frances Separovic,
The University of Melbourne, Australia
Diana Lousa,
New University of Lisbon, Portugal

****Correspondence:***
Sónia Troeira Henriques
sonia.henriques@qut.edu.au

Specialty section:
This article was submitted to Pharmaceutical Innovation, a section of the journal Frontiers in Medical Technology

Received: *28 September 2020*
Accepted: *20 November 2020*
Published: *11 December 2020*

Citation:
Benfield AH and Henriques ST (2020) Mode-of-Action of Antimicrobial Peptides: Membrane Disruption vs. Intracellular Mechanisms. Front. Med. Technol. 2:610997. doi: 10.3389/fmedt.2020.610997

INTRODUCTION

Antibiotic resistant bacteria are rapidly emerging while the development of new antimicrobial agents is decelerating (1–3). To fight infections caused by resistant bacteria, it is essential to develop new compounds. Antimicrobial peptides (AMPs) have attracted attention as potential alternative antimicrobial agents, as these small biological molecules kill bacteria using a mode-of-action (MOA) distinct from those used by traditional antibiotics (4).

AMPs are produced in almost all species (5), kill a broad spectrum of bacteria, fungi, protozoa and viruses, have anticancer properties (6, 7), and can kill antibiotic-resistant bacteria (8, 9). In general, AMPs are positively charged amphipathic molecules able to selectively target bacteria and kill them using two broad MOAs. In the first mechanism AMPs induce membrane disruption, leading to cell lysis and death. In the second MOA, AMPs enter cells without membrane disruption and inhibit essential intracellular functions by binding to nucleic acids or intracellular proteins (10–12).

Peptide-based antimicrobials, such as Tyrothricin, Gramicidin S (13), Vancomycin and Telavancin (14), are used in the clinic as therapeutics. Nevertheless, the widespread application of AMPs is limited by a perception that peptides are expensive to produce, susceptible to proteases, and display high cytotoxicity (15–17). Peptide production costs have decreased over the past years due to advances in solid- and liquid-phase peptide synthesis (18, 19), and production of recombinant peptides in *Escherichia coli* (20) and yeast (21). Peptides can be engineered to increase their chemical and proteolytic stability via backbone cyclization (22), side chain-to-side chain cyclization (23), or the inclusion of stereochemical amino acids (24). Furthermore, toxicity to the host can be reduced, and potency can be improved, if we understand their MOA (16, 25–28).

In this mini-review, we highlight some experimental biophysical techniques that can be employed to investigate the complex MOA of AMPs. Identifying whether particular AMPs act by disrupting bacterial membranes, or by interfering with an intracellular pathway, is key to rationally improve efficacy, stability and safety of AMPs, and develop novel antimicrobial therapeutics.

CHARACTERIZATION OF PEPTIDE-LIPID BINDING USING MODEL MEMBRANES

AMPs generally target and bind bacterial membranes via peptide-lipid interactions. Model membrane systems, including Langmuir monolayers, liposomes, and solid supported bilayers, have been used to screen peptide-membrane interactions and investigate the effect of peptides on the structure of lipid bilayers. Although they are less complex than bacterial membranes, model membranes are useful to investigate individual membrane components (29, 30). They can be produced with defined lipid compositions, biophysical properties, and conditions (e.g., size, charge, pH, ionic strength); thereby reducing the variables present in biological assays.

Liposomes are particularly useful as a model membrane: they are versatile, easy to prepare, and can be used in several methodologies. Liposomes can be prepared with synthetic lipids present in bacterial membranes, such as phospholipids with phosphatidylglycerol-, or phosphatidylethanolamine-headgroups and cardiolipin (31) or can be prepared with lipids extracted directly from bacterial membranes. Liposomes are unilamellar or multilamellar structures obtained by suspending lipids in an aqueous solution and by sonicating, or extruding them through a membrane filter with a defined pore size, such as 50 nm, 100 nm and 1 μm, to prepare small, large and giant vesicles, respectively.

Surface plasmon resonance (SPR) (**Figure 1A**) can be used to study peptide-lipid binding affinity in real-time and without requiring fluorescently labeled peptide. In this assay, liposomes are deposited onto the surface of a sensor chip covered with polydextran (e.g., L1 Sensor Chip from GE Biacore systems) to form a stable lipid bilayer (32). Peptide solution is injected over the lipid bilayer and peptide-lipid binding is monitored via variation of refractive index over time. Sensorgrams can be used to calculate peptide-lipid binding association (k_{on}), dissociation (k_{off}) rate constants, equilibrium dissociation constant (K_D) and membrane partition coefficients (K_p) (32, 33). It is possible to predict cytotoxic properties of AMPs by comparing their peptide-lipid binding affinity. AMPs with high binding affinity for negatively charged membranes and with weak affinity for zwitterionic membranes are normally selective toward bacteria and not toxic to host cells (34).

Many AMPs kill bacteria by inducing membrane disruption and leakage of bacterial content. Leakage assays with model membranes (**Figure 1B**) can be used to investigate the ability of AMPs to disrupt lipid bilayers. In these assays, an aqueous soluble fluorescent dye, such as carboxyfluorescein (35–37) or calcein (38, 39), is entrapped into large unilamellar vesicles at self-quenching concentrations. Dye-loaded vesicles are resuspended in buffer by gel filtration and their lipid concentration quantified using the Stewart assay (40). If peptides permeabilize vesicles, the fluorescent dye is released into solution, resulting in increased fluorescence emission signal. This assay can be performed in a 96-well plate format to reduce the volume of reagents and peptides (41). It can also be used to investigate membrane selectivity in a competitive lipid environment (42). For example, AMPs can be incubated with a mixture of liposomes of distinct composition to quantify selective disruption of negatively charged over neutral liposomes. Although leakage assays do not provide information about the disruption mechanism involved (e.g., toroidal pore, barrel pore, or carpet mechanism), they inform on whether AMPs can disrupt lipid bilayers, can be used to investigate membrane selectivity (42).

Molecular dynamic simulations using atomistic or coarse-grained models of lipid bilayers, can also be used to characterize peptide-lipid interactions and to gain information on the disruption mechanism used by specific AMPs (43–46). More complex bacterial cell wall models (e.g., peptidoglycan network, outer membrane of Gram-negative bacteria) (47–49) have been developed and can be used to simulate interactions of peptides with bacterial cell walls, and predict membrane disruption properties (50).

EXAMINING INTEGRITY AND FUNCTION OF BACTERIAL MEMBRANES USING MEMBRANE DYES

Membrane dyes and fluorescence spectrophotometer plate readers can be used with bacteria cells to study the effect of AMPs on the integrity of specific layers of bacterial membranes. For instance, the fluorescence of the lipophilic dye *N*-phenyl-1-napthylamine (NPN) can inform on the ability of AMPs to permeabilize the outer membrane of Gram-negative bacteria (**Figure 1C**). NPN emits weak fluorescence in aqueous environment and is highly fluorescent in hydrophobic environment found in lipid membranes. NPN cannot insert into intact bacteria membranes; however, when AMPs disturb the outer membrane of Gram-negative bacteria, NPN gains access to lipid layers in the outer membrane and/or in the cytoplasmic membrane (51–53) and its fluorescence emission intensity increases. This assay can be done using a 96-well plate format in a fluorescence spectrophotometer plate reader, in which peptides are added to bacterial suspensions.

Cell membranes of viable bacteria are polarized (i.e., they have a negative transmembrane potential), and some cationic AMPs kill bacteria by depolarizing their membranes (10, 54). The dye 3,3′-Dipropylthiadicarbocyanine iodide [$DiSC_3(5)$] is cationic, membrane-permeable, fluorescent in aqueous environment and can be used to examine the ability of specific AMPs to depolarize bacterial membranes (53, 55, 56). DiSC3(5) has a stable and low fluorescence emission signal when bound to viable bacteria with polarized membranes; if an AMP induces membrane depolarization, the dye is released, and its fluorescence emission intensity increases (**Figure 1D**). In this assay, it is important to optimize cell density, dye concentration and ensure that tested

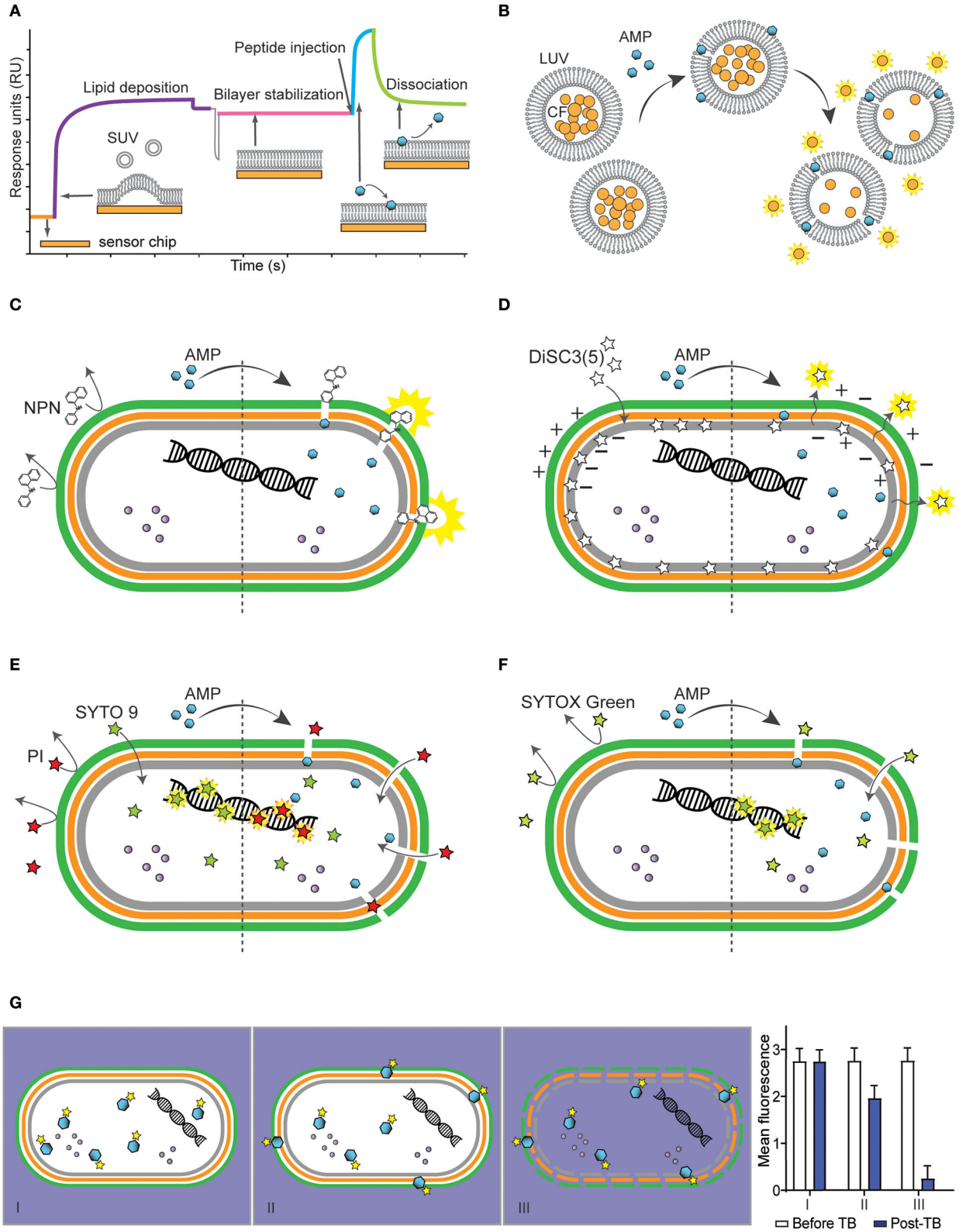

FIGURE 1 | Methodologies to determine interactions of antimicrobial peptides (AMPs) with bacterial membranes using model membranes **(A,B)** and bacterial cells **(C-G)**. **(A)** Schematic representation of a sensorgram obtained with surface plasmon resonance (SPR) to monitor peptide-lipid interactions. The response units (RU) increase when small unilamellar vesicles (SUV) are injected to cover the chip (orange) and form a bilayer (purple). Once the bilayer is stabilized (pink), AMPs are injected

(Continued)

FIGURE 1 | and association with the lipid bilayer (blue) is monitored in real time. The stronger the binding of the antimicrobial peptide (AMP) to the lipid system, the higher the response units. When the peptide injection stops, it is possible to monitor the dissociation of the peptides from the lipid bilayer (green). **(B)** Illustration of the leakage assay using large unilamellar vesicles (LUV) filled with carboxyfluorescein (CF), whose fluorescence is self-quenched when packed inside LUVs at high concentration. In the presence of permeabilizing AMPs, CF escapes into the aqueous environment and becomes fluorescent. **(C–F)** Schematic of a Gram-negative bacterium with inner membrane (gray), peptidoglycan layer (orange), outer membrane (green) and intracellular content such as proteins (purple spheres) and nucleic acids (helix) and the effect of fluorescent dyes before (left) and after (right) treatment with a membrane-active AMP. **(C)** Illustration of *N*-phenyl-1-napthylamine (NPN) becoming highly fluorescent when in hydrophobic environment such as lipid membranes, subsequently damaged by AMPs. **(D)** Illustration of 3,3′-Dipropylthiadicarbocyanine iodide [$DiSC_3(5)$] packed within inner membrane of bacterium. DiSC3(5) is released into the aqueous environment and becomes highly fluorescent (right) once membrane is depolarized by binding of AMPs. **(E)** Illustration of bacterial cells incubated with propidium iodide (PI) and SYTO 9, to label lysed/dead and viable cells, respectively. Left side shows PI unable to go through intact membrane, unlike SYTO 9 that can penetrate intact membrane and bind to DNA. Once AMP damages membrane, PI enters the cell and displaces SYTO 9 (right). **(F)** Illustration of SYTOX Green which is highly fluorescent if bound to DNA, however, unable to go through bacterial membrane unless membrane is damaged by the AMP. **(G)** Schematic of internalization of bacterial cell by fluorescently labeled AMP and graph showing fluorescence measurement before and after addition of trypan blue (TB). Panel I shows an AMP able to enter bacteria cells without damaging membrane, panel II shows an AMP entering cells with a portion located on the membrane, and panel III shows internalization of an AMP and permeabilization of bacterial membrane resulting in drop of fluorescence readings after addition of TB quenching fluorescence of labeled AMP.

AMPs do not quench the fluorescence of the dye, as this assay is based on fluorescence quenching (57).

EXAMINING BACTERIAL MEMBRANE INTEGRITY USING FLOW CYTOMETRY

Flow cytometry combines fluidic, optical and electronic parameters to analyze physical properties (e.g., size and granularity) and fluorescence of individual cells within a population of cells. Each cell goes through a set of lasers and produces scattered and fluorescent light signals that are detected and analyzed by a computer (58).

Bacteria with permeabilized membranes can be distinguished from viable bacterial cells using two fluorescent dyes [e.g., propidium iodide (PI) and SYTO 9] and by analyzing cells using flow cytometry (59). PI and SYTO 9 become fluorescent when intercalating with DNA. However, PI is a red-fluorescent dye, non-permeable to intact plasma membranes and cannot enter viable cells, whereas SYTO 9 is a green-fluorescent dye that can enter both live and dead bacterial cells (**Figure 1E**). PI has stronger affinity for nucleic acids than SYTO 9; therefore, when both dyes have access to nucleic acids inside bacteria, PI displaces SYTO 9 (60).

There are some factors that might interfere with correct readings, such as photobleaching of SYTO 9, variable binding affinities of SYTO 9 to live and dead cells, background fluorescence and bleed-through (61). Moreover, some bacteria strains have efflux pumps that can remove PI from the cell (60). Nevertheless, this is a rapid and high-throughput assay to quantify the effect of AMPs on the cell membrane integrity within a large population of cells (62).

SYTOX Green is another high-affinity nucleic acid stain that can be used to investigate cell membrane integrity in bacteria using flow cytometry. This dye only enters cells with compromised plasma membrane (**Figure 1F**). The binding of SYTOX green to nucleic acids results in >500-fold increase in fluorescence emission intensity (63). SYTOX green and PI have similar molecular weight (i.e., 600 and 688 Da), and entry of these two dyes into bacteria is unlikely to be discriminated based on their size. Nevertheless, the detection of permeabilized cells and distinction from non-permeabilized cells is superior when using SYTOX Green. This dye has a higher quantum yield and molar extinction coefficient compared to that of PI (63). These advantages might explain why many studies used SYTOX green to investigate bacterial membrane integrity in the presence of AMPs, instead of the combination of SYTO 9 and PI (53, 64–69).

CONFIRMING WHETHER MEMBRANE DISRUPTION IS THE CAUSE OF DEATH

It is important to investigate whether peptide concentrations required to lyse bacterial membranes correlate with concentrations required to kill bacteria. Some AMPs display a minimal inhibitory concentration (MIC) below the concentration required to disrupt membranes, suggesting that bacteria are being killed/inactivated by a mechanism not directly related to cell membrane disruption. This can be investigated by treating bacteria with various concentrations of peptide and quantifying viable cells (e.g., using plate colony count method) in parallel with permeabilized cells (e.g., using a flow cytometry assay with SYTOX Green) (67, 70). Interestingly, some bacteria species seem to be more resistant to membrane damage, as suggested by a study with the AMP maculatin 1.1. This peptide induces uptake of SYTOX Green in *E. coli* and *Staphylococcus aureus* at similar concentrations, but is more potent at inhibiting the growth of *S. aureus* (67).

When AMPs inhibit bacterial growth at non-permeabilizing concentrations, their MOA is likely to involve entry in the cell and ability to interact with an intracellular target; therefore, it is important to investigate whether they can enter inside bacteria. These non-lytic AMPs able to cross bacterial membranes can also be referred to as cell-penetrating peptides (66).

DISTINGUISHING INTERNALIZED AND MEMBRANE-BOUND PEPTIDE VIA FLOW CYTOMETRY

Uptake into bacterial cells can be investigated using flow cytometry and peptides labeled with a fluorophore, such as Alexa Fluor® 488, fluorescein isothiocyanate (FITC), bodipy or rhodamine. Care must be taken when choosing

the fluorophore, as some can alter peptide physicochemical properties (e.g., increase of overall hydrophobicity), peptide-peptide intermolecular interactions, binding affinity for lipid bilayers, activity, or cellular uptake (71–75).

There are also some challenges in conjugating peptides with fluorescent labels, as the most common strategies involve amide bond ligation with labels derivatized with succinimidyl esters and require a free amine (66, 69). Therefore, the peptide requires an uncapped N-terminal, or a Lys residue within the amino acid sequence if the peptide is backbone-cyclised. Moreover, when the peptide has more than one Lys, several isomers with one or more label molecules might be obtained (76). To decrease the number of possible isomers and avoid changes in the overall charge of Lys-rich peptides after labeling, the dye can be conjugated using site-directed strategies. Some examples include conjugation of alkyne-derivatized dyes onto azide-containing peptides with copper-catalyzed azide-alkyne cycloaddition, and conjugation of dyes containing hydroxylamine with acetone-linked peptides using oxime ligation (77).

Fluorescently labeled AMP molecules located inside bacteria can be distinguished from those bound to the bacteria surface by screening peptide-treated cells via flow cytometry (**Figure 1G**). Fluorescence emission intensity and percentage of fluorescent bacteria are recorded before and after addition of trypan blue (TB), an aqueous fluorescence quencher unable to enter cells with intact membranes. A similar fluorescence emission signal before and after addition of TB indicates that the peptide is inside the bacteria. A decrease in fluorescence emission signal suggests that a proportion of peptide molecules is surface exposed and accessible to TB. A significant decrease in the percentage of fluorescent bacteria and in the fluorescence emission intensity indicate that cells are permeabilized, which enabled TB to enter and quench the fluorescence emission of peptide inside cells (66, 78, 79).

USING MICROSCOPY TO VISUALIZE BACTERIA MORPHOLOGY AND PEPTIDE LOCATION

Changes in cell morphology induced by AMPs can be visualized using electron microscopy and atomic force microscopy (AFM). Bacterial cells incubated with sub-lethal and/or lethal concentrations of AMPs are imaged to identify whether the membrane surface is intact, becomes wrinkly, has blebs, or is lysed (28, 80–82). AMPs inducing visible damages are likely to act on the membrane, whereas lack of morphological changes at lethal concentrations suggests interference with an internal component.

The location of labeled AMPs inside bacteria can be visualized using confocal microscopy. For instance, AMPs NCR247 and NCR235 bind to the membrane of both *Salmonella* and *Listeria*, but can only reach the cytosol of *Salmonella* (83, 84). In another study, the authors showed localization of an AMP inside *E. coli* using confocal microscopy, SYTOX green and rhodamine-labeled AMP, and confirmed changes in the *E. coli* morphology using AFM (70). These examples demonstrate how diverse and versatile microscopy techniques are to evaluate peptide location within bacteria, and effect on their membrane.

DETECTION OF AMP AND NUCLEIC ACID INTERACTIONS USING ELECTROPHORETIC MOBILITY SHIFT ASSAYS

Some AMPs kill bacteria by interacting with DNA or RNA, and therefore interfere with their synthesis, replication, and translational processes (10, 85). It is debatable whether AMPs can target specific portions of DNA/RNA, as positively charged AMPs might bind unspecifically to negatively charged nucleic acids via strong electrostatic attractions (86). In addition, binding to nucleic acids can be unrelated to the cell death mechanism, as it can occur as a result of AMPs entering bacteria after disrupting their membranes. Thus, studies to investigate interaction with DNA/RNA are more appropriate with non-lytic AMPs.

The gel electrophoretic mobility shift assay (EMSA) is a rapid and sensitive methodology used to detect interactions between proteins, or peptides, with DNA/RNA (87). In this assay, the peptide is incubated with nucleic acids and the reaction is electrophoresed on an agarose or native polyacrylamide gel to detect whether a peptide-nucleic acid complex is formed based on a slower migration than that of free nucleic acid. The complex can be detected using a range of approaches, including fluorescence, chemiluminescence, immunohistochemical and highly sensitive radioisotope-labeled nucleic acids (**Figure 2A**). One limitation to consider during the electrophoresis is that samples are not at chemical equilibrium and therefore rapid dissociation during this time might prevent detection of the complex. Antimicrobial peptides such as indolicin (88), LL-37 (89), Burforin II (90) and Frenatin 2.3S peptide (91) have been shown to bind bacterial DNA using EMSAs.

PROTEOMICS TO SEARCH FOR A PUTATIVE INTRACELLULAR TARGET OR/AND DIFFERENCES IN PROTEIN EXPRESSION

Non-lytic AMPs that translocate through bacterial membranes might inhibit intracellular processes by interacting with essential proteins and enzymes (92). Mass spectrometry and proteome microarray are examples of methodologies used to identify protein targets of AMPs and/or the subsequent changes in protein expression due to peptide entry inside bacteria.

Mass spectrometry is a powerful tool to examine changes in protein expression of bacteria treated with AMPs. In the unlabeled approach, after co-incubation of bacteria with AMPs, proteins are extracted, digested and fractionated, and the whole proteome is analyzed by mass spectrometry (**Figure 2B**). A recent study used this approach to show the effect of LL-37 peptide on the proteome of *Streptococcus pneumoniae* D39, and identified alteration in the expression of 105 proteins (93). Treatment with LL-37 induced upregulation of proteins involved in cell surface

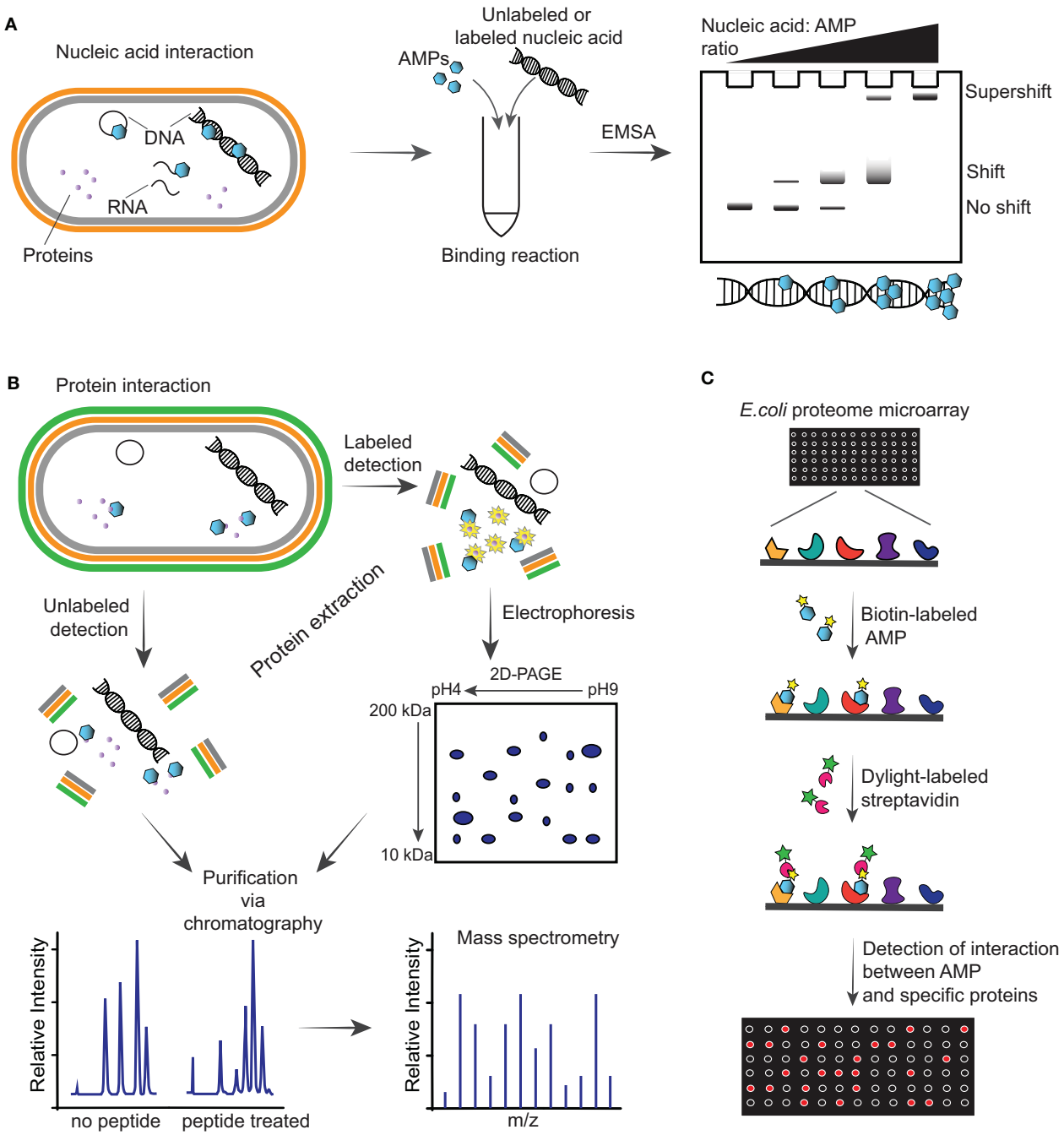

FIGURE 2 | Illustrations of methodologies for detection of intracellular targets of antimicrobial peptides (AMPs). **(A)** Schematic of detection of an AMP able to interact with nucleic acid including DNA, plasmid DNA and RNA of a Gram-negative bacterium via electrophoretic mobility shift assay (EMSA). This assay consists of running incubation reactions between increasing ratios of AMPs with specific nucleic acid (labeled or unlabeled) and running the reactions through an agarose gel. Depending on the affinity of the AMP with the nucleic acid, a shift or supershift in the EMSA is observed. **(B)** Interaction of AMPs with intracellular proteins can be detected by incubating the peptides with bacteria, followed by protein extraction, purification, and mass spectrometry analysis. Alternatively, cells can be incubated with AMPs followed by addition of radioactive labels to incorporate labels to the newly synthesized proteins and performing a two-dimensional polyacrylamide gel (2D-PAGE), from which spots are analyzed via mass spectrometry. **(C)** Schematic representation of *E. coli* proteome microarray and workflow. Biotinylated AMPs are probed on the microarray followed by Dylight-labeled streptavidin to tag the biotin linked on the AMPs and signals are obtained by scanning the chip with a laser scanner to show interaction between AMPs and specific proteins on the chip.

modification, including increasing membrane surface charge, and an abundance of ABC transporters. These modifications are likely to help removing LL-37 from the bacterial membrane. Using a similar workflow, lipidomics studies can be used to investigate changes in the lipid composition of bacterial membranes after treatment with AMPs, as recently reviewed (94).

Wenzel et al. (95) reported a radio-labeling approach to facilitate the identification of proteins that are up/down regulated upon treatment with peptide (**Figure 2B**). In this study, *Bacillus subtilis* cultures were incubated with RW-rich peptides, followed by addition of radioactive methionine to incorporate a radioactive label into newly synthesized proteins. Proteins were extracted from cells and separated on a two-dimensional polyacrylamide gel (2D-PAGE) where up/down regulated proteins were identified, excised from the gel and identified by mass spectrometry (95).

Proteome microarray is another powerful and high-throughput tool with potential to screen the entire proteome and identify targets in a single experiment. This has been exemplified with a biotin-labeled AMP and incubated with an *E. coli* K12 proteome microarray chip, followed by detection of the biotinylated AMPs with Dylight-labeled streptavidin (92) (**Figure 2C**). The signals detected on a microarray scanner show binding between specific proteins and AMPs. Fabricated *E. coli* K12 proteome microarrays have been used to identify intracellular protein targets of several AMPs, such as bactenecin 7, a hybrid of pleurocidin and dermaseptin, and proline-arginine-rich peptide (96). However, the coverage of the microarray, differences between the proteins immobilized on microarrays and their counterpart in physiological conditions, and the cost are limitations for a broader use of protein microarrays (97).

DISCUSSION

AMPs are promising leads to develop new antimicrobial drugs to treat bacterial infections. The number of AMPs reported to date is high, and some candidates reached clinical trials (98, 99). Understanding the MOA used by AMPs to kill bacteria is important to advance their development. Here we describe some experimental biophysical tools that can be used to investigate whether AMPs act by disrupting bacterial membranes, or by modulating intracellular activities. An overview of multiple AMPs, their MOA and the biophysical techniques employed to characterize them, is summarized in a recent review (100).

Determining whether an AMP disrupts bacterial membranes can be straightforward; however, finding specific intracellular targets is more complex. Pinpointing whether AMPs act by interfering with DNA, RNA or proteins remains challenging, as some AMPs not only act on the membrane they can also activate a cascade of reactions within the bacteria (12, 85). Advances in transcriptomics, proteomics, lipidomics and continued development of high-throughput techniques will facilitate these MOA studies.

Computational tools, such as molecular dynamics simulations, machine learning, and AMPs databases [such as https://dbaasp.org/ (101)] are also important to identify new AMPs, characterize their MOA, and predict lead candidates (102, 103). Computer-based and wet-lab based methodologies can be integrated to better understand the MOA of AMPs, and to rationally design novel AMPs with a required MOA. For example, when searching for AMPs to target intracellular pathogens, it is desirable to have peptides with cell-penetrating properties able to enter host cells and kill bacteria by modulating specific bacterial components, without disrupting the membrane of host cells. On the other hand, when targeting mixed-species biofilms, membrane-lytic AMPs with a broad-spectrum activity are likely to be more effective at the infection site, compared to AMPs that selectively inhibit an intracellular target.

MOA studies *in vitro* and *in silico*, together with efficacy, safety and pharmacology studies *in vivo* and *ex vivo*, are essential to convert AMP leads into therapeutics used in the clinic. In particular, MOA studies help in identifying off-targets in host cells, understanding spectrum of activity, finding intrinsically resistant bacteria, and overcoming challenges associated with delivery of peptides. Therefore, the biophysical tools here described can assist the development of novel antibiotics.

AUTHOR CONTRIBUTIONS

AB and STH conceptualized the manuscript. AB wrote the original draft. STH reviewed and edited the manuscript. Both authors contributed to the article and approved the submitted version.

FUNDING

STH was an Australian Research Council (ARC) Future Fellow (FT150100398). The Translational Research Institute was supported by a grant from the Australian Government. The authors are supported by the Australian Research Council Centre of Excellence for Innovations in Peptide and Protein Science (CE200100012).

REFERENCES

1. Ventola CL. The antibiotic resistance crisis: part 1: causes and threats. *P T.* (2015) 40:277–83.
2. Ghosh C, Sarkar P, Issa R, Haldar J. Alternatives to conventional antibiotics in the era of antimicrobial resistance. *Trends Microbiol.* (2019) 27:323–38. doi: 10.1016/j.tim.2018.12.010
3. Ventola CL. The antibiotic resistance crisis: part 2: management strategies and new agents. *P T.* (2015) 40:344–52.
4. Lei J, Sun L, Huang S, Zhu C, Li P, He J, et al. The antimicrobial peptides and their potential clinical applications. *Am J Transl Res.* (2019) 11:3919–31.
5. Zasloff M. Antimicrobial peptides of multicellular organisms. *Nature.* (2002) 415:389–95. doi: 10.1038/415389a

6. Hancock RE, Diamond G. The role of cationic antimicrobial peptides in innate host defences. *Trends Microbiol.* (2000) 8:402–10. doi: 10.1016/S0966-842X(00)01823-0
7. Zhang LJ, Gallo RL. Antimicrobial peptides. *Curr Biol.* (2016) 26:R14–R19. doi: 10.1016/j.cub.2015.11.017
8. Ageitos JM, Sanchez-Perez A, Calo-Mata P, Villa TG. Antimicrobial peptides (AMPs): ancient compounds that represent novel weapons in the fight against bacteria. *Biochem Pharmacol.* (2017) 133:117–38. doi: 10.1016/j.bcp.2016.09.018
9. Mourtada R, Herce HD, Yin DJ, Moroco JA, Wales TE, Engen JR, et al. Design of stapled antimicrobial peptides that are stable, nontoxic and kill antibiotic-resistant bacteria in mice. *Nat Biotechnol.* (2019) 37:1186–97. doi: 10.1038/s41587-019-0222-z
10. Brogden KA. Antimicrobial peptides: pore formers or metabolic inhibitors in bacteria? *Nat Rev Microbiol.* (2005) 3:238–50. doi: 10.1038/nrmicro1098
11. Sani MA, Separovic F. How membrane-active peptides get into lipid membranes. *Acc Chem Res.* (2016) 49:1130–8. doi: 10.1021/acs.accounts.6b00074
12. Le CF, Fang CM, Sekaran SD. Intracellular targeting mechanisms by antimicrobial peptides. *Antimicrob Agents Chemother.* (2017) 61:e02340–16. doi: 10.1128/AAC.02340-16
13. Wenzel M, Rautenbach M, Vosloo JA, Siersma T, Aisenbrey CHM, Zaitseva E, et al. The multifaceted antibacterial mechanisms of the pioneering peptide antibiotics tyrocidine and gramicidin S. *mBio.* (2018) 9:e00802–18. doi: 10.1128/mBio.00802-18
14. Binda E, Marinelli F, Marcone GL. Old and new glycopeptide antibiotics: action and Resistance. *Antibiotics.* (2014) 3:572–94. doi: 10.3390/antibiotics3040572
15. Mahlapuu M, Hakansson J, Ringstad L, Bjorn C. Antimicrobial peptides: an emerging category of therapeutic agents. *Front Cell Infect Microbiol.* (2016) 6:194. doi: 10.3389/fcimb.2016.00194
16. Mishra B, Reiling S, Zarena D, Wang G. Host defense antimicrobial peptides as antibiotics: design and application strategies. *Curr Opin Chem Biol.* (2017) 38:87–96. doi: 10.1016/j.cbpa.2017.03.014
17. Chen CH, Lu TK. Development and challenges of antimicrobial peptides for therapeutic applications. *Antibiotics.* (2020) 9:24. doi: 10.3390/antibiotics9010024
18. Isidro-Llobet A, Kenworthy MN, Mukherjee S, Kopach ME, Wegner K, Gallou F, et al. Sustainability challenges in peptide synthesis and purification: from RandD to production. *J Org Chem.* (2019) 84:4615–28. doi: 10.1021/acs.joc.8b03001
19. Magana M, Pushpanathan M, Santos AL, Leanse L, Fernandez M, Ioannidis A, et al. The value of antimicrobial peptides in the age of resistance. *Lancet Infect Dis.* (2020) 20:e216–e230. doi: 10.1016/S1473-3099(20)30327-3
20. Gaglione R, Pane K, Dell'olmo E, Cafaro V, Pizzo E, Olivieri G, et al. Cost-effective production of recombinant peptides in *Escherichia coli*. *N Biotechnol.* (2019) 51:39–48. doi: 10.1016/j.nbt.2019.02.004
21. Cao J, De La Fuente-Nunez C, Ou RW, Torres MT, Pande SG, Sinskey AJ, et al. Yeast-based synthetic biology platform for antimicrobial peptide production. *ACS Synth Biol.* (2018) 7:896–902. doi: 10.1021/acssynbio.7b00396
22. Clark RJ, Fischer H, Dempster L, Daly NL, Rosengren KJ, Nevin ST, et al. Engineering stable peptide toxins by means of backbone cyclization: stabilization of the alpha-conotoxin MII. *Proc Natl Acad Sci USA.* (2005) 102:13767–72. doi: 10.1073/pnas.0504613102
23. Schafmeister CE, Po J, Verdine GL. An all-hydrocarbon cross-linking system for enhancing the helicity and metabolic stability of peptides. *J Am Chem Soc.* (2000) 122:5891–2. doi: 10.1021/ja000563a
24. Tugyi R, Uray K, Ivan D, Fellinger E, Perkins A, Hudecz F. Partial D-amino acid substitution: improved enzymatic stability and preserved Ab recognition of a MUC2 epitope peptide. *Proc Natl Acad Sci USA.* (2005) 102:413–8. doi: 10.1073/pnas.0407677102
25. Zelezetsky I, Tossi A. Alpha-helical antimicrobial peptides–using a sequence template to guide structure-activity relationship studies. *Biochim Biophys Acta.* (2006) 1758:1436–49. doi: 10.1016/j.bbamem.2006.03.021
26. Badosa E, Ferre R, Planas M, Feliu L, Besalu E, Cabrefiga J, et al. A library of linear undecapeptides with bactericidal activity against phytopathogenic bacteria. *Peptides.* (2007) 28:2276–85. doi: 10.1016/j.peptides.2007.09.010
27. Mangoni ML, Shai Y. Short native antimicrobial peptides and engineered ultrashort lipopeptides: similarities and differences in cell specificities and modes of action. *Cell Mol Life Sci.* (2011) 68:2267–80. doi: 10.1007/s00018-011-0718-2
28. Torcato IM, Huang YH, Franquelim HG, Gaspar D, Craik DJ, Castanho MA, et al. Design and characterization of novel antimicrobial peptides, R-BP100 and RW-BP100, with activity against gram-negative and gram-positive bacteria. *Biochim Biophys Acta.* (2013) 1828:944–55. doi: 10.1016/j.bbamem.2012.12.002
29. Knobloch J, Suhendro DK, Zieleniecki JL, Shapter JG, Koper I. Membrane-drug interactions studied using model membrane systems. *Saudi J Biol Sci.* (2015) 22:714–8. doi: 10.1016/j.sjbs.2015.03.007
30. Hollmann A, Martinez M, Maturana P, Semorile LC, Maffia PC. Antimicrobial peptides: interaction with model and biological membranes and synergism with chemical antibiotics. *Front Chem.* (2018) 6:204. doi: 10.3389/fchem.2018.00204
31. Epand RM, Epand RF. Bacterial membrane lipids in the action of antimicrobial agents. *J Pept Sci.* (2011) 17:298–305. doi: 10.1002/psc.1319
32. Figueira TN, Freire JM, Cunha-Santos C, Heras M, Goncalves J, Moscona A, et al. Quantitative analysis of molecular partition towards lipid membranes using surface plasmon resonance. *Sci Rep.* (2017) 7:45647. doi: 10.1038/srep45647
33. Benfield AH, Defaus S, Lawrence N, Chaousis S, Condon N, Cheneval O, et al. Cyclic gomesin, a stable redesigned spider peptide able to enter cancer cells. *Biochim Biophys Acta Biomembr.* (2020) 1863:183480. doi: 10.1016/j.bbamem.2020.183480
34. Maturana P, Martinez M, Noguera ME, Santos NC, Disalvo EA, Semorile L, et al. Lipid selectivity in novel antimicrobial peptides: implication on antimicrobial and hemolytic activity. *Colloids Surf B Biointerfaces.* (2017) 153:152–9. doi: 10.1016/j.colsurfb.2017.02.003
35. Weinstein JN, Klausner RD, Innerarity T, Ralston E, Blumenthal R. Phase transition release, a new approach to the interaction of proteins with lipid vesicles. Application to lipoproteins. *Biochim Biophys Acta.* (1981) 647:270–84. doi: 10.1016/0005-2736(81)90255-8
36. Rex S. Pore formation induced by the peptide melittin in different lipid vesicle membranes. *Biophys Chem.* (1996) 58:75–85. doi: 10.1016/0301-4622(95)00087-9
37. Ambroggio EE, Separovic F, Bowie JH, Fidelio GD, Bagatolli LA. Direct visualization of membrane leakage induced by the antibiotic peptides: maculatin, citropin, and aurein. *Biophys J.* (2005) 89:1874–81. doi: 10.1529/biophysj.105.066589
38. Kendall DA, Macdonald RC. A fluorescence assay to monitor vesicle fusion and lysis. *J Biol Chem.* (1982) 257:13892–5.
39. Won A, Ianoul A. Interactions of antimicrobial peptide from C-terminus of myotoxin II with phospholipid mono- and bilayers. *Biochim Biophys Acta.* (2009) 1788:2277–83. doi: 10.1016/j.bbamem.2009.07.012
40. Stewart JC. Colorimetric determination of phospholipids with ammonium ferrothiocyanate. *Anal Biochem.* (1980) 104:10–4. doi: 10.1016/0003-2697(80)90269-9
41. Huang YH, Colgrave ML, Daly NL, Keleshian A, Martinac B, Craik DJ. The biological activity of the prototypic cyclotide kalata b1 is modulated by the formation of multimeric pores. *J Biol Chem.* (2009) 284:20699–707. doi: 10.1074/jbc.M109.003384
42. Sani MA, Gagne E, Gehman JD, Whitwell TC, Separovic F. Dye-release assay for investigation of antimicrobial peptide activity in a competitive lipid environment. *Eur Biophys J.* (2014) 43:445–50. doi: 10.1007/s00249-014-0970-0
43. Cruz VL, Ramos J, Melo MN, Martinez-Salazar J. Bacteriocin AS-48 binding to model membranes and pore formation as revealed by coarse-grained simulations. *Biochim Biophys Acta.* (2013) 1828:2524–31. doi: 10.1016/j.bbamem.2013.05.036
44. Bennett WF, Hong CK, Wang Y, Tieleman DP. Antimicrobial peptide simulations and the influence of force field on the free energy for pore formation in lipid bilayers. *J Chem Theory Comput.* (2016) 12:4524–33. doi: 10.1021/acs.jctc.6b00265

45. Aghazadeh H, Ganjali Koli M, Ranjbar R, Pooshang Bagheri K. Interactions of GF-17 derived from LL-37 antimicrobial peptide with bacterial membranes: a molecular dynamics simulation study. *J Comput Aided Mol Des.* (2020) 34:1261–73. doi: 10.1007/s10822-020-00348-4
46. Su J, Marrink SJ, Melo MN. Localization preference of antimicrobial peptides on liquid-disordered membrane domains. *Front Cell Dev Biol.* (2020) 8:350. doi: 10.3389/fcell.2020.00350
47. Piggot TJ, Holdbrook DA, Khalid S. Electroporation of the *E. coli* and *S Aureus* membranes: molecular dynamics simulations of complex bacterial membranes. *J Phys Chem B.* (2011) 115:13381–8. doi: 10.1021/jp207013v
48. Kim S, Pires MM, Im W. Insight into elongation stages of peptidoglycan processing in bacterial cytoplasmic membranes. *Sci Rep.* (2018) 8:17704. doi: 10.1038/s41598-018-36075-y
49. Vaiwala R, Sharma P, Puranik M, Ayappa KG. Developing a coarse-grained model for bacterial cell walls: evaluating mechanical properties and free energy barriers. *J Chem Theory Comput.* (2020) 16:5369–84. doi: 10.1021/acs.jctc.0c00539
50. Jiang X, Yang K, Yuan B, Gong B, Wan L, Patil NA, et al. Simulations of octapeptin-outer membrane interactions reveal conformational flexibility is linked to antimicrobial potency. *J. Biol. Chem*. (2020) 295:15902–12. doi: 10.1074/jbc.RA120.014856
51. Hancock RE, Farmer SW. Mechanism of uptake of deglucoteicoplanin amide derivatives across outer membranes of *Escherichia coli* and *Pseudomonas aeruginosa*. *Antimicrob Agents Chemother.* (1993) 37:453–6. doi: 10.1128/AAC.37.3.453
52. Lee DL, Powers JP, Pflegerl K, Vasil ML, Hancock RE, Hodges RS. Effects of single D-amino acid substitutions on disruption of beta-sheet structure and hydrophobicity in cyclic 14-residue antimicrobial peptide analogs related to gramicidin S. *J Pept Res.* (2004) 63:69–84. doi: 10.1046/j.1399-3011.2003.00106.x
53. Velkov T, Gallardo-Godoy A, Swarbrick JD, Blaskovich M. A. T., Elliott, A. G., et al. (2018). Structure, function, and biosynthetic origin of octapeptin antibiotics active against extensively drug-resistant gram-negative bacteria. *Cell Chem Biol.* 25:380–391.e5. doi: 10.1016/j.chembiol.2018.01.005
54. Yeaman MR, Yount NY. Mechanisms of antimicrobial peptide action and resistance. *Pharmacol Rev.* (2003) 55:27–55. doi: 10.1124/pr.55.1.2
55. Wu M, Maier E, Benz R, Hancock RE. Mechanism of interaction of different classes of cationic antimicrobial peptides with planar bilayers and with the cytoplasmic membrane of *Escherichia coli*. *Biochemistry*. (1999) 38:7235–42. doi: 10.1021/bi9826299
56. Cheng M, Huang JX, Ramu S, Butler MS, Cooper MA. Ramoplanin at bactericidal concentrations induces bacterial membrane depolarization in *Staphylococcus aureus*. *Antimicrob Agents Chemother.* (2014) 58:6819–27. doi: 10.1128/AAC.00061-14
57. Te Winkel JD, Gray DA, Seistrup KH, Hamoen LW, Strahl H. Analysis of antimicrobial-triggered membrane depolarization using voltage sensitive dyes. *Front Cell Dev Biol.* (2016) 4:29. doi: 10.3389/fcell.2016.00029
58. Mckinnon KM. Flow cytometry: an overview. *Curr Protoc Immunol.* (2018) 120:5.1.1–5.1.11. doi: 10.1002/cpim.40
59. Freire JM, Gaspar D, De La Torre BG, Veiga AS, Andreu D, Castanho MA. Monitoring antibacterial permeabilization in real time using time-resolved flow cytometry. *Biochim Biophys Acta.* (2015) 1848:554–60. doi: 10.1016/j.bbamem.2014.11.001
60. Stocks SM. Mechanism and use of the commercially available viability stain, BacLight. *Cytometry A.* (2004) 61:189–95. doi: 10.1002/cyto.a.20069
61. Stiefel P, Schmidt-Emrich S, Maniura-Weber K, Ren Q. Critical aspects of using bacterial cell viability assays with the fluorophores SYTO9 and propidium iodide. *BMC Microbiol.* (2015) 15:36. doi: 10.1186/s12866-015-0376-x
62. O'Brien-Simpson NM, Pantarat N, Attard TJ, Walsh KA, Reynolds EC. A rapid and quantitative flow cytometry method for the analysis of membrane disruptive antimicrobial activity. *PLoS ONE.* (2016) 11:e0151694. doi: 10.1371/journal.pone.0151694
63. Roth BL, Poot M, Yue ST, Millard PJ. Bacterial viability and antibiotic susceptibility testing with SYTOX green nucleic acid stain. *Appl Environ Microbiol.* (1997) 63:2421–31. doi: 10.1128/AEM.63.6.2421-2431.1997
64. Rathinakumar R, Walkenhorst WF, Wimley WC. Broad-spectrum antimicrobial peptides by rational combinatorial design and high-throughput screening: the importance of interfacial activity. *J Am Chem Soc.* (2009) 131:7609–17. doi: 10.1021/ja8093247
65. Kaplan CW, Sim JH, Shah KR, Kolesnikova-Kaplan A, Shi W, Eckert R. Selective membrane disruption: mode of action of C16G2, a specifically targeted antimicrobial peptide. *Antimicrob Agents Chemother.* (2011) 55:3446–52. doi: 10.1128/AAC.00342-11
66. Torcato IM, Huang YH, Franquelim HG, Gaspar DD, Craik DJ, Castanho MA, et al. The antimicrobial activity of Sub3 is dependent on membrane binding and cell-penetrating ability. *Chembiochem.* (2013) 14:2013–22. doi: 10.1002/cbic.201300274
67. Sani MA, Henriques ST, Weber D, Separovic F. Bacteria may cope differently from similar membrane damage caused by the australian tree frog antimicrobial peptide maculatin 1.1. *J Biol Chem.* (2015) 290:19853–62. doi: 10.1074/jbc.M115.643262
68. Dias SA, Freire JM, Perez-Peinado C, Domingues MM, Gaspar D, Vale N, et al. New potent membrane-targeting antibacterial peptides from viral capsid proteins. *Front Microbiol.* (2017) 8:775. doi: 10.3389/fmicb.2017.00775
69. Troeira Henriques S, Lawrence N, Chaousis S, Ravipati AS, Cheneval O, Benfield AH, et al. Redesigned spider peptide with improved antimicrobial and anticancer properties. *ACS Chem Biol.* (2017) 12:2324–34. doi: 10.1021/acschembio.7b00459
70. Perez-Peinado C, Dias SA, Domingues MM, Benfield AH, Freire JM, Radis-Baptista G, et al. Mechanisms of bacterial membrane permeabilization by crotalicidin (Ctn) and its fragment Ctn(15-34), antimicrobial peptides from rattlesnake venom. *J Biol Chem.* (2018) 293:1536–49. doi: 10.1074/jbc.RA117.000125
71. Henriques ST, Costa J, Castanho MA. Re-evaluating the role of strongly charged sequences in amphipathic cell-penetrating peptides: a fluorescence study using pep-1. *FEBS Lett.* (2005) 579:4498–502. doi: 10.1016/j.febslet.2005.06.085
72. Szeto HH, Schiller PW, Zhao K, Luo G. Fluorescent dyes alter intracellular targeting and function of cell-penetrating tetrapeptides. *FASEB J.* (2005) 19:118–20. doi: 10.1096/fj.04-1982fje
73. Hughes LD, Rawle RJ, Boxer SG. Choose your label wisely: water-soluble fluorophores often interact with lipid bilayers. *PLoS ONE.* (2014) 9:e87649. doi: 10.1371/journal.pone.0087649
74. Hedegaard SF, Derbas MS, Lind TK, Kasimova MR, Christensen MV, Michaelsen MH, et al. Fluorophore labeling of a cell-penetrating peptide significantly alters the mode and degree of biomembrane interaction. *Sci Rep.* (2018) 8:6327. doi: 10.1038/s41598-018-24154-z
75. Cavaco M, Perez-Peinado C, Valle J, Silva RDM, Correia JDG, Andreu D, et al. To what extent do fluorophores bias the biological activity of peptides? A practical approach using membrane-active peptides as models. *Front Bioeng Biotechnol.* (2020) 8:552035. doi: 10.3389/fbioe.2020.552035
76. Philippe GJ, Gaspar D, Sheng C, Huang YH, Benfield AH, Condon ND, et al. Cell membrane composition drives selectivity and toxicity of designed cyclic helix-loop-helix peptides with cell penetrating and tumor suppressor properties. *ACS Chem Biol.* (2019) 14:2071–87. doi: 10.1021/acschembio.9b00593
77. Lawrence N, Philippe GJB, Harvey PJ, Condon ND, Benfield AH, Cheneval O, et al. Cyclic peptide scaffold with ability to stabilize and deliver a helical cell-impermeable cargo across membranes of cultured cancer cells. *RSC Chem Biol.* (2020). doi: 10.1039/D0CB00099J
78. Benincasa M, Pacor S, Gennaro R, Scocchi M. Rapid and reliable detection of antimicrobial peptide penetration into gram-negative bacteria based on fluorescence quenching. *Antimicrob Agents Chemother.* (2009) 53:3501–4. doi: 10.1128/AAC.01620-08
79. Mardirossian M, Perebaskine N, Benincasa M, Gambato S, Hofmann S, Huter P, et al. The dolphin proline-rich antimicrobial peptide Tur1A inhibits protein synthesis by targeting the bacterial ribosome. *Cell Chem Biol.* (2018) 25:530–539.e7. doi: 10.1016/j.chembiol.2018.02.004
80. Hartmann M, Berditsch M, Hawecker J, Ardakani MF, Gerthsen D, Ulrich AS. Damage of the bacterial cell envelope by antimicrobial peptides gramicidin S and PGLa as revealed by transmission and scanning electron microscopy. *Antimicrob Agents Chemother.* (2010) 54:3132–42. doi: 10.1128/AAC.00124-10

81. Schneider VA, Coorens M, Ordonez SR, Tjeerdsma-Van Bokhoven JL, Posthuma G, Van Dijk A, et al. Imaging the antimicrobial mechanism(s) of cathelicidin-2. *Sci Rep.* (2016) 6:32948. doi: 10.1038/srep32948
82. Chen RB, Zhang K, Zhang H, Gao CY, Li CL. Analysis of the antimicrobial mechanism of porcine beta defensin 2 against *E. coli* by electron microscopy and differentially expressed genes. *Sci Rep.* (2018) 8:14711. doi: 10.1038/s41598-018-32822-3
83. Farkas A, Maroti G, Durgo H, Gyorgypal Z, Lima RM, Medzihradszky KF, et al. Medicago truncatula symbiotic peptide NCR247 contributes to bacteroid differentiation through multiple mechanisms. *Proc Natl Acad Sci USA.* (2014) 111:5183–8. doi: 10.1073/pnas.1404169111
84. Farkas A, Maroti G, Kereszt A, Kondorosi E. Comparative analysis of the bacterial membrane disruption effect of two natural plant antimicrobial peptides. *Front Microbiol.* (2017) 8:51. doi: 10.3389/fmicb.2017.00051
85. Cardoso MH, Meneguetti BT, Costa BO, Buccini DF, Oshiro KGN, Preza SLE, et al. Non-lytic antibacterial peptides that translocate through bacterial membranes to act on intracellular targets. *Int J Mol Sci.* (2019) 20:4877. doi: 10.3390/ijms20194877
86. Snoussi M, Talledo JP, Del Rosario NA, Mohammadi S, Ha BY, Kosmrlj A, et al. Heterogeneous absorption of antimicrobial peptide LL37 in *Escherichia coli* cells enhances population survivability. *eLife.* (2018) 7:e38174. doi: 10.7554/eLife.38174.023
87. Hellman LM, Fried MG. Electrophoretic mobility shift assay (EMSA) for detecting protein-nucleic acid interactions. *Nat Protoc.* (2007) 2:1849–61. doi: 10.1038/nprot.2007.249
88. Hsu CH, Chen C, Jou ML, Lee AY, Lin YC, Yu YP, et al. Structural and DNA-binding studies on the bovine antimicrobial peptide, indolicidin: evidence for multiple conformations involved in binding to membranes and DNA. *Nucleic Acids Res.* (2005) 33:4053–64. doi: 10.1093/nar/gki725
89. Limoli DH, Rockel AB, Host KM, Jha A, Kopp BT, Hollis T, et al. Cationic antimicrobial peptides promote microbial mutagenesis and pathoadaptation in chronic infections. *PLoS Pathog.* (2014) 10:e1004083. doi: 10.1371/journal.ppat.1004083
90. Park CB, Kim HS, Kim SC. Mechanism of action of the antimicrobial peptide buforin II: buforin II kills microorganisms by penetrating the cell membrane and inhibiting cellular functions. *Biochem Biophys Res Commun.* (1998) 244:253–7. doi: 10.1006/bbrc.1998.8159
91. Munoz-Camargo C, Salazar VA, Barrero-Guevara L, Camargo S, Mosquera A, Groot H, et al. Unveiling the multifaceted mechanisms of antibacterial activity of buforin II and frenatin 2.3S peptides from skin micro-organs of the orinoco lime treefrog (*Sphaenorhynchus lacteus*). *Int J Mol Sci.* (2018) 19:2170. doi: 10.3390/ijms19082170
92. Shah P, Hsiao FS, Ho YH, Chen CS. The proteome targets of intracellular targeting antimicrobial peptides. *Proteomics.* (2016) 16:1225–37. doi: 10.1002/pmic.201500380
93. Mucke PA, Maass S, Kohler TP, Hammerschmidt S, Becher D. Proteomic adaptation of streptococcus pneumoniae to the human antimicrobial peptide *LL*-37. *Microorganisms.* (2020) 8:413. doi: 10.3390/microorganisms8030413
94. Lee TH, Hofferek V, Separovic F, Reid GE, Aguilar MI. The role of bacterial lipid diversity and membrane properties in modulating antimicrobial peptide activity and drug resistance. *Curr Opin Chem Biol.* (2019) 52:85–92. doi: 10.1016/j.cbpa.2019.05.025
95. Wenzel M, Schriek P, Prochnow P, Albada HB, Metzler-Nolte N, Bandow JE. Influence of lipidation on the mode of action of a small RW-rich antimicrobial peptide. *Biochim Biophys Acta.* (2016) 1858:1004–11. doi: 10.1016/j.bbamem.2015.11.009
96. Ho YH, Shah P, Chen YW, Chen CS. Systematic analysis of intracellular-targeting antimicrobial peptides, bactenecin 7, hybrid of pleurocidin and dermaseptin, proline-arginine-rich peptide, and lactoferricin b, by using *Escherichia coli* proteome microarrays. *Mol Cell Proteomics.* (2016) 15:1837–47. doi: 10.1074/mcp.M115.054999
97. Qi H, Wang F, Tao SC. Proteome microarray technology and application: higher, wider, and deeper. *Expert Rev Proteomics.* (2019) 16:815–27. doi: 10.1080/14789450.2019.1662303
98. Koo HB, Seo J. Antimicrobial peptides under clinical investigation. *Peptide Sci.* (2019) 111:e24122. doi: 10.1002/pep2.24122
99. Browne K, Chakraborty S, Chen R, Willcox MD, Black DS, Walsh WR, et al. A new era of antibiotics: the clinical potential of antimicrobial peptides. *Int J Mol Sci.* (2020) 21:7047. doi: 10.3390/ijms21197047
100. Raheem N, Straus SK. Mechanisms of action for antimicrobial peptides with antibacterial and antibiofilm functions. *Front Microbiol.* (2019) 10:2866. doi: 10.3389/fmicb.2019.02866
101. Pirtskhalava M, Amstrong AA, Grigolava M, Chubinidze M, Alimbarashvili E, Vishnepolsky B, et al. DBAASP v3: database of antimicrobial/cytotoxic activity and structure of peptides as a resource for development of new therapeutics. *Nucleic Acids Res.* (2020) 5:gkaa991. doi: 10.1093/nar/gkaa991
102. Lee EY, Lee MW, Fulan BM, Ferguson AL, Wong GCL. What can machine learning do for antimicrobial peptides, and what can antimicrobial peptides do for machine learning? *Interface Focus.* (2017) 7:20160153. doi: 10.1098/rsfs.2016.0153
103. Cardoso MH, Orozco RQ, Rezende SB, Rodrigues G, Oshiro KGN, Candido ES, et al. Computer-aided design of antimicrobial peptides: are we generating effective drug candidates? *Front Microbiol.* (2019) 10:3097. doi: 10.3389/fmicb.2019.03097

Conflict of Interest: The authors declare that the research was conducted in the absence of any commercial or financial relationships that could be construed as a potential conflict of interest.

frontiers in Medical Technology

MINI REVIEW
published: 15 December 2020
doi: 10.3389/fmedt.2020.606079

Application of Biophysical Techniques to Investigate the Interaction of Antimicrobial Peptides With Bacterial Cells

Maria Luisa Gelmi[1], *Luca Domenico D'Andrea*[2] *and Alessandra Romanelli*[1]*

[1] *Department of Pharmaceutical Sciences, University of Milan, Milan, Italy,* [2] *Institute of Biostructures and Bioimaging, CNR, Turin, Italy*

Gaining new understanding on the mechanism of action of antimicrobial peptides is the basis for the design of new and more efficient antibiotics. To this aim, it is important to detect modifications occurring to both the peptide and the bacterial cell upon interaction; this will help to understand the peptide structural requirement, if any, at the base of the interaction as well as the pathways triggered by peptides ending in cell death. A limited number of papers have described the interaction of peptides with bacterial cells, although most of the studies published so far have been focused on model membrane-peptides interactions. Investigations carried out with bacterial cells highlighted the limitations connected to the use of oversimplified model membranes and, more importantly, helped to identify molecular targets of antimicrobial peptides and changes occurring to the bacterial membrane. In this review, details on the mechanism of action of antimicrobial peptides, as determined by the application of spectroscopic techniques, as well as scattering, microscopy, and calorimetry techniques, to complex systems such as peptide/bacteria mixtures are discussed.

Keywords: peptide, antimicrobial, bacteria, biophysical techniques, mechanism of action

OPEN ACCESS

Edited by:
Lorenzo Stella,
University of Rome Tor Vergata, Italy

Reviewed by:
William Wimley,
Tulane University, United States
Thomas Gutsmann,
Research Center Borstel (LG), Germany

***Correspondence:**
Alessandra Romanelli
alessandra.romanelli@unimi.it

Specialty section:
This article was submitted to Pharmaceutical Innovation, a section of the journal Frontiers in Medical Technology

Received: *14 September 2020*
Accepted: *25 November 2020*
Published: *15 December 2020*

Citation:
Gelmi ML, D'Andrea LD and Romanelli A (2020) Application of Biophysical Techniques to Investigate the Interaction of Antimicrobial Peptides With Bacterial Cells. Front. Med. Technol. 2:606079. doi: 10.3389/fmedt.2020.606079

INTRODUCTION

Antimicrobial peptides (AMPs) are produced by all organisms and represent the first line of defense against attack by external pathogens (1). They are expressed or may be produced upon encountering a stimulus; interestingly, each organism produces its own set of peptides, tailored for the "enemy" that has to be killed. A feature that is common to most antimicrobial peptides is the presence of positively charged amino acids, which are essential for establishing an interaction with the negatively charged cell wall of bacteria and fungi. The distribution of charged and hydrophobic residues within the peptide sequence is thought to be functional to the interaction of peptides with bacteria and to their activity. In this review we focus on biophysical studies aimed at exploring the interaction of peptides with bacterial cells. It is our opinion that, although more complicated to set up, these studies will result in a more reliable picture of the mechanism of action of AMPs as compared to studies with systems that mimic cell membranes. Model systems are mainly composed of lipid mixtures, whereas bacterial cells contain a variety of molecules, including those other than lipids, sugars, and proteins. In principle, interactors of antimicrobial peptides could be found among all these molecules; in addition, the behavior of any of these molecules within the bacterial membrane may be different as compared to that of the same isolated molecules.

The different chemical composition of membranes also affects their fluidity, which is crucial to different biological processes and is tuned by cells depending on external conditions. Results obtained with model membranes are strictly dependent on the set up of the experiment; it is demonstrated that the composition of the lipid mixture affects the structure of peptides, their dynamic, and their orientation with respect to membranes (2). For example, the peptide maculatin 1.1 is reported to insert into neutral phosphatidylcholine membranes assuming a helical conformation, whereas it remains locked on the surface of bilayers when anionic lipids are used. The helical content is dependent on the lipid composition (3).

Challenges imposed by the use of live bacterial cells derive from the need to adapt biophysical techniques to heterogeneous and evolving samples; ideally, measurements should be carried out on live cells, therefore experimental conditions compatible with measurements and cell life need to be sought out (4). In many cases, high background noise due to the presence of salts or micrometric cells may be an issue. Another critical issue is that not all bacteria may be managed in all laboratories, which limits the studies that can be performed in a standard chemistry lab. Biosafety levels of bacteria need to be carefully checked; in general, bacteria that present minimal potential hazards for the lab user and the environment (biosafety level 1, as certified by ATCC), such as non-pathogenic *E. coli* strains, may be managed with proper care in most laboratories. In the last few years, an increasing number of publications have appeared and details on the mechanism of action of peptides are being discovered with the support of biophysical techniques.

Mechanism studies can be carried out starting from two different perspectives: either by looking at changes occurring to peptides or by looking at changes occurring to cells. **Figure 1** groups biophysical techniques in three main families: one including techniques exploited to monitor changes occurring at peptides in the presence of bacterial cells, one including techniques used to detect changes occurring at bacterial cells in the presence of AMPs, and one including techniques useful for both scopes. Understanding the changes occurring to the peptides upon contact with bacterial cells yields information at the molecular level on the factors that determine the initial interaction and trigger cell death. On the other hand, studies carried out looking at cells yield information on the effect of the AMPs on features such as the morphology of the cell; in many cases, these changes can be related to molecular events triggered by peptides. For example, the appearance of filaments in bacterial cells treated with AMPs is associated to the inhibition of cell division, that in turn depends on the interaction of AMPs with specific targets (5–7). Some techniques are suitable to investigate changes occurring both to peptides and cells; as an example, Nuclear Magnetic Resonance (NMR), that looks at changes in the chemical shift of magnetically active nuclei such as ^{1}H, ^{13}C, and ^{31}P, is exploited to determine the structure of peptides that interact with cells, but is also used to detect the binding of peptides to cells (8–11). Similarly, fluorescence microscopy can be used to follow labeled peptides inside cells or to monitor the permeabilization of bacterial cells expressing fluorescent proteins able to cross damaged membranes (12–18). Other techniques, such as scattering techniques (DLS, SANS, SAXS) or AFM or TEM, are employed to monitor only changes at bacterial cells (19, 20). In this review, we describe the application of selected biophysical techniques to the study of the mechanism of action of AMPs.

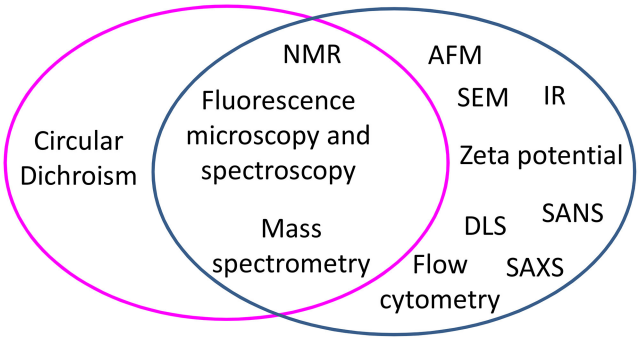

FIGURE 1 | Biophysical techniques applied to study the mechanism of action of peptides in experiments performed with bacterial cells, grouped by techniques used to monitor changes occurring to peptides (magenta circle) and techniques used to monitor changes at bacterial cells (blue circle). At the cross, techniques useful to both aims are listed.

STRUCTURAL STUDIES OF PEPTIDES INTERACTING WITH BACTERIAL CELLS

Structural changes of peptides may be investigated by different techniques, such as **Circular Dichroism** (CD) that affords information on the secondary structure of peptides, or **NMR** that gives information on their three-dimensional structure. Most of the studies are reported for peptides that interact with *E. coli* cells, some studies are reported for peptides interacting with fungi and, to the best of our knowledge, only one paper reports the structure of peptides in the presence of a Gram-positive bacterium such as *S. epidermidis* (21–24). CD studies were initially reported on magainin 2 and cecropin A in the presence of *E. coli* cells, revealing that these peptides do not show a preferred conformation in buffer, but rapidly fold into α helices upon interaction with cells (21). A comparison with data obtained for the same peptides in the presence of *E. coli* lipopolysaccharide (LPS) reveals similar secondary structures, driving to the conclusion that the folding process depends to a large extent on the interaction of peptides with LPS, that is also the main component of the Gram-negative bacterial outer membrane. Similar behavior was observed for temporin L, TBKKG6A, and LG-21 (11, 22, 23). Interestingly, the peptide temporin B that is inactive against *E. coli* folds with purified LPS but not with cells (11). The peptide PG-1 is reported to fold into a beta hairpin upon interaction with *E. coli* cells (24).

CD studies to detect structural changes of peptides incubated with the Gram-positive *S. epidermidis* cells are reported for TBKKG6A, temporin B, and temporin L; in the presence of cells the first two peptides remain unfolded, while temporin L shows weak signals, suggesting the presence of a helical structure

(22). Electrostatic interactions seem to drive peptide folding, being crucial for establishing contact with Gram-negative bacterial cells; in the case of Gram-positive bacteria, whose outer membrane shows a lower negative charge, hydrophobic interactions seem to play a more important role (25). CD studies have also been carried out with fungi: peptides MAP and cecropin B are reported to fold into helices in the presence of *C. albicans*; the protein NFAP from *N. fischeri* or its synthetic derivative spanning NFAP γ core, which possesses a very stable β pleated structure stabilized by disulfide bonds, do not change their conformation when incubated with *C. herbarium* (26, 27).

More detailed information on the structure of peptides has been derived from NMR studies. The three-dimensional structure of the peptide TBKKG6A determined by NMR either with *E. coli* LPS or with *E. coli* cells reveals that the peptide appears as a straight helix in the presence of LPS, while it is a kinked helix when incubated with cells (11, 28). These data support the idea that different components of the bacterial membrane concur to stabilize the interaction of AMPs with bacterial cells. **Rotational-echo double-resonance (REDOR) NMR** was applied to characterize complexes formed between ^{19}F labeled vancomycin-like peptides and *S. aureus* cells labeled at the peptidoglycan (PG) with ^{15}N and ^{13}C (10). The ^{13}C-^{19}F and ^{15}N-^{19}F distances from the REDOR experiments were used to build model structures for all glycopeptide-PG complexes, allowing for the dissection of the vancomycin in five distinct fragments and assignment to each of a role in the interaction with PG.

BINDING STUDIES

The binding of peptides to cells can be investigated by NMR, fluorescence, zeta potential measurements, and Isothermal Titration Calorimetry (ITC). Through NMR, changes occurring at membranes in live bacterial cells upon AMP binding can be detected. **Solid state ^{31}P NMR** is used to examine the interaction of peptides with the phospholipids of live bacteria. As the number of phosphate groups in a bacterial membrane is estimated to overwhelm that found in bacterial RNA, ^{31}P is a suitable probe of membrane dynamics. The first paper on this topic dates back to 2000 and reports on the interactions of caerin 1.1, caerin 4.1, and maculatin 1.1 with the Gram-positive bacteria *B. cereus* and *S. epidermidis*. Caerin 4.1, which is not active against *B. cereus* and *S. epidermidis*, does not affect the ^{31}P spectra. Caerin 1.1 and maculatin 1.1 instead induce isotropic peak formation, due to membrane disruption (9). More recently, **^{2}H solid state NMR** has been exploited to detect the interaction of the peptide MSI-78 with *E. coli* cells that incorporated high levels of ^{2}H labels specifically into membranes (8). These special cells, obtained by genetic manipulation, do not synthesize or metabolize fatty acids and are able to incorporate ^{2}H labeled palmitic acid from the growth media and produce ^{2}H labeled saturated phospholipids. Lipid bilayer disruption is followed by the analysis of spectral moments; interestingly this phenomenon is observed in NMR at a peptide concentration well below that needed to inhibit cell growth. Furthermore, the peptide/lipid ratio required to induce lipid disordering in bacterial cells is much higher as compared to that needed to obtain the same effect in model lipid systems. This effect is likely due to the interaction of the peptide with other components of the cell envelope, such as LPS. Solid state ^{2}H NMR studies are also reported to detect the interaction of caerin 1.1 and aurein 1.2 with ^{2}H labeled *E. coli* and *B. subtilis* cells. In this case, membrane disordering effects were observed at MIC and were in agreement with data collected on model membranes.

Fluorescence spectroscopy using labeled peptides is used to determine the binding stoichiometry and binding constant of peptides to cells. Studies reported for TBKKG6A labeled with nitrobenzodiazole show that this peptide binds to *E. coli* cells in a 1×10^6:1 (peptide:cell) stoichiometry; similar values are reported in the literature for other peptides (29–31). The binding constant of TBKKG6A to cells, expressed as a dissociation constant, reveals a very tight binding. Interestingly, this constant results to be higher as compared to that measured when *E. coli* LPS was used instead of cells. Experiments performed on the peptide temporin B, which is not active against *E. coli* cells, reveal no binding to cells but to LPS. Altogether, fluorescence data indicate that active peptides cover the entire bacterial surface; this hypothesis is sustained by data collected using techniques that are instead focused on detecting changes occurring to cells such as **Zeta potential** measurements. These measurements are used to determine the net surface charge of bacteria, which is a function of the media in which it is observed, depending on the concentration of molecules able to establish electrostatic interactions with cells. An increase in the zeta potential of *E. coli* cells incubated with antimicrobial peptides was observed, consistent with the idea that the peptides overlay the bacterial outer membrane. Neutralization may occur at different concentrations, as demonstrated for peptides BP100, pepR, and crotalicidin with *E. coli* cells (32, 33). BP100 neutralization occurs at MIC, while for pepR and crotalicidin (Ctn) zero-potential precedes the MIC; this different behavior suggests that in the case of pepR and Ctn cell death is triggered by factors other than membrane neutralization.

In addition, the binding of peptides to bacterial cells may be followed by IR, monitoring the fluidity of lipopolysaccharides and phospholipids within the membrane. In the **IR,** the 2851–2853 cm^{-1} band that is characteristic of the acyl chain order moves to lower wavelengths upon binding of peptides; gel-to-liquid phase transition temperatures also show minor changes (34, 35).

Thermodynamic investigations of the peptide-cell binding are also performed by **isothermal titration calorimetry (ITC)** (34). ITC experiments performed on the peptide Pep19-2.5 with Gram-negative and Gram-positive bacteria reveal that the binding process is exothermic; the amount of released heat is higher for Gram-negative than for Gram positive bacteria. Electrostatic interactions between the negative charges of LPS phosphates and positive charges of peptides lead to a strong exothermic reaction. In the case of Gram-positive bacteria, the cell wall contains teichoic acids, lipoteichoic acids and lipoproteins; the latest have phosphates in the form of diesters, shielded by the cell wall and therefore less accessible to peptides. This results in a lower energy release.

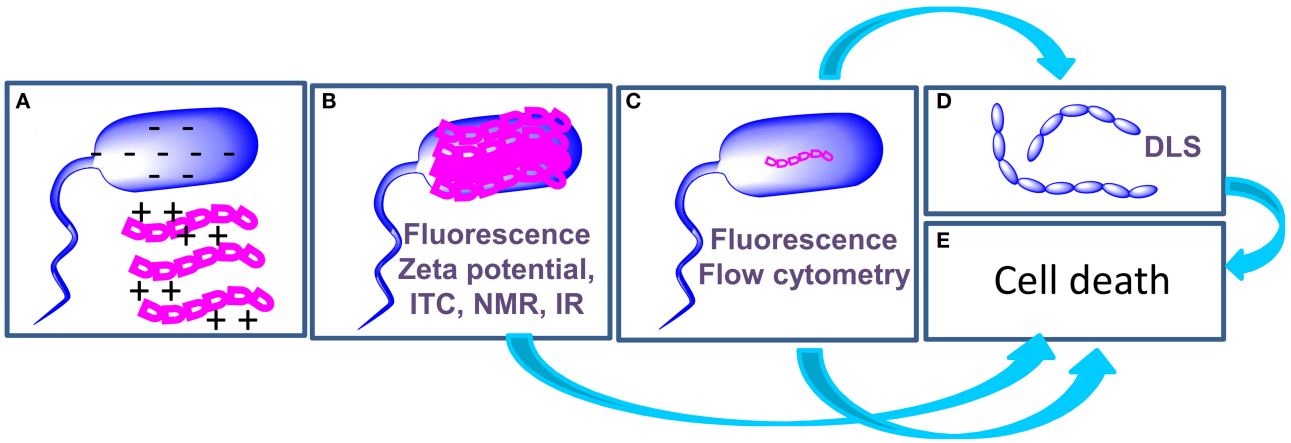

FIGURE 2 | Schematic representation of the mechanism of action of AMPs and of the techniques (highlighted in purple in each panel) employed to investigate each step. AMPs (magenta) interact with bacterial cells (blue) through electrostatic interactions **(A)**. AMPs cover the surface of bacterial cells **(B)**; in some cases, this step triggers cell death **(E)**, in other cases AMPs enter the cell **(C)** to hit their targets and this step determines cell death **(E)**. When AMPs target proteins involved in cell division, agglutination occurs **(D)**.

DETECTION OF EFFECTS OCCURRING AT THE MEMBRANE/CELL SURFACE

Fluorescence microscopy is widely used to follow peptides inside cells and visualize bacterial membranes permeabilization. Using *E. coli* cells expressing cytoplasmic GFP, it is possible to follow outer membrane (OM) permeabilization by the GFP signal decay; increase of the signal of the DNA stain Sytox green or Sytox red is related to cytoplasmic membrane (CM) permeabilization (13, 14). Using single cell fluorescence microscopy, it has been demonstrated in *E. coli* that mutations to the core oligosaccharide affect OM and CM permeabilization by cecropin A (12). In a different study, OM permeabilization has been detected by the profluorophore JF646, a small molecule (702 Da) emitting weak fluorescence in aqueous solution. When the AMP permeabilizes the outer membrane, JF646 enters the cytoplasm and covalently binds to the HaloTag protein emitting red fluorescence; permeabilization onset is detected with a 3s resolution (15, 16). When peptides are labeled, information on the localization and distribution of peptides may be obtained (17). Recently, laser scanning **Stimulated Emission Depletion** (STED) fluorescence microscopy was employed to detect the localization of BDP-FL labeled thanatin in *E. coli* cells: localization of the peptide in islands at the poles and across the cell was related to the interaction of the peptide with outer membrane proteins, a hypothesis confirmed by photoaffinity labeling experiments and *in vivo* by Bacterial Adenylate Cyclase Two-Hybrid (BACTH) system (18, 36). Using time-lapse **Fluorescence Lifetime Imaging Microscopy** (FLIM) on a fluorescently tagged melittin analog, transient disruption of the *E. coli* membrane was observed (37). Interestingly, the same experiment performed on synthetic membranes suggested the formation of stable pores.

By phase-contrast and time lapse microscopy, using fluorescent LL-37, the distribution, translocation, and retention of the AMP in *E. coli* cells was investigated (38). Snoussi observed that inhibition of bacterial growth is followed by a rapid translocation of peptides into cells. Experiments carried out at different peptide concentrations (above MIC and sub-MIC) reveal the relationship between the mean concentration of free peptides and the mean concentration of growing bacteria (inoculum effect); this relationship is also described by a mathematical model.

Permeabilization is also investigated by time-resolved **Flow Cytometry Assay** (FCA). Freire et al. demonstrated that pepR binds in a cooperative fashion and faster to the *E. coli* 25922 strain than to the *E. coli* K-12 strain, which presents a truncated LPS, while permeabilization takes place at a higher rate in *E. coli* K-12 than in *E. coli* 25922 (39). These studies highlight the role of the LPS composition in permeabilization kinetic by AMPs. Using labeled peptides, it is possible to correlate permeabilization and internalization kinetics. Time-resolved FCAs performed on Rhodamine B labeled Ctn and Ctn (15–34) show that binding and internalization processes occur until an equilibrium is reached; Ctn(15-34) uptake is faster and precedes bacterial membrane damage, suggesting that permeabilization occurs only upon achievement of a threshold surface concentration (33). In line with this, single cell images show that both peptides are mostly localized on the *E. coli* surface, but a small percentage co-localizes with the dye SYTOX green, suggesting a partial internalization.

Changes occurring to the bacterial cells surface are detected by microscopy (AFM; TEM, SEM). **Atomic Force Microscopy** (AFM) is frequently used to detect surface roughness and cell height; when measurements are carried out on dry samples, it is quite difficult to separate the effect due to drying from those caused by the AMPs. In some applications, images are taken on liquid samples. In a study on the peptide CM15, bacteria are imaged in aqueous solution; using high-speed atomic force, microscopy dynamic changes at a single cell level are recorded at a nanometric resolution (19). Following the average surface

corrugation with the time, the authors proposed that bacterial death mediated by CM15 occurs in two stages: an incubation time, followed by an execution phase in which 50% of the damage occurring to cell happens. Mularski reports that melittin affects *K. pneumoniae* turgor pressure and cell wall elasticity, while it does not alter bacterial capsule thickness and organization, leading to the hypothesis that the capsule does not offer protection to *K. pneumoniae* against antimicrobial peptides (20).

Light scattering measurements are employed to detect aggregation of bacteria following treatment with AMPs (**Figure 2D**): Di Somma et al. report the formation of *E. coli* elongated structures with dimensions over 6000 nm upon incubation with temporin L (TL) (7). In the same work, changes to the structure of bacterial cells occurring at a nanoscale level, in the range of 2 to 300 nm, were observed by **Small Angle Neutron Scattering** measurements that disclose a change in the spatial arrangement of a protein involved in the interaction with TL.

TARGET IDENTIFICATION

Identification of AMP targets in bacterial cells is the most challenging task in mechanism studies and usually requires integration of data from different experiments. While in many cases AMPs act by disrupting the bacterial membrane (33, 40), in other cases intracellular targets, such as DNA, RNA, and proteins, have been identified. Mass spectrometry is one of the most useful techniques to achieve this goal. As an example of application of mass spectrometry to the detection of protein targets in living bacterial cells, we here report on *in vivo* photolabelling. These experiments are based on the use of peptides containing a photoprobe (a L-4,4-diazarinylproline in place of one proline) and a biotin tag; these peptides are incubated with bacterial cells. Upon irradiation, the photoprobe captures the protein target of the AMP. Photolabelled proteins are separated by gel electrophoresis, digested in gel, and identified by tandem mass spectrometry. Identification of proteins involved in the biogenesis of the bacterial outer membrane as the interactors of antimicrobial peptides, such as L27-11 and thanatin, was achieved in this way (18, 41, 42).

CONCLUSIONS

The application of biophysical techniques to study the interactions of AMPs with bacterial cells enabled the highlighting of some steps that are common to the mechanism of action of many peptides (**Figure 2**): (a) the initial interaction of AMPs with bacterial cells is mediated by electrostatic forces between peptides and the outer leaflet of bacteria. These interactions may result in a change in the structure of the peptide; (b) AMPs cover the outer surface of bacteria; (c) Internalization occurs with mechanisms and kinetics that depend on the composition of the bacterial membrane. Intracellular targets of AMPs are various, including proteins involved in cell division or in the synthesis/transport of LPS. (d) AMPs may cause cell agglutination; (e) AMPs may also cause cell death depending on the target. In order to draw conclusions on the mechanism of action of AMPs, the integration of data deriving from biophysical experiments with results of microbiological and genetic tests is of fundamental importance. We are confident that results of these studies will contribute to the exploitation of AMPs as drugs and to the design of new biomedical devices (43–46).

AUTHOR CONTRIBUTIONS

AR contributed to the conception of the manuscript. AR, LD'A, and MG contributed to the preparation and editing of the manuscript and approved the submitted version. All authors contributed to the article and approved the submitted version.

REFERENCES

1. Mookherjee N, Anderson MA, Haagsman HP, Davidson DJ. Antimicrobial host defence peptides: functions and clinical potential. *Nat Rev Drug Dis.* (2020) 19:311–32. doi: 10.1038/s41573-019-0058-8
2. Laadhari M, Arnold AA, Gravel AE, Separovic F, Marcotte I. Interaction of the antimicrobial peptides caerin 1.1 and aurein 1.2 with intact bacteria by (2)H solid-state NMR. *Biochim Biophys Acta.* (2016) 1858:2959–64. doi: 10.1016/j.bbamem.2016.09.009
3. Sani MA, Whitwell TC, Separovic F. Lipid composition regulates the conformation and insertion of the antimicrobial peptide maculatin 1.1. *Biochim Biophys Acta.* (2012) 1818:205–11. doi: 10.1016/j.bbamem.2011.07.015
4. Freire JM, Gaspar D, Veiga AS, Castanho MA. Shifting gear in antimicrobial and anticancer peptides biophysical studies: from vesicles to cells. *J Pept Sci.* (2015) 21:178–85. doi: 10.1002/psc.2741
5. Ray S, Dhaked HP, Panda D. Antimicrobial peptide CRAMP (16-33) stalls bacterial cytokinesis by inhibiting FtsZ assembly. *Biochemistry.* (2014) 53:6426–9. doi: 10.1021/bi501115p
6. Yadavalli SS, Carey JN, Leibman RS, Chen AI, Stern AM, Roggiani M, et al. Antimicrobial peptides trigger a division block in *Escherichia coli* through stimulation of a signalling system. *Nat Commun.* (2016) 7:12340. doi: 10.1038/ncomms12340
7. Di Somma A, Avitabile C, Cirillo A, Moretta A, Merlino A, Paduano L, et al. The antimicrobial peptide Temporin L impairs *E. coli* cell division by interacting with FtsZ and the divisome complex. *Biochim Biophys Acta.* (2020) 1864:6. doi: 10.1016/J.Bbagen.2020.129606
8. Booth V, Warschawski DE, Santisteban NP, Laadhari M, Marcotte I. Recent progress on the application of H-2 solid-state NMR to probe the interaction of antimicrobial peptides with intact bacteria. *Biochim Biophys Acta.* (2017) 1865:1500–511. doi: 10.1016/j.bbapap.2017.07.018
9. Chia BCS, Lam YH, Dyall-Smith M, Separovic F, Bowie JH. A P-31 NMR study of the interaction of amphibian antimicrobial peptides with the membranes of live bacteria. *Lett Pept Sci.* (2000) 7:151–6. doi: 10.1023/A:1008982605521
10. Kim SJ, Cegelski L, Preobrazhenskaya M, Schaefer J. Structures of *Staphylococcus aureus* cell-wall complexes with vancomycin, eremomycin, and chloroeremomycin derivatives by C-13{F-19} and N-15{F-19} rotational-echo double resonance. *Biochemistry.* (2006) 45:5235–50. doi: 10.1021/bi052660s
11. Malgieri G, Avitabile C, Palmieri M, D'Andrea LD, Isernia C, Romanelli A, et al. Structural basis of a temporin 1b analogue antimicrobial activity against gram negative bacteria determined by CD and NMR techniques in cellular environment. *Acs Chemical Biol.* (2015) 10:965–9. doi: 10.1021/cb501057d
12. Agrawal A, Weisshaar JC. Effects of alterations of the *E. coli* lipopolysaccharide layer on membrane permeabilization events

induced by Cecropin A. *Biochim Biophys Acta.* (2018) 1860:1470–9. doi: 10.1016/j.bbamem.2018.04.009
13. Sochacki KA, Barns KJ, Bucki R, Weisshaar JC. Real-time attack on single Escherichia coli cells by the human antimicrobial peptide LL-37. *Proc Natl Acad Sci USA.* (2011) 108:E77–E81. doi: 10.1073/pnas.1101130108
14. Rangarajan N, Bakshi S, Weisshaar JC. Localized permeabilization of *E-coli* membranes by the antimicrobial peptide cecropin A. *Biochemistry.* (2013) 52:6584–94. doi: 10.1021/bi400785j
15. Los GV, Encell LP, McDougall MG, Hartzell DD, Karassina N, Zimprich C, et al. HatoTag: a novel protein labeling technology for cell imaging and protein analysis. *Acs Chem Biol.* (2008) 3:373–82. doi: 10.1021/cb800025k
16. Yang ZL, Weisshaar JC. HaloTag assay suggests common mechanism of *E. coli* membrane permeabilization induced by cationic peptides. *Acs Chem Biol.* (2018) 13:2161–9. doi: 10.1021/acschembio.8b00336
17. Chileveru HR, Lim SA, Chairatana P, Wommack AJ, Chiang IL, Nolan EM. Visualizing attack of *Escherichia coli* by the antimicrobial peptide human defensin 5. *Biochemistry.* (2015) 54:1767–77. doi: 10.1021/bi501483q
18. Vetterli SU, Zerbe K, Muller M, Urfer M, Mondal M, Wang SY, et al. Thanatin targets the intermembrane protein complex required for lipopolysaccharide transport in *Escherichia coli*. *Sci Adv.* (2018) 4:2634. doi: 10.1126/sciadv.aau2634
19. Fantner GE, Barbero RJ, Gray DS, Belcher AM. Kinetics of antimicrobial peptide activity measured on individual bacterial cells using high-speed atomic force microscopy. *Nat Nanotechnol.* (2010) 5:280–85. doi: 10.1038/nnano.2010.29
20. Mularski A, Wilksch JJ, Wang HB, Hossain MA, Wade JD, Separovic F, et al. Atomic force microscopy reveals the mechanobiology of lytic peptide action on bacteria. *Langmuir.* (2015) 31:6164–71. doi: 10.1021/acs.langmuir.5b01011
21. Avitabile C, D'Andrea LD, Romanelli A. Circular dichroism studies on the interactions of antimicrobial peptides with bacterial cells. *Sci Rep.* (2014) 4:4293. doi: 10.1038/srep04293
22. Avitabile C, D'Andrea LD, Saviano M, Romanelli A. Determination of the secondary structure of peptides in the presence of Gram positive bacterium *S. epidermidis* cells. *Rsc Adv.* (2016) 6:51407–10. doi: 10.1039/c6ra06877d
23. Mohanram H, Bhattacharjya S. 'Lollipop'-shaped helical structure of a hybrid antimicrobial peptide of temporin B-lipopolysaccharide binding motif and mapping cationic residues in antibacterial activity. *Biochim Biophys Acta.* (2016) 1860:1362–72. doi: 10.1016/j.bbagen.2016.03.025
24. Soundrarajan N, Park S, Le Van Chanh Q, Cho HS, Raghunathan G, Ahn B, et al. Protegrin-1 cytotoxicity towards mammalian cells positively correlates with the magnitude of conformational changes of the unfolded form upon cell interaction. *Sci Rep.* (2019) 9:11569. doi: 10.1038/s41598-019-47955-2
25. Halder S, Yadav KK, Sarkar R, Mukherjee S, Saha P, Haldar S, et al. Alteration of Zeta potential and membrane permeability in bacteria: a study with cationic agents. *Springerplus*. (2015) 4:672. doi: 10.1186/S40064-015-1476-7
26. Gong ZF, Ikonomova SP, Karlsson AJ. Secondary structure of cell-penetrating peptides during interaction with fungal cells. *Protein Sci.* (2018) 27:702–13. doi: 10.1002/pro.3364
27. Toth L, Varadi G, Boros E, Borics A, Ficze H, Nagy I, et al. Biofungicidal potential of neosartorya (Aspergillus) fischeri antifungal protein NFAP and novel synthetic gamma-core peptides. *Front Microbiol.* (2020) 11:820. doi: 10.3389/Fmicb.2020.00820
28. Avitabile C, Netti F, Orefice G, Palmieri M, Nocerino N, Malgieri G, et al. Design, structural and functional characterization of a Temporin-1b analog active against Gram-negative bacteria. *Biochim Biophys Acta.* (2013) 1830:3767–75. doi: 10.1016/j.bbagen.2013.01.026
29. Roversi D, Luca V, Aureli S, Park Y, Mangoni ML, Stella L. How many antimicrobial peptide molecules kill a bacterium? The case of PMAP-23. *Acs Chem Biol.* (2014) 9:2003–7. doi: 10.1021/cb500426r
30. Avitabile C, D'Andrea LD, Saviano M, Olivieri M, Cimmino A, Romanelli A. Binding studies of antimicrobial peptides to *Escherichia coli* cells. *Biochem Biophys Res Commun.* (2016) 478:149–53. doi: 10.1016/j.bbrc.2016.07.077
31. Correa W, Brandenburg J, Behrends J, Heinbockel L, Reiling N, Paulowski L, et al. Inactivation of bacteria by γ-irradiation to investigate the interaction with antimicrobial peptides. *Biophys J.* (2019) 117:1805–19. doi: 10.1016/j.bpj.2019.10.012
32. Alves CS, Melo MN, Franquelim HG, Ferre R, Planas M, Feliu L, et al. *Escherichia coli* cell surface perturbation and disruption induced by antimicrobial peptides BP100 and pepR. *J Biol Chem.* (2010) 285:27536–44. doi: 10.1074/jbc.M110.130955
33. Perez-Peinado C, Dias SA, Domingues MM, Benfield AH, Freire JM, Radis-Baptista G, et al. Mechanisms of bacterial membrane permeabilization by crotalicidin (Ctn) and its fragment Ctn(15-34), antimicrobial peptides from rattlesnake venom. *J Biol Chem.* (2018) 293:1536–49. doi: 10.1074/jbc.RA117.000125
34. Correa W, Heinbockel L, Behrends J, Kaconis Y, Barcena-Varela S, Gutsmann T, et al. Antibacterial action of synthetic antilipopolysaccharide peptides (SALP) involves neutralization of both membrane-bound and free toxins. *Febs J.* (2019) 286:1576–93. doi: 10.1111/febs.14805
35. Zdybicka-Barabas A, Staczek S, Pawlikowska-Pawlega B, Mak P, Luchowski R, Skrzypiec K, et al. Studies on the interactions of neutral *Galleria mellonella* cecropin D with living bacterial cells. *Amino Acids.* (2019) 51:175–91. doi: 10.1007/s00726-018-2641-4
36. Moura ECCM, Baeta T, Romanelli A, Laguri C, Martorana AM, et al. Thanatin impairs lipopolysaccharide transport complex assembly by targeting LptC-LptA interaction and decreasing LptA stability. *Front Microbiol.* (2020) 11:909. doi: 10.3389/Fmicb.2020.00909
37. Gee ML, Burton M, Grevis-James A, Hossain MA, McArthur S, Palombo EA, et al. Imaging the action of antimicrobial peptides on living bacterial cells. *Sci Rep.* (2013) 3:1557. doi: 10.1038/Srep01557
38. Snoussi M, Talledo JP, Del Rosario NA, Mohammadi S, Ha BY, Košmrlj A, et al. Heterogeneous absorption of antimicrobial peptide LL37 in *Escherichia coli* cells enhances population survivability. *ELife.* (2018) 7:e38174. doi: 10.7554/eLife.38174
39. Freire JM, Gaspar D, de la Torre BG, Veiga AS, Andreu D, Castanho ARB, et al. Monitoring antibacterial permeabilization in real time using time-resolved flow cytometry. *Biochim Biophys Acta.* (2015) 1848:554–60. doi: 10.1016/j.bbamem.2014.11.001
40. Yasir M, Dutta D, Willcox MDP. Comparative mode of action of the antimicrobial peptide melimine and its derivative Mel4 against *Pseudomonas aeruginosa*. *Sci Rep.* (2019) 9:7063. doi: 10.1038/s41598-019-42440-2
41. Srinivas N, Jetter P, Ueberbacher BJ, Werneburg M, Zerbe K, Steinmann J, et al. Peptidomimetic antibiotics target outer-membrane biogenesis in *Pseudomonas aeruginosa*. *Science.* (2010) 327:1010–13. doi: 10.1126/science.1182749
42. Andolina G, Bencze LC, Zerbe K, Muller M, Steinmann J, Kocherla H, et al. A peptidomimetic antibiotic interacts with the periplasmic domain of LptD from *Pseudomonas aeruginosa*. *Acs Chem Biol.* (2018) 13:666–75. doi: 10.1021/acschembio.7b00822
43. Kang HK, Kim C, Seo CH, Park Y. The therapeutic applications of antimicrobial peptides (AMPs): a patent review. *J Microbiol.* (2017) 55:1–12. doi: 10.1007/s12275-017-6452-1
44. Riool M, de Breij A, Drijfhout JW, Nibbering PH, Zaat SAJ. Antimicrobial peptides in biomedical device manufacturing. *Front Chem.* (2017) 5:63. doi: 10.3389/Fchem.2017.00063
45. Sperandeo P, Bosco F, Clerici F, Polissi A, Gelmi ML, Romanelli A. Covalent grafting of antimicrobial peptides onto microcrystalline cellulose. *ACS Appl Biomater.* (2020) 3:4895–901. doi: 10.1021/acsabm.0c00412
46. Weishaupt R, Zund JN, Heuberger L, Zuber F, Faccio G, Robotti F, et al. Antibacterial, cytocompatible, sustainably sourced: cellulose membranes with bifunctional peptides for advanced wound dressings. *Adv Healthcare Mater.* (2020) 9:1901850doi: 10.1002/Adhm.201901850

Conflict of Interest: The authors declare that the research was conducted in the absence of any commercial or financial relationships that could be construed as a potential conflict of interest.

frontiers in Medical Technology

MINI REVIEW
published: 17 December 2020
doi: 10.3389/fmedt.2020.610203

In-cell Solid-State NMR Studies of Antimicrobial Peptides

Frances Separovic[1,2], *David W. Keizer*[2] *and Marc-Antoine Sani*[1,2*]

[1] School of Chemistry, University of Melbourne, Melbourne, VIC, Australia, [2] Bio21 Molecular Science and Biotechnology Institute, University of Melbourne, Melbourne, VIC, Australia

Antimicrobial peptides (AMPs) have attracted attention as alternatives to classic antibiotics due to their expected limited pressure on bacterial resistance mechanisms. Yet, their modes of action, in particular *in vivo*, remain to be elucidated. *In situ* atomistic-scale details of complex biomolecular assemblies is a challenging requirement for deciphering the complex modes of action of AMPs. The large diversity of molecules that modulate complex interactions limits the resolution achievable using imaging methodology. Herein, the latest advances in in-cell solid-state NMR (ssNMR) are discussed, which demonstrate the power of this non-invasive technique to provide atomic details of molecular structure and dynamics. Practical requirements for investigations of intact bacteria are discussed. An overview of recent *in situ* NMR investigations of the architecture and metabolism of bacteria and the effect of AMPs on various bacterial structures is presented. In-cell ssNMR revealed that the studied AMPs have a disruptive action on the molecular packing of bacterial membranes and DNA. Despite the limited number of studies, in-cell ssNMR is emerging as a powerful technique to monitor *in situ* the interplay between bacteria and AMPs.

Keywords: antimicrobial peptides, bacteria, solid-state NMR, in-cell NMR, mode of action

OPEN ACCESS

Edited by:
Miguel A. R. B. Castanho, University of Lisbon, Portugal

Reviewed by:
Stephan L. Grage, Karlsruhe Institute of Technology (KIT), Germany
Leandro Ramos Souza Barbosa, University of São Paulo, Brazil
Fabio Almeida, Federal University of Rio de Janeiro, Brazil

***Correspondence:**
Marc-Antoine Sani
msani@unimelb.edu.au

Specialty section:
This article was submitted to Pharmaceutical Innovation, a section of the journal Frontiers in Medical Technology

Received: *25 September 2020*
Accepted: *30 November 2020*
Published: *17 December 2020*

Citation:
Separovic F, Keizer DW and Sani M-A (2020) In-cell Solid-State NMR Studies of Antimicrobial Peptides. Front. Med. Technol. 2:610203. doi: 10.3389/fmedt.2020.610203

INTRODUCTION

Antimicrobial peptides (AMPs) are found in all living organisms, serving as an arsenal against pathogens and as modulators of the host immune system. These peptides serve as sentinels but are also produced in response to infectious and inflammatory stimuli (1). Thousands of AMPs have been discovered [APD (http://aps.unmc.edu/AP/)], mainly isolated from evolved immune systems that need to cohabit with a large array of pathogens (i.e., other cells) some have been designed *in silico* and many remain to be discovered. Indeed, new AMPs are constantly being investigated as the search for potent antimicrobial therapeutics is a high priority for providing alternatives as antibiotic resistance increases. Resistance also evolves naturally as cohabitation between microorganisms leads to competition for and production of antibiotics. A pressing problem is acquired-resistance in hospital environments, responsible for millions of premature deaths and a trillion dollar cost to the global economy (http://amr-review.org/). The acquired-resistance phenomenon can be seen as an accelerated selection process where pathogens have either mutated or incorporated genetic material to survive an increased antibiotic pressure. The difficult task of managing antibiotic-resistance in clinical practice is complex. For instance, some infected patients may tolerate higher antibiotic levels to overcome the resistance, while others could develop health threatening side-effects. Likewise, the level of drug that is actually taken up at the site of infection, particularly for deep-seated pathogens, can differ between *in vitro*

and *in vivo* environments (2). Overall, these scenarios stress that it is essential to study antimicrobial agents in their inherent environment so as to understand their mechanism of action.

AMPs have been considered as a potent alternative to antibiotics because they act fast, exploit a specific affinity for bacterial lipid membranes and often have multiple intracellular targets, which together are likely to reduce the development of AMP resistance. However, very few AMPs have reached the clinic, partly due to the pharmacokinetic discrepancies between their *in vitro* and *in vivo* behaviors (3), limiting systemic administration and instead favoring topical applications. AMPs range from *ca.* 10 to over 40 amino acids long with mainly cationic and amphipathic properties, which unifies them in targeting negatively charged lipid membranes, and often lead to bilayer disruption (4). The molecular mechanism of action is thought to be correlated with the structure of AMPs when in contact with the pathogens; thus structure elucidation techniques are key to the determination of critical structural features that modulate the potency of AMPs *in situ*. The ability to extract atomic details of molecular interactions within functioning cells is the utmost challenge in biology. There are many challenges to face when in-cell studies are performed, from the lifetime of the cells to the resolution of the signal.

STRUCTURE ELUCIDATION TECHNIQUES

X-ray diffraction has been the method of choice to determine the structure of crystalized proteins with resolution well below 2 Å. In systems where AMPs co-crystalize with their target, X-ray can provide high-resolution structures, as demonstrated by the recent structures of peptides complexed with *Pseudomonas aeruginosa* protein LecB (5). The requirement of a crystalline environment, however, has excluded this technique from in-cell studies, which has limited our understanding of the impact of the cellular environments on intricate interactions. This hurdle is gradually being phased out with the development of soft X-ray tomography, a fast progressing field, for generating high-resolution images of cellular systems in a similar fashion to cryo-electron microscopy (EM) tomography. Indeed, recent images of cells at 30–50 nm resolution have been reported (6, 7).

Cryo-EM has drastically improved the capability to determine the structure of proteins with <3 Å resolution, as recently reported by Herzik et al. (8). This imaging technique is particular well-suited for cellular environments and large complexes since labeling is not required for signal detection and is not impeded by conformational heterogeneity (9, 10). For instance, the structures of bacterial ribosomes have been investigated as they are good candidates for drug targeting (11). Cryo-EM can also provide a wealth of information on the topology of cell structures, such as the architecture of organelles at membrane contact sites (12) or how membrane-active molecules, such as AMPs, can alter the cell morphology (13). However, high-resolution cryo-EM of peptides and proteins is often limited if X-ray or NMR derived structures are not available to assist computer-guided structural fitting of images, known as single particle analysis. Furthermore, cryo-EM is unable to provide information on the dynamic interactions between biomolecules such as receptor-ligand interplays. Ultimately, in-cell structural studies of membrane-active peptides and small membrane proteins remain rare and difficult, mainly due to their size.

Imaging using fluorescent probes has also been successful in providing structural details of cellular components. Resolution is constantly improving with the latest single particle methodology at the forefront (14). In-cell fluorescence has a severe limitation, however, due to the necessity of a fluorescent probe which is invasive and challenging to target in a crowded cellular environment.

NMR, and in particular ssNMR, is well suited to tackle in-cell studies as, like EM, it is not limited by the nature of the environment and does not require a perturbing label for signal detection. Notably, the majority of the AMP structures deposited in the RSCB Protein Data Bank (PDB) have been determined by solution-state NMR, albeit in membrane mimetics or mixed solvents. In-cell NMR has provided the first structure of a protein at atomic resolution in an intact cellular environment (15). In addition to its capability to provide high-resolution structures, NMR is particularly powerful for investigating dynamics, which opens a window to view the mechanism of complex *in situ* physiological processes. NMR has provided deep insights into protein-protein, protein-lipid, and protein-ligand interactions, with particular success in monitoring transient interactions (16). NMR is the most powerful high-resolution technique for determining binding constants, folding thermodynamics and kinetics of biomolecular interactions. However, NMR has rather low sensitivity and background signals can contribute significantly: difficulties that impose long experimental times compounded by limited cell viability. These practical challenges and ways around them for in-cell NMR studies will be discussed in the following section.

IN-CELL SOLID-STATE NMR

Practical Challenges

A key physical property necessary for high-resolution NMR is the rapid reorientation, or rotational tumbling, of the macromolecules within the magnetic field. Large molecules tumble slowly and display severely broadened NMR signals, which could become undetectable in solution-state experiments. Indeed, most cellular components are not detected by solution-state NMR although, interestingly, the viscosity of the intracellular environment is only moderately higher (1.2–2-fold) than the usual buffers used *in vitro* (17, 18). In fact, it has been determined that weak and non-specific interactions that slow down molecular motions of soluble molecules—termed quinary structures (19)—are mostly responsible for the absence of these NMR signals (20).

ssNMR is not limited by slow molecular motion, which places this non-invasive technique as ideal for investigating the interplay between AMPs and bacteria, fungi or other cell systems. However, the intrinsic slow molecular tumbling combined with the strong anisotropy lead to lower sensitivity in comparison to solution-state NMR. Thus, greater amounts of material and longer experimental times would be necessary to obtain

structural information with high resolution. ssNMR uses magic angle spinning (rotation of the sample at 54.74° relative to the magnetic field) to partially reintroduce motional averaging thereby providing enhanced resolution. However, to fully average the broadening interactions with the magnetic field, such as the dipolar couplings or the chemical shift anisotropy, the rotor must be spun above 110 kHz for solid samples. This is achievable with latest NMR probe developments with rotors of 0.9 mm diameter but remains limited to particular samples, such as microcrystals. This highlights a limiting factor in ssNMR as the sample volumes are generally well below 100 μL, which is a challenge for live cell experiments. Indeed, most of the sample volume will be occupied by the aqueous phase, resulting in less signal from molecules of interest, e.g., lipids. Furthermore, cellular background is usually significant in ssNMR since all molecules, regardless of their tumbling rate, are contributing to the NMR signal. However, filtering techniques using specific pulse sequences can be used to select rigid (Hartmann-Hahn cross-polarization transfer, CP) vs. mobile (insensitive nuclei enhanced by polarization transfer, INEPT) molecules (21), opening strategies to design NMR experiments.

In addition to the spectral broadening due to the biomolecular tumbling rates, other factors contribute to reducing the resolution of the NMR signals of cellular components. The heterogenous environments in cells induce gradients of magnetic susceptibility and cellular degradation is changing the signal during acquisition. It becomes apparent that fast signal acquisition and/or signal enhancement are important challenges to be tackled in order to develop in-cell ssNMR further. The development of dynamic nuclear polarization (DNP) has provided tremendous NMR signal enhancement, requiring spin labels and cryogenic conditions, thereby enabling in-cell studies of peptides and proteins while cell integrity is preserved under cryoprotection during experimental time (22). Many challenges remain before in-cell studies using DNP-enhanced NMR techniques become routine, mainly due to lower signal resolution at cryogenic temperatures (100 K). Still, the technology is rapidly improving with reduced rotor sizes for faster spinning speed and development of DNP at high magnetic fields (23). A recent review on DNP NMR of large biomolecular assemblies has emphasized that cellular preparations do not provide as high signal enhancements asmi crocrystals or precipitates and require particular isotopic enrichment to alleviate the background signal (24).

NMR studies of naturally abundant metabolites and molecules with high copy levels have provided useful *in vivo* details of physiological processes, albeit with a limited resolution and greater complexity of signal interpretation, which often requires heavy statistical analysis, such as principal component analysis (25). In-cell NMR differs as it focuses typically on a specific molecule with high resolution. To achieve this specificity, the molecule of interest needs to be labeled with isotopes that are otherwise in very low abundance at natural level or not present in biomolecules. ^{13}C (1.1% natural abundance), ^{15}N (0.4% natural abundance), ^{2}H (0.01% natural abundance) and ^{19}F (100% natural abundance but not found in biological environments) have been successfully incorporated into biomolecules to provide specific monitoring within complex environments (**Figure 1**). Procedures are now commonly available to design labeling schemes for proteins over-expressed in prokaryotic cells (26) and less so in eukaryotic cells, although methodology to deliver labeled ubiquitin into mammalian cells recently was achieved for in-cell NMR studies (27). The production of isotopically enriched recombinant AMPs for structural studies has not been extensively reported, but a similar strategy could be applied and has been for commercial production of several AMPs (28). Synthetic methods have also been used to introduce selective labeling within peptides, but this remains a costly method that is often limited to labeled hydrophobic amino acids. A few studies have reported the expression of AMPs in decent yields, by using a fusion partner thereby limiting the toxicity toward the host system and post-translation modification or degradation (29, 30). It is noteworthy that AMPs are often naturally C-amidated, which confers higher stability from serum degradation. One expression system attempted to generate C-amidated AMPs by using an intein fusion tag. The self-splicing tag is removed under reducing conditions and high concentration of ammonium bicarbonate, thereby introducing the amide group at the cleavage site (31). An issue of the method, however, is the low final yield as the fusion tag can easily represent 90% of the expressed fusion protein molecular weight, which drastically reduces the amount of recovered peptide, and additional purification of the carboxylic vs. amidated C-terminus peptides may be required.

As seen in **Figure 1**, several potential targets by AMPs can be monitored by ssNMR using either naturally abundant reporters, such as ^{31}P, or by enriching cellular components with isotopes, such as ^{2}H. Phosphorus is naturally found in high content as phosphate moieties are used as a building block in phospholipids but also in nucleic acids (NA) and other metabolites such as ATP. ^{2}H has been introduced into bacterial phospholipids by feeding bacteria with ^{2}H labeled fatty acids (32, 33). Cell wall components have also been labeled by introducing ^{13}C, ^{15}N and even ^{19}F into the peptidoglycan structure (34). Peptides and proteins can be ^{13}C, ^{15}N and even ^{2}H isotopically enriched to improve sensitivity and resolution of NMR studies (26, 30).

Overall, ssNMR studies of AMPs in whole bacterial cells have been scarce due to the necessity of introducing biochemical labeling steps. However, recent studies have demonstrated that in-cell NMR can provide new insights into the mode of action of AMPs, not otherwise accessible within *in vitro* environments.

AMPs' First Encounter, the Gram-Positive Cell Wall or the Gram-Negative LPS Layer

Bacteria have a protective external layer around their phospholipid membranes: the cell wall for Gram-positive and the lipopolysaccharide layer (LPS) for Gram-negative bacteria. Knowledge of these structures is important for understanding how AMPs either get through to target the phospholipid membranes or how they inhibit cellular processes by remaining in these external layers.

The cell wall is made of a peptidoglycan (PGN) sacculus anchored within phospholipid membranes by teichoic acids. ^{13}C ssNMR studies of *Staphylococcus aureus* and *Bacillus subtilis*

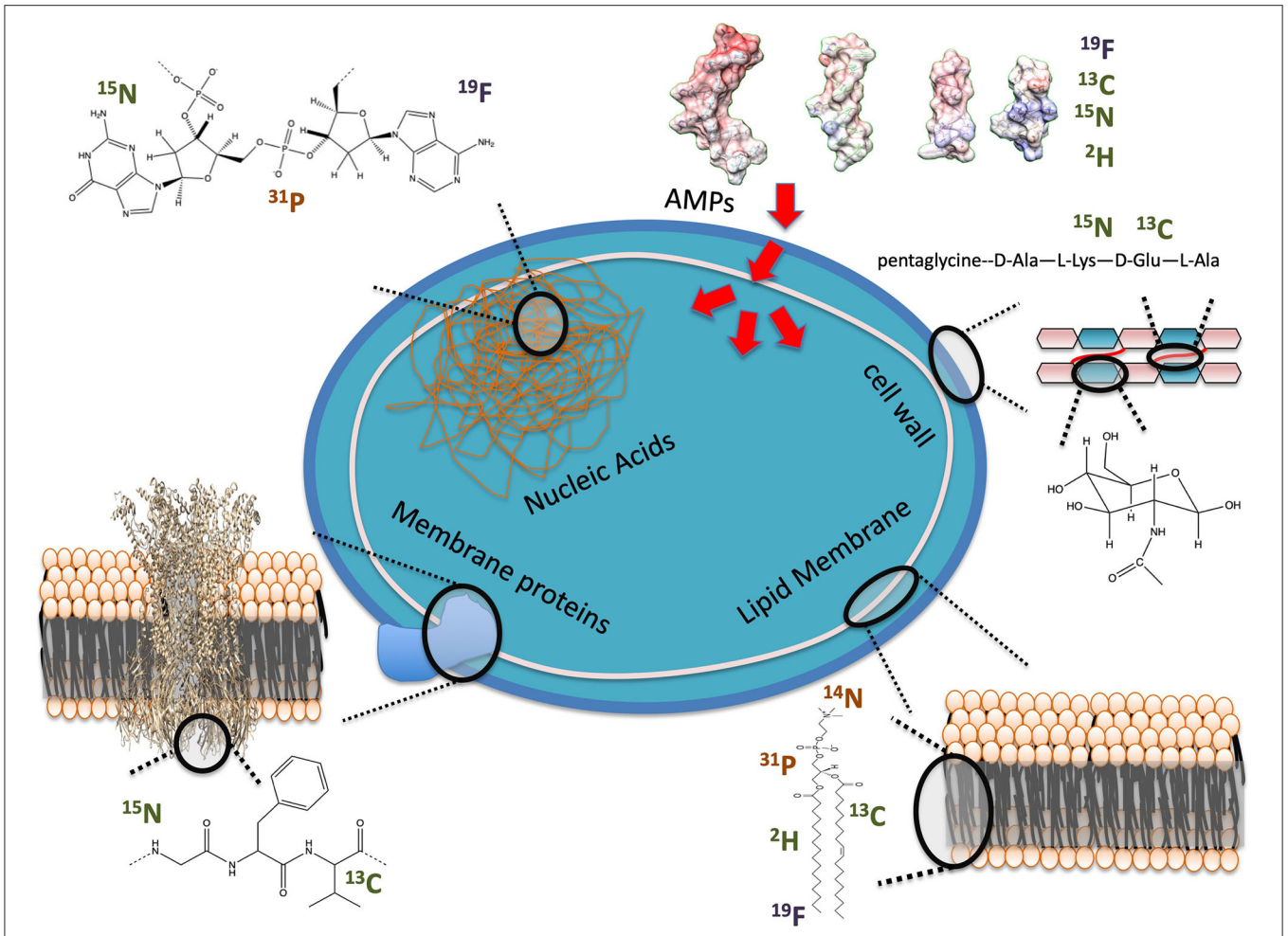

FIGURE 1 | Examples of NMR observables for in-cell studies of AMP interactions with bacteria. Nuclei are labeled as present in cells at high (orange) or low (green) natural abundance or unnatural (blue).

(**Figure 2**) have determined that the PGN mesh structure is formed by the disaccharide backbone four-fold screw helical symmetry with each PGN stem oriented 90° from the previous stem (37). Most AMPs are not retained by the PGN mesh partially due to the neutral charge of the structure vs. the highly negatively charged surface of the Gram-positive phospholipid membranes. Yet, AMPs, such as the human cationic polypeptide ECP (eosinophilic cationic protein), have shown strong interactions with the PGN, which interfere with the cell replication process (38). Cegelski *et al.* have reported methods to label the PGN of Gram-positive bacteria and have monitored the binding of antibiotics to the cell wall of *S. aureus* (34). A similar achievement was obtained using the DNP ssNMR approach where lipid II binding antibiotics were investigated *in situ*. The importance of a native environment was highlighted for pore formation of nisin with increased plasticity of the peptide observed in native bacteria (39).

The outer leaflet of the outer membrane (OM) of Gram-negative bacteria is mainly made of LPS, whose complex structure is species specific (40). LPS can contain various amount of phosphate and pyrophosphate groups, which can modulate the negative charge density, and thus electrostatic interactions with cationic AMPs (41). NMR has provided a wealth of structural details on LPS incorporated into micelles (42) and isolated OMs have been used to investigate AMP interactions with LPS (43). These studies have demonstrated that external LPS often limits the activity of AMPs by strongly binding to the peptides thereby preventing interior access to Gram-negative bacteria. Yet, high-resolution in-cell NMR studies of intact Gram-negative bacteria remain to be performed so as to specifically address AMP interactions with the complex LPS layer under native conditions. This may require specific labeling of the LPS to enable signal separation between it and other intracellular molecules such as the phospholipids.

Bacterial Lipid Membrane, the Main Target for AMPs

AMPs have displayed a remarkable affinity for negatively charged membranes of bacteria vs. neutral eukaryotic membranes (44). ^{31}P is a natural highly abundant nucleus that can report on the

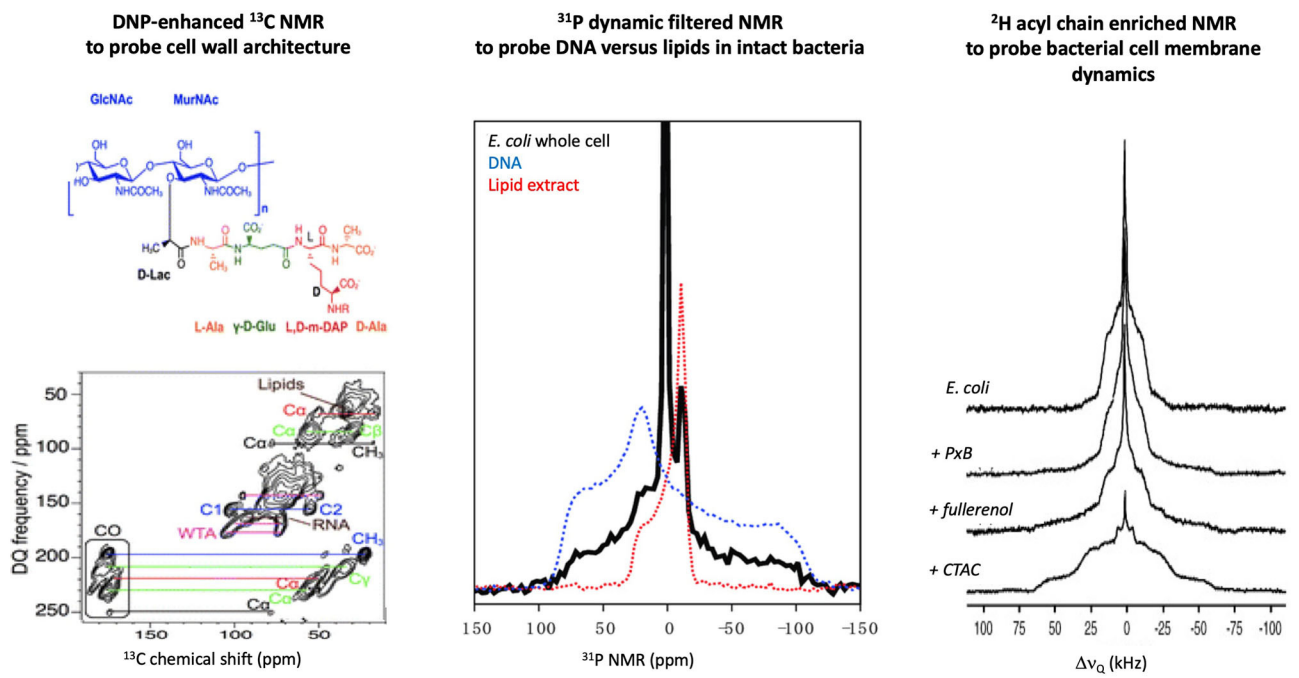

FIGURE 2 | Examples of in-cell solid-state NMR studies of intact bacteria. **(Lef)t** Using DNP-enhanced ^{13}C NMR, the cell wall of *B. Subtilis* was investigated and signals from several cell components could be assigned, which allowed the impact of AMPs on these structures to be monitored [adapted from (35)]. **(Middle)** ^{31}P NMR of *E. coli* can differentiate DNA vs. lipid signals due to the difference in intramolecular dynamics, which allowed direct monitoring of AMP impact on cell membranes or secondary targets such as DNA [adapted from (36)]. **(Right)** ^{2}H NMR of *E. coli* fed with ^{2}H enriched fatty acids has allowed monitoring the effect of membrane active molecules (PxB, polymyxin B; fullerenol, nanoparticle; CTAC, cetyltrimethylammonium chloride) on the dynamic of the bacterial membranes [adapted from (32)].

architecture of the lipid bilayers and the dynamics of the lipid headgroup (45). A recent ^{31}P NMR study of intact *Escherichia coli* (36) has reported that the AMP maculatin 1.1 increases the dynamics of the membrane lipids, which is direct evidence of the disruptive effect that AMPs trigger in membranes of live bacteria.

Not only the charge but also the nature of the lipid acyl chains has been shown to modulate AMPs activity. Incorporation of ^{2}H labeled fatty acids into the growth media of bacteria has allowed specific monitoring of AMPs perturbation of the hydrophobic core of bacterial (32, 33). ^{2}H NMR spectra can provide a more direct measure of how deep AMPs perturb the dynamics along the lipid acyl chain as methyl deuterons found at the chain terminus and deuterons near the glycerol region at the water interface are usually well resolved (**Figure 2**). Although a small subset of AMPs and bacteria have been investigated by in-cell ^{2}H NMR, similar observations have been reported, i.e., AMPs increase the acyl chain dynamics by inserting into the hydrophobic core of the bacterial membranes. However, the degree of perturbation of *E. coli* vs. *B. subtilis* for a series of AMPs having different charges and lengths was quite disparate, which supports the importance of studying the impact of AMPs *in situ* (46, 47).

Intracellular Targets, AMPs Secondary Targets?

^{31}P NMR studies of *E. coli* bacteria with the AMP maculatin 1.1 revealed that the phospholipid membranes were significantly perturbed but, unexpectedly, that DNA packing was also impacted (36). NMR is able to filter between the rigid DNA and the mobile phospholipid membrane which allowed the multiple effects induced on the bacteria under the AMP action to be monitored (**Figure 2**). This study showcased that AMPs can have multiple targets and, unlike *in vitro* systems, by monitoring the entire cellular response, the full spectrum of the bactericidal mechanism may be tracked.

AMPs Structure and Self-Assembly in Bacteria: the Key to Understanding AMPs Mode of Action

Most cationic linear AMPs are unstructured in an aqueous environment but adopt a secondary structure when in contact with a lipid membrane (48). Do these *in vitro* observations hold in bacteria? To obtain the *in situ* structure of an AMP, higher amounts of ^{13}C and ^{15}N labeled peptides and longer experimental times are necessary to extract the intricate dipolar network of the amino acid residues. This is a hurdle since labeling is tedious (and costly) and long experimental times are detrimental for cell integrity. DNP-NMR has opened new possibilities to tackle these practical issues. By significantly enhancing the NMR signal using spin labels under cryogenic conditions, in-cell DNP-NMR experiments of *E. coli* incubated with ^{13}C,^{15}N synthetically enriched labeled AMPs at specific residues is achievable. The ^{13}C to ^{15}N atomic distances obtained by REDOR NMR (49,

50) are used to provide restraints for structure calculation, i.e., determining if AMPs retained the expected helical pitch between residue i to residue i + 3 in bacteria (51). Once large-scale expression systems for C-amidated AMPs are optimized, AMP structures and peptide-peptide contact maps will be achievable by in-cell solid-state DNP-NMR studies.

PERSPECTIVES

Understanding the mode of action of AMPs based on their primary sequence, deciphering their self-assembly mechanism and tracking their interactions with multiple intracellular targets in intact bacteria are crucial in order to develop new therapeutics. Although at an early stage, in-cell ssNMR has demonstrated the capability to provide important structural details, such as how cell membranes and/or DNA of bacteria respond to AMPs. This additional knowledge will give rise to further questions and in turn stimulate new biochemical engineering that further will extend *in situ* ssNMR studies. From the production of isotopically enriched AMPs to identifying specific NMR signals in bacteria, ssNMR offers exciting prospects to image the interplay of AMPs with bacteria and plays an important role in complementing other imaging techniques and biochemical assays.

AUTHOR CONTRIBUTIONS

M-AS, FS, and DK conceived and wrote the paper. All authors contributed to the article and approved the submitted version.

FUNDING

The authors thank the Australian Research Council for funding (DP160100959 to FS and LE160100120 to FS, DK, and M-AS).

ACKNOWLEDGMENTS

The authors would like to thank the Bio21 Institute for support of the in-cell NMR work related in this manuscript.

REFERENCES

1. Hancock RE. Cationic peptides: effectors in innate immunity and novel antimicrobials. *Lancet Infect Dis.* (2001) 1:156–64. doi: 10.1016/S1473-3099(01)00092-5
2. Nannini EC, Singh KV, Arias CA, Murray BE. *In vivo* effects of cefazolin, daptomycin, and nafcillin in experimental endocarditis with a methicillin-susceptible *Staphylococcus aureus* strain showing an inoculum effect against cefazolin. *Antimicrob Agents Chemother.* (2013) 57:4276–81. doi: 10.1128/AAC.00856-13
3. Jenssen H, Hamill P, Hancock RE. Peptide antimicrobial agents. *Clin Microbiol Rev.* (2006) 19:491–511. doi: 10.1128/CMR.00056-05
4. Sani MA, Separovic F. How membrane-active peptides get into lipid membranes. *Acc Chem Res.* (2016) 49:1130–8. doi: 10.1021/acs.accounts.6b00074
5. Baeriswyl S, Gan BH, Siriwardena TN, Visini R, Robadey M, Javor S, et al. X-ray crystal structures of short antimicrobial peptides as *Pseudomonas aeruginosa* lectin B complexes. *ACS Chem Biol.* (2019) 14:758–66. doi: 10.1021/acschembio.9b00047
6. Larabell CA, Nugent KA. Imaging cellular architecture with X-rays. *Curr Opin Struct Biol.* (2010) 20:623–31. doi: 10.1016/j.sbi.2010.08.008
7. Weinhardt V, Chen JH, Ekman A, Mcdermott G, Le Gros MA, Larabell C. Imaging cell morphology and physiology using X-rays. *Biochem Soc Trans.* (2019) 47:489–508. doi: 10.1042/BST20180036
8. Herzik MAJr, Wu M, Lander GC. High-resolution structure determination of sub-100 kDa complexes using conventional cryo-EM. *Nat Commun.* (2019) 10:1032. doi: 10.1038/s41467-019-08991-8
9. Nogales E, Scheres SH. Cryo-EM: a unique tool for the visualization of macromolecular complexity. *Mol Cell.* (2015) 58:677–89. doi: 10.1016/j.molcel.2015.02.019
10. Cheng Y. Single-particle cryo-EM-how did it get here and where will it go. *Science.* (2018) 361:876–80. doi: 10.1126/science.aat4346
11. Morgan CE, Huang W, Rudin SD, Taylor DJ, Kirby JE, Bonomo RA, et al. Cryo-electron microscopy structure of the *Acinetobacter baumannii* 70S ribosome and implications for new antibiotic development. *mBio.* (2020) 11:e03117-19. doi: 10.1128/mBio.03117-19
12. Collado J, Fernandez-Busnadiego R. Deciphering the molecular architecture of membrane contact sites by cryo-electron tomography. *Biochim Biophys Acta Mol Cell Res.* (2017) 1864:1507–12. doi: 10.1016/j.bbamcr.2017.03.009
13. Sani MA, Whitwell TC, Gehman JD, Robins-Browne RM, Pantarat N, Attard TJ, et al. Maculatin 1.1 disrupts *Staphylococcus aur*eus lipid membranes via a pore mechanism. *Antimicrob Agents Chemother.* (2013) 57:3593–600. doi: 10.1128/AAC.00195-13
14. Yu J. Single-molecule studies in live cells. *Annu Rev Phys Chem.* (2016) 67:565–85. doi: 10.1146/annurev-physchem-040215-112451
15. Sakakibara D, Sasaki A, Ikeya T, Hamatsu J, Hanashima T, Mishima M, et al. Protein structure determination in living cells by in-cell NMR spectroscopy. *Nature.* (2009) 458:102–5. doi: 10.1038/nature07814
16. Sani M-A, Separovic F, (editors). *Solid-state NMR: Applications in Biomembrane Structure.* Bristol, UK: IOP Publishing (2020). p. 416.
17. Moonen CT, Van Zijl PC, Le Bihan D, Despres D. *In vivo* NMR diffusion spectroscopy: 31P application to phosphorus metabolites in muscle. *Magn Reson Med.* (1990) 13:467–77. doi: 10.1002/mrm.1910130314
18. Williams SP, Haggie PM, Brindle KM. 19F NMR measurements of the rotational mobility of proteins *in vivo*. *Biophys J.* (1997) 72:490–8. doi: 10.1016/S0006-3495(97)78690-9
19. Mcconkey EH. Molecular evolution, intracellular organization, and the quinary structure of proteins. *Proc Natl Acad Sci USA.* (1982) 79:3236–40. doi: 10.1073/pnas.79.10.3236
20. Cohen RD, Pielak GJ. Electrostatic contributions to protein quinary structure. *J Am Chem Soc.* (2016) 138:13139–42. doi: 10.1021/jacs.6b07323
21. Gopinath T, Veglia G. Probing membrane protein ground and conformationally excited states using dipolar- and J-coupling mediated MAS solid state NMR experiments. *Methods.* (2018) 148:115–22. doi: 10.1016/j.ymeth.2018.07.003
22. Sani MA, Zhu S, Hofferek V, Separovic F. Nitroxide spin-labeled peptides for DNP-NMR in-cell studies. *FASEB J.* (2019) 33:11021–7. doi: 10.1096/fj.201900931R
23. Bernard GM, Michaelis VK. Instrumentation for high-field dynamic nuclear polarization NMR spectroscopy. In: Harris RK, Wasylishen RL, Editors. *eMagRes, Vol: 8.* John Wiley & Sons, Ltd. (2019). doi: 10.1002/9780470034590.emrstm1560
24. Jaudzems K, Polenova T, Pintacuda G, Oschkinat H, Lesage A. DNP NMR of biomolecular assemblies. *J Struct Biol.* (2019) 206:90–8. doi: 10.1016/j.jsb.2018.09.011
25. Glader O, Puljula E, Jokioja J, Karonen M, Sinkkonen J, Hytonen J. NMR metabolome of *Borrelia burgdorferi in vitro* and *in vivo* in mice. *Sci Rep.* (2019) 9:8049. doi: 10.1038/s41598-019-44540-5
26. Acton TB, Xiao R, Anderson S, Aramini J, Buchwald WA, Ciccosanti C, et al. Preparation of protein samples for NMR structure, function, and small-molecule screening studies. *Methods Enzymol.* (2011) 493:21–60. doi: 10.1016/B978-0-12-381274-2.00002-9

27. Narasimhan S, Scherpe S, Lucini Paioni A, Van Der Zwan J, Folkers GE, Ovaa H, et al. DNP-supported solid-state NMR spectroscopy of proteins inside mammalian cells. *Angew Chem Int Ed Engl.* (2019) 58:12969–73. doi: 10.1002/anie.201903246
28. Sinha R, Shukla P. Antimicrobial peptides: recent insights on biotechnological interventions and future perspectives. *Protein Pept Lett.* (2019) 26:79–87. doi: 10.2174/0929866525666181026160852
29. Zorko M, Jerala R. Production of recombinant antimicrobial peptides in bacteria. *Methods Mol Biol.* (2010) 618:61–76. doi: 10.1007/978-1-60761-594-1_5
30. Ishida H, Nguyen LT, Gopal R, Aizawa T, Vogel HJ. Overexpression of antimicrobial, anticancer, and transmembrane peptides in *Escherichia coli* through a calmodulin-peptide fusion system. *J Am Chem Soc.* (2016) 138:11318–26. doi: 10.1021/jacs.6b06781
31. Cottingham IR, Millar A, Emslie E, Colman A, Schnieke AE, Mckee C. A method for the amidation of recombinant peptides expressed as intein fusion proteins in *Escherichia coli. Nat Biotechnol.* (2001) 19:974–7. doi: 10.1038/nbt1001-974
32. Tardy-Laporte C, Arnold AA, Genard B, Gastineau R, Morancais M, Mouget JL, et al. A (2)H solid-state NMR study of the effect of antimicrobial agents on intact *Escherichia coli* without mutating. *Biochim Biophys Acta.* (2013) 1828:614–22. doi: 10.1016/j.bbamem.2012.09.011
33. Santisteban NP, Morrow MR, Booth V. Protocols for studying the interaction of MSI-78 with the membranes of whole gram-positive and gram-negative bacteria by NMR. *Methods Mol Biol.* (2017) 1548:217–30. doi: 10.1007/978-1-4939-6737-7_15
34. Romaniuk JA, Cegelski L. Bacterial cell wall composition and the influence of antibiotics by cell-wall and whole-cell NMR. *Philos Trans R Soc Lond B Biol Sci.* (2015) 370:20150024. doi: 10.1098/rstb.2015.0024
35. Takahashi H, Ayala I, Bardet M, De Paepe G, Simorre JP, Hediger S. Solid-state NMR on bacterial cells: selective cell wall signal enhancement and resolution improvement using dynamic nuclear polarization. *J Am Chem Soc.* (2013) 135:5105–10. doi: 10.1021/ja312501d
36. Overall SA, Zhu S, Hanssen E, Separovic F, Sani MA. *In situ* monitoring of bacteria under antimicrobial stress using (31)P solid-state NMR. *Int J Mol Sci.* (2019) 20:181. doi: 10.3390/ijms20010181
37. Kim SJ, Chang J, Singh M. Peptidoglycan architecture of Gram-positive bacteria by solid-state NMR. *Biochim Biophys Acta.* (2015) 1848:350–62. doi: 10.1016/j.bbamem.2014.05.031
38. Torrent M, Navarro S, Moussaoui M, Nogues MV, Boix E. Eosinophil cationic protein high-affinity binding to bacteria-wall lipopolysaccharides and peptidoglycans. *Biochemistry.* (2008) 47:3544–55. doi: 10.1021/bi702065b
39. Medeiros-Silva J, Jekhmane S, Paioni AL, Gawarecka K, Baldus M, Swiezewska E, et al. High-resolution NMR studies of antibiotics in cellular membranes. *Nat Commun.* (2018) 9:3963. doi: 10.1038/s41467-018-06314-x
40. Ruiz N, Kahne D, Silhavy TJ. Advances in understanding bacterial outer-membrane biogenesis. *Nat Rev Microbiol.* (2006) 4:57–66. doi: 10.1038/nrmicro1322
41. Lanne ABM, Goode A, Prattley C, Kumari D, Drasbek MR, Williams P, et al. Molecular recognition of lipopolysaccharide by the lantibiotic nisin. *Biochim Biophys Acta Biomembr.* (2019) 1861:83–92. doi: 10.1016/j.bbamem.2018.10.006
42. Bhattacharjya S. NMR structures and interactions of antimicrobial peptides with lipopolysaccharide: connecting structures to functions. *Curr. Top. Med. Chem.* (2016) 16:4–15. doi: 10.2174/1568026615666150703121943
43. Wu EL, Engstrom O, Jo S, Stuhlsatz D, Yeom MS, Klauda JB, et al. Molecular dynamics and NMR spectroscopy studies of *E. coli* lipopolysaccharide structure and dynamics. *Biophys J.* (2013) 105:1444–55. doi: 10.1016/j.bpj.2013.08.002
44. Sani MA, Gagne E, Gehman JD, Whitwell TC, Separovic F. Dye-release assay for investigation of antimicrobial peptide activity in a competitive lipid environment. *Eur Biophys J.* (2014) 43:445–50. doi: 10.1007/s00249-014-0970-0
45. Dufourc EJ, Bonmatin JM, Dufourcq J. Membrane structure and dynamics by 2H- and 31P-NMR. Effects of amphipatic peptidic toxins on phospholipid and biological membranes. *Biochimie.* (1989) 71:117–23. doi: 10.1016/0300-9084(89)90141-7
46. Laadhari M, Arnold AA, Gravel AE, Separovic F, Marcotte I. Interaction of the antimicrobial peptides caerin 1.1 and aurein 1.2 with intact bacteria by (2)H solid-state NMR. *Biochim Biophys Acta.* (2016) 1858:2959–64. doi: 10.1016/j.bbamem.2016.09.009
47. Santisteban NP, Morrow MR, Booth V. Effect of AMPs MSI-78 and BP100 on the lipid acyl chains of (2)H-labeled intact Gram positive bacteria. *Biochim Biophys Acta Biomembr.* (2020) 1862:183199. doi: 10.1016/j.bbamem.2020.183199
48. Sani MA, Whitwell TC, Separovic F. Lipid composition regulates the conformation and insertion of the antimicrobial peptide maculatin 1.1. *Biochim Biophys Acta.* (2012) 1818:205–11. doi: 10.1016/j.bbamem.2011.07.015
49. Toke O, Cegelski L, Schaefer J. Peptide antibiotics in action: investigation of polypeptide chains in insoluble environments by rotational-echo double resonance. *Biochim Biophys Acta.* (2006) 1758:1314–29. doi: 10.1016/j.bbamem.2006.02.031
50. Gehman JD, Separovic F, Lu K, Mehta AK. Boltzmann statistics rotational-echo double-resonance analysis. *J Phys Chem B.* (2007) 111:7802–11. doi: 10.1021/jp072504q
51. Kang X, Elson C, Penfield J, Kirui A, Chen A, Zhang L, et al. Integrated solid-state NMR and molecular dynamics modeling determines membrane insertion of human beta-defensin analog. *Commun Biol.* (2019) 2:402. doi: 10.1038/s42003-019-0653-6

Conflict of Interest: The authors declare that the research was conducted in the absence of any commercial or financial relationships that could be construed as a potential conflict of interest.

frontiers in Medical Technology

REVIEW
published: 21 December 2020
doi: 10.3389/fmedt.2020.615494

Revealing the Mechanisms of Synergistic Action of Two Magainin Antimicrobial Peptides

Burkhard Bechinger[1,2]*, *Dennis Wilkens Juhl*[1†], *Elise Glattard*[1] and *Christopher Aisenbrey*[1]

[1] University of Strasbourg/CNRS, UMR7177, Institut de Chimie de Strasbourg, Strasbourg, France, [2] Institut Universitaire de France (IUF), Paris, France

The study of peptide-lipid and peptide-peptide interactions as well as their topology and dynamics using biophysical and structural approaches have changed our view how antimicrobial peptides work and function. It has become obvious that both the peptides and the lipids arrange in soft supramolecular arrangements which are highly dynamic and able to change and mutually adapt their conformation, membrane penetration, and detailed morphology. This can occur on a local and a global level. This review focuses on cationic amphipathic peptides of the magainin family which were studied extensively by biophysical approaches. They are found intercalated at the membrane interface where they cause membrane thinning and ultimately lysis. Interestingly, mixtures of two of those peptides namely magainin 2 and PGLa which occur naturally as a cocktail in the frog skin exhibit synergistic enhancement of antimicrobial activities when investigated together in antimicrobial assays but also in biophysical experiments with model membranes. Detailed dose-response curves, presented here for the first time, show a cooperative behavior for the individual peptides which is much increased when PGLa and magainin are added as equimolar mixture. This has important consequences for their bacterial killing activities and resistance development. In membranes that carry unsaturations both peptides align parallel to the membrane surface where they have been shown to arrange into mesophases involving the peptides and the lipids. This supramolecular structuration comes along with much-increased membrane affinities for the peptide mixture. Because this synergism is most pronounced in membranes representing the bacterial lipid composition it can potentially be used to increase the therapeutic window of pharmaceutical formulations.

Keywords: PGLa, membrane topology, membrane pore, membrane macroscopic phase, SMART model, carpet model, peptide-lipid interactions, molecular shape concept

OPEN ACCESS

Edited by:
Miguel A. R. B. Castanho, University of Lisbon, Portugal

Reviewed by:
Octavio Luiz Franco, Catholic University of Brasilia (UCB), Brazil
Davor Juretić, MEDILS - Mediterranean Institute for Life Sciences, Croatia

***Correspondence:**
Burkhard Bechinger
bechinge@unistra.fr

***Present address:**
Dennis Wilkens Juhl, Department of Chemistry, Aarhus University, Aarhus, Denmark

Specialty section:
This article was submitted to Pharmaceutical Innovation, a section of the journal Frontiers in Medical Technology

Received: *09 October 2020*
Accepted: *30 November 2020*
Published: *21 December 2020*

Citation:
Bechinger B, Juhl DW, Glattard E and Aisenbrey C (2020) Revealing the Mechanisms of Synergistic Action of Two Magainin Antimicrobial Peptides. Front. Med. Technol. 2:615494. doi: 10.3389/fmedt.2020.615494

INTRODUCTION

Antimicrobial peptides (AMPs) are part of the innate immune system of higher organisms which provides a powerful and responsive first line of defense against a multitude of pathogenic microorganisms (1, 2). Several years after the discovery of penicillin in 1928 (3) gramicidin S was extracted from soil bacteria and used to treat gunshot wounds during world-war II (4–6). Furthermore, other peptidic compounds with antimicrobial activities have been detected in microorganisms (7, 8), but antimicrobial peptides also exist in many species of the plant and animal

kingdom, including humans (9). The first of these peptides have been discovered decades ago and have been investigated ever since (4, 10–12). The list of amino acid sequences with antimicrobial activities is continuously increasing and they are accessible through various data bases (13–16). To understand their mechanisms of action several of them have been investigated by a variety of biological, biochemical, and biophysical approaches (17, 18).

During recent years the rapid increase in multiresistant pathogens (19) has brought back research on AMPs (20, 21), because their mechanisms of action has been shown to be less prone to microbial resistance when compared to conventional treatments (2, 22, 23). Although peptides are quickly digested by proteases (24–26) this limitation in their applicability can be overcome by unnatural building blocks, their protection inside nanostructures or when linked to surfaces (27–29). Furthermore, based on mechanistic studies of cationic amphipathic antimicrobial peptides small amphipathic molecules (30, 31), foldamer and pseudopeptides (32–40), and polymers (41) with potent antimicrobial properties have been designed.

Peptides have been found early on in the skin of toads and frogs (10, 42) and magainins from *Xenopus laevis* were among the first, for which the potential usefulness of their antimicrobial activity has been described (**Table 1**) (11). Soon after their discovery a multitude of investigations have been performed that reveal that magainins and other cationic amphipathic peptides interfere with the barrier function of bacterial membranes which by itself causes bacterial killing (43–45). Notably, related peptides have been shown to also enter the cell interior where further action can take place (46–48). Furthermore, many peptides are involved in modulating the immune response of the host organisms thereby adding an additional layer of efficiency and they are therefore also referred to as "host defense peptides" (49–52).

A membrane-active mechanism has been confirmed by the study of all-D analogs of AMPs which exhibit the same activity than their naturally occurring counter-part indicating that they do not interact with chiral proteinaceous receptors (47). Indeed, their amphipathic nature and in most cases an accumulation of cationic residues has been shown essential for membrane interaction and selectivity, rather than a specific amino acid composition (2). Peptides with helical (17, 18), cyclic (40, 53–55) and/or β-sheet arrangements have been investigated (56–60).

Abbreviations: AMP, antimicrobial peptide; ATR FTIR, attenuated total reflection Fourier transform infrared; CFU, colony-forming unit; CD, circular dichroism; CL, cardiolipin; DCP, dicetylphosphate; DOPC, 1, 2-dioleoyl-*sn*-glycero-3-phosphocholine; DOPG, 1, 2-dioleoyl-*sn*-glycero-3- phospho-(1′-*rac*-glycerol); GUV, giant unilamellar vesicle; ITC, isothermal titration calorimetry; LUV, large unilamellar vesicle; MD, molecular dynamics; MIC, minimal inhibitory concentration; NMR, nuclear magnetic resonance; PC, phosphatidylcholine; PE, phosphatidylethanolamine; PG, phosphatidylglycerol; PS, phosphatidylserine; POPC, 1-palmitoyl-2-oleoyl-*sn*-glycero-3-phosphocholine; POPE, 1-palmitoyl-2-oleoyl-*sn*-glycero-3-phosphoethanolamine; POPG, 1-palmitoyl-2-oleoyl -*sn*-glycero-3- phospho-(1′-*rac*-glycerol); POPS, 1-palmitoyl-2-oleoyl-*sn*-glycero-3-phosphoserine; SMART, Soft Membranes Adapt and Respond, also Transiently; TM, transmembrane.

TABLE 1 | Amino acid sequences of selected antimicrobial peptides.

Magainin 1	GIGKF LHSAG KFGKA FVGEI MKS
Magainin 2	GIGKF LHSAK KFGKA FVGEI MNS
PGLa	GMASK AGAIA GKIAK VALKA L-NH_2
LAH4	KKALL ALALH HLAHL ALHLA LALKK A-NH_2
LL37	LLGDF FRKSK EKIGK EFKRI VQRIK DFLRN LVPRT ES
Cecropin P1	SWLSK TAKKL ENSAK KRISE GIAIA IQGGP R
Cecropin A	KWKLF KKIEK VGQNI RDGII KAGPA VAVVG QATQI AK-NH_2
Melittin	GIGAV LKVLT TGLPA LISWI KRKRQ Q-NH_2

Magainins and related sequences have been developed up to phase IIb/III clinical trials (61, 62), and in parallel, have been explored in considerable detail by biophysical approaches [e.g., (63–66)]. The data from these studies were often unexpected and resulted in the need to introduce novel mechanisms to explain the activities of these peptides (67–69). Because the peptides and/or their biophysical investigations have been reviewed recently (20, 21, 70), this paper will only shortly summarize some of the key discoveries made with magainins and then focus on the synergistic interactions between PGLa and magainins. Combining antimicrobial peptides provides an interesting and little exploited alternative strategy to enhance their efficiency and to further reduce their susceptibility to bacterial resistance.

MAGAININS FORM MEMBRANE OPENINGS

Magainins exhibit pore-forming and lytic activities when added to membranes which have also been studied by single-channel measurements (45, 71). On a macroscopic scale, magainin pore formation was investigated by fluorophore release experiments. For example, this allowed to measure the release kinetics from individual DOPC/DOPG giant unilamellar vesicles (GUV) at different peptide-to-lipid molar ratios (72). While after peptide addition it takes minutes before the release of fluorophores sets-in, once the pores have formed the micrometer vesicles empty within 30 s (73). It has been measured that fluorophore release is a two-stage process starting with the transient formation of very large pores corresponding to the equilibration of the peptide concentration between the outer and inner leaflets (74). Thereafter a slower but persistent release of fluorophore is observed through pores of 3 nm hydrodynamic radius, large enough to allow passage of globular proteins > 20 kDa (74).

The spatio-temporal events when antimicrobial peptides attach to live bacteria have been investigated by microscopic imaging techniques. Interestingly, the human peptide LL37 (**Table 1**) preferentially attacks septating *E. coli* cells at the septum and at the curved regions of the outer membrane (75). In non-septating cells, the peptide accumulates at one of the endcaps. As expected permeabilization starts with the outer membrane and after a short delay cytoplasmic membrane permeabilization occurs. The openings at both membranes occur in a localized and persistent manner (76). Related events are observed when

cationic polymers, longer or shorter peptides such as LL37, cecropin A, or melittin are studied (**Table 1**) even though the exact details vary with the antimicrobial compound (77). Finally, the peptides enter the cells where they interact with anionic polymers including nucleic acids and proteins that are abundant in the cell interior (46, 48, 78).

MAGAININ STRUCTURAL INVESTIGATIONS

Structural investigations show that magainins undergo a random coil to helix transition when they partition into the membrane (79). Interestingly the energies associated with this refolding have been identified to be one of the main driving forces for membrane association (80). During the same time period when the antimicrobial activity of magainins was investigated solid-state NMR approaches applied to uniaxially oriented lipid bilayers were under development (63). The latter technique measures angular constraints from polypeptides reconstituted into uniaxially oriented phospholipid bilayers to calculate their structure, topology, and dynamics (81–84). Because the ^{15}N chemical shift of peptide bonds alone already provides an approximate tilt angle of helical domains (85) the very first experiments with magainin 2 and PGLa were indicative that these helices are oriented parallel to the membrane surface (63, 86–88). A membrane alignment parallel to the lipid bilayer surface has been confirmed for magainin 2 (89), for magainin analogs (90, 91) and for several other linear cationic antimicrobial peptides (22, 92–95). Later on oriented CD spectra and fluorescence quenching experiments confirmed such a topology of the magainin helix where the latter approach also shows an interfacial localization of the magainin 2 helix (64, 96). A parallel alignment of cecropin P1 (**Table 1**) using ATR FTIR was later on described by the "carpet model" (97). Notably, this peripheral membrane topology assures that the peptides can exchange between the membrane and the aqueous phase (89).

Whereas, the magainin 2 helix has been found to partition into the membrane parallel to its surface regardless of membrane lipid composition (64, 89), its relative PGLa (**Table 1**) exhibits a much wider range of topologies but only in membranes where all fatty acyl chains are saturated (89, 98, 99). In the presence of magainin 2 PGLa adopts transmembrane alignments (98–101) and early on this configuration has been suggested to be part of a synergistic complex between the two peptides (100, 102). However, in the presence of lipid unsaturations (such as palmitoyl-oleoyl-phosphatidylethanolamine), both PGLa and magainin 2 are aligned along the bilayer surface under all conditions so far investigated (98, 99, 101). Because unsaturations are an integral part of bacterial membranes it is highly likely that both magainin and PGLa exert their antimicrobial activity in a state with their amphipathic helices aligned within the membrane plane [e.g., data obtained with membranes made from *E. coli* lipid extracts (103)]. Correspondingly, alternative models explaining synergism have been suggested (69, 103) (**Figure 1**).

Notably, recent fluorescence self-quenching investigations have demonstrated the formation of nematic phases at the membrane surface by magainin, PGLa, and the LAH4 amphipathic designer peptide (**Figure 1**, **Table 1**). Formation of these supramolecular arrangements is dependent on the lipid composition and the salt concentration of the surrounding buffer suggesting that electrostatic but also lipophobic interactions contribute (69, 104).

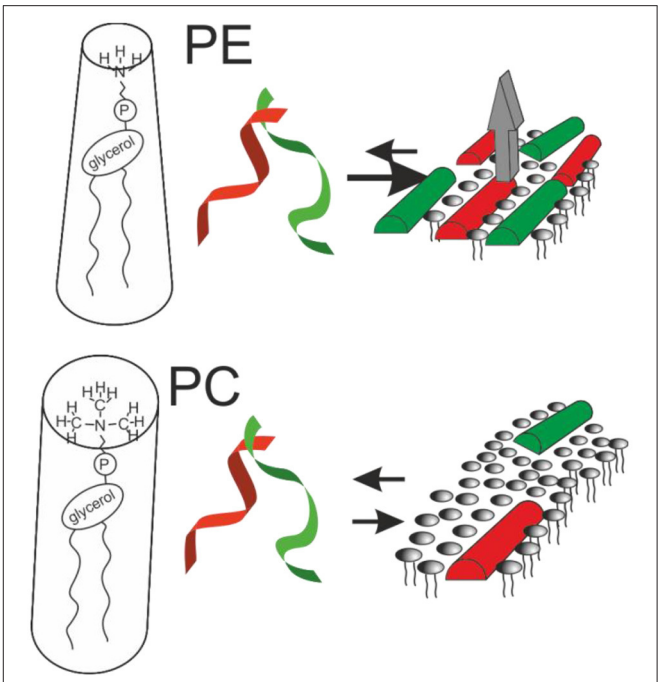

FIGURE 1 | Sketches the structural findings made with magainin 2 (red) and PGLa (green). Both peptides adopt helical conformations that are oriented parallel to the membrane surface in membranes carrying lipid unsaturations. The peptides arrange in nematic mesophases which when added together result in increased membrane affinity and synergistic calcein release activity from POPE-containing liposomes (gray arrow; cf. text for details).

An amphipathic peptide that partitions into the membrane interface takes up the place of a few lipids but penetrates only to the depth of the head group and glycerol region (64). Thereby the packing of the hydrophobic region becomes more disordered and the membrane thickness is reduced (105, 106). The resulting changes of the macroscopic phase properties, the bilayer packing and the dynamics of the lipids has been monitored by ^{2}H and ^{31}P solid-state NMR spectroscopy (107). Thereby magainin peptides have been shown to introduce curvature into membranes (106), to cause a considerable decreases in the fatty acyl chain order parameters in particular of lipid segments well into the bilayer interior (101, 108–110), and at higher peptide concentrations membrane disruption into micellar or bicellar structures (111). Such bilayer disordering has been estimated to reach over a diameter of 10 nm (112, 113).

Atomistic views how in-plane oriented peptides potentially form water-filled openings in lipid bilayers have been obtained from molecular dynamics simulations (114–116). A reoccurring limitation of the computational approaches is the limited time span covered by the simulations which does not allow

to reach equilibrium of statistically relevant numbers or peptides. Therefore, at the present stage the results remain dependent on the starting conditions and careful comparison with experimental data an important control (115–117). Furthermore, for magainins the importance of the very details of the lipid composition has only become apparent about a decade ago (69, 98, 118, 119), therefore, only few such simulations have been performed with lipid compositions such as POPE/POPG 3/1 that closely mimic bacterial membranes. All-atom simulations covering 100 ns show a stable in-plane topology of magainin, some oligomerization, but no pore or supramolecular rearrangement within this time frame (120). Stable in-plane alignments and an interfacial localization in such membranes were also observed in more recent coarse-grain and all-atom simulations (116, 117). In summary, pores rather form through stochastic rearrangements of peptides and lipids rather than well-defined channel structures although some peptide-peptide interactions are sometimes apparent. Because of the relatively small size of the membrane patches and the short time frame covered by the simulations the membrane lytic nature of the peptides or the formation of large pores apparent in dye release experiments do not become visible (73, 74).

The molecular shape concept provides a rationale for the bilayer disruptive properties of in-plane aligned amphipathic helices partitioning into the interface (121, 122). Geometrical considerations originally developed for lipids explain why PC lipids, that have the shape of cylinders, spontaneously arrange into extended bilayers. In contrast, PE exhibits a cone shape with a tendency to adopt hexagonal phases and detergents are inverted cones that arrange into micelles. In an analogous manner, surfactin, a cyclic peptide with a long fatty acyl chain (55), or the magainin 2 in-planar interfacial helix use up much more space in the head group than in the hydrophobic core region of the membrane, therefore, the molecular shape concept has recently been elaborated in some detail for amphipathic antimicrobial peptides (122).

Thus, magainins and other cationic amphipathic antimicrobial peptides appear to fulfill the criteria of the "carpet" model where peptides cover the membrane surface at alignments parallel to the surface (67) ultimately causing membrane lysis (111, 123). At lower peptide-to-lipid ratios the lipid membranes can adapt and compensate for the disruptive properties of the peptides, however from time to time openings form locally and transiently thereby resulting in channel-like recordings (124). The structural changes of the membrane have been monitored in the presence of magainin 2 in real-time revealing intermediate states, lysis and recovery (125). The peptides and lipids show a high degree of structural plasticity thus membranes can adopt a broad range of possible morphologies a behavior that is best described by phase diagrams which can take into account the peptide concentration, the membrane composition and other parameters (126). Such features are summarized in the SMART model where "Soft Membranes Adapt and Respond, also Transiently" (127). In line with this model, AMPs have been proposed to affect the membrane line tension (125, 128).

Magainin and PGLa carry several positive charges (nominal charge +4 to +5) and have been shown to interact better with negatively charged membranes. Such preferential association driven by electrostatic attraction is thought to be a reason for the selective killing of bacteria or tumor cells, that expose negative charges while they do not affect healthy eukaryotic cells which expose an overall charge neutral surface (129–133). Indeed, Joachim Seelig and co-workers have quantitatively dissected the interactions of membrane-association into an attractive electrostatic component and a hydrophobic insertion (with a partitioning constant around of the latter of 1,000 M^{-1}) (130, 134). Notably, the apparent membrane association is more than an order of magnitude increased for bilayers mimicking the overall anionic composition of bacterial membranes (66). However, this relatively modest membrane association is boosted by electrostatic attraction to negatively charged surfaces which can dominate the association process (122, 135). Furthermore, the membrane association of multicationic antimicrobial peptides has been suggested to result in the interference of electrostatic attractions that keep peripheral membrane proteins in place and consequently antimicrobial action (68).

MAGAININ 2—PGLa MIXTURES SHOW SYNERGISTIC ENHANCEMENT IN BIOLOGICAL ASSAYS

Interestingly combinations of antimicrobial compounds are sometimes much more potent than the individual components (49, 136). These observations have been made with mixtures of peptides (137), of peptides with conventional antibiotics (41, 138–142), with blood plasma components (143), or with ions (144). In particular magainin 2 has been shown to interact synergistically with PGLa (45) and with tachyplesin I a cyclic β-sheet peptide (145).

Because magainin and PGLa peptides (**Table 1**) are produced together and stored as a cocktail in the skin of *Xenopus laevis* frogs, very early on antimicrobial assays have been performed with mixtures of the two peptides. It was soon realized that the peptides exert cooperative behavior (26, 44, 45, 146, 147). These studies involved *E. coli* (24, 26, 43, 148), mitochondria (43), tumor cells (26), calcein loaded liposomes (26, 45), cytochrome oxidase liposomes (24), and hamster spermatozoa (44). Notably, in the latter case only the mixture exhibits detectable activity at all. More recent papers also report synergism of magainin and PGLa on a few selected bacterial species (*E. coli, S. aureus,* and *S. epidermis*) with somehow varying enhancement factors (102, 103, 119, 149).

In particular, the early investigations revealed the poration of membranes, loss of membrane potential, uncoupling of membranes concomitant with effects on respiratory control and thereby interference with energy production and cell survival [e.g., (26, 44, 45, 146)]. In a most recent investigation it was shown that both PGLa and magainin are capable to form fibers at physiological conditions (150). These fibers are somewhat less active in antimicrobial assays but maintain the synergy. Because the peptides are stored in the granules of the frog skin at

high concentrations it was speculated that they form functional amyloids for protease protection and graded release (150).

In further studies these investigations have been extended to variants of the peptides and/or other bacteria and the combination index CI has been used as a quantitative measure of synergism (103, 151):

$$CI = \frac{0.5\ MIC_{50}^{a+b}}{MIC_{50}^{a}} + \frac{0.5\ MIC_{50}^{a+b}}{MIC_{50}^{b}}, \quad (1)$$

where MIC^{i} is the MIC value determined for peptide i alone (i = a or b), and MIC^{a+b} is the total peptide concentration at the MIC determined for the combination. For values < 1 synergistic enhancement occurs whereas values > 1 correspond to antagonism (152). In other work the fractional inhibitory concentration index (FICI) has been used which follows a related definition (102).

In order to analyze bacterial growth curves in a quantitative manner, we have early on started to fit the dose-dependence curves to sigmoidal functions of the type:

$$G_{(c_p)} = \frac{G_{\max}}{1 + \left(\frac{c_p}{MIC_{50}}\right)^{m}} \quad (2)$$

where c_p is the peptide concentration, G is the growth, m the slope, and G_{max} is the maximal growth of the bacteria. In a subsequent step the additive curves (CI = 1) are simulated, which can then be compared to the observed dose-dependent bacterial killing when both peptides are present in the mixture (103). Notably during the transition, the normalized bacterial density (y-axis) is particularly sensitive to even small changes in peptide concentration. Because of the steep dependence of bacterial growth on peptide concentration a small error in peptide concentration (along the x-axis) translates into a pronounced standard deviation when the growth is measured in replicates [i.e., a big error bar in y-axis; cf. (103)].

Whereas, in case of a steep dose-response the slope *m* of the sigmoidal cannot be calculated from a 2-fold dilution series and was initially chosen arbitrarily (103) it turns out that this cooperativity index bears additional information of interest once more data points around the MIC_{50} reveal interesting differences between the peptides. **Figure 2** and **Table 2** present so far unpublished data and a more elaborate scheme for the investigation of antimicrobial activities and synergism. Instead of the often applied 2-fold dilution series more data points are included (1.5 dilution series) thus revealing the slope m of the transition.

Four individual dilution series were fitted to Equation (2), from which averages for the MIC_{50}, the slope *m,* and G_{max} were calculated and these were used to calculate the fits represented by the continuous lines in blue, red, and green.

It has been shown that at sub-MIC only a fraction of bacteria is killed and their debris including anionic polymers from the cell interior neutralizes much of the peptide added (153, 154). As a consequence, with some delay the survivors catch up in such laboratory suspensions and may reach the full cell density (151). Given the complete coverage of bacteria with peptides at the cell densities used in standardized antimicrobial activity assays, it is unlikely that the fractional killing is due to statistical variations in peptide density. Therefore, it has been suggested that fractional killing is a consequence of phenotypic variations of single cells which makes them more or less susceptible to the antibacterial activity of AMPs (153). The same authors have estimated that under sub-MIC conditions shortly after peptide addition a relatively small number of bacteria persists in a well thus such fluctuations potentially become apparent.

Therefore, in the experiments shown in **Figures 2**, **3** the incubation of bacteria after addition of peptide was kept to 18 h which prevents that bacteria that are delayed in their growth by the peptides can catch up to full density. It is also interesting to note that the values $G_{max} > 1$ indicate that at low peptide concentrations and low to standard inoculum ($<10^6$ CFU/mL) addition of peptide stimulates the bacterial growth.

Interestingly the slope *m* in the presence of PGLa is different from that of magainin (**Figure 2**). Most strikingly for the synergistic mixture the onset of activity is not that different but it has the deepest slope which brings the MIC_{100} from about 10 μM for the individual peptides to about 1 μM for the mixture. This 10-fold synergistic enhancement when the MIC_{100} is taken as an indicator decreases to a factor of 2.3 when the 50% killing is taken into consideration, i.e., the midpoint of the transition (**Figure 2**). Thus, a quantitative evaluation of synergy not only depends on the detailed experimental conditions but also the very details of how bacterial killing or growth are evaluated.

Because near the MIC_{50} only a fraction of the bacteria is killed the survivors are selected and take over, which may cause resistance development (153). It has been suggested that AMPs have a high Hill coefficient which explains why bacteria are less prone to develop resistance development (23). Here we show that the synergistic magainin 2/PGLa mixture exhibits even steeper slopes and hence adds an additional advantage (**Figures 2**, **3**). It is possible that because the peptides affect bacterial subpopulations differently, there are less survivors that can fill the gap. The data also suggest that at least part of what is considered the synergistic interaction between the peptides is related to the steeper slope of the dose-response.

In a general sense *m* means some sort of cooperative or anti-cooperative behavior (i.e., non-linearity) (155) and in the case of a cooperative coefficient indicates that more than one molecule is required for a given activity. This can happen through oligomerization, but it could also mean that several peptides have to come into proximity on the bacterial surface (79), or that they form loosely packed lipid-peptide supramolecular structures (69). On the other hand, the slope of the curve can flatten should aggregation occur in solution at high peptide concentrations.

When the cell density is increased the MIC_{50} increases (**Figures 3D–F**, so far unpublished data). This is well-known phenomenon and has been associated with peptide adsorption to cell debris including anionic biopolymers and membranes (153, 156). Furthermore, cooperativity, especially of PGLa is reduced when the CFU per ml are increased. This probably reflects a larger phenotypic variability of cells with differences

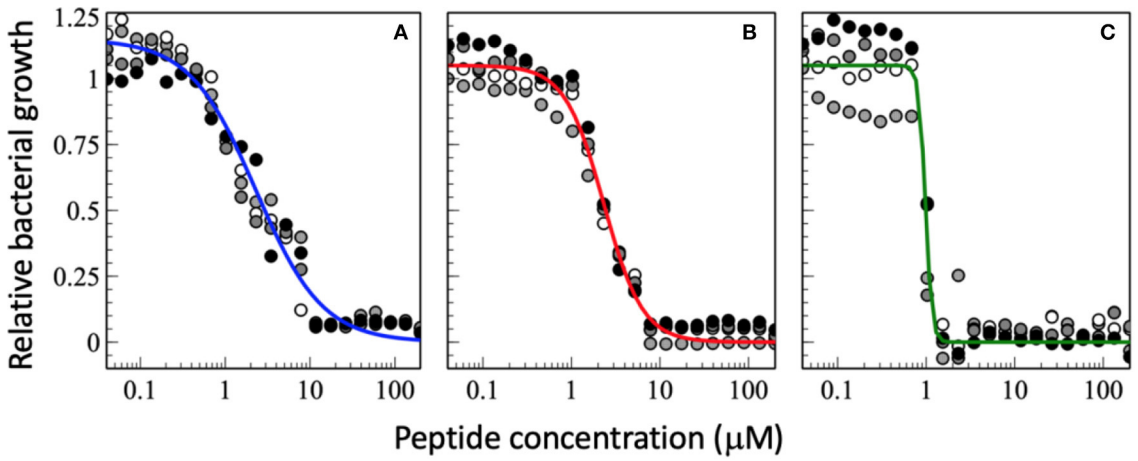

FIGURE 2 | Dose-response curve of relative bacterial growth in the presence of **(A)** magainin 2a, **(B)** PGLa, and **(C)** the equimolar mixture of both. Bacterial supensions in MH medium (8.3 x 10^5 CFU/mL) are added to a serial dilution of peptides and the optical density at 600 nm is recorderd after an 18 h inclubation at 37°C. The experiments were performed on 96-well microplates (F-bottom sterile non-treated polystyrene, Thermo Scientific Nunc A/S, Roskilde, Denmark). Starting from a 200 μM peptide concentration a sequential dilution series was performed with a dilution factor of 1.5 in 22 steps yielding final peptide concentrations ranging from 200 to 0.040 μM (after addition of bacteria). Each condition was done in quadruplet and each experiment is represented by different symbols in the plots (i.e., white, gray, and black circles represent a different experiment). The sequential dilution series were normalized to the bacterial growth without treatment on the same plate. The data shown have not been published before.

TABLE 2 | This table shows the fit parameters of the blue, red, and green curves of **Figure 2**.

Peptide	MIC_{50} (mM)	m	G_{max}
magainin 2a	2.31 ± 0.52	1.11 ± 0.10	1.15 ± 0.07
PGLa	2.32 ± 0.04	1.98 ± 0.09	1.05 ± 0.06
mix (1:1)	0.98 ± 0.05	11.8 ± 5.3	1.06 ± 0.12

The data shown have not been published before.

in AMP susceptibility (153). Furthermore, the synergy factor obtained by comparing the MIC_{50} values increases to 4.8 whereas it remains around 10 when the MIC_{100} are considered. Because at very high inoculum the peptides distribute on many more cells it may be more difficult to reach a high enough density to kill (154, 157, 158). Thereby, one may speculate that at high cell density the increased binding affinity and the mesophase structures when the two peptides are added conjointly (69) help to reestablish local hot spots and synergy. In this context it is noteworthy that the peptides have been shown to redistribute unevenly on the bacterial surface (159). Alternatively, it may also be possible that at high cell densities the ratio of surviving subpopulations increases thus it is easier to replenish the bacteria killed by a single antibiotic. This phenomenon would be less apparent when the combined action of two peptides keeps killing a large fraction of bacteria. Clearly, more experiments are needed to elaborate on these observations.

Interestingly, the best MICs are in the 1 μM range which agrees with observations made previously (103). As a consequence the synergistic factor is usually small for peptides that exhibit already high antimicrobial activity when investigated alone (103). This is also observed for the experimental series at a low CFU of 1.46 x 10^2 CFU/mL where the synergy factor by comparing the MIC_{50} is 1.7 but again higher for the MIC_{100} (**Figures 3A–C**, so far unpublished data). However, it was recently pointed out that peptides also stick to surfaces of the test equipment thus the available concentration is probably significantly lower especially at low peptide concentrations (158).

MAGAININ 2—PGLa MIXTURES SHOW SYNERGISTIC ENHANCEMENT IN MODEL MEMBRANES

Such synergistic enhancements in antibacterial assays can occur through specific interactions (49, 160) but also when one compound helps the antimicrobial effector to reach its target (161). Thereby the PGLa/magainin 2 case is of particular interest because it works in pure lipid model membranes where the mode of action can be studied in biophysical detail (26, 119, 122, 162, 163). When the release of fluorophores from liposomal preparations was investigated these were made of well-defined lipid compositions thus revealing interesting lipid dependences.

First of all negative charges are important to assure a high local peptide concentration close to the membrane surface and thereby and increased membrane association (130, 134). Whereas, in the absence of negatively charged lipids the membrane partitioning coefficients of AMPs are in the 10^3 M^{-1} range they apparently increase by more than an order of magnitude due to negative membrane surface charges (66). In some cases the association of antimicrobial peptides seems solely driven by electrostatic attraction until charge compensation is achieved (122, 135). This observation explains the lack of

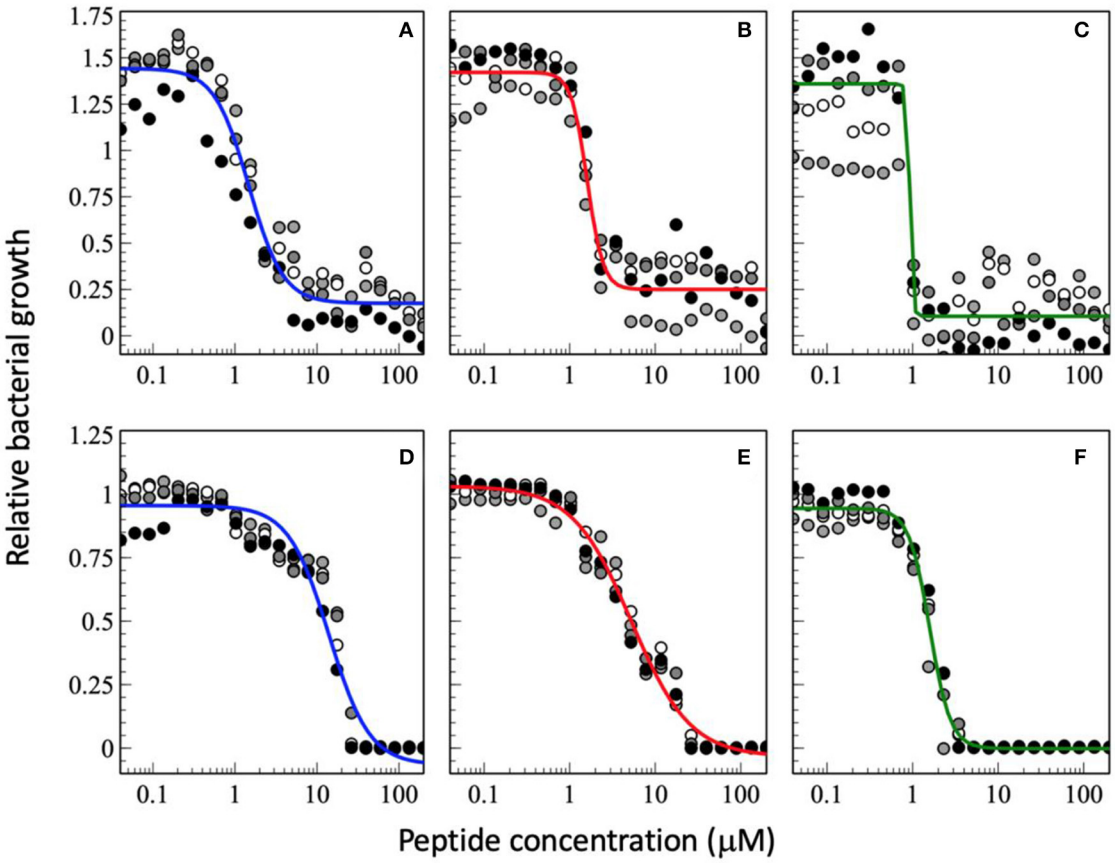

FIGURE 3 | Dose-response curve of relative bacterial growth in the presence of antimicrobial peptides as a function of inocculum. The peptides were added to a bacterial supension in MH medium at low inocculum of 1.46 x 10^2 CFU/mL **(A–C)** or at high inocculum at 1.51 x 10^7 CFU/mL **(D–F)** and the optical density at 600 nm recorderd after an 18 h inclubation at 37°C. The peptides tested are magainin 2 **(A,D)**, PGLa **(B,E),** and the equimolar mixture of both **(C,F)**. The experimental conditions are those of **Figure 2**. The data shown have not been published before.

structuration when the peptides were investigated by optical techniques in dilute suspension of zwitterionic liposomes (122, 164). Electrostatic effects also contribute to their selectivity in killing of bacteria which exhibit a negative surface over healthy eukaryotic cells which appear electrically neutral to the outside (129–133). Therefore, when association and pore formation to zwitterionic membranes is very low the peptides may be too dilute in the membrane to interact with each other (119).

When fluorophore release and peptide synergy are investigated in a P/L ratio-dependent manner it becomes clear that a quantitative evaluation of synergy also depends on the detailed conditions of the experiment (**Figure 4**). For example, inspection of **Figure 4B** shows the absence of synergy at low peptide concentrations, but this value continuously increases at $\geq$0.4 μM. Notably either the amount of leakage after a few minutes (102, 119, 162) or the initial leakage rate (45, 163) have been taken as indicators of synergy.

From a combination of fluorescence-based biophysical experiments Matsuzaki and co-workers suggested early on that the rate of pore formation is slower for magainin, but the openings are more stable than those of PGLa (162). Thereby, synergism arises from fast pore formation and moderate stability. A more recent paper by Heerklotz and co-workers suggests that the combination of making large enough pores that are well distributed among the liposomes causes synergism in vesicle dye release experiments (165). According to these models the size of the vesicles or of the bacterial cells and the heterogeneity of the peptide distribution have an effect on the observed synergism (165).

ON DEFINITIONS TO QUANTITATIVELY DEFINE SYNERGISTIC ACTIVITY

A quantitative comparison of synergistic enhancement is further complicated not only due to differences in the experimental systems investigated but also by the different definitions used to quantitatively compare the activities of the mixture and individual peptide solutions. For example, Matsuzaki and co-workers compare the P/L ratio where 50% of the dye is released (162): $= \frac{\frac{P}{L_{50,\ calculated}}}{\frac{P}{L_{50,\ observed}}}$.

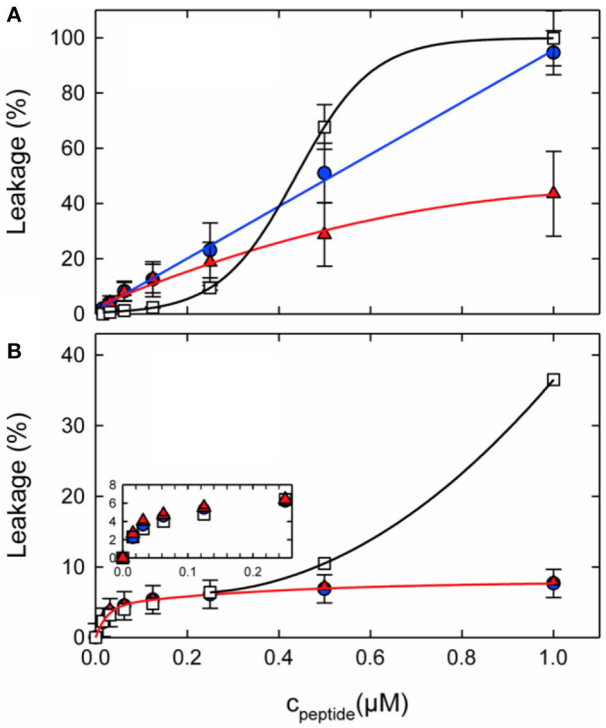

FIGURE 4 | Calcein leakage from 100 nm unilamellar vesicles made from **(A)** POPC/POPG (3:1 mol/mol) or **(B)** POPE/POPG (3:1 mol/mol) as a function of peptide concentration. L18W-PGLa (blue circles), magainin 2a (red triangles), or their equimolar mixture (open squares) were added to 50 μM lipid. The lines were added to guide the eye. Taken from Leber et al. (119).

In this definition the calculated values are the average of the P/L_{50} ratios obtained from the individual peptides. This approach is similar to the calculated MICs published by Glattard et al. (103).

In contrast, rather than comparing the peptide concentration needed to reach a defined functional activity (e.g., 50% leakage) Zerweck et al. use the (variable) leakage values (L) at a fixed 100 μM lipid concentration and a fixed P/L. Typically conditions are chosen where a good range of activities is observed (i.e., 3 μM peptide for PE/PG/CL 72/23/5 and 0.6 μM for PC/PG 3/1). From this data a synergy factor is calculated according to $SF = \frac{L_{(P+M)}}{L_{(P)}+L_{(M)}}$.

Furthermore, from the same team the P/L of the mixture was twice that of the individual peptides in one publication (102) but kept constant in a prior paper (163). Finally, Leber et al. use "Peptide Synergy" $\Sigma = 1/SF$ at the "highest peptide concentration" (cf. **Figure 4** showing data up to 1 μM) and 50 μM lipid (119). The total peptide concentration when peptides are tested individually is half of that of the mixture. This definition of synergy is based on the assumption that a heterodimer complex forms (G. Pabst, personal communication). While all of these definitions have their justification comparing the data quantitatively becomes impossible. For example, for PE-rich membranes the values include Σ =0.4 (corresponding to SF=2.5) (119) and SF = 22 (102). Furthermore, the PGLa-driven calcein release from PC/PE/PS 2:5:3 vesicles requires 25 to 43-fold less PGLa when 3.7 μM magainin are present (50 μg/ml lipid in 0.5 M NaCl, 10 mM PIPES, pH 7) (164). At this concentration magainin exhibits no activity when added alone (164).

CORRELATING SYNERGISM WITH STRUCTURAL INVESTIGATIONS AND LIPID COMPOSITION

Structural investigations were performed to develop a model how the peptides interact and thereby enhance their antimicrobial/pore-forming activities. When studied by solid-state NMR methods PGLa and magainin are both aligned along the surface of membranes when these carry at least one unsaturation per phospholipid (98, 99, 116, 166), including *E. coli* lipid extracts (103). Thus, in such membranes the helix topology resembles those of magainin or PGLa alone, i.e., in the absence of the other peptide (89, 98). In contrast, when magainin 2/PGLa mixtures are studied in fully saturated lipid bilayers magainin remains oriented along the membrane surface whereas PGLa adopts transmembrane alignments (98, 99). However, it should be noted that unsaturations are abundant in biological membranes thus a mechanism for synergistic antibacterial activities should consider an alignment of both peptides along the bilayer surface (98, 101, 103).

Not only the lipid fatty acyl chain but also the lipid head group composition seems of considerable importance for the synergistic enhancement to develop. Notably, in recent investigations it was demonstrated that for lipids with intrinsic negative curvature such as PE or PC/cholesterol the pore forming activity of the individual peptides is reduced when compared to PC/PG membranes. However, much of the activity was restored when adding the peptide mixture. This behavior results in a significant synergetic enhancement of activities in PE/PG but not in PC/PG membranes (**Figure 4**). In this context it should be noted that the antimicrobial activities of PGLa or magainin individually are much lower in PE/PG than in PC/PG, thereby synergetic enhancement in the bacterial membrane mimetic abolishes the differences observed for the individual peptides when investigated in membranes of different composition (cf. **Figure 4** at 1 μM). This agrees with observations made when the antimicrobial activity of magainin and PGLa as well as derivatives thereof were investigated and the highest synergy was observed for peptides with intrinsically low activities (103).

Notably, a fluorescence quenching investigation has revealed the formation of mesophase structures along the membrane surface and correlated diffusion of both peptides (69). Fluorescence quenching occurs when the fluorophores, which were added to the amino-terminus of either magainin 2 or PGLa, approach each other within the nm range, i.e., closer than expected from a statistical distribution (104). These experimental observations are in-line with a recently published MD simulation of the peptide mixture where in stacked membranes a string of interacting peptides and lipids has been observed (117). Interestingly, the observed mesophases and diffusion correlation come along with a much increased membrane partitioning of the

peptides when the mixture is investigated in PE/PG but not in the presence of PC/PG membranes (69). Because the membrane disruptive properties of magainin 2 extends over several layers of lipids (ca 0.8 nm in diameter) (112, 113) the formation of mesophases with interpeptide distances < 1 nm (104) suggests a concerted action of several peptides in destabilizing the membrane (69). In this context is it interesting that microscopic imaging approaches have revealed an uneven distribution of antimicrobial peptides with preferential association with curved regions of the bacterial membrane such as pole caps or the septum of dividing cells (47, 77).

During early work on magainin/PGLa synergism little attention was given to the lipid compositions of the model systems investigated. With new data pointing to important effects of lipids exhibiting intrinsic negative membrane curvature it is of interest to review earlier publications. Indeed, the very early investigations were performed in PC/dicetylphosphate membranes of different (PC/DCA ratios) where dicetylphosphate is a small negatively charged "head group" made of phosphate carrying two C16 chains (26, 45). Thus, in a lipid membrane the molecule exhibits an inverted cone shape which is associated with negative curvature [cf. (122)]. Furthermore, experiments were performed with azolectin a soy bean lipid mixture which contains PC, PE, and PIs (45). Synergistic enhancements of fluorophore release were also observed with BBPS or egg-PC membranes (162), and thereby do not seem to fit the requirements of negative curvature observed by Leber et al. (119). However, it should be noted that the synergy factors published in this work are only 3.5 and thereby relatively low when compared to the antibacterial tests presented in the same paper where a factor of 8 was observed (162). For EYPC very high P/L ratios of 0.57, 0.14, and 0.05, respectively, were required to measure the S value. Thereby, although typically 100 nm vesicles are used for most of the dye release experiments (102, 119, 162) the detailed conditions are otherwise quite different and the values may not easily be compared, in particular as the dose response curves are not linear (**Figure 4**).

BIOPHYSICAL MEASUREMENTS OF PGLa—MAGAININ INTERACTIONS IN MEMBRANES

Spectral changes that occur upon membrane partitioning can be used to derive membrane association constants of polypeptides (69, 135, 167, 168). From such data the interaction between the membrane associated peptides can be derived including quantitative estimates of the energies involved. However, these values are only valid in the context of an assumed molecular model. In this manner favorable PGLa-magainin interaction energies were obtained in egg-PG membranes (162). Notably the quantitative evaluation of the data depends how many peptides are assumed to be involved in the interaction process. Energies for homo- and hetero-dimer formation have also been published for fully saturated membranes where PGLa exhibits a transition into the TM state (163). Therefore, this analysis probably includes many energy contributions (101, 169) which remain unimportant when synergy occurs between peptides that reside along the membrane surface of a bacterial membrane (103).

In a more recent investigation association of the two peptides with LUVs made of POPE/POPG 3/1 at pH 7 as a bacterial membrane mimetic were investigated by Isothermal Titration Calorimetry (ITC) (70) indicating strong membrane association with apparent membrane association constants in the 10^6 M^{-1} range (apparent stoichiometry P/L $\approx$ 1.7 mole%). Whereas, the membrane association of magainin and PGLa is characterized by an endothermic reaction enthalpy an additional exothermic contribution becomes apparent when the peptide mixture is titrated. Thus, these ITC data reveal an additional model-independent ΔH in the range of -2 kcal/mole in the magainin 2/PGLa mixture when compared to the peptides individually. This reaction enthalpy could be due to e.g., vesicle agglutination as observed by DLS experiments conducted on the same system (70). Peptide-driven intermembrane interactions were also apparent by a reduction in the bilayer repeat distance of mechanically oriented membranes (110, 117). Furthermore, the formation of loosely packed supramolecular assemblies also contributes to an energetic contribution in particular as these have been shown to correlate with an order of magnitude increased membrane affinity in the presence of POPE/POPG (69). Notably, when the proximity and thereby the interactions between magainin 2 and PGLa when associated to POPE/POPG 3/1 or POPC/POPS 3/1 membranes was tested by fluorescence spectroscopy a FRET effect was observed at high P/L ratios where close encounters of the peptides happen statistically (170). However, this effect diminishes and disappears when diluting the peptide with more lipid indicating that possible interactions between the peptides are rather weak.

SEQUENCE SPECIFICITY OF MAGAININ 2—PGLa SYNERGY

In order to define key structural elements of the synergistic interactions and residues that may be involved in the magainin 2—PGLa interactions the peptide sequences have been modified and tested. When the F16W or E19Q modifications of magainin 2 were studied for fluorophore release from egg PC/PG (1:1) liposomes a reduced synergistic activity was observed whereas the F5W alteration did not exhibit any effect (162). Introducing a positive charge at position 19 much abolished the synergistic interactions (102). In contrast, neutralizing the magainin 2 carboxyterminus by amidation has no effect on its synergism with PGLa (102, 103, 170, 171) although the antimicrobial activity of the peptide is increased (171, 172). Similar observations were made with the hydrophobic face of the magainin 2 helix (173).

Furthermore, when PGLa is modified the synergistic activity with magainin 2 is maintained even when a proline is added to the N-terminus and a negative charge to the C-terminus of PGL (171). When key residues of PGLa were searched exchanging the positive charges of lysines 15 and 19 by glutamines abolish synergistic enhancement whereas a more moderate reduction is measured for K5E and K12E (102) and L18W is tolerated (119, 162).

Such potential electrostatic interactions between the membrane-associated peptides have been suggested early on and are visualized in coarse grain and all-atom MD simulations even though the membranes used in the older simulations do not fulfill the criteria of a physiological composition (116, 117, 174, 175).

Furthermore, residues G7, G11, and L18 of PGLa have been shown important (102). Glycines 7 and 11 form a GxxxG motif which has been suggested to promote dimerization in highly apolar environments (176). However, the PGLa localization at the membrane interface (98, 103) may not be suitable for stable PGLa homodimer interactions. A detailed structural analysis of the peptide mixture in a lipid bilayer is required to resolve such ambiguities. In summary, the charges located at the carboxyterminal ends of the peptides have the strongest effects on synergy and an important role was also associated with G7, G11, and L18 of PGLa which needs further investigation.

LESSONS LEARNED FROM PEPTIDE DIMERS

In previous publications the question how the oligomerization of peptides along the membrane surface influences activity was already discussed (122, 177). In the context of models proposed for the mechanisms of synergistic enhancement the comparison with covalently linked dimers is also of interest. Therefore, in a first step possible interactions between membrane-associated PGLa and magainin 2 were tested by preparing peptides carrying GGC extensions and cross linking experiments (178). In PC/PG (1/1) bilayers parallel dimers preferentially form (178), therefore, dimers linked through C-terminal GGC extensions were prepared and investigated. When compared to the same amount of unmodified peptides in a mixture all of, the (PGLa-GGC)$_2$ and (magainin-GGC)$_2$ homodimers as well as the magainin-GGC/PGLa-GGC heterodimer were all more active in calcein release experiments from POPE/POPG 3/1 liposomes (119). However, only the PGLa-homodimer and the PGLa-magainin heterodimer, but not the individual peptides or their mixture, showed significant dye release from POPC/Cholesterol 3/1 liposomes (119). When the antimicrobial activities of the wildtype magainin/PGLa mixture and the dimer of the GCC-derivatives are compared to each other a complication arises from the fact that the GGC extensions itself make the monomeric peptides more active (103, 149). Furthermore, a dimer linked through a carboxyterminal lysine extension was considerably more active than the monomer whereas the amino-terminal linkage through glutamic acid has no effect (179).

Furthermore, a cystine-linked magainin 2 dimer has been shown more active in membrane permeabilization and antimicrobial activities (180). From the ensemble of data it seems that the increased activity of the dimers is based on an increased membrane perturbation by the larger peptide aggregates rather than due to a particular structure of the PGLa-magainin 2 dimer (122, 180, 181). In line with such a model is the observation that the homotarsinin homo-dimer (2 x 24 residues) is more active in antibacterial assays than the corresponding amount of monomer (181).

Another dimer that has been studied is distinctin a heterodimer which forms a compact dimer of two dimers in solution which has been suggested to protect the protein from proteolytic digestion (182) thereby resulting in a slightly increased antimicrobial activity of the dimer when compared to the monomers (183). Its solution structure unfolds in the presence of membranes thus the 25-residue chain 2-helix partitions into the membrane parallel to the membrane surface. In contrast, the 22-residue chain 1 associates only loosely with the membrane (92, 184). Thereby the dimer acts similar to a monomeric linear cationic peptide.

MODEL FOR SYNERGISTIC PGLa—MAGAININ INTERACTIONS

In order to develop a model for antimicrobial synergism focus should be on structural data obtained in membranes carrying unsaturations and PE head groups such as they occur in bacterial membranes. Structural data indicate that the highly cationic peptides adopt amphipathic α-helical conformations and that these peptides are aligned parallel to the membrane surface (98, 101, 103). MD simulation and diffraction data show that the peptides partition into the interface of POPE/POPG 3/1 membranes with the large hydrophobic face of PGLa being inserted somewhat deeper than magainin 2 (103, 116, 117). Electrostatic interactions involving the dipolar charge distribution along the peptides (102, 103, 162) and interactions involving anionic lipids (104) and/or anions of the surrounding buffers (185) help in the formation of nematic phase arrangements along the membrane surface (**Figure 1**).

Furthermore, when the peptides partition into the membrane interface they have been shown to have a large disordering effect on the fatty acyl chains of the surrounding lipids (101). Interestingly, such and related changes in the membrane packing and structure have been postulated to result in lipid-mediated interactions over several molecular layers (186–188). The peptides disturb the finely tuned equilibrium of van-der Waals, hydrogen bonding and electrostatic interactions, entropic contributions of the lipid fatty acyl chains and of the membrane-associated water, that assure the lipid bilayer packing into well-defined supramolecular arrangements. Therefore, it is possible that the pronounced lipid disordering observed in the presence of magainin 2, PGLa, and the mixture constitutes an important driving force to bring peptides into closer proximity (**Figure 5**). Thereby new supramolecular arrangements of the lipids and peptides form which have been detected by fluorescence quenching techniques and MD simulations (69, 117). Notably, zones of high peptide density have also been observed when bacteria were imaged (159) but these measurements work on very different length scales and it is not clear if these observations correlate. Notably, the formation of supramolecular arrangements within POPE/POPG membranes and the correlation observed between PGLa and magainin 2 comes along with an order of magnitude increase in membrane partitioning of the peptides (**Figure 5**). The much-increased membrane affinity due to the presence of the other peptide by

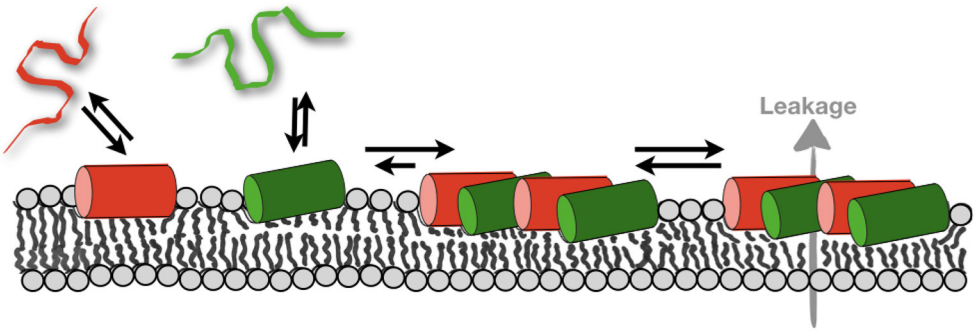

FIGURE 5 | Schematically illustrates the membrane partitioning equilibria of magainin 2 (red) and PGLa (green). The formation of mesophases deletes the pool of monomeric peptides thereby more peptide can bind. As a consequence, the total amount of membrane-associated peptide increases and supramolecular structures that facilitate leakage form (69).

itself could explain the synergistic enhancement of activities, but the formation of peptide-lipid mesophases results in high local peptide concentrations which can also involve a modulation of activities.

While extensive studies have been performed to define the range of pathogens and tumor cells susceptible to be killed by magainin antimicrobial peptides or the lack of toxicity against healthy human (or frog) cells (61, 62, 172, 189) much less data on toxicity or antimicrobial action are published about the synergistic mixture of PGLa and magainin 2 (26, 44, 190). For the individual peptides selectivity of bacteria over healthy eukaryotic cells has been explained by the negatively charged surface of bacteria and a high negative inside membrane potential of their plasma membrane assuring a high density of polycationic peptides at the bacterial membrane (129, 191). Furthermore, eukaryotic cells are protected from membrane lysis by these peptides due to the presence of cholesterol (62, 192). Because in this model the preferential killing of bacteria over healthy human cells is driven by the physico-chemical properties of the membrane similar considerations should also be applicable to the peptide mixtures. In this context it is notable that the synergistic enhancement of activities works for PE-rich (bacterial) membranes but not when this lipid is replaced by PC (eukaryotic membranes). Thereby, such biophysical findings suggest that the therapeutic window of these peptides potentially increase when added in combination.

AUTHOR CONTRIBUTIONS

EG and DJ performed experiments. BB wrote the manuscript. All authors contributed to writing the manuscript and in the preparation of Figures.

FUNDING

The financial support by the Agence Nationale de la Recherche (projects MemPepSyn 14-CE34-0001-01, Biosupramol 17-CE18-0033-3 and the LabEx Chemistry of Complex Systems 10-LABX-0026_CSC), the University of Strasbourg, the CNRS, the Région Alsace and the RTRA International Center of Frontier Research in Chemistry is much appreciated.

ACKNOWLEDGMENTS

We are grateful to Lorenzo Stella for valuable discussion.

REFERENCES

1. Boman HG. Peptide antibiotics and their role in innate immunity. *Annu Rev Immunol.* (1995) 13:61–92. doi: 10.1146/annurev.iy.13.040195.000425
2. Zasloff M. Antimicrobial peptides of multicellular organisms. *Nature.* (2002) 415:389–95. doi: 10.1038/415389a
3. Aldridge S, Parascandola J, Sturchio JL. *The Discovery and Development of Penicillin 1928-1945.* (1999). Royal Society of Chemistry, London and National Historic Chemical Landmarks Program of the American Chemical Society. Available online at: https://www.acs.org/content/acs/en/education/whatischemistry/landmarks/flemingpenicillin.html
4. Dubos RJ, Hotchkiss RD. The production of bactericidal substances by aerobic sporulating bacilli. *J Exp Med.* (1941) 73:629–40. doi: 10.1084/jem.73.5.629
5. Gause GF. Gramicidin S. *Lancet.* (1946) 2:46. doi: 10.1016/S0140-6736(46)90004-9
6. Gall YM, Konashev MB. The discovery of Gramicidin S: the intellectual transformation of G.F. Gause from biologist to researcher of antibiotics and on its meaning for the fate of Russian genetics. *Hist Philos Life Sci.* (2001) 23:137–50.
7. Leitgeb B, Szekeres A, Manczinger L, Vagvolgyi C, Kredics L. The history of alamethicin: a review of the most extensively studied peptaibol. *Chem Biodivers.* (2007) 4:1027–51. doi: 10.1002/cbdv.200790095
8. Rautenbach M, Troskie AM, Vosloo JA. Antifungal peptides: to be or not to be membrane active. *Biochimie.* (2016) 130:132–45. doi: 10.1016/j.biochi.2016.05.013
9. Agerberth B, Gunne H, Odeberg J, Kogner P, Boman HG, Gudmundsson GH. FALL-39, a putative human peptide antibiotic, is cysteine-free and expressed in bone marrow and testis. *Proc Natl Acad Sci USA.* (1995) 92:195–9. doi: 10.1073/pnas.92.1.195
10. Kiss G, Michl H. Über das Giftsekret der Gelbbauchunke *Bombina variegata* L. *Toxicon.* (1962) 1:33–9. doi: 10.1016/0041-0101(62)90006-5

11. Zasloff M. Magainins, a class of antimicrobial peptides from Xenopus skin: Isolation, characterization of two active forms, and partial cDNA sequence of a precursor. *Proc Natl Acad Sci USA*. (1987) 84:5449–53. doi: 10.1073/pnas.84.15.5449
12. Juhl DW, Van Rensburg W, Bossis X, Vosloo JA, Rautenbach M, Bechinger B. Tyrocidine A interactions with saccharides investigated by CD and NMR spectroscopies. *J Pept Sci.* (2019) 25:e3163. doi: 10.1002/psc.3163
13. Pirtskhalava M, Gabrielian A, Cruz P, Griggs HL, Squires RB, Hurt DE, et al. DBAASP v.2: an enhanced database of structure and antimicrobial/cytotoxic activity of natural and synthetic peptides. *Nucleic Acids Res.* (2016) 44:D1104–12. doi: 10.1093/nar/gkv1174
14. Wang G, Li X, Wang Z. APD3: the antimicrobial peptide database as a tool for research and education. *Nucleic Acids Res.* (2016) 44:D1087–93. doi: 10.1093/nar/gkv1278
15. Liu S, Fan L, Sun J, Lao X, Zheng H. Computational resources and tools for antimicrobial peptides. *J Pept Sci.* (2017) 23:4–12. doi: 10.1002/psc.2947
16. Aguilera-Mendoza L, Marrero-Ponce Y, Garcia-Jacas CR, Chavez E, Beltran JA, Guillen-Ramirez HA, et al. Automatic construction of molecular similarity networks for visual graph mining in chemical space of bioactive peptides: an unsupervised learning approach. *Sci Rep.* (2020) 10:18074. doi: 10.1038/s41598-020-75029-1
17. Sansom MSP. The biophysics of peptide models of ion channels. *Prog Biophys Mol Biol.* (1991) 55:139–235. doi: 10.1016/0079-6107(91)90004-C
18. Bechinger B. Structure and functions of channel-forming polypeptides: magainins, cecropins, melittin and alamethicin. *J Membr Biol.* (1997) 156:197–211. doi: 10.1007/s002329900201
19. Chang S, Sievert DM, Hageman JC, Boulton ML, Tenover FC, Downes FP, et al. Infection with vancomycin-resistant *Staphylococcus aureus* containing the vanA resistance gene. *N Engl J Med.* (2003) 348:1342–7. doi: 10.1056/NEJMoa025025
20. Koo HB, Seo J. Antimicrobial peptides under clinical investigation. *J Peptide Sci.* (2019) 111:e24122. doi: 10.1002/pep2.24122
21. Mookherjee N, Anderson MA, Haagsman HP, Davidson DJ. Antimicrobial host defence peptides: functions and clinical potential. *Nat Rev Drug Discov.* (2020) 19:311–32. doi: 10.1038/s41573-019-0058-8
22. Bechinger B, Gorr SU. Antimicrobial peptides: mechanisms of action and resistance. *J Dent Res.* (2017) 96:254–60. doi: 10.1177/0022034516679973
23. Lazzaro BP, Zasloff M, Rolff J. Antimicrobial peptides: Application informed by evolution. *Science.* (2020) 368:eaau5480. doi: 10.1126/science.aau5480
24. Juretic D, Chen HC, Brown JH, Morell JL, Hendler RW, Westerhoff HV. Magainin 2 amide and analogues. Antimicrobial activity, membrane depolarization and susceptibility to proteolysis. *FEBS Lett.* (1989) 249:219–23. doi: 10.1016/0014-5793(89)80627-1
25. Resnick NM, Maloy WL, Guy HR, Zasloff M. A novel endopeptidase from *Xenopus* that recognizes alpha-helical secondary structure. *Cell.* (1991) 66:541–54. doi: 10.1016/0092-8674(81)90017-9
26. Westerhoff HV, Zasloff M, Rosner JL, Hendler RW, De Waal A, Vaz G, et al. Functional synergism of the magainins PGLa and magainin-2 in *Escherichia coli*, tumor cells and liposomes. *Eur J Biochem.* (1995) 228:257–64. doi: 10.1111/j.1432-1033.1995.00257.x
27. Yang D, Zou R, Zhu Y, Liu B, Yao D, Jiang J, et al. Magainin II modified polydiacetylene micelles for cancer therapy. *Nanoscale.* (2014) 6:14772–83. doi: 10.1039/C4NR04405C
28. Yuksel E, Karakecili A. Antibacterial activity on electrospun poly(lactide-co-glycolide) based membranes via Magainin II grafting. *Mater Sci Eng C Mater Biol Appl.* (2014) 45:510–8. doi: 10.1016/j.msec.2014.10.004
29. Reijmar K, Edwards K, Andersson K, Agmo Hernandez V. Characterizing and controlling the loading and release of cationic amphiphilic peptides onto and from PEG-stabilized lipodisks. *Langmuir.* (2016) 32:12091–9. doi: 10.1021/acs.langmuir.6b03012
30. Arnusch CJ, Albada HB, Van Vaardegem M, Liskamp RMJ, Sahl HG, Shadkchan Y, et al. Trivalent ultrashort lipopeptides are potent pH dependent antifungal agents. *J Med Chem.* (2012) 55:1296–302. doi: 10.1021/jm2014474
31. Ghosh C, Harmouche N, Bechinger B, Haldar J. Aryl-alkyl-lysines interact with anionic lipid components of bacterial cell envelope eliciting anti-inflammatory and anti-biofilm properties. *ACS Omega.* (2018) 3:9182–90. doi: 10.1021/acsomega.8b01052
32. Porter EA, Weisblum B, Gellman SH. Mimicry of host-defense peptides by unnatural oligomers: antimicrobial beta-peptides. *J Am Chem Soc.* (2002) 124:7324–30. doi: 10.1021/ja0260871
33. Patch JA, Barron AE. Helical peptoid mimics of magainin-2 amide. *J Am Chem Soc.* (2003) 125:12092–3. doi: 10.1021/ja037320d
34. Kuroda K, Degrado WF. Amphiphilic polymethacrylate derivatives as antimicrobial agents. *J Am Chem Soc.* (2005) 127:4128–9. doi: 10.1021/ja044205+
35. Violette A, Fournel S, Lamour K, Chaloin O, Frisch B, Briand JP, et al. Mimicking helical antibacterial peptides with nonpeptidic folding oligomers. *Chem Biol.* (2006) 13:531–8. doi: 10.1016/j.chembiol.2006.03.009
36. Makovitzki A, Baram J, Shai Y. Antimicrobial lipopolypeptides composed of palmitoyl Di- and tricationic peptides: *in vitro* and *in vivo* activities, self-assembly to nanostructures, and a plausible mode of action. *Biochemistry.* (2008) 47:10630–6. doi: 10.1021/bi8011675
37. Scott RW, Degrado WF, Tew GN. De novo designed synthetic mimics of antimicrobial peptides. *Curr Opin Biotechnol.* (2008) 19:620–7. doi: 10.1016/j.copbio.2008.10.013
38. Rotem S, Mor A. Antimicrobial peptide mimics for improved therapeutic properties. *Biochim Biophys Acta.* (2009) 1788:1582–92. doi: 10.1016/j.bbamem.2008.10.020
39. Palermo EF, Kuroda K. Structural determinants of antimicrobial activity in polymers which mimic host defense peptides. *Appl Microbiol Biotechnol.* (2010) 87:1605–15. doi: 10.1007/s00253-010-2687-z
40. Laurencin M, Simon M, Fleury Y, Baudy-Floc'h M, Bondon A, Legrand B. Selectivity modulation and structure of alpha/aza-beta(3) cyclic antimicrobial peptides. *Chemistry.* (2018) 24:6191–201. doi: 10.1002/chem.201800152
41. Rank LA, Walsh NM, Liu R, Lim FY, Bok JW, Huang M, et al. A cationic polymer that shows high antifungal activity against diverse human pathogens. *Antimicrob Agents Chemother.* (2017) 61:e00204-17. doi: 10.1128/AAC.00204-17
42. Giovannini MG, Poulter L, Gibson BW, Williams DH. Biosynthesis and degradation of peptides derived from *Xenopus laevis* prohormones. *Biochem J.* (1987) 243:113–20. doi: 10.1042/bj2430113
43. Westerhoff HV, Juretic D, Hendler RW, Zasloff M. Magainins and the disruption of membrane-linked free-energy transduction. *Proc Natl Acad Sci USA.* (1989) 86:6597–601. doi: 10.1073/pnas.86.17.6597
44. De Waal A, Gomes AV, Mensink A, Grootegoed JA, Westerhoff HV. Magainins affect respiratory control, membrane potential and motility of hamster spermatozoa. *FEBS Lett.* (1991) 293:219–23. doi: 10.1016/0014-5793(91)81191-A
45. Vaz Gomes A, De Waal A, Berden JA, Westerhoff HV. Electric potentiation, cooperativity, and synergism of magainin peptides in protein-free liposomes. *Biochemistry.* (1993) 32:5365–72. doi: 10.1021/bi00071a011
46. Moulay G, Leborgne C, Mason AJ, Aisenbrey C, Kichler A, Bechinger B. Histidine-rich designer peptides of the LAH4 family promote cell delivery of a multitude of cargo. *J Pept Sci.* (2017) 23:320–8. doi: 10.1002/psc.2955
47. Savini F, Bobone S, Roversi D, Mangoni ML, Stella L. From liposomes to cells: filling the gap between physicochemical and microbiological studies of the activity and selectivity of host-defense peptides. *Pept Sci.* (2018) 110:e24041. doi: 10.1002/pep2.24041
48. Zhu YY, Mohapatra S, Weisshaar JC. Rigidification of the *E. coli* cytoplasm by the human antimicrobial peptide Ll-37 revealed by superresolution fluorescence microscopy. *Biophys J.* (2019) 116:138a. doi: 10.1016/j.bpj.2018.11.765
49. Mccafferty DG, Cudic P, Yu MK, Behenna DC, Kruger R. Synergy and duality in peptide antibiotic mechanisms. *Curr Opin Chem Biol.* (1999) 3:672–80. doi: 10.1016/S1367-5931(99)00025-3
50. Holzl MA, Hofer J, Steinberger P, Pfistershammer K, Zlabinger GJ. Host antimicrobial proteins as endogenous immunomodulators. *Immunol Lett.* (2008) 119:4–11. doi: 10.1016/j.imlet.2008.05.003
51. Diamond G, Beckloff N, Weinberg A, Kisich KO. The roles of antimicrobial peptides in innate host defense. *Curr Pharm Des.* (2009) 15:2377–92. doi: 10.2174/138161209788682325
52. Steinstraesser L, Kraneburg U, Jacobsen F, Al-Benna S. Host defense peptides and their antimicrobial-immunomodulatory duality. *Immunobiology.* (2010) 216:322–33. doi: 10.1016/j.imbio.2010.07.003

53. Cao P, Yang Y, Uche FI, Hart SR, Li WW, Yuan C. Coupling plant-derived cyclotides to metal surfaces: an antibacterial and antibiofilm study. *Int J Mol Sci.* (2018) 19:793. doi: 10.3390/ijms19030793
54. Tsutsumi LS, Elmore JM, Dang UT, Wallace MJ, Marreddy R, Lee RB, et al. Solid-phase synthesis and antibacterial activity of cyclohexapeptide wollamide B analogs. *ACS Comb Sci.* (2018) 20:172–85. doi: 10.1021/acscombsci.7b00189
55. Zhao P, Xue Y, Gao W, Li J, Zu X, Fu D, et al. Bacillaceae-derived peptide antibiotics since 2000. *Peptides.* (2018) 101:10–6. doi: 10.1016/j.peptides.2017.12.018
56. Hong M, Su Y. Structure and dynamics of cationic membrane peptides and proteins: insights from solid-state NMR. *Protein Sci.* (2011) 20:641–55. doi: 10.1002/pro.600
57. Salnikov E, Aisenbrey C, Balandin SV, Zhmak MN, Ovchinnikova AY, Bechinger B. Structure and alignment of the membrane-associated antimicrobial peptide arenicin by oriented solid-state NMR spectroscopy. *Biochemistry.* (2011) 50:3784–95. doi: 10.1021/bi1018732
58. Rautenbach M, Troskie AM, Vosloo JA, Dathe ME. Antifungal membranolytic activity of the tyrocidines against filamentous plant fungi. *Biochimie.* (2016) 130:122–31. doi: 10.1016/j.biochi.2016.06.008
59. Sychev SV, Sukhanov SV, Panteleev PV, Shenkarev ZO, Ovchinnikova TV. Marine antimicrobial peptide arenicin adopts a monomeric twisted beta-hairpin structure and forms low conductivity pores in zwitterionic lipid bilayers. *Biopolymers.* (2017). doi: 10.1002/bip.23093. [Epub ahead of print].
60. Usachev KS, Kolosova OA, Klochkova EA, Yulmetov AR, Aganov AV, Klochkov VV. Oligomerization of the antimicrobial peptide Protegrin-5 in a membrane-mimicking environment. Structural studies by high-resolution NMR spectroscopy. *Eur Biophys J.* (2017) 46:293–300. doi: 10.1007/s00249-016-1167-5
61. Jacob L, Zasloff M. Potential therapeutic applications of magainins and other antimicrobial agents of animal origin. [Review]. *Ciba Found Sympos.* (1994) 186:197–216; discussion 216. doi: 10.1002/9780470514658.ch12
62. Maloy WL, Kari UP. Structure-activity studies on magainins and other host defense peptides. *Biopolymers.* (1995) 37:105–22. doi: 10.1002/bip.360370206
63. Bechinger B, Kim Y, Chirlian LE, Gesell J, Neumann JM, Montal M, et al. Orientations of amphipathic helical peptides in membrane bilayers determined by solid- state NMR spectroscopy. *J Biomol NMR.* (1991) 1:167–73. doi: 10.1007/BF01877228
64. Matsuzaki K, Murase O, Tokuda H, Funakoshi S, Fujii N, Miyajima K. Orientational and aggregational states of magainin 2 in phospholipid bilayers. *Biochemistry.* (1994) 33:3342–9. doi: 10.1021/bi00177a027
65. Ludtke SJ, He K, Heller WT, Harroun TA, Yang L, Huang HW. Membrane pores induced by magainin. *Biochemistry.* (1996) 35:13723–8. doi: 10.1021/bi9620621
66. Wieprecht T, Apostolov O, Beyermann M, Seelig J. Membrane binding and pore formation of the antibacterial peptide PGLa: thermodynamic and mechanistic aspects. *Biochemistry.* (2000) 39:442–52. doi: 10.1021/bi992146k
67. Shai Y. Mechanism of the binding, insertion, and destabilization of phospholipid bilayer membranes by alpha-helical antimicrobial and cell non-selective lytic peptides. *Biochim Biophys Acta.* (1999) 1462:55–70. doi: 10.1016/S0005-2736(99)00200-X
68. Wenzel M, Chiriac AI, Otto A, Zweytick D, May C, Schumacher C, et al. Small cationic antimicrobial peptides delocalize peripheral membrane proteins. *Proc Natl Acad Sci USA.* (2014) 111:E1409–18. doi: 10.1073/pnas.1319900111
69. Aisenbrey C, Amaro M, Pospisil P, Hof M, Bechinger B. Investigation of the supramolecular complexes formed by Magainin 2, PGLa and lipids. *Sci Rep.* (2020) 10:11652. doi: 10.1038/s41598-020-68416-1
70. Marquette A, Bechinger B. Biophysical investigations elucidating the mechanisms of action of antimicrobial peptides and their synergism. *Biomolecules.* (2018) 8:18. doi: 10.3390/biom8020018
71. Duclohier H. Antimicrobial peptides and peptaibols, substitutes for conventional antibiotics. *Curr Pharm Des.* (2010) 16:3212–23. doi: 10.2174/138161210793292500
72. Islam MZ, Alam JM, Tamba Y, Karal MS, Yamazaki M. The single GUV method for revealing the functions of antimicrobial, pore-forming toxin, and cell-penetrating peptides or proteins. *Phys Chem Chem Phys.* (2014) 16:15752–67. doi: 10.1039/C4CP00717D
73. Gregory SM, Cavenaugh A, Journigan V, Pokorny A, Almeida PFF. A quantitative model for the all-or-none permeabilization of phospholipid vesicles by the antimicrobial peptide cecropin A. *Biophys J.* (2008) 94:1667–80. doi: 10.1529/biophysj.107.118760
74. Tamba Y, Ariyama H, Levadny V, Yamazaki M. Kinetic Pathway of antimicrobial peptide Magainin 2-induced pore formation in lipid membranes. *J Phys Chem B.* (2010) 114:12018–26. doi: 10.1021/jp104527y
75. Barns KJ, Weisshaar JC. Real-time attack of LL-37 on single *Bacillus subtilis* cells. *Biochim Biophys Acta.* (2013) 1828:1511–20. doi: 10.1016/j.bbamem.2013.02.011
76. Rangarajan N, Bakshi S, Weisshaar JC. Localized permeabilization of *E. coli* membranes by the antimicrobial peptide Cecropin A. *Biochemistry.* (2013) 52:6584–94. doi: 10.1021/bi400785j
77. Yang Z, Choi H, Weisshaar JC. Melittin-induced permeabilization, re-sealing, and re-permeabilization of *E. coli* membranes. *Biophys J.* (2018) 114:368–79. doi: 10.1016/j.bpj.2017.10.046
78. Scocchi M, Mardirossian M, Runti G, Benincasa M. Non-membrane permeabilizing modes of action of antimicrobial peptides on bacteria. *Curr Top Med Chem.* (2016) 16:76–88. doi: 10.2174/1568026615666150703121009
79. Bechinger B. The structure, dynamics and orientation of antimicrobial peptides in membranes by multidimensional solid-state NMR spectroscopy. *Biochim Biophys Acta.* (1999) 1462:157–83. doi: 10.1016/S0005-2736(99)00205-9
80. Wieprecht T, Apostolov O, Beyermann M, Seelig J. Thermodynamics of the alpha-helix-coil transition of amphipathic peptides in a membrane environment: implications for the peptide-membrane binding equilibrium. *J Mol Biol.* (1999) 294:785–94. doi: 10.1006/jmbi.1999.3268
81. Das N, Dai J, Hung I, Rajagopalan MR, Zhou HX, Cross TA. Structure of CrgA, a cell division structural and regulatory protein from *Mycobacterium tuberculosis*, in lipid bilayers. *Proc Natl Acad Sci USA.* (2015) 112:E119–26. doi: 10.1073/pnas.1415908112
82. Gopinath T, Mote KR, Veglia G. Simultaneous acquisition of 2D and 3D solid-state NMR experiments for sequential assignment of oriented membrane protein samples. *J Biomol NMR.* (2015) 62:53–61. doi: 10.1007/s10858-015-9916-9
83. Itkin A, Salnikov ES, Aisenbrey C, Raya J, Raussens V, Ruysschaert JM, et al. Evidence for heterogeneous conformations of the gamma cleavage site within the amyloid precursor proteins transmembrane domain *ACS Omega.* (2017) 2:6525–34. doi: 10.1021/acsomega.7b00619
84. Salnikov ES, Anantharamaiah GM, Bechinger B. Supramolecular organization of apolipoprotein A-I - derived peptides within disc-like arrangements. *Biophys J.* (2018) 115:467–77. doi: 10.1016/j.bpj.2018.06.026
85. Bechinger B, Sizun C. Alignment and structural analysis of membrane polypeptides by 15N and 31P solid-state NMR spectroscopy. *Concepts Magn Reson.* (2003) 18A:130–45. doi: 10.1002/cmr.a.10070
86. Bechinger B, Shon K, Eck H, Zasloff M, Opella SJ. NMR studies of magainin peptide antibiotics in membranes. *Biol Chem Hoppe Seyler.* (1990) 371:758–758.
87. Bechinger B, Zasloff M, Opella SJ. Structure and interactions of magainin antibiotic peptides in lipid bilayers: a solid-state NMR investigation. *Biophys J.* (1992) 62:12–4.
88. Bechinger B, Zasloff M, Opella SJ. Structure and orientation of the antibiotic peptide magainin in membranes by solid-state NMR spectroscopy. *Protein Sci.* (1993) 2:2077–84.
89. Bechinger B. Insights into the mechanisms of action of host defence peptides from biophysical and structural investigations. *J Pept Sci.* (2011) 17:306–14. doi: 10.1002/psc.1343
90. Ramamoorthy A, Thennarasu S, Lee DK, Tan A, Maloy L. Solid-state NMR investigation of the membrane-disrupting mechanism of antimicrobial peptides MSI-78 and MSI-594 derived from magainin 2 and melittin. *Biophys J.* (2006) 91:206–16. doi: 10.1529/biophysj.105.073890
91. Mason AJ, Moussaoui W, Abdelrhaman T, Boukhari A, Bertani P, Marquette A, et al. Structural determinants of antimicrobial and antiplasmodial activity and selectivity in histidine rich amphipathic cationic peptides. *J Biol Chem.* (2009) 284:119–33. doi: 10.1074/jbc.M806201200
92. Resende JM, Moraes CM, Munhoz VHDO, Aisenbrey C, Verly RM, Bertani P, et al. Membrane structure and conformational changes of the antibiotic

heterodimeric peptide distinctin by solid-state NMR spectroscopy. *Proc Natl Acad Sci USA*. (2009) 106:16639–44. doi: 10.1073/pnas.0905069106
93. Resende JM, Verly RM, Aisenbrey C, Amary C, Bertani P, Pilo-Veloso D, et al. Membrane interactions of Phylloseptin-1,−2, and−3 peptides by oriented solid-state NMR spectroscopy. *Biophys J.* (2014) 107:901–11. doi: 10.1016/j.bpj.2014.07.014
94. Hayden RM, Goldberg GK, Ferguson BM, Schoeneck MW, Libardo MD, Mayeux SE, et al. Complementary effects of host defense peptides piscidin 1 and piscidin 3 on DNA and lipid membranes: biophysical insights into contrasting biological activities. *J Phys Chem B.* (2015) 119:15235–46. doi: 10.1021/acs.jpcb.5b09685
95. Sani MA, Separovic F. Antimicrobial peptide structures: from model membranes to live cells. *Chemistry.* (2018) 24:286–91. doi: 10.1002/chem.201704362
96. Ludtke SJ, He K, Wu Y, Huang HW. Cooperative membrane insertation of maginin correlated with its cytolytic activity. *Biochim Biophys Acta.* (1994) 1190:181–4.
97. Gazit E, Miller IR, Biggin PC, Sansom MSP, Shai Y. Structure and orientation of the mammalian antibacterial peptide cecropin P1 within phospholipid membranes. *J Mol Biol.* (1996) 258:860–70.
98. Salnikov E, Bechinger B. Lipid-controlled peptide topology and interactions in bilayers: structural insights into the synergistic enhancement of the antimicrobial activities of PGLa and magainin 2. *Biophys J.* (2011) 100:1473–80. doi: 10.1016/j.bpj.2011.01.070
99. Strandberg E, Zerweck J, Wadhwani P, Ulrich AS. Synergistic insertion of antimicrobial magainin-family peptides in membranes depends on the lipid spontaneous curvature. *Biophys J.* (2013) 104:L9–11. doi: 10.1016/j.bpj.2013.01.047
100. Tremouilhac P, Strandberg E, Wadhwani P, Ulrich AS. Synergistic transmembrane alignment of the antimicrobial heterodimer PGLa/magainin. *J Biol Chem.* (2006) 281:32089–94. doi: 10.1074/jbc.M604759200
101. Harmouche N, Bechinger B. Lipid-mediated interactions between the amphipathic antimicrobial peptides magainin 2 and PGLa in phospholipid bilayers. *Biophys J.* (2018) 115:1033–44. doi: 10.1016/j.bpj.2018.08.009
102. Zerweck J, Strandberg E, Kukharenko O, Reichert J, Burck J, Wadhwani P, et al. Molecular mechanism of synergy between the antimicrobial peptides PGLa and magainin 2. *Sci Rep.* (2017) 7:13153. doi: 10.1038/s41598-017-12599-7
103. Glattard E, Salnikov ES, Aisenbrey C, Bechinger B. Investigations of the synergistic enhancement of antimicrobial activity in mixtures of magainin 2 and PGLa. *Biophys Chem.* (2016) 210:35–44. doi: 10.1016/j.bpc.2015.06.002
104. Aisenbrey C, Bechinger B. Molecular packing of amphipathic peptides on the surface of lipid membranes. *Langmuir.* (2014) 30:10374–83. doi: 10.1021/la500998g
105. Ludtke S, He K, Huang H. Membrane thinning caused by magainin 2. *Biochemistry.* (1995) 34:16764–9. doi: 10.1021/bi00051a026
106. Kim C, Spano J, Park EK, Wi S. Evidence of pores and thinned lipid bilayers induced in oriented lipid membranes interacting with the antimicrobial peptides, magainin-2 and aurein-3.3. *Biochim Biophys Acta.* (2009) 1788:1482–1496. doi: 10.1016/j.bbamem.2009.04.017
107. Bechinger B, Salnikov ES. The membrane interactions of antimicrobial peptides revealed by solid-state NMR spectroscopy. *Chem Phys Lipids.* (2012) 165:282–301. doi: 10.1016/j.chemphyslip.2012.01.009
108. Hallock KJ, Lee DK, Omnaas J, Mosberg HI, Ramamoorthy A. Membrane composition determines pardaxin's mechanism of lipid bilayer disruption. *Biophys J.* (2002) 83:1004–13. doi: 10.1016/S0006-3495(02)75226-0
109. Salnikov ES, Mason AJ, Bechinger B. Membrane order perturbation in the presence of antimicrobial peptides by 2 H solid-state NMR spectroscopy. *Biochimie.* (2009) 91:743. doi: 10.1016/j.biochi.2009.01.002
110. Grage SL, Afonin S, Kara S, Buth G, Ulrich AS. Membrane thinning and thickening induced by membrane-active amphipathic peptides. *Front Cell Dev Biol.* (2016) 4:65. doi: 10.3389/fcell.2016.00065
111. Bechinger B. Detergent-like properties of magainin antibiotic peptides: a 31P solid-state NMR study. *Biochim Biophys Acta.* (2005) 1712:101–8. doi: 10.1016/j.bbamem.2005.03.003
112. Chen FY, Lee MT, Huang HW. Evidence for membrane thinning effect as the mechanism for Peptide-induced pore formation. *Biophys J.* (2003) 84:3751–8. doi: 10.1016/S0006-3495(03)75103-0
113. Mecke A, Lee DK, Ramamoorthy A, Orr BG, Banaszak Holl MM. Membrane thinning due to antimicrobial peptide binding: an atomic force microscopy study of MSI-78 in lipid bilayers. *Biophys J.* (2005) 89:4043–50. doi: 10.1529/biophysj.105.062596
114. Vacha R, Frenkel D. Simulations suggest possible novel membrane pore structure. *Langmuir.* (2014) 30:1304–10. doi: 10.1021/la402727a
115. Farrotti A, Bocchinfuso G, Palleschi A, Rosato N, Salnikov ES, Voievoda N, et al. Molecular dynamics methods to predict peptide location in membranes: LAH4 as a stringent test case. *Biochim Biophys Acta.* (2015) 1848:581–92. doi: 10.1016/j.bbamem.2014.11.002
116. Pachler M, Kabelka I, Appavou MS, Lohner K, Vacha R, Pabst G. Magainin 2 and PGLa in bacterial membrane mimics I: peptide-peptide and lipid-peptide interactions. *Biophys J.* (2019) 117:1858–69. doi: 10.1016/j.bpj.2019.10.022
117. Kabelka I, Pachler M, Prevost S, Letofsky-Papst I, Lohner K, Pabst G, et al. Magainin 2 and PGLa in bacterial membrane mimics II: membrane fusion and sponge phase formation. *Biophys J.* (2020) 118:612–23. doi: 10.1016/j.bpj.2019.11.1985
118. Huang HW. Action of antimicrobial peptides: two-state model. *Biochemistry.* (2000) 39:8347–52. doi: 10.1021/bi000946l
119. Leber R, Pachler M, Kabelka I, Svoboda I, Enkoller D, Vácha R, et al. Synergism of antimicrobial frog peptides couples to membrane intrinsic curvature Strain. *Biophys J.* (2018) 114:1945–54. doi: 10.1016/j.bpj.2018.03.006
120. Amos ST, Vermeer LS, Ferguson PM, Kozlowska J, Davy M, Bui TT, et al. Antimicrobial peptide potency is facilitated by greater conformational flexibility when binding to gram-negative bacterial inner membranes. *Sci Rep.* (2016) 6:37639. doi: 10.1038/srep37639
121. Israelachvili JN, Marcelja S, Horn RG. Physical principles of membrane organization. *Q Rev Biophys.* (1980) 13:121–200.
122. Aisenbrey C, Marquette A, Bechinger B. The mechanisms of action of cationic antimicrobial peptides refined by novel concepts from biophysical investigations. *Adv Exp Med Biol.* (2019) 1117:33–64. doi: 10.1007/978-981-13-3588-4_4
123. Cruciani RA, Barker JL, Zasloff M, Chen HC, Colamonici O. Antibiotic magainins exert cytolytic activity transformed cell lines through channel formation. *Proc Natl Acad Sci USA.* (1991) 88:3792–6.
124. Cruciani RA, Barker JL, Raghunathan G, Guy HR, Zasloff M, Stanley EF. Magainin 2, a natural antibiotic from frog skin, forms ion channels in lipid bilayer membranes. *Eur J Pharmacol.* (1992) 226:287–96.
125. Hall K, Lee TH, Mechler AI, Swann MJ, Aguilar MI. Real-time measurement of membrane conformational states induced by antimicrobial peptides: balance between recovery and lysis. *Sci Rep.* (2014) 4:5479. doi: 10.1038/srep05479
126. Bechinger B, Lohner K. Detergent-like action of linear cationic membrane-active antibiotic peptides. *Biochim Biophys Acta.* (2006) 1758:1529–39. doi: 10.1016/j.bbamem.2006.07.001
127. Bechinger B. The SMART model: soft membranes adapt and respond, also transiently, to external stimuli. *J Pept Sci.* (2015) 21:346–55. doi: 10.1002/psc.2729
128. Henderson JM, Waring AJ, Separovic F, Lee KYC. Antimicrobial peptides share a common interaction driven by membrane line tension reduction. *Biophys J.* (2016) 111:2176–89. doi: 10.1016/j.bpj.2016.10.003
129. Matsuzaki K, Harada M, Funakoshi S, Fujii N, Miyajima K. Physicochemical determinants for the interactions of magainins 1 and 2 with acidic lipid bilayers. *Biochim Biophys Acta.* (1991) 1063:162–70.
130. Wenk M, Seelig J. Magainin 2 amide interaction with lipid membranes: calorimetric detection of peptide binding and pore formation. *Biochemistry.* (1998) 37:3909–16.
131. Bechinger B. Membrane-lytic peptides. *Crit Rev Plant Sci.* (2004) 23:271–92. doi: 10.1080/07352680490452825
132. Klocek G, Seelig J. Melittin interaction with sulfated cell surface sugars. *Biochemistry.* (2008) 47:2841–9. doi: 10.1021/bi702258z

133. Lohner K. New strategies for novel antibiotics: peptides targeting bacterial cell membranes. *Gen Physiol Biophys.* (2009) 28:105–16. doi: 10.4149/gpb_2009_02_105
134. Wieprecht T, Beyermann M, Seelig J. Binding of antibacterial magainin peptides to electrically neutral membranes: thermodynamics and structure. *Biochemistry.* (1999) 38:10377–8.
135. Voievoda N, Schulthess T, Bechinger B, Seelig J. Thermodynamic and biophysical analysis of the membrane-association of a histidine-rich peptide with efficient antimicrobial and transfection activities. *J Phys Chem B.* (2015) 119:9678–87. doi: 10.1021/acs.jpcb.5b04543
136. Acar JF. Antibiotic synergy and antagonism. *Med Clin North Am.* (2000) 84:1391–406. oi: 10.1016/S0025-7125(05)70294-7
137. Mangoni ML, Shai Y. Temporins and their synergism against Gram-negative bacteria and in lipopolysaccharide detoxification. *Biochim Biophys Acta.* (2009) 1788:1610–9. doi: 10.1016/j.bbamem.2009.04.021
138. Chou S, Shao C, Wang J, Shan A, Xu L, Dong N, et al. Short, multiple-stranded beta-hairpin peptides have antimicrobial potency with high selectivity and salt resistance. *Acta Biomater.* (2016) 30:78–93. doi: 10.1016/j.actbio.2015.11.002
139. Bolosov IA, Kalashnikov AA, Panteleev PV, Ovchinnikova TV. Analysis of synergistic effects of antimicrobial peptide arenicin-1 and conventional antibiotics. *Bull Exp Biol Med.* (2017) 162:765–8. doi: 10.1007/s10517-017-3708-z
140. Kim EY, Rajasekaran G, Shin SY. LL-37-derived short antimicrobial peptide KR-12-a5 and its d-amino acid substituted analogs with cell selectivity, anti-biofilm activity, synergistic effect with conventional antibiotics, and anti-inflammatory activity. *Eur J Med Chem.* (2017) 136:428–41. doi: 10.1016/j.ejmech.2017.05.028
141. Payne JE, Dubois AV, Ingram RJ, Weldon S, Taggart CC, Elborn JS, et al. Activity of innate antimicrobial peptides and ivacaftor against clinical cystic fibrosis respiratory pathogens. *Int J Antimicrob Agents.* (2017) 50:427–35. doi: 10.1016/j.ijantimicag.2017.04.014
142. Sakoulas G, Kumaraswamy M, Kousha A, Nizet V. Interaction of antibiotics with innate host defense factors against *Salmonella enterica* serotype newport. *mSphere.* (2017) 2:e00410–17. doi: 10.1128/mSphere.00410-17
143. Citterio L, Franzyk H, Palarasah Y, Andersen TE, Mateiu RV, Gram L. Improved in vitro evaluation of novel antimicrobials: potential synergy between human plasma and antibacterial peptidomimetics, AMPs and antibiotics against human pathogenic bacteria. *Res Microbiol.* (2016) 167:72–82. doi: 10.1016/j.resmic.2015.10.002
144. Walkenhorst WF, Sundrud JN, Laviolette JM. Additivity and synergy between an antimicrobial peptide and inhibitory ions. *Biochim Biophys Acta.* (2014) 1838:2234–42. doi: 10.1016/j.bbamem.2014.05.005
145. Kobayashi S, Hirakura Y, Matsuzaki K. Bacteria-selective synergism between the antimicrobial peptides alpha-helical magainin 2 and cyclic beta-sheet tachyplesin I: toward cocktail therapy. *Biochemistry.* (2001) 40:14330–5. doi: 10.1021/bi015626w
146. Juretic D, Hendler RW, Zasloff M, Westerhoff HV. Cooperative action of magainins in disrupting membrane-linked free-energy transduction. *Biophys J.* (1989) 55:W-Pos313.
147. Juretić D. Antimicrobial peptides of the magainin family: membrane depolarization studies on *E. coli* and cytochrome oxidase liposomes. *Stud Biophys.* (1990) 138:79–86.
148. Juretic D, Hendler RW, Kamp F, Caughey WS, Zasloff M, Westerhoff HV. Magainin oligomers reversibly dissipate delta microH+ in cytochrome oxidase liposomes. *Biochemistry.* (1994) 33:4562–70.
149. Nishida M, Imura Y, Yamamoto M, Kobayashi S, Yano Y, Matsuzaki K. Interaction of a magainin-PGLa hybrid peptide with membranes: insight into the mechanism of synergism. *Biochemistry.* (2007) 46:14284–90. doi: 10.1021/bi701850m
150. Juhl DW, Glattard E, Lointier M, Bampilis P, Bechinger B. The antimicrobial and synergistic activities of PGLa and magainin 2 fibrils. *Front Cell Infect Microbiol.* (2020) 10:526459. doi: 10.3389/fcimb.2020.526459
151. Yu G, Baeder DY, Regoes RR, Rolff J. Combination effects of antimicrobial peptides. *Antimicrob Agents Chemother.* (2016) 60:1717–24. doi: 10.1128/AAC.02434-15
152. Chou TC. Theoretical basis, experimental design, and computerized simulation of synergism and antagonism in drug combination studies. *Pharmacol Rev.* (2006) 58:621–81. doi: 10.1124/pr.58.3.10
153. Jepson AK, Schwarz-Linek J, Ryan L, Ryadnov MG, Poon WCK. What is the 'minimum inhibitory concentration' (MIC) of pexiganan acting on *Escherichia coli*?—A cautionary case study. *Adv Exp Med Biol.* (2016) 915:33–48. doi: 10.1007/978-3-319-32189-9_4
154. Snoussi M, Talledo JP, Del Rosario NA, Mohammadi S, Ha BY, Kosmrlj A, et al. Heterogeneous absorption of antimicrobial peptide LL37 in *Escherichia coli* cells enhances population survivability. *Elife.* (2018) 7:e38174. doi: 10.7554/eLife.38174
155. Hill AV. The possible effects of the aggregation of the molecules of hemoglobin on its dissociation curves. *J Physiol.* (1910) 40:4–7.
156. Savini F, Loffredo MR, Troiano C, Bobone S, Malanovic N, Eichmann TO, et al. Binding of an antimicrobial peptide to bacterial cells: Interaction with different species, strains and cellular components. *Biochim Biophys Acta.* (2020) 1862:183291. doi: 10.1016/j.bbamem.2020.183291
157. Savini F, Luca V, Bocedi A, Massoud R, Park Y, Mangoni ML, et al. Cell-density dependence of host-defense peptide activity and selectivity in the presence of host cells. *ACS Chem Biol.* (2017) 12:52–6. doi: 10.1021/acschembio.6b00910
158. Loffredo MR, Savini F, Bobone S, Casciaro B, Franzyk H, Mangoni ML, et al. Inoculum effect of antimicrobial peptides. *bioRxiv preprint.* (2020). doi: 10.1101/2020.08.21.260620
159. Choi H, Rangarajan N, Weisshaar JC. Lights, camera, action! antimicrobial peptide mechanisms imaged in space and time. *Trends Microbiol.* (2016) 24:111–22. doi: 10.1016/j.tim.2015.11.004
160. Mor A, Hani K, Nicolas P. The vertebrate peptide antibiotics dermaseptins have overlapping structural features but target specific microorganisms. *J Biol Chem.* (1994) 269:31635–41.
161. Giacometti A, Cirioni O, Del Prete MS, Paggi AM, D'errico MM, Scalise G. Combination studies between polycationic peptides and clinically used antibiotics against Gram-positive and Gram-negative bacteria. *Peptides.* (2000) 21:1155–60. doi: 10.1016/S0196-9781(00)00254-0
162. Matsuzaki K, Mitani Y, Akada K, Murase O, Yoneyama S, Zasloff M, et al. Mechanism of synergism between antimicrobial peptides magainin 2 and PGLa. *Biochemistry.* (1998) 37:15144–53.
163. Zerweck J, Strandberg E, Burck J, Reichert J, Wadhwani P, Kukharenko O, et al. Homo- and heteromeric interaction strengths of the synergistic antimicrobial peptides PGLa and magainin 2 in membranes. *Eur Biophys J.* (2016) 45:535–47. doi: 10.1007/s00249-016-1120-7
164. Williams RW, Starmann R, Taylor KMP, Gable K, Beeler T, Zasloff M, et al. Raman spectroscopy of synthetic antimicrobial frog peptides magainin 2a and PGLa. *Biochemistry.* (1990) 29:4490–6.
165. Patel H, Huynh Q, Barlehner D, Heerklotz H. Additive and synergistic membrane permeabilization by antimicrobial (Lipo)peptides and detergents. *Biophys J.* (2014) 106:2115–25. doi: 10.1016/j.bpj.2014.04.006
166. Salnikov ES, Aisenbrey C, Aussenac F, Ouari O, Sarrouj H, Reiter C, et al. Membrane topologies of the PGLa antimicrobial peptide and a transmembrane anchor sequence by Dynamic Nuclear Polarization/solid-state NMR spectroscopy. *Sci Rep.* (2016) 6:20895. doi: 10.1038/srep20895
167. Aisenbrey C, Bechinger B. Equilibria governing the membrane insertion of polypeptides and their interactions with other biomacromolecules. In: Moreno Pirajan JC, editor. *Thermodynamics/Book 2.* Rijeka: IntechOpen (2011). p. 381–402.
168. Matsuzaki K, Nakamura A, Murase O, Sugishita K, Fujii N, Miyajima K. Modulation of magainin 2-lipid bilayer interactions by peptide charge. *Biochemistry.* (1997) 36:2104–11.
169. Bechinger B. Towards membrane protein design: pH-sensitive topology of histidine-containing polypeptides. *J Mol Biol.* (1996) 263:768–75.
170. Marquette A, Salnikov E, Glattard E, Aisenbrey C, Bechinger B. Magainin 2-PGLa interactions in membranes - two peptides that exhibit synergistic enhancement of antimicrobial activity. *Curr Top Med Chem.* (2015) 16:65–75. doi: 10.2174/1568026615666150703115701
171. Juhl DW, Glattard E, Aisenbrey C, Bechinger B. Antimicrobial peptides: mechanism of action and lipid-mediated synergistic interactions within membranes. *Faraday Discuss.* (2020).

172. Cuervo JH, Rodriguez B, Houghten RA. The Magainins: sequence factors relevant to increased antimicrobial activity and decreased hemolytic activity. *Pept Res.* (1988) 1:81–6.
173. Strandberg E, Zerweck J, Horn D, Pritz G, Berditsch M, Bürck J, et al. Influence of hydrophobic residues on the activity of the antimicrobial peptide magainin 2 and its synergy with PGLa. *J Pept Sci.* (2015) 21:436–45. doi: 10.1002/psc.2780
174. Han E, Lee H. Synergistic effects of magainin 2 and PGLa on their heterodimer formation, aggregation, and insertion into the bilayer. *RSC Adv.* (2015) 5:2047–55. doi: 10.1039/C4RA08480B
175. Pino-Angeles A, Leveritt JM III, Lazaridis T. Pore structure and synergy in antimicrobial peptides of the magainin family. *PLoS Comput Biol.* (2016) 12:e1004570. doi: 10.1371/journal.pcbi.1004570
176. Russ WP, Engelman DM. The GxxxG motif: a framework for transmembrane helix-helix association. *J Mol Biol.* (2000) 296:911–9. doi: 10.1006/jmbi.1999.3489
177. Bechinger B, Kinder R, Helmle M, Vogt TB, Harzer U, Schinzel S. Peptide structural analysis by solid-state NMR spectroscopy. *Biopolymers.* (1999) 51:174–90.
178. Hara T, Kodama H, Kondo M, Wakamatsu K, Takeda A, Tachi T, et al. Effects of peptide dimerization on pore formation: antiparallel disulfide-dimerized magainin 2 analogue. *Biopolymers.* (2001) 58:437–46. doi: 10.1002/1097-0282(20010405)58:4<437::AID-BIP1019>3.0.CO;2-I
179. Lorenzon EN, Santos-Filho NA, Ramos MA, Bauab TM, Camargo IL, Cilli EM. C-terminal lysine-linked magainin 2 with increased activity against multidrug-resistant bacteria. *Protein Pept Lett.* (2016) 23:738–47. doi: 10.2174/0929866523666160511150907
180. Dempsey CE, Ueno S, Avison MB. Enhanced membrane permeabilization and antibacterial activity of a disulfide-dimerized magainin analogue. *Biochemistry.* (2003) 42:402–9. doi: 10.1021/bi026328h
181. Verly RM, Resende JM, Junior EFC, De Magalhães MTC, Guimarães CFCR, Munhoz VHO, et al. Structure and membrane interactions of the homodimeric antibiotic peptide homotarsinin. *Sci Rep.* (2017) 7:40854. doi: 10.1038/srep40854
182. Raimondo D, Andreotti G, Saint N, Amodeo P, Renzone G, Sanseverino M, et al. A folding-dependent mechanism of antimicrobial peptide resistance to degradation unveiled by solution structure of distinctin. *Proc Natl Acad Sci USA.* (2005) 102:6309–14. doi: 10.1073/pnas.0409004102
183. Dalla Serra M, Cirioni O, Vitale RM, Renzone G, Coraiola M, Giacometti A, et al. Structural features of distinctin affecting peptide biological and biochemical properties. *Biochemistry.* (2008) 47:7888–99. doi: 10.1021/bi800616k
184. Verardi R, Traaseth NJ, Shi L, Porcelli F, Monfregola L, De Luca S, et al. Probing membrane topology of the antimicrobial peptide distinctin by solid-state NMR spectroscopy in zwitterionic and charged lipid bilayers. *Biochim Biophys Acta.* (2011) 1808:34–40. doi: 10.1016/j.bbamem.2010.08.008
185. Vermeer LS, Hamon L, Schirer A, Schoup M, Cosette J, Majdoul S, et al. The transduction enhancing peptide vectofusin-1 forms pH-dependent α-helical coiled-coil nanofibrils, trapping viral particles. *Acta Biomater.* (2017) 64:259–68. doi: 10.1016/j.actbio.2017.10.009
186. Lague P, Zuckermann MJ, Roux B. Lipid-mediated interactions between intrinsic membrane proteins: dependence on protein size and lipid composition. *Biophys J.* (2001) 81:276–84. doi: 10.1016/S0006-3495(01)75698-6
187. Duneau JP, Sturgis JN. Lateral organization of biological membranes: role of long-range interactions. *Eur Biophys J.* (2013) 42:843–50. doi: 10.1007/s00249-013-0933-x
188. Bitbol A-F, Constantin D, Fournier J-B. Membrane-mediated interactions. *arXiv preprint* arXiv:1903.05712 (2018).
189. Chen H-C, Brown JH, Morell JL, Huang CM. Synthetic magainin analogues with improved antimicrbial activity. *FEBS Lett.* (1988) 236:462–6.
190. Bevins CL, Zasloff M. Peptides from frog skin. *Annu Rev Biochem.* (1990) 59:395–441.
191. Wieprecht T, Apostolov O, Seelig J. Binding of the antibacterial peptide magainin 2 amide to small and large unilamellar vesicles. *Biophys Chem.* (2000) 85:187–98. doi: 10.1016/S0301-4622(00)00120-4
192. Bechinger B. Rationalizing the membrane interactions of cationic amphipathic antimicrobial peptides by their molecular shape. *Curr Opin Colloid Interface Sci Surf.* (2009) 14:349–55. doi: 10.1016/j.cocis.2009.02.004

Conflict of Interest: The authors declare that the research was conducted in the absence of any commercial or financial relationships that could be construed as a potential conflict of interest.

frontiers in Medical Technology

MINI REVIEW
published: 11 January 2021
doi: 10.3389/fmedt.2020.621572

Deuterium Solid State NMR Studies of Intact Bacteria Treated With Antimicrobial Peptides

*Valerie Booth**

Department of Biochemistry and Department of Physics and Physical Oceanograpy, Memorial University of Newfoundland, St. John's, NL, Canada

Solid state NMR has been tremendously useful in characterizing the structure and dynamics of model membranes composed of simple lipid mixtures. Model lipid studies employing solid state NMR have included important work revealing how membrane bilayer structure and dynamics are affected by molecules such as antimicrobial peptides (AMPs). However, solid state NMR need not be applied only to model membranes, but can also be used with living, intact cells. NMR of whole cells holds promise for helping resolve some unsolved mysteries about how bacteria interact with AMPs. This mini-review will focus on recent studies using ^{2}H NMR to study how treatment with AMPs affect membranes in intact bacteria.

Keywords: HDP, AMP, intact bacteria, whole cell NMR, solid state NMR, magic angle spinning (MAS), lipid membrane, bilayer

OPEN ACCESS

Edited by:
Lorenzo Stella,
University of Rome Tor Vergata, Italy

Reviewed by:
Tuo Wang,
Louisiana State University, United States
Francesca M. Marassi,
Sanford Burnham Prebys Medical Discovery Institute, United States

***Correspondence:**
Valerie Booth
vbooth@mun.ca

Specialty section:
This article was submitted to Pharmaceutical Innovation, a section of the journal Frontiers in Medical Technology

Received: *26 October 2020*
Accepted: *10 December 2020*
Published: *11 January 2021*

Citation:
Booth V (2021) Deuterium Solid State NMR Studies of Intact Bacteria Treated With Antimicrobial Peptides. Front. Med. Technol. 2:621572. doi: 10.3389/fmedt.2020.621572

BRIDGING BIOPHYSICAL AND FUNCTIONAL STUDIES

Much attention has been given to the mechanisms by which AMPs disrupt the membrane bilayers of bacterial cells, permeabilizing them and dissipating the membrane potential (1–3). However, not all AMPs disrupt membranes via the same mechanism and some AMPs have been shown to have targets other than membranes (4–6). Additionally, there are AMPs that have been shown to modulate the immune response of the host organism (7, 8), in which case they are more properly referred to as host defense peptides (HDPs).

A major challenge in AMP research has been in developing a unified picture of AMP mechanism(s) that is consistent, at least for the particular AMP under scrutiny, with the results from a spectrum of experimental approaches, from simple model systems to whole cells to whole organisms. For example, on the one hand, function is often studied via minimal inhibitory concentration (MIC) assays with bacteria, which indicate the minimum concentration of AMP needed to prevent bacterial growth (9–11). On the other hand, NMR and other biophysical studies provide details of AMP structure and AMP-induced alterations to the bilayer structure, such as bilayer thinning, formation of toroidal pores, solubilizing the membrane into micellar structures, or lipid clustering (1, 12–14). Such "biophysical" studies typically employ model lipid systems with ∼1–3 different types of lipids. Likewise, relating an AMP's membrane disruption mechanism in one model lipid system with its behavior in a different model lipid system is not always straightforward. As pointed out by Bechinger and Lohner (3, 15, 16) the lipid structure promoted by a particular AMP is perhaps best thought of in terms of a phase diagram, where the lipid arrangement promoted by the AMP is a function of several parameters including peptide-to-lipid ratio, intrinsic curvature of the lipids, temperature, salt, and pH. This way of thinking has the potential to unify findings when a particular AMP is observed to promote one type of lipid structure under one set of conditions, but a different type of lipid structure under a different set of conditions.

In order to compare AMP study results from cells to those from liposomes, a number of workers have tried to determine, from experimental data, the molar AMP to lipid (AMP:L) ratio needed to see growth inhibition in cells and the AMP:L ratio needed to see liposome disruption *in vitro*. A decade ago, Wimley estimated that for typical experimental conditions the molar bound AMP:L ratio was about 1:200 for liposomes and about 10–100:1 for cells (17). Around the same time, Melo et al. (18) used partition constants to link the two types of experiments. For the two AMPs for which they had both *in vitro* and *in vivo* data, omiganan and melittin, they found that the cell-bound AMP:L ratio was 2.3–9.2 times higher than the threshold needed to see effects on liposomes. As reviewed in (19), the amount of cell-bound AMP at the minimum bactericidal concentration (MBC) has been measured via fluorescently labeled AMP or via separation of unbound and cell-bound AMP via centrifugation. Depending on the peptide, the AMP:L ratios for binding to *E. coli* ranged from ∼1:3 to 5:1.

There are a number of potential reasons for a difference in AMP:L ratios between *in vitro* and *in vivo* studies. For instance, some AMPs may bind targets in addition to lipids, including intracellular targets (20–25), and/or non-lipid components of the cell envelope, such as lipopolysaccharide (LPS), peptidoglycan (PGN), teichoic acids (TA), or membrane proteins (**Figures 1E,F**) (26–30). With regards to cell envelope interactions, two divergent potential effects have been suggested. One possibility is that non-lipid cell envelope components may entrap AMPs, sequestering them away from the lipid bilayer and thus protecting the cell. On the other hand, the non-lipid cell envelope components, especially those with a net negative charge, may attract more AMPs toward cells, leading to more AMP accumulating on the lipid bilayer and thus more damage.

Another aspect of AMP studies where it is vital to link the basic research with model lipid systems that probe AMP mechanism to AMP behavior in more complex systems, is in optimizing AMPs for systemic use in humans. Physiological levels of salt may substantially reduce the membrane-disrupting activities of AMPs (31, 32). AMP binding to serum proteins may reduce their availability to bind the target cells, e.g., bacteria or cancer cells (33, 34). Protease activity may reduce the half-life of peptides in the bloodstream, which, interestingly, could be counteracted by AMP aggregation (34–36). Particularly for histidine-rich peptides, pH can have a large impact on activity (9, 37–39), which can be exploited to confer increased AMP activity around tumors where the pH is low (40, 41) or in helping AMPs escape lysosomes/endosomes (42–44). And of course, optimizing the selectivity of AMPs toward the target cells and minimizing host cell toxicity is always of paramount concern.

In order to understand the fundamentals of how this important class of molecules function, as well as to effectively deploy AMPs in the clinic, it is critical to address the afore-mentioned gaps between the *in vivo* function of AMPs, with detailed studies of AMP mechanism in model lipid systems. This objective is starting to be addressed with a variety of approaches that provided high resolution data on AMPs interacting with whole cells, including atomic force microscopy (45–47), electron microscopy (48, 49), Fourier Transform InfraRed (FTIR) spectroscopy (46), differential scanning calorimetry (DSC) (21), and confocal microscopy with fluorescently labeled peptides (50, 51). However, the rest of this mini-review will focus on ^{2}H solid state NMR studies of AMPs interacting with whole cells.

NMR APPROACHES FOR STUDYING AMPs INTERACTING WITH WHOLE CELLS

NMR has a number of advantages for studying AMP mechanisms: (1) it provides atomic resolution data on the structure of both the peptide and lipid components of the system; (2) NMR can be used to characterize the dynamical behavior of peptides and lipids; (3) NMR experiments can be carried out in physiological-like solution conditions; (4) the isotope labels on the lipids and peptides have very little potential to disturb the systems under study, in contrast to, for example, fluorescent labeling; and (5) isotope labels provide the ability to observe selected molecules, i.e., peptides or the lipids, within the context of much more complicated systems, including whole bacteria. For these reasons, there are many NMR studies of AMPs in the literature, although by far the greatest number are in model systems, rather than in whole cells.

There are a variety of ways NMR has traditionally been employed to study AMPs in model systems (**Figures 1A–D**). Solution NMR can supply atomic resolution structures of AMPs in solution or, more commonly, in membrane-mimetic systems such as detergent or lyso-lipid micelles (**Figure 1A**) (52–56). Solid state NMR of ^{15}N- or ^{13}C- labeled AMPs in physically oriented bilayers provides residue-specific information on the helicity of the AMP as well as the angle between the helical segment(s) and the bilayer normal (**Figure 1B**) (3, 57–60). Complementary to the information provided by NMR-active nuclei within the AMP, solid state NMR in liposome or oriented lipid samples also offers structural and dynamical data on the lipids in the system. ^{31}P-NMR is frequently used to report on the behavior of the lipid headgroups (**Figure 1C**), while ^{2}H-NMR with acyl chain deuterated lipids reveals the structure and dynamics at specific locations along the acyl chain (**Figure 1D**). With ^{31}P-NMR one can learn about AMP-induced changes in phospholipid headgroup structure and dynamics, as well as probe for preferential interactions between the AMP and individual components of lipid mixtures (60–62). ^{2}H-NMR is commonly used to observe AMP-induced alterations in the order parameter profile of the deuterated lipid acyl chains and in many cases indicates that the presence of the AMP disturbs the acyl chains in a manner consistent with the AMP positioning near the polar/apolar interface (63–65). Solid state REDOR NMR is used to measure the distance between an isotope labeled nucleus on an AMP to specific atoms in the lipids, e.g., ^{31}P or ^{13}C (66, 67). ^{1}H and ^{19}F spin diffusion have been used to measure AMP to lipid distances and determine AMP oligomeric state in the bilayer (68, 69).

NMR approaches have been adapted for the study of whole cells in a variety of ways. One relatively well-developed approach is the application of solution NMR to proteins or nucleic acids inside whole cells that range from bacterial to human cells (70,

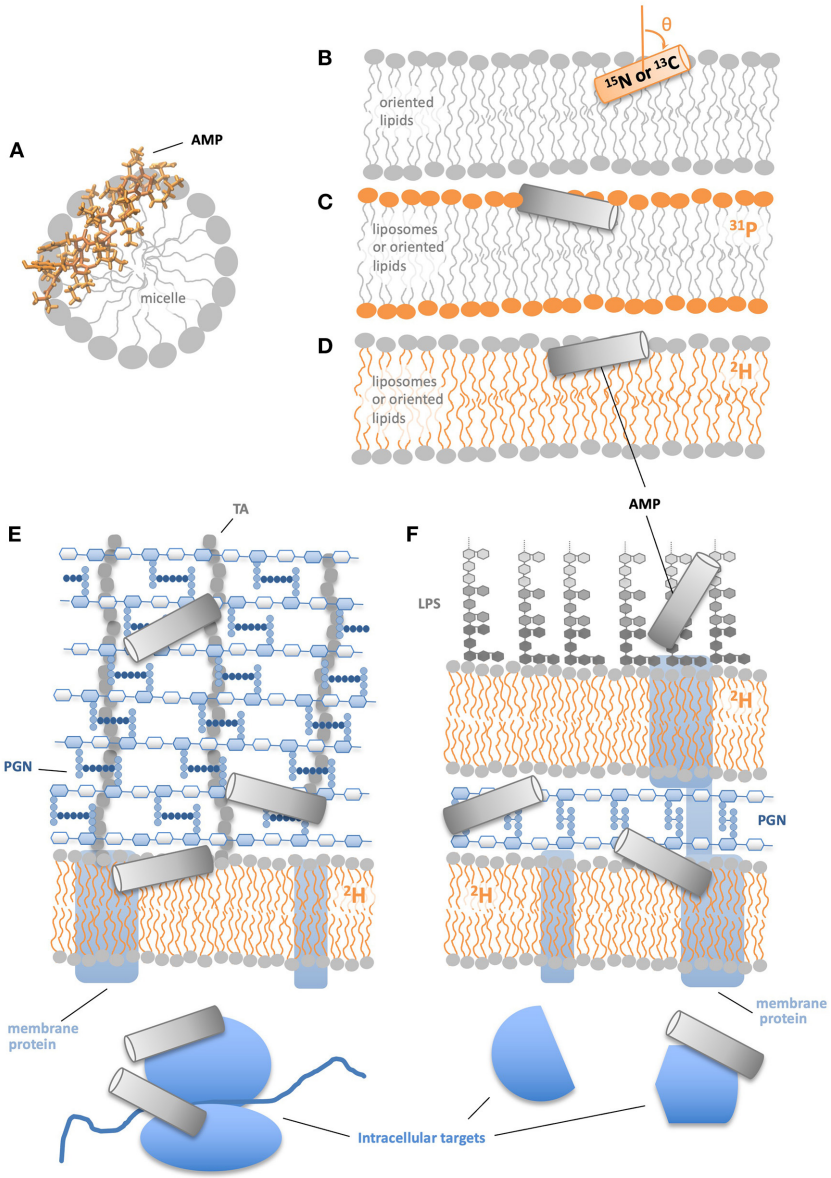

FIGURE 1 | NMR approaches to study AMP structural mechanisms. **(A)** Solution NMR provides atomic resolution structures of AMPs in micelles. **(B)** Solid state NMR of ^{15}N or ^{13}C labeled peptides in physically oriented bilayers indicates residue-specific helicity and angle of helical segments relative to the bilayer. **(C)** ^{13}P solid state NMR of bilayers with a AMPs shows the effect of AMPs on lipid head groups. **(D)** ^{2}H solid state NMR of AMPs in bilayers show the effect of AMPs on lipid acyl chains. ^{2}H NMR of membrane deuterated Gram(+) **(E)** and Gram(–) bacteria **(F)** indicate how AMPs' effects on lipid acyl chains are modified by non-lipid cell components.

71). Solution NMR strategies include recombinant expression of the protein of interest, or delivery of the proteins from the outside via electroporation or linkage to cell penetrating peptides (72–74). Solution NMR has also been employed to probe AMP binding to the fungus *C. neoformans* as well as to probe AMP-DNA binding via ^{1}H NMR of whole cells (75). Membrane proteins and large, soluble proteins in whole cells and whole organelles have been studied with solid state NMR techniques and have benefited from developments like amino acid selective isotope labeling and sensitivity enhancement from dynamic nuclear polarization (76–79). Magic Angle Spinning (MAS)-NMR has been used to study the carbohydrates in the cell envelopes of both unlabelled and selectively isotope-labeled bacteria, including how the carbohydrates are affected by antimicrobial agents (80–82). The molecular architecture of intact fungal cell walls has been probed via ^{13}C correlation spectroscopy (83, 84). ^{13}C MAS spectra report on both the PGN and TA components of cell envelopes and ^{15}N MAS reveals details of the peptidic components of the cell envelope. Two-dimensional ^{13}C NMR has also been used to study starch granules

in intact cells (85). Overall et al. (86) have shown how ^{31}P can be used to study AMPs' interactions with whole cells. In this context ^{31}P reports primarily on nucleic acids, but also contains some information on phospholipid headgroups. The Booth and Marcotte groups independently pioneered ^{2}H-NMR methods to study AMPs interacting with membrane-deuterated bacteria (87, 88). The remainder of this mini-review will focus on the ^{2}H-NMR work in intact cells.

^{2}H NMR OF MEMBRANE-DEUTERATED BACTERIA

The first ^{2}H-NMR spectra of membrane-deuterated bacteria were attained in the early 80s by the Davis group (89). In more recent work aimed at using ^{2}H-NMR to study how AMPs interact with bacteria (**Figures 1E,F**), researchers have employed two different approaches to incorporating ^{2}H-labels into the bacterial membranes. The first strategy uses a mutant strain of *Escherichia coli (E. coli)*, unable to either metabolize or synthesize fatty acids (87). The mutant bacteria are grown in the presence of deuterated palmitic acid (PA) and un-deuterated oleic acid. The second approach employs unmutated bacteria [Gram(+) or Gram(–)] which, during growth, are supplied with deuterated PA complexed with dodecylphosphocholine (DPC) micelles to facilitate uptake of the PA (88, 90). For the bacteria to remain healthy and maintain a normal acyl chain composition in their membranes, it is important to also provide oleic acids in the correct proportion to PA, which varies depending on the type of bacteria (90, 91). The two methods of isotope labeling lead to very similar, but not identical spectra of *E. coli*, likely due to variations in lipid composition introduced by the different growth protocols (Kumari, Morrow, and Booth, publication in preparation). Thus far, the approach has been applied to both Gram(–) and Gram(+) bacteria in the absence and presence of AMPs, as well as to microalgae (87, 90–98). The viability of the bacteria during NMR data acquisition depends both on optimization of the growth conditions, as well as the length of the NMR experiment, but, with care, ∼80% of the bacteria remain able to metabolize and divide, even after 8 h in the NMR spectrometer at 37°C (87). Moreover, the NMR spectra obtained from the cells remain largely unchanged up to ∼10 h after the cells are prepared.

Two types of NMR spectra can be obtained from the membrane-deuterated bacteria, static spectra and MAS spectra. Both types of experiments provide information of key importance to understanding how AMPs interact with membranes. From the NMR spectra, it is possible to derive the degree of acyl chain order and thus the amount of membrane disruption induced by the AMP. **Figure 2** shows static spectra for the Gram (–) bacteria *E. coli* and the Gram (+) bacteria *Bacillus subtilis (B. subtilis)*, MAS spectra for *E. coli,* and for comparison, a static spectrum with lipids alone. Starting with the lipid-only spectrum, the key features to note are as follows. There is a prominent edge at ∼±12.5 kHz that derives largely from the acyl chain deuterons located near the lipid head groups. The deuterons at the opposite end of the acyl chain, i.e., the methyl groups, give rise to the intense pair of peaks near the center of the spectrum. Offering attention to these two regions of the spectra serves to illustrate the most important feature of ^{2}H-NMR of lipids, especially as applied to the study of AMPs; large splittings correspond to greater orientational ordering of the lipid acyl chains with respect to the bilayer normal, while small splittings indicate disorder. Thus, the deuterated methyl groups in the disordered center of the bilayer give rise to small splittings, whereas the deuterons on the acyl chains near the head groups are more ordered and thus contribute to peaks with larger splittings. The essential takeaway for application of the technique to AMPs, is that the bilayer disruptions caused by AMPs are generally observed as a narrowing in the splittings.

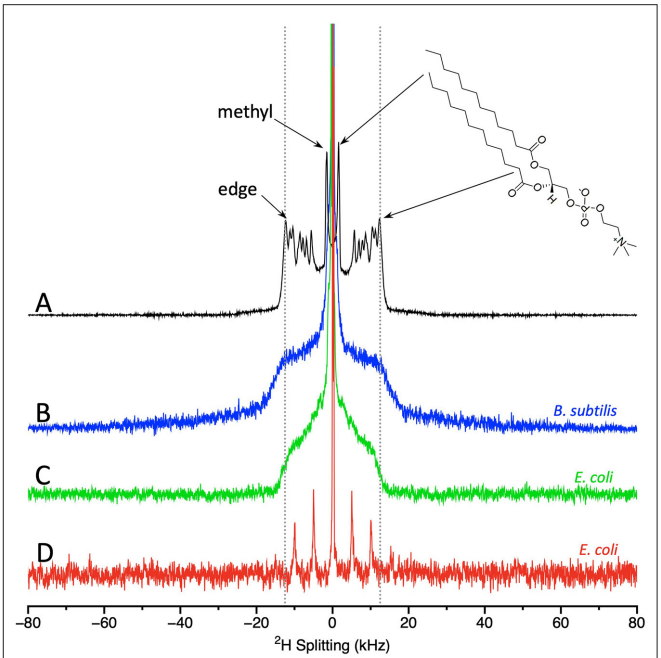

FIGURE 2 | Static solid state NMR spectra of **(A)** model lipids, i.e., dilauroyl phosphatidylcoholine-d_{46} (DLPC-d_{46}); **(B)** ^{2}H-labeled *B. subtilis;* and **(C)** ^{2}H-membrane labeled *E. coli*. MAS NMR spectra of **(D)** ^{2}H-membrane labeled *E. coli*. DLPC spectra acquired at 25°C and the bacterial spectra acquired at 37°C. DLPC spectrum provided by Michael Morrow and Tim Porter. *B. subtilis and E. coli* static spectra as in (91, 99) provided by Nury Paula Sanisteban. MAS *E. coli* spectrum provided by Sarika Kumari.

Turning to the static spectra of the membrane deuterated bacteria (**Figures 2B,C**), it is clear that many of the finer details seen in the lipid-only spectra are lost. This outcome is not surprising given that in bacteria the deuterons will be found on different types of phospholipids, and even the same phospholipids may well be located in different microenvironments. However, some key features of the spectra are retained. The prominent edge at ∼±12.5 kHz (from deuterons near the headgroup) can still be observed with the same splitting as for the lipid-only samples. The methyl groups can also be observed in the spectra of *E. coli.* Although the spectra from *E. coli* and *B. subtilis* share the prominent edge at ∼±12.5 kHz, consistent with lipids in liquid crystalline phase,

there are differences in the shape of the bacterial spectra between ∼±4–8 kHz. MAS NMR of *E. coli* provide similar information to the static spectra and have the significant advantage of a much shorter acquisition time (98). The MAS spectrum of *E. coli* display a central peak plus 3 pairs of spinning sidebands (**Figure 2D**). To compare the spectra, especially those from MAS to those acquired statically, it is useful to extract quantitative measures from the spectra.

The measures in common use are the first and second moments, M_1 and M_2, as well as Δ_2, a parameter derived from M_1 and M_2 (right-hand panel of **Figure 3**). M_1 and M_2 are proportional to the frequency-weighted averages of the lipid acyl chain order parameters. Thus, larger values of M_1 and M_2 indicate relatively well-ordered lipid acyl chains. Δ_2 is a useful measure of the overall shape of the spectra (95, 100). As an example, these quantitative parameters provide a way to assess an important issue for living, complex and sensitive biological samples, i.e., how consistent the spectra and moments are from sample to sample. This has been characterized, in particular by Santisteban et al. (91) who found that for 6 sample preparations of *B. subtilis*, the standard deviation in Δ_2 was 5%, while for 5 sample preparations of *E. coli it* was 9% (99).

WHAT ^{2}H-NMR OF WHOLE CELLS HAS TAUGHT US ABOUT AMP-CELL INTERACTIONS SO FAR

Addition of AMPs to bacteria leads to striking changes in the ^{2}H NMR spectra, indicating substantial disruption of the lipid bilayers. Static spectra of *B. subtilis* and *E. coli* with and without 20% (by dry weight of bacteria) of the AMP MSI-78 are shown in **Figure 3**. MSI-78 causes a reduction in the intensity at large splittings with a concomitant increase in intensity at the smaller splittings, indicating the peptide induces disorder in the lipid acyl chains. These changes can be quantified as reduction in M_1 and M_2, and an increase in Δ_2 with the addition of AMP (**Figure 3**). Similar AMP-induced changes are seen in ^{2}H spectra of model lipids, e.g., (101). What is remarkable is that the same observation can be made in the context of whole, intact, living bacteria.

In addition to MSI-78 (87, 90–92, 95), ^{2}H-NMR of membrane deuterated bacteria has also been performed with the AMPs CAME, BP100 (91, 95), caerin 1.1 and aurein 1.2 (94), as well as antibiotics polymyxin B and fullerenol nanoparticles (88). All the AMPs tested thus far induce similar changes in the NMR spectra, consistent with similar peptide-lipid interactions. One way to consider the uniqueness of AMPs' effects on lipid bilayers in bacteria is to compare their effects to other means of disrupting lipids. Neither mechanical lysis of cells, nor organic solvent lipid extraction leads to alterations in the ^{2}H NMR spectra (91, 99). Hence it appears the AMPs' effects on lipids are quite distinctive, and that intact, living cells are unable to repair the damage from AMPs, unlike the self-repair of the bilayer that happens after mechanical lysis or lipid extraction.

Perhaps the most instructive aspect of the work thus far is the consideration of the bound AMP:L ratios needed to see changes in the ^{2}H-NMR spectra of intact bacteria. Assuming that most of the MSI-78 binds to the cells, which is reasonable given the large positive charge of the peptide, the high concentration of cells during treatment, and low amount of protein measured in the supernatant after the AMP-treated cells are centrifuged, about thirty times more peptide is required to see lipid disruption in intact cells than is needed in ^{2}H-NMR studies of AMPs in model lipid systems (87, 101). Consequently, there must be something present in the cells that is protecting the bilayer from disruption, either by directly stabilizing the bilayer, and/or by sequestering AMPs away from the bilayer. And whichever cell component(s) this effect is coming from, it seems to be present in both Gram(+) and Gram(–) cells. Possibilities abound (**Figures 1E,F**). Non-lipid components of the cell envelope such as LPS, PGN, or TA could be stabilizing the bilayer and/or sequestering the AMPs away from the bilayer. Membrane proteins and intracellular molecules are also potential targets for AMPs. In fact, MSI-78 has been shown to disrupt the thermal stability of ribosomes and inhibit transcription (21). Thus, the work with the limited selection of AMPs proved via ^{2}H-labeled whole cell NMR so far is consistent with a multi-hit mechanism (1, 5, 17, 20, 102–104). Conversely, there are several AMPs for which the biological activity of the L- and D-amino acid versions of the peptide are similar [reviewed in Savini et al. (19)], arguing that if these peptides have additional targets beyond the membrane, the interactions are not specific enough to be disrupted by the switch to the alternate enantiomer.

Turning next to the other end of the AMP:L ratio spectrum, for MSI-78 the AMP:L ratio needed to see membrane disruption in ^{2}H-NMR spectra (∼1:1) of intact cells is of the same order, but slightly greater, than the predicted values of cell-bound AMP:L (1:2.5–28:1) for a suite of 6 AMPs (18) and the observed membrane-bound PMAP-23 at the MBC in cells (19, 105). We have used flow cytometry to analyze cells treated with MSI-78 under conditions identical to the NMR experiments and found that for the AMP:L concentration shown in **Figure 3**, there is no MSI-78-induced increase in cell permeability. Since the NMR experiments reveal major disruptions to the lipid bilayer at AMP:lipid ratios lower than what is lethal, it seems possible that AMP is getting across the bilayer to the inside of the cells (**Figures 1E,F**). Again, this is consistent with the suggestion that at least some AMPs have intra-cellular targets, and that for at least some AMPs, membrane disruption may not the only mechanism by which the AMP harms cells.

FUTURE PROSPECTS

^{2}H-NMR of membrane-deuterated bacteria could be expanded in a variety of potentially fruitful ways. Firstly, given that different AMPs are likely to function via different mechanisms or sets of mechanisms, it is important not to over-generalize the results from the limited number of AMPs probed so far. Performing similar experiments with a greater variety of AMPs may help reveal variations in lipid interactions with whole cells. Similarly, it will be interesting to expand the work from AMPs to cell penetrating peptides (CPPs) which transverse the bilayer, but

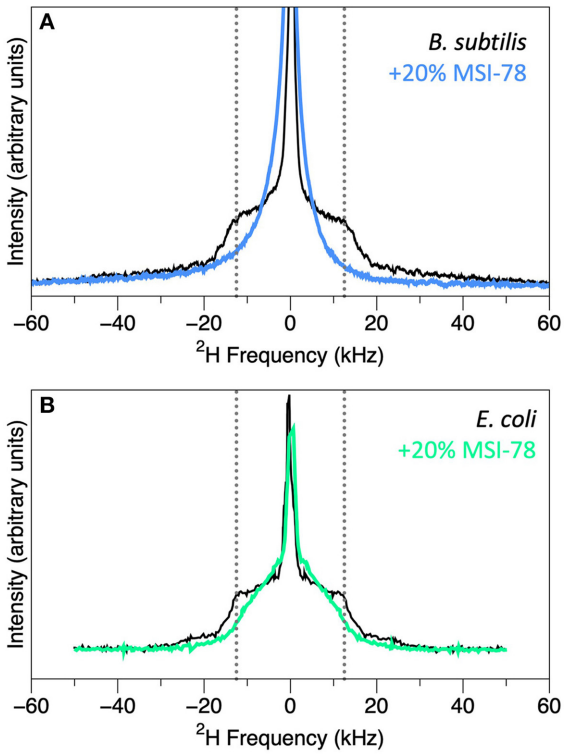

	M_1 ($\times 10^4$ s^{-1})	M_2 ($\times 10^9$ s^{-2})	Δ_2
B. subtilis	6.2	8.4	0.59
+20% MSI-78	4.4	6.5	1.45

	M_1 ($\times 10^4$ s^{-1})	M_2 ($\times 10^9$ s^{-2})	Δ_2
E. coli	4.6	3.7	0.27
+20% MSI-78	3.6	2.5	0.37

FIGURE 3 | Spectra of membrane-deuterated *B. subtilis* **(A)** and *E. coli* **(B)** without (black) and with the addition of 20% (by weight) of AMP MSI-78 (blue and green), along with the M_1, M_2, and Δ_2 values calculated from the spectra. *B. subtilis* spectra from Nury Paula Santisteban as in (91) and *E. coli* spectra from James Pius as in (87).

do not induce the membrane permeabilization characteristic of many AMPs (22, 106–108).

The ^{2}H-NMR approach can also be adapted to probe the role of non-lipid cell components in modulating AMP-lipid interactions. Preliminary work in our group has been done to manipulate LPS and PGN layers to monitor how disrupting these components affects the cytoplasmic membrane in the absence and presence of AMPs. Gentle disruption of the carbohydrate portion of LPS in Gram(−) bacteria results in a slight increase in lipid bilayer disorder, and slightly sensitizes cells to lipid membrane disruption by AMPs. Similarly, disruption of the PGN component of Gram(+) bacteria causes a slight increase in membrane disorder, but unlike LPS disruption, has no detectable effect on AMP-lipid interactions. Since Gram(+) bacterial cell envelopes also have negatively charged TA, it will be interesting to see how disrupting TA affects interactions with positively charged AMPs.

Another exciting prospect is to broaden the approach from bacteria to eukaryotic cells. Such experiments will need to be optimized to incorporate sufficient levels of deuteration into eukaryotic cell membranes. Given the much larger size of most eukaryotic cells compared to bacteria, and the consequent decrease in the ratio of amount of cytoplasmic membrane to the rest of the biomolecules in the cells, signal-to-noise in the NMR spectra may prove to be a challenge. Focussing on smaller types of eukaryotic cells, or organelles such as mitochondria, may be a more achievable. Another feasible prospect would be to carry out experiments with AMPs and deuterated bacteria in the presence of unlabelled eukaryotic cells, which would give a sense of the selectivity of the AMP for the bacterial membranes. Furthermore, studying AMP-resistant cells with NMR may help reveal how the cell envelope alterations of the resistant cells affect the ability of the AMP to disrupt the lipid membranes.

AUTHOR CONTRIBUTIONS

The author confirms being the sole contributor of this work and has approved it for publication.

ACKNOWLEDGMENTS

The author gratefully acknowledges continuing support from the National Sciences and Engineering Council of Canada (NSERC) (RG PIN 05154), as well as a long-term collaboration with Dr. Michael Morrow and many helpful discussions about ^{2}H NMR and AMP-lipid interactions.

REFERENCES

1. Nguyen LT, Haney EF, Vogel HJ. The expanding scope of antimicrobial peptide structures and their modes of action. *Trends Biotechnol.* (2011) 29:464–72. doi: 10.1016/j.tibtech.2011.05.001
2. Faust JE, Yang PY, Huang HW. Action of antimicrobial peptides on bacterial and lipid membranes: a direct comparison. *Biophys J.* (2017) 112:1663–72. doi: 10.1016/j.bpj.2017.03.003
3. Aisenbrey C, Marquette A, Bechinger B. The mechanisms of action of cationic antimicrobial peptides refined by novel concepts from biophysical investigations. In: Matsuzaki K, editor. *Antimicrobial Peptides, Advances in Experimental Medicine and Biology, 1117*. Singapore: Springer Nature (2019). p. 33–64. doi: 10.1007/978-981-13-3588-4_4
4. Brogden KA. Antimicrobial peptides: pore formers or metabolic inhibitors in bacteria? *Nat Rev Microbiol.* (2005) 3:238–50. doi: 10.1038/nrmicro1098
5. Marcos JF, Gandia M. Antimicrobial peptides: to membranes and beyond. *Expert Opin Drug Discov.* (2009) 4:659–71. doi: 10.1517/17460440902992888
6. Scocchi M, Mardirossian M, Runti G, Benincasa M. Non-membrane permeabilizing modes of action of antimicrobial peptides on bacteria. *Curr Top Med Chem.* (2016) 16:76–88. doi: 10.2174/1568026615666150703121009
7. Niyonsaba F, Kiatsurayanon C, Chieosilapatham P, Ogawa H. Friends or Foes? Host defense (antimicrobial) peptides and proteins in human skin diseases. *Exp Dermatol.* (2017) 26:989–98. doi: 10.1111/exd.13314
8. Haney EF, Straus SK, Hancock REW. Reassessing the host defense peptide landscape. *Front Chem.* (2019) 7:43. doi: 10.3389/fchem.2019.00043
9. McDonald M, Mannion M, Pike D, Lewis K, Flynn A, Brannan AM, et al. Structure-function relationships in histidine-rich antimicrobial peptides from Atlantic cod. *Biochim Biophys Acta.* (2015) 1848:1451–61. doi: 10.1016/j.bbamem.2015.03.030
10. Chen X, Zhang L, Ma C, Zhang Y, Xi X, Wang L, et al. A novel antimicrobial peptide, Ranatuerin-2PLx, showing therapeutic potential in inhibiting proliferation of cancer cells. *Biosci Rep.* (2018) 38:BSR20180710. doi: 10.1042/BSR20180710
11. Barroso C, Carvalho P, Carvalho C, Santarém N, Gonçalves JFM, Rodrigues PNS, et al. The diverse piscidin repertoire of the European sea bass (*dicentrarchus labrax*): molecular characterization and antimicrobial activities. *Int J Mol Sci.* (2020) 21:4613. doi: 10.3390/ijms21134613
12. Shai Y. Mechanism of the binding, insertion and destabilization of phospholipid bilayer membranes by alpha-helical antimicrobial and cell non-selective membrane-lytic peptides. *Biochim Biophys Acta.* (1999) 1462:55–70. doi: 10.1016/S0005-2736(99)00200-X
13. Mahlapuu M, Håkansson J, Ringstad L, Björn C. Antimicrobial peptides: an emerging category of therapeutic agents. *Front Cell Infect Microbiol.* (2016) 6:194. doi: 10.3389/fcimb.2016.00194
14. Epand RM. Anionic lipid clustering model. *Adv Exp Med Biol.* (2019) 1117:65–71. doi: 10.1007/978-981-13-3588-4_5
15. Bechinger B, Lohner K. Detergent-like actions of linear amphipathic cationic antimicrobial peptides. *Biochim Biophys Acta.* (2006) 1758:1529–39. doi: 10.1016/j.bbamem.2006.07.001
16. Bechinger B. Insights into the mechanisms of action of host defence peptides from biophysical and structural investigations. *J Pept Sci.* (2011) 17:306–14. doi: 10.1002/psc.1343
17. Wimley WC. Describing the mechanism of antimicrobial peptide action with the interfacial activity model. *ACS Chem Biol.* (2010) 5:905–17. doi: 10.1021/cb1001558
18. Melo MN, Ferre R, Castanho MA. Antimicrobial peptides: linking partition, activity and high membrane-bound concentrations. *Nat Rev Microbiol.* (2009) 7:245–50. doi: 10.1038/nrmicro2095
19. Savini F, Bobone S, Roversi D, Mangoni Maria L, Stella L. From liposomes to cells: filling the gap between physicochemical and microbiological studies of the activity and selectivity of host-defense peptides. *Pept Sci.* (2018) 110:e24041. doi: 10.1002/pep2.24041
20. Jenssen H, Hamill P, Hancock RE. Peptide antimicrobial agents. *Clin Microbiol Rev.* (2006) 19:491–511. doi: 10.1128/CMR.00056-05
21. Brannan AM, Whelan WA, Cole E, Booth V. Differential scanning calorimetry of whole *Escherichia coli* treated with the antimicrobial peptide MSI-78 indicate a multi-hit mechanism with ribosomes as a novel target. *PeerJ.* (2015) 3:e1516. doi: 10.7717/peerj.1516
22. Sani MA, Separovic F. How membrane-active peptides get into lipid membranes. *Acc Chem Res.* (2016) 49:1130–8. doi: 10.1021/acs.accounts.6b00074
23. Libardo MDJ, Bahar AA, Ma B, Fu R, McCormick LE, Zhao J, et al. Nuclease activity gives an edge to host-defense peptide piscidin 3 over piscidin 1, rendering it more effective against persisters and biofilms. *FEBS J.* (2017) 284:3662–83. doi: 10.1111/febs.14263
24. Vasilchenko AS, Rogozhin EA. Sub-inhibitory effects of antimicrobial peptides. *Front Microbiol.* (2019) 10:1160. doi: 10.3389/fmicb.2019.01160
25. Savini F, Loffredo MR, Troiano C, Bobone S, Malanovic N, Eichmann TO, et al. Binding of an antimicrobial peptide to bacterial cells: interaction with different species, strains and cellular components. *Biochim Biophys Acta Biomembr.* (2020) 1862:183291. doi: 10.1016/j.bbamem.2020.183291
26. Freire JM, Gaspar D, Veiga AS, Castanho MA. Shifting gear in antimicrobial and anticancer peptides biophysical studies: from vesicles to cells. *J Pept Sci.* (2015) 21:178–85. doi: 10.1002/psc.2741
27. Malanovic N, Lohner K. Gram-positive bacterial cell envelopes: the impact on the activity of antimicrobial peptides. *Biochim Biophys Acta.* (2016) 1858:936–46. doi: 10.1016/j.bbamem.2015.11.004
28. Rashid R, Veleba M, Kline KA. Focal targeting of the bacterial envelope by antimicrobial peptides. *Front Cell Dev Biol.* (2016) 4:55. doi: 10.3389/fcell.2016.00055
29. Bechinger B, Gorr SU. Antimicrobial peptides: mechanisms of action and resistance. *J Dent Res.* (2017) 96:254–60. doi: 10.1177/0022034516679973
30. Li J, Koh JJ, Liu S, Lakshminarayanan R, Verma CS, Beuerman RW. Membrane active antimicrobial peptides: translating mechanistic insights to design. *Front Neurosci.* (2017) 11:73. doi: 10.3389/fnins.2017.00073
31. Walkenhorst WF, Klein JW, Vo P, Wimley WC. The pH dependence of microbe sterilization by cationic antimicrobial peptides: not just the usual suspects. *Antimicrob Agents Chemother.* (2013) 57:3312–20. doi: 10.1128/AAC.00063-13
32. Westerfield J, Gupta C, Scott HL, Ye Y, Cameron A, Mertz B, et al. Ions modulate key interactions between pHLIP and lipid membranes. *Biophys J.* (2019) 117:920–9. doi: 10.1016/j.bpj.2019.07.034
33. Hilchie AL, Hoskin DW, Power Coombs MR. Anticancer activities of natural and synthetic peptides. In: ed Matsuzaki K, editor. *Antimicrobial Peptides, Advances in Experimental Medicine and Biology, 1117*. Singapore: Sptringer Nature (2019). p. 131–47. doi: 10.1007/978-981-13-3588-4_9
34. Mishra B, Lakshmaiah Narayana J, Lushnikova T, Wang X, Wang G. Low cationicity is important for systemic *in vivo* efficacy of database-derived peptides against drug-resistant gram-positive pathogens. *Proc Natl Acad Sci USA.* (2019) 116:13517–22. doi: 10.1073/pnas.1821410116
35. Oliva R, Chino M, Pane K, Pistorio V, De Santis A, Pizzo E, et al. Exploring the role of unnatural amino acids in antimicrobial peptides. *Sci Rep.* (2018) 8:8888. doi: 10.1038/s41598-018-27231-5
36. Vaezi Z, Bortolotti A, Luca V, Perilli G, Mangoni ML, Khosravi-Far R, et al. Aggregation determines the selectivity of membrane-active anticancer and antimicrobial peptides: the case of killerFLIP. *Biochim Biophys Acta Biomembr.* (2020) 1862:183107. doi: 10.1016/j.bbamem.2019.183107
37. Kacprzyk L, Rydengard V, Morgelin M, Davoudi M, Pasupuleti M, Malmsten M, et al. Antimicrobial activity of histidine-rich peptides is dependent on acidic conditions. *Biochim Biophys Acta.* (2007) 1768:2667–80. doi: 10.1016/j.bbamem.2007.06.020
38. Kharidia R, Tu Z, Chen L, Liang JF. Activity and selectivity of histidine-containing lytic peptides to antibiotic-resistant bacteria. *Arch Microbiol.* (2012) 194:769–78. doi: 10.1007/s00203-012-0810-5
39. Khatami MH, Bromberek M, Saika-Voivod I, Booth V. Molecular dynamics simulations of histidine-containing cod antimicrobial peptide paralogs in self-assembled bilayers. *Biochim Biophys Acta.* (2014) 1838:2778–87. doi: 10.1016/j.bbamem.2014.07.013
40. Hoskin DW, Ramamoorthy A. Studies on anticancer activities of antimicrobial peptides. *Biochim Biophys Acta.* (2008) 1778:357–75. doi: 10.1016/j.bbamem.2007.11.008
41. Capozzi E, Aureli S, Minicozzi V, Rossi GC, Stellato F, Morante S. Designing effective anticancer-radiopeptides. A molecular dynamics study of their interaction with model tumor and healthy cell membranes. *Biochim Biophys Acta Biomembr.* (2018) 1860:2348–55. doi: 10.1016/j.bbamem.2018.05.021

42. Wiedman G, Wimley WC, Hristova K. Testing the limits of rational design by engineering pH sensitivity into membrane-active peptides. *Biochim Biophys Acta.* (2015) 1848:951–7. doi: 10.1016/j.bbamem.2014.12.023
43. Liu N, Bechinger B, Süss R. The histidine-rich peptide LAH4-L1 strongly promotes PAMAM-mediated transfection at low nitrogen to phosphorus ratios in the presence of serum. *Sci Rep.* (2017) 7:9585. doi: 10.1038/s41598-017-10049-y
44. Wolf J, Aisenbrey C, Harmouche N, Raya J, Bertani P, Voievoda N, et al. pH-dependent membrane interactions of the histidine-rich cell-penetrating peptide LAH4-L1. *Biophys J.* (2017) 113:1290–300. doi: 10.1016/j.bpj.2017.06.053
45. Torcato IM, Huang YH, Franquelim HG, Gaspar DD, Craik DJ, Castanho MA, et al. The antimicrobial activity of Sub3 is dependent on membrane binding and cell-penetrating ability. *Chembiochem.* (2013) 14:2013–22. doi: 10.1002/cbic.201300274
46. Quilès F, Saadi S, Francius G, Bacharouche J, Humbert F. *In situ* and real time investigation of the evolution of a pseudomonas fluorescens nascent biofilm in the presence of an antimicrobial peptide. *Biochim Biophys Acta.* (2016) 1858:75–84. doi: 10.1016/j.bbamem.2015.10.015
47. Hammond K, Ryadnov MG, Hoogenboom BW. Atomic force microscopy to elucidate how peptides disrupt membranes. *Biochim Biophys Acta Biomembr.* (2020) 1863:183447. doi: 10.1016/j.bbamem.2020.183447
48. Hartmann M, Berditsch M, Hawecker J, Ardakani MF, Gerthsen D, Ulrich AS. Damage of the bacterial cell envelope by antimicrobial peptides gramicidin S and PGLa as revealed by transmission and scanning electron microscopy. *Antimicrob Agents Chemother.* (2010) 54:3132–42. doi: 10.1128/AAC.00124-10
49. Schneider VA, Coorens M, Ordonez SR, Tjeerdsma-van Bokhoven JL, Posthuma G, van Dijk A, et al. Imaging the antimicrobial mechanism(s) of cathelicidin-2. *Sci Rep.* (2016) 6:32948. doi: 10.1038/srep32948
50. Choi H, Rangarajan N, Weisshaar JC. Lights, camera, action! antimicrobial peptide mechanisms imaged in space and time. *Trends Microbiol.* (2016) 24:111–22. doi: 10.1016/j.tim.2015.11.004
51. Zhang X, Wang Y, Liu L, Wei Y, Shang N, Zhang X, et al. Two-peptide bacteriocin PlnEF causes cell membrane damage to *Lactobacillus plantarum*. *Biochim Biophys Acta.* (2016) 1858:274–80. doi: 10.1016/j.bbamem.2015.11.018
52. Bourbigot S, Dodd E, Horwood C, Cumby N, Fardy L, Welch WH, et al. Antimicrobial peptide RP-1 structure and interactions with anionic versus zwitterionic micelles. *Biopolymers.* (2009) 91:1–13. doi: 10.1002/bip.21071
53. Haney EF, Hunter HN, Matsuzaki K, Vogel HJ. Solution NMR studies of amphibian antimicrobial peptides: linking structure to function? *Biochim Biophys Acta.* (2009) 1788:1639–55. doi: 10.1016/j.bbamem.2009.01.002
54. Legrand B, Laurencin M, Sarkis J, Duval E, Mouret L, Hubert JF, et al. Structure and mechanism of action of a *de novo* antimicrobial detergent-like peptide. *Biochim Biophys Acta.* (2011) 1808:106–16. doi: 10.1016/j.bbamem.2010.08.020
55. Shenkarev ZO, Balandin SV, Trunov KI, Paramonov AS, Sukhanov SV, Barsukov LI, et al. Molecular mechanism of action of beta-hairpin antimicrobial peptide arenicin: oligomeric structure in dodecylphosphocholine micelles and pore formation in planar lipid bilayers. *Biochemistry.* (2011) 50:6255–65. doi: 10.1021/bi200746t
56. Vermeer LS, Lan Y, Abbate V, Ruh E, Bui TT, Wilkinson LJ, et al. Conformational flexibility determines selectivity and antibacterial, antiplasmodial, and anticancer potency of cationic alpha-helical peptides. *J Biol Chem.* (2012) 287:34120–33. doi: 10.1074/jbc.M112.359067
57. Bechinger B, Aisenbrey C, Bertani P. The alignment, structure and dynamics of membrane-associated polypeptides by solid-state NMR spectroscopy. *Biochim Biophys Acta.* (2004) 1666:190–204. doi: 10.1016/j.bbamem.2004.08.008
58. Bourbigot S, Fardy L, Waring AJ, Yeaman MR, Booth V. Structure of chemokine-derived antimicrobial peptide interleukin-8alpha and interaction with detergent micelles and oriented lipid bilayers. *Biochemistry.* (2009) 48:10509–21. doi: 10.1021/bi901311p
59. Perrin BS Jr, Tian Y, Fu R, Grant CV, Chekmenev EY, Wieczorek WE, et al. High-resolution structures and orientations of antimicrobial peptides piscidin 1 and piscidin 3 in fluid bilayers reveal tilting, kinking, and bilayer immersion. *J Am Chem Soc.* (2014) 136:3491–504. doi: 10.1021/ja411119m
60. Fillion M, Marise O, Auger M. Solid-state NMR studies of the interactions and structure of antimicrobial peptides in model membranes. In: Webb GA, editor. *Modern Magnetic Resonance*. Cham: Springer International Publishing (2016). p. 1-18 doi: 10.1007/978-3-319-28275-6_63-1
61. Lee DK, Bhunia A, Kotler SA, Ramamoorthy A. Detergent-type membrane fragmentation by MSI-78, MSI-367, MSI-594, and MSI-843 antimicrobial peptides and inhibition by cholesterol: a solid-state nuclear magnetic resonance study. *Biochemistry.* (2015) 54:1897–907. doi: 10.1021/bi501418m
62. Zhu S, Sani MA, Separovic F. Interaction of cationic antimicrobial peptides from Australian frogs with lipid membranes. *Pept Sci.* (2018) 110:e24061. doi: 10.1002/pep2.24061
63. Sherman PJ, Jackway RJ, Gehman JD, Praporski S, McCubbin GA, Mechler A, et al. Solution structure and membrane interactions of the antimicrobial peptide fallaxidin 4.1a: an NMR and QCM study. *Biochemistry.* (2009) 48:11892–901. doi: 10.1021/bi901668y
64. Harmouche N, Bechinger B. Lipid-mediated interactions between the antimicrobial peptides magainin 2 and PGLa in bilayers. *Biophys J.* (2018) 115:1033–44. doi: 10.1016/j.bpj.2018.08.009
65. Sandhu G, Booth V, Morrow MR. Role of charge in lipid vesicle binding and vesicle surface saturation by gaduscidin-1 and gaduscidin-2. *Langmuir.* (2020) 36:9867–77. doi: 10.1021/acs.langmuir.0c01497
66. Hong M, Su Y. Structure and dynamics of cationic membrane peptides and proteins: insights from solid-state NMR. *Protein Sci.* (2011) 20:641–55. doi: 10.1002/pro.600
67. Sani MA, Separovic F. Progression of NMR studies of membrane-active peptides from lipid bilayers to live cells. *J Magn Reson.* (2015) 253:138–42. doi: 10.1016/j.jmr.2014.11.016
68. Mani R, Cady SD, Tang M, Waring AJ, Lehrer RI, Hong M. Membrane-dependent oligomeric structure and pore formation of a beta-hairpin antimicrobial peptide in lipid bilayers from solid-state NMR. *Proc Natl Acad Sci USA.* (2006) 103:16242–7. doi: 10.1073/pnas.0605079103
69. Kang X, Elson C, Penfield J, Kirui A, Chen A, Zhang L, et al. Integrated solid-state NMR and molecular dynamics modeling determines membrane insertion of human β-defensin analog. *Commun Biol.* (2019) 2:402. doi: 10.1038/s42003-019-0653-6
70. Luchinat E, Banci L. In-cell NMR: a topical review. *IUCrJ.* (2017) 4:108–18. doi: 10.1107/S2052252516020625
71. Narasimhan S, Folkers GE, Baldus M. When small becomes too big: expanding the use of in-cell solid-state NMR spectroscopy. *Chempluschem.* (2020) 85:760–8. doi: 10.1002/cplu.202000167
72. Serber Z, Selenko P, Hänsel R, Reckel S, Löhr F, Ferrell JE, et al. Investigating macromolecules inside cultured and injected cells by in-cell NMR spectroscopy. *Nat Protoc.* (2006) 1:2701–9. doi: 10.1038/nprot.2006.181
73. Inomata K, Ohno A, Tochio H, Isogai S, Tenno T, Nakase I, et al. High-resolution multi-dimensional NMR spectroscopy of proteins in human cells. *Nature.* (2009) 458:106–9. doi: 10.1038/nature07839
74. Burmann BM, Gerez JA, Matečko-Burmann I, Campioni S, Kumari P, Ghosh D, et al. Regulation of α-synuclein by chaperones in mammalian cells. *Nature.* (2020) 577:127–32. doi: 10.1038/s41586-019-1808-9
75. Datta A, Yadav V, Ghosh A, Choi J, Bhattacharyya D, Kar RK, et al. Mode of action of a designed antimicrobial peptide: high potency against cryptococcus neoformans. *Biophys J.* (2016) 111:1724–37. doi: 10.1016/j.bpj.2016.08.032
76. Kaplan M, Cukkemane A, van Zundert GC, Narasimhan S, Daniëls M, Mance D, et al. Probing a cell-embedded megadalton protein complex by DNP-supported solid-state NMR. *Nat Methods.* (2015) 12:649–52. doi: 10.1038/nmeth.3406
77. Yamamoto K, Caporini MA, Im SC, Waskell L, Ramamoorthy A. Cellular solid-state NMR investigation of a membrane protein using dynamic nuclear polarization. *Biochim Biophys Acta.* (2015) 1848:342–9. doi: 10.1016/j.bbamem.2014.07.008
78. Albert BJ, Gao C, Sesti EL, Saliba EP, Alaniva N, Scott FJ, et al. Dynamic nuclear polarization nuclear magnetic resonance in human cells using fluorescent polarizing agents. *Biochemistry.* (2018) 57:4741–6. doi: 10.1021/acs.biochem.8b00257
79. Narasimhan S, Scherpe S, Lucini Paioni A, van der Zwan J, Folkers GE, Ovaa H, et al. DNP-supported solid-state NMR spectroscopy of proteins

inside mammalian cells. *Angew Chem Int Ed Engl.* (2019) 58:12969–73. doi: 10.1002/anie.201903246
80. Cegelski L, Steuber D, Mehta AK, Kulp DW, Axelsen PH, Schaefer J. Conformational and quantitative characterization of oritavancin-peptidoglycan complexes in whole cells of *Staphylococcus aureus* by *in vivo* 13C and 15N labeling. *J Mol Biol.* (2006) 357:1253–62. doi: 10.1016/j.jmb.2006.01.040
81. Zhou X, Cegelski L. Nutrient-dependent structural changes in *S. aureus* peptidoglycan revealed by solid-state NMR spectroscopy. *Biochemistry.* (2012) 51:8143–53. doi: 10.1021/bi3012115
82. Romaniuk JAH, Cegelski L. Peptidoglycan and teichoic acid levels and alterations in *Staphylococcus aureus* by cell-wall and whole-cell nuclear magnetic resonance. *Biochemistry.* (2018) 57:3966–75. doi: 10.1021/acs.biochem.8b00495
83. Chatterjee S, Prados-Rosales R, Itin B, Casadevall A, Stark RE. Solid-state NMR reveals the carbon-based molecular architecture of cryptococcus neoformans fungal eumelanins in the cell wall. *J Biol Chem.* (2015) 290:13779–90. doi: 10.1074/jbc.M114.618389
84. Kang X, Kirui A, Muszyński A, Widanage MCD, Chen A, Azadi P, et al. Molecular architecture of fungal cell walls revealed by solid-state NMR. *Nat Commun.* (2018) 9:2747. doi: 10.1038/s41467-018-05199-0
85. Poulhazan A, Arnold AA, Warschawski DE, Marcotte I. Unambiguous *ex situ* and in cell 2D. *Int J Mol Sci.* (2018) 19:3817. doi: 10.3390/ijms19123817
86. Overall SA, Zhu S, Hanssen E, Separovic F, Sani MA. *In situ* monitoring of bacteria under antimicrobial stress using ^{31}P solid-state NMR. *Int J Mol Sci.* (2019) 20:181. doi: 10.3390/ijms20010181
87. Pius J, Morrow MR, Booth V. (2)H solid-state nuclear magnetic resonance investigation of whole *Escherichia coli* interacting with antimicrobial peptide MSI-78. *Biochemistry.* (2012) 51:118–25. doi: 10.1021/bi201569t
88. Tardy-Laporte C, Arnold AA, Genard B, Gastineau R, Morancais M, Mouget JL, et al. A (2)H solid-state NMR study of the effect of antimicrobial agents on intact *Escherichia coli* without mutating. *Biochim Biophys Acta.* (2013) 1828:614–22. doi: 10.1016/j.bbamem.2012.09.011
89. Davis JH. The description of membrane lipid conformation, order and dynamics by 2H-NMR. *Biochim Biophys Acta.* (1983) 737:117–71. doi: 10.1016/0304-4157(83)90015-1
90. Santisteban NP, Morrow MR, Booth V. Protocols for studying the interaction of MSI-78 with the membranes of whole gram-positive and gram-negative bacteria by NMR. *Methods Mol Biol.* (2017) 1548:217–30. doi: 10.1007/978-1-4939-6737-7_15
91. Santisteban NP, Morrow MR, Booth V. Effect of AMPs MSI-78 and BP100 on the lipid acyl chains of ^{2}H-labeled intact gram positive bacteria. *Biochim Biophys Acta Biomembr.* (2020) 1862:183199. doi: 10.1016/j.bbamem.2020.183199
92. Marcotte I, Booth V. 2H solid-state NMR study of peptide-membrane interactions in intact bacteria. In: Separovic F, Naito A, editors. *Advances in Biological Solid-State NMR: Proteins and Membrane-Active Peptides.* London: RSC Books (2014) 459–475. doi: 10.1039/9781782627449-00459
93. Warnet XL, Arnold AA, Marcotte I, Warschawski DE. In-cell solid-state NMR: an emerging technique for the study of biological membranes. *Biophys J.* (2015) 109:2461–6. doi: 10.1016/j.bpj.2015.10.041
94. Laadhari M, Arnold AA, Gravel AE, Separovic F, Marcotte I. Interaction of the antimicrobial peptides caerin 1.1 and aurein 1.2 with intact bacteria by (2)H solid-state NMR. *Biochim Biophys Acta.* (2016) 1858:2959–64. doi: 10.1016/j.bbamem.2016.09.009
95. Booth V, Warschawski DE, Santisteban NP, Laadhari M, Marcotte I. Recent progress on the application of (2)H solid-state NMR to probe the interaction of antimicrobial peptides with intact bacteria. *Biochim Biophys Acta.* (2017) 1865:1500–11. doi: 10.1016/j.bbapap.2017.07.018
96. Arnold AA, Bourgouin JP, Genard B, Warschawski DE, Tremblay R, Marcotte I. Whole cell solid-state NMR study of chlamydomonas reinhardtii microalgae. *J Biomol NMR.* (2018) 70:123–31. doi: 10.1007/s10858-018-0164-7
97. Bouhlel Z, Arnold AA, Warschawski DE, Lemarchand K, Tremblay R, Marcotte I. Labelling strategy and membrane characterization of marine bacteria vibrio splendidus by *in vivo*. *Biochim Biophys Acta Biomembr.* (2019) 1861:871–8. doi: 10.1016/j.bbamem.2019.01.018
98. Warnet XL, Laadhari M, Arnold AA, Marcotte I, Warschawski DE. A 2H magic-angle spinning solid-state {NMR} characterisation of lipid membranes in intact bacteria. *Biochim Biophys Acta Biomembr.* (2016) 1858:146–52. doi: 10.1016/j.bbamem.2015.10.020
99. Santisteban NP. *Interaction of Antimicrobial Peptides With Bacterial Cell Envelopes.* (Ph.D. Dissertation), Department of Physics and Physical Oceanography, Memorial University of Newfoundland, Canada (St. John's, NL). (2019).
100. Booth V. Deuterium solid-state NMR of whole bacteria: Sample preparation and effects of cell envelope manipulation. In: Separovic F, Sani M, editors. *Solid-State NMR: Applications in Biomembrane Structure*. Bristol: IOP Publishing (2020). p. 1–121. doi: 10.1088/978-0-7503-2532-5ch3
101. Ramamoorthy A, Thennarasu S, Lee DK, Tan A, Maloy L. Solid-state NMR investigation of the membrane-disrupting mechanism of antimicrobial peptides MSI-78 and MSI-594 derived from magainin 2 and melittin. *Biophys J.* (2006) 91:206–16. doi: 10.1529/biophysj.105.073890
102. Friedrich CL, Moyles D, Beveridge TJ, Hancock RE. Antibacterial action of structurally diverse cationic peptides on gram-positive bacteria. *Antimicrob Agents Chemother.* (2000) 44:2086–92. doi: 10.1128/AAC.44.8.2086-2092.2000
103. Hancock RE, Sahl HG. Antimicrobial and host-defense peptides as new anti-infective therapeutic strategies. *Nat Biotechnol.* (2006) 24:1551–7. doi: 10.1038/nbt1267
104. Baeder DY, Yu G, Hozé N, Rolff J, Regoes RR. Antimicrobial combinations: bliss independence and loewe additivity derived from mechanistic multi-hit models. *Philos Trans R Soc Lond B Biol Sci.* (2016) 371:20150294. doi: 10.1098/rstb.2015.0294
105. Roversi D, Luca V, Aureli S, Park Y, Mangoni ML, Stella L. How many antimicrobial peptide molecules kill a bacterium? The case of PMAP-23. *ACS Chem Biol.* (2014) 9:2003–7. doi: 10.1021/cb500426r
106. Splith K, Neundorf I. Antimicrobial peptides with cell-penetrating peptide properties and vice versa. *Eur Biophys J.* (2011) 40:387–97. doi: 10.1007/s00249-011-0682-7
107. Milletti F. Cell-penetrating peptides: classes, origin, and current landscape. *Drug Discov Today.* (2012) 17:850–60. doi: 10.1016/j.drudis.2012.03.002
108. Avci FG, Akbulut BS, Ozkirimli E. Membrane active peptides and their biophysical characterization. *Biomolecules.* (2018) 8:77. doi: 10.3390/biom8030077

Conflict of Interest: The author declares that the research was conducted in the absence of any commercial or financial relationships that could be construed as a potential conflict of interest.

frontiers in Medical Technology

REVIEW
published: 21 January 2021
doi: 10.3389/fmedt.2020.628552

Spectroscopic and Microscopic Approaches for Investigating the Dynamic Interactions of Anti-microbial Peptides With Membranes and Cells

*Andrew H. A. Clayton**

Cell Biophysics Laboratory, Optical Sciences Centre, Department of Physics and Astronomy, School of Science, Swinburne University of Technology, Melbourne, VIC, Australia

The emergence of microbes resistant to conventional antibiotics is a burgeoning threat to humanity with significant impacts on the health of people and on the health system itself. Antimicrobial peptides (AMPs) hold promise as potential future alternatives to conventional drugs because they form an integral part of the defense systems of other species in the animal, plant, and fungal kingdoms. To aid the design of the next generation of AMPs optimized for human use, we must first understand the mechanism of action of existing AMPs with their targets, ideally in the context of the complex landscape of the living (microbial) cell. Advances in lasers, optics, detectors, fluid dynamics and various probes has enabled the experimentalist to measure the kinetics of molecule–membrane, molecule–molecule, and molecule–cell interactions with increasing spatial and temporal resolution. The purpose of this review is to highlight studies into these dynamic interactions with a view to improving our understanding of AMP mechanisms.

Keywords: anti-microbial, peptide–cell interaction, peptide–peptide interaction, microscopy, fluorescence lifetime imaging (FLIM)-FRET microscopy, spectroscopy

OPEN ACCESS

Edited by:
Lorenzo Stella,
University of Rome Tor Vergata, Italy

Reviewed by:
James Carl Weisshaar,
University of Wisconsin-Madison, United States
Thorsten Wohland,
National University of Singapore, Singapore

***Correspondence:**
Andrew H. A. Clayton
aclayton@swin.edu.au

Specialty section:
This article was submitted to Pharmaceutical Innovation, a section of the journal Frontiers in Medical Technology

Received: *12 November 2020*
Accepted: *30 December 2020*
Published: *21 January 2021*

Citation:
Clayton AHA (2021) Spectroscopic and Microscopic Approaches for Investigating the Dynamic Interactions of Anti-microbial Peptides With Membranes and Cells. Front. Med. Technol. 2:628552. doi: 10.3389/fmedt.2020.628552

INTRODUCTION

Antimicrobial peptides (AMPs) are part of the innate immune defense system of many organisms in the animal, plant, and fungal kingdoms (1). AMPs found in nature, typically consist of a small number of amino acids (10–30) and are predominantly cationic. The cationic nature of AMPs is thought to facilitate the association with the negatively charged membranes of microbial cells, such as bacteria. Of the 3,000 or so AMPs so far isolated from nature, only a relatively small number of structures have been obtained by high-resolution x-ray or NMR spectroscopy in a membrane environment (2–8). These seminal structural studies have revealed that some AMPs can form pores and/or channels in membranes, disrupting the barrier function of the membrane essential to the life of the cell. Biophysical studies on other classes of AMPs with model membranes have revealed alternative structures where peptides reside on the surface of the membrane, as opposed to passing through it in a transmembrane pore. This has led to alternative membrane-disruption mechanisms, as in the carpet model (9). Variations on pore models (10) or on the carpet model (11), have also been proposed. Some researchers have proposed completely different models altogether (12, 13). A common theme to all the models seems to be some sort of AMP-induced perturbation or disruption of the membrane, either transient, permanent, or both.

How microbes are actually killed by AMPs seems to be less well-understood. Some scientists have proposed different models for cell killing that do not involve pore formation or substantial membrane disruption but may involve peptide translocation and binding to intracellular targets. Bacterial and fungal cells are considerably more complex than phospholipid membranes. End-point assays commonly used in AMP studies with bacteria or fungi can address cell population growth, dead/live cell fractions, or examine cell morphology using methods such as electron microscopy. However, measurements taken at a single time point cannot track intermediate states that may be important in the cell killing mechanism. Studies that dynamically track the interactions of AMPs with targets on or inside cells have the potential to answer this question with a greater degree of confidence.

Here we provide an overview of studies addressing the dynamics of peptide interactions with membranes and cells. Because molecule-molecule, as well as molecule-membrane and molecule-cell interactions are important, we will highlight studies that address the dynamics of these interactions in particular. We will first discuss some key insights gleaned from model membrane studies and then move onto studies conducted on live cells. We conclude with further questions and outlook.

MODEL MEMBRANE STUDIES

Model membranes afford the advantages that the chemical composition and physical phase state can be controlled or varied systematically, and that a large range of physical techniques can be applied to them. Membranes of varying morphology and size can be prepared including vesicles and planar membranes.

The interaction of peptides with membranes is the very first step in a series of processes leading to microbial killing. Studies on model membranes have enabled some of the subsequent steps in the membrane to be elucidated.

The interaction of peptides with membranes can entail a number of structural changes both in the peptide and in the membrane. First, many peptides are unstructured in aqueous solution but can adopt regular secondary structures, such as α-helix or β-sheet when associated with the membrane. Peptide folding, akin to protein folding, is a key dynamic process. Second, peptides usually adopt one of two orientations on/in the membrane. One orientation is with the peptide long axis parallel to the membrane surface. Another common orientation is with the peptide long axis oriented normal to the membrane surface. Orientation changes can be important in processes such as pore formation or peptide translocation through membranes. Third, peptides often associate to form oligomeric complexes or nanoclusters in the membrane. A typical case is pore formation, wherein peptides associate in a transmembrane orientation to form a pore.

There are a few studies aimed at measuring the folding dynamics of monomeric alpha-helices in bilayer membranes. Using a combination of stopped flow fluorescence and stopped flow circular dichroism, Constantinescu and Lafleur (14) detected biphasic kinetics on time scales of tens of milliseconds and seconds for the interaction of the AMP melittin (derived from the sting from a honey Bee), with lipid vesicles. Melittin is a suitable peptide for these studies because in its monomeric form it is predominantly random coil in aqueous solution but adopts an alpha-helix in membranes. The authors showed that the peptide insertion into the bilayer, as measured by quenching of the intrinsic tryptophan fluorescence from the melittin by a brominated-quencher in the bilayer, appeared to precede the full folding of the melittin, as detected by circular dichroism. The authors concluded that changes in apparent folding rates (circular dichroism), promoted by changes in lipid composition, were mainly a reflection of different rates of peptide insertion. These results suggest that insertion and folding are strongly coupled processes, with the former being a rate limiting step.

Tucker et al. (15) used stopped-flow fluorescence spectroscopy to examine the membrane assisted folding of magainin 2, an AMP derived from the skin of an African frog. The authors introduced a special amino acid (p-cyano-phenylalanine) and replaced a phenylalanine with a tryptophan residue to enable detection of coil-helix transition through Forster resonance energy transfer from p-cyano-phenylalanine to tryptophan. The authors detected biphasic fluorescence kinetics with time constants of 10 and 100 ms, attributed to coupled-binding-folding process at the membrane. As for the melittin study mentioned above, the authors here concluded that the measured appearance of the folded helical state is limited by the rate of peptide association with or insertion in the lipid membrane. To explore this aspect further, Tang et al. (16) use a stopped-flow FRET approach with AMP mastaporan X and derivatives with nucleated α-helix formation. The authors concluded that mastaporan associates with the lipid bilayer initially in a non-helical conformation, which rapidly converts into a helical state within the complex anisotropic environment of the lipid bilayer. Taken together, these studies show that while binding and helix formation are coupled events, the determination of the rate of coil-helix transitions in the membrane is difficult owing to the rate limiting peptide-bilayer binding/insertion process. Nevertheless, we can tentatively conclude that the helix formation step is faster than milliseconds and certainly not a rate-limiting process in the overall scheme of AMP activity.

A number of approaches have been employed to examine changes in helix orientation within the lipid bilayer. The pH low insertion peptides (or pHLIPs) developed by Engelman et al. (17) contain hydrophobic residues and have high affinity for membranes at normal or high pH, but at low pH fold and insert across membranes in a transmembrane orientation. Rapid pH modulation provides a means to measure the kinetics of the reorientation step using stopped-flow fluorescence techniques. These studies have revealed two steps in the process, the first being formation of a α-helix at the membrane interface and the second being reorientation of the peptide to form a transmembrane helix. The first step was characterized with a time constant of about 0.1 s, whereas the timescale for the second step ranged from 0.1 to 100 s, dependent on the sequence of the peptide and the composition of the lipid membrane. While not strictly anti-microbial in nature, these model peptides are useful

tools for examining helix insertion processes, which are relevant to some AMPs.

Linear dichroism can provide important information on changes in orientation of peptides when associating with lipid bilayers. In one such study, the Rodgers group (18) used cyclic peptides and a combination of circular dichroism and linear dichroism to track changes in peptide secondary structure and peptide orientation during the interaction of peptide with lipid bilayers. After addition of liposomes, the circular dichroism signal indicated a rapid formation of β-structure with no further change throughout the experiment. In contrast, the linear dichroism signal displayed complex kinetics with time constants in the range of seconds, minutes to 100 min. The authors interpreted the changes in LD signal due to rearrangements of the peptide in the lipid bilayer. Interestingly the time-scale for these changes was comparable with the folding of β-barrel outer-membrane proteins suggesting that these model peptides may provide to be good model systems for examining these processes.

The Gai lab (19) used a two probe approach with stopped-flow fluorescence to investigate the binding, insertion and helix–helix association of a peptide (TM anti-αIIb homodimer) known to spontaneously insert and form dimers in bilayers. The complex fluorescence kinetics, observed over a time-scale of milliseconds to seconds, was described by a kinetic model involving peptide binding, insertion, and dimerization within the membrane as well as peptide dimer formation in solution. Interestingly the helix–helix association, to form the homodimer, was the slowest step in the process occurring on a time-scale of seconds and orders of magnitude slower than a diffusion-controlled dimerization process. Thus, the dimerization process itself was the rate-limiting step in this instance.

Anderluh's laboratory (20) used a multi-probe approach to investigate binding, insertion, and oligomerization of a pore-forming α-helical toxin (Equinatoxin II) in membranes. Intrinsic tryptophan fluorescence was used to measure the initial association of the toxin with membranes. NBD fluorescence (from an NBD probe covalently attached to an engineered cysteine derivative) provided insight into the kinetics of helix insertion into the membrane, while AlexaFluor488 fluorescence self-quenching quantitated the extent of helix–helix association (i.e., oligomerization). Impressively, the authors were able to track the kinetics of these fundamental processes in real time, using stopped-flow fluorescence techniques. Protein binding to the membrane was rapid (<1 s), helix insertion took place on the time-scale of seconds, while oligomerization was on the time-scale of tens of seconds. Examination of an engineered protein mutant, which could not insert α-helix into the membrane, bound to the membrane and oligomerized but could not form a functional pore in the membrane. This study brings up an important point that membrane associated proteins and peptides are likely to have multiple states on and in the membrane with the possibility that only some of those states are the biologically active ones (biologically active here means forming a functional pore).

The aforementioned studies have mainly utilized small unilamellar vesicles (either in stopped-flow or flow-aligned (Couette flow) for linear dichroism) as the model membrane system (typical diameter: 50–100 nm). These are very convenient for spectroscopic studies because light scattering is kept to a minimum (relative to studies with cell-sized vesicles) and vesicles survive the shear conditions of rapid fluid mixing or flow. We will next highlight some of the studies performed using giant unilamellar vesicles as the model membrane system. Giant unilamellar vesicles can be prepared to have diameters comparable with the dimensions of biological cells (typical diameter: 1–100 μm) and afford visualization with a microscope so that single objects and single events can be detected.

The Huang laboratory (7) has employed microscopic visualization of melittin action on single giant unilamellar vesicles. Using AlexaFluor488-tagged melittin and calcein-entrapped giant unilamellar vesicles, melittin binding to and calcein release from single vesicles could be observed using fluorescence microscopy. Simultaneous measurements of membrane area was also performed. Melittin binding was observed over a time-scale of 100s s while calcein release was observed only after the majority of melittin was bound to the membrane. In oriented circular dichroism experiments, the authors revealed that at low peptide concentrations melittin forms α-helix aligned parallel to the membrane surface and as the peptide concentration increased, the helices began to align perpendicular to the membrane surface. Lastly, the authors used x-ray diffraction to observe toroidal pores of melittin. Taken together this study revealed that the melittin initially absorbs to the membrane causing an increase in membrane surface area (and thinning of the membrane), this then reduces the energetic cost of forming a transmembrane orientation. Once enough peptide is absorbed to the membrane, the helices then orient to form transmembrane toroidal pores, which allow leakage of large species into the extra-vesicular space. The study here reveals the utility of combining different but related techniques to provide mechanistic information.

Almeida's lab (21) has utilized giant unilamellar vesicles to design useful assays for probing the mechanism of AMP membrane actions and peptide translocations. In one approach, they examined the binding of daptomycin to mixed membranes composed of phosphatidylcholine and phosphatidylglycerol and subsequent effects on the membrane. Using robust colocalization analysis of 1,000s of individual vesicles, they concluded that daptomycin causes formation of daptomycin-phosphatidylgylcerol membrane domains (lipid clusters) in the membrane which eventually cause destabilization and vesicle collapse.

Oreopoulos et al. (22) were able to view membrane domains and phase separation using advanced imaging methods and planar supported lipid bilayers. The authors used atomic microscopy to reveal topographic features of the peptide-induced membrane domains and total-internal reflection fluorescence polarization microscopy to reveal the extent of orientational order of membrane-imbedded probes.

In other series of studies, Almeida's lab developed an assay for examining peptide translocation (23). This assay relies on the creation of vesicles inside giant unilamellar vesicles (vesicles in vesicles). The authors were able to observe peptide and dye influx using confocal microscopy. They were able to identify peptide-assisted influx of dye molecules across giant vesicles, and across

the membranes of intra-vesicular vesicles. They observed time scales of influx of the order of tens of minutes (dependent on peptide). They also identified a silent mode of peptide transport, i.e., transport across the giant vesicle and binding to an internal vesicle, which did not cause dye influx. This suggested that a small proportion of the total population of peptides were able to translocate the membrane without causing membrane damage.

Paterson et al. (24) have developed a high throughput giant unilamellar vesicle system suitable for examining the detailed behavior of peptides and used this system to contrast the mechanistic behaviors of melittin and magainin on vesicles with differing membrane compositions. The authors were able to show a spectrum of peptide-induced effects including no effect, burst behavior, pore formation, and carpet-like disruption. The authors interpreted the data in the context of topological and charge effects in the peptides and the lipids, and in terms of a negative feedback model for pore formation. Studies such as these have the potential to provide useful design criteria for the next generation of peptides with enhanced activity and selectivity.

Recently the Huang lab has introduced advances in membrane models and techniques to allow comparison of actions of different anti-microbial agents (25). One of the widely used methods to assess *in vitro* activity of peptides is to use efflux or influx of fluorescent dyes with vesicles. However, the permeability of membranes to dyes is usually time-dependent owing to the time-dependent nature of the peptide-interaction with membranes, making measurements of dye fluxes problematic from conventional fluorescence measurements. Therefore, Huang's team developed a fluorescence recovery after photobleaching protocol to determine dye fluxes through membranes. To compare different AMPs and also to move toward a more realistic membrane system, Huang utilized spheroplasts derived from bacteria. Spheroplasts are created by using antibiotics which cause the bacteria to shed the outer membrane leaving the cytoplasmic membrane. Spheroplasts can also be created to have sizes suitable for observation by microscopy. Using the fluorescence recovery after photobleaching assay revealed that the AMPs known to form pores have similar performance with regard to dye flux in giant unilamellar vesicles as compared with the spheroplasts prepared from bacteria, although differences were noted in the concentration dependence of the phenomena. These conclusions suggest that for the peptides tested, model membranes provide a useful test-bed for pore formation processes occurring at the cytoplasmic membrane.

Wimley's laboratory has been interested in how the performance of peptides as measured by model membrane disruption translates into useful anti-microbial activity against bacteria (26). To this end they designed a peptide library and used a stringent vesicle disruption screen to select the most potent pore forming peptides. They used these peptides of varying membrane disruption abilities to test the hypothesis that better membrane disruption would correlate with improved bacterial sterilization properties. Unfortunately the hypothesis was rejected. The better pore forming peptides were only marginally better in anti-bacterial activity and were more cytotoxic. The authors suggested that the approaches used with vesicles were useful for an initial screen and that conditions that better mimic conditions found in nature are needed in the search for improved AMPs. In the quest for a therapeutic peptide, the Wimley lab have identified a number of barriers to implementation. These barriers include low solubility, degradation by proteases, cell lysis (and associated toxicity), and inhibition due to host cell binding (27).

CELLULAR STUDIES

Leaving the relatively well-studied confines of model membranes we now turn to studies of AMP action on living cells. Imaging and microscopy methods become important in this context since they can reveal the locations, interactions and symptoms of AMPs as they navigate the complex cellular landscape (28).

The Wohland lab (29) utilized single molecule and fluorescence correlation spectroscopy techniques to examine the mechanism of action of quantum-dot labeled a-helical peptide, Sushi-1, on single *Escherichia coli* bacterial cells. The authors identified four steps in the killing mechanism, peptide binding to membrane (as deduced from change in diffusion coefficient of peptide), peptide–peptide association on the membrane (as deduced from decrease in peptide diffusion coefficient as peptide concentration was increased), membrane disruption [without lipopolysaccharide (LPS) detachment] and cytoplasmic leakage through large defects in the membrane [through cytoplasmic Green Fluorescent Protein (GFP) release]. The use of highly sensitive fluorescence detection allowed examination of the peptide behavior at the single molecule level and at very low densities on the membrane. Great care was also taken to ensure that the peptide label did not influence the biological activity of the peptide.

The Weisshaar lab has developed a number of impressive microscope-based assays to examine the mechanisms of AMP actions on single bacteria (30–36). By cleverly combining different genetically encoded and synthetic fluorescence probes, they can track the sequence of events leading to different peptide-induced effects. A particularly ingenious development was the use of a genetically encoded GFP fusion which is trafficked to the periplasmic region of gram negative bacteria. This probe can be used to detect inner membrane disruption, through an increase in the GFP fluorescence from the bacterial cytoplasm. Outer membrane disruption, in contrast, will lead to loss of GFP fluorescence from the bacteria cell entirely. This GFP probe can be combined with other probes, such as cell impermeable nucleic acid-binding dyes, which detect permeability of the cytoplasmic membranes and can be monitored through an increase in fluorescence in the interior of the cell. Probes of other cell states, such as intracellular pH or oxidative stress can also be used. By controlling the delivery of dyes and peptides to the bacteria by means of a microfluidic device, the laboratory can investigate the action of AMPs at different stages of bacterial growth or growth cycle on demand. Microfluidic delivery also allows the use of different concentration profiles of peptides to examine recovery or reversibility of peptide effects. Using these approaches the lab has investigated several peptides including

alamethicin, melittin, LL-37, and the cecropin A on *E. coli* cells and *Bacillus subtilis* cells. In the case of the prototypical peptide melittin, the laboratory has shown different features of the membrane disruption mechanism in bacterial cells which involve some combination of changes to outer-membrane permeability (opening and re-sealing and opening again), inner-membrane permeability (opening and re-sealing and opening again) and formation of periplasmic bubbles. The assays developed by the laboratory allowed them to document the ordering and dynamics of these processes, which occurred on the time-scale of minutes to tens of minutes, congruent with the complex interplay of molecular interactions and concentration fluxes over the cellular landscape.

To better understand the nexus between peptide-peptide interactions, as implied in some membrane disruption mechanisms, and cytoplasmic contents release, the Clayton laboratory developed a single-color assay based on fluorescence lifetime imaging microscopy (37). The method relies on the unique lifetime "fingerprints" of fluorescently-tagged peptides in monomeric membrane-bound and oligomerized states, and the lifetime of cytoplasmic GFP (cells) or synthetic fluorophore (membranes), and can track quantitatively the relative amounts of these species in real time. The time-lapse fluorescence lifetime imaging microscopy approach has been applied to a fluorescently tagged melittin derivative upon interaction with single giant unilamellar vesicles, single giant multilamellar vesicles, and *E. coli* bacterial cells (38). Quenching of the lifetime of the fluorescence tag on the melittin peptide was observed over a time scale of minutes, assigned to a progressive increase in peptide–peptide interactions at the membrane. For the unilamellar giant vesicles, once the peptide–peptide interactions reached a threshold level (i.e., once the monomeric and oligomerized peptides were equi-molar at the membrane), release of an intra-vesicular dye occurred rapidly, consistent with pore formation. For the multi-lamellar giant vesicles, dye release was more gradual, which was assigned to the requirement of peptide accumulation at each membrane, pore formation, pore closure and peptide translocation. For the bacterial cells, peptide-peptide interactions increased over time, as for the model membrane systems, but GFP release was not complete, attributed to the complexity of the membranes in the bacteria, and the capacity of the living cell to resist membrane attack. In view of the Weisshaar lab's observations (36), it is likely that the incomplete release may be due to membrane re-sealing events.

AMPs can also transit through cellular membranes without apparent disruption of membrane integrity. Park et al. (39) compared the activities of the AMP burforin II and magainin 2 on *E. coli* cells. Buforin II killed *E. coli* without lysing the cell membrane even at five times minimal inhibitory concentration (MIC) at which buforin II reduced the viable cell numbers by 6 orders of magnitude. However, magainin 2 lysed the cells, resulting in cell death under the same condition. FITC-labeled buforin II was found to penetrate the cell membrane and accumulate inside *E. coli* even below its MIC, whereas FITC-labeled magainin 2 remained outside or on the cell wall even at its MIC. These results are consistent with a mechanism where buforin II translocates across the cell membrane to bind to intracellular DNA and RNA targets.

Shagaghi et al. (40) used a combination of techniques, including fluorescence lifetime imaging microscopy, to address the mechanism of action of a tryptophan-rich peptide thought to act either by pore formation or binding to internal DNA or both. Using a membrane permeant DNA binding dye, which serves as a quencher for FITC fluorescence, the authors detected binding of the puroA-FITC peptide to DNA in the nucleus of a *Candida albicans* yeast cell within 1 min of addition. A propidium iodide assay confirmed that the membranes of the yeast cell were not breached at this point, suggesting that peptide translocation to the nucleus caused only transient membrane damage. About 25–45 min later, puroA-FITC was found to accumulate at the outer membrane of the yeast cell causing a quenching in the lifetime of the FITC fluorescence, due to peptide–peptide interactions (assigned as pore formation) which also coincided with propidium iodide entry into the cells soon afterwards. Changes in cell size, observed at this later step, indicated that the cell integrity was compromised. The kinetics of the pore formation, loss of membrane integrity, shrinkage of cell diameter matched fairly well the kinetics of killing of the cell population indicating that these processes are causally linked. However, the peptide also bound to DNA/nucleic acids (as detected by lifetime quenching) inside the cell before and after membrane disruption and caused cell cycle arrest. Thus, this peptide likely has a dual mode of action involving both intracellular and membrane targets.

A recent study (41) demonstrated the use of fluorescence lifetime imaging microscopy, Fourier transform infrared spectroscopy and atomic force microscopy to examine the interaction of the peptide cecropin D with *E. coli* bacterial cells. Fluorescence lifetime imaging microscopy of FITC-tagged cecropin D revealed a rapid decrease (within minutes) in fluorescence lifetime owing to binding of the peptide to the cells. Fourier infrared spectroscopy revealed changes consistent with peptide interaction with the LPS layer of the outer cell membrane, and a lipid ordering effect. Accordingly, surface topography and nano-mechanical properties were also altered, as revealed by atomic force microscopy, but over a longer time-period of up to an hour.

While single cell assays using microscopic image approaches are clearly powerful at elucidating events at the single cell level, the ultimate goal of an AMP as a therapeutic is to destroy the relevant microbe (fungi or bacteria) at the population level. Some interesting studies have combined single cell with population level assays to examine how peptides function on a "community" level.

Wu and Tan (42), and Snoussi et al. (43) in two separate studies, combined single cell microscopy, population level experiments with mathematical modeling to show that the AMP LL-37 kills a sub-population of bacterial cells, forming dead (or growth arrested) cells, which then absorb the remaining LL-37 from the medium. These authors show that one strain of bacteria can effectively protect another strain of bacteria via this mechanism, although cell-to-cell communication is unlikely to be involved. The results of these two studies reveal the power of combining single cell and population approaches to elucidate emergent behavior on a cell population growth behavior from an

AMP. It would be interesting to see if this mechanism applies to other AMPs as well.

Biofilms are often challenging to treat clinically because of resistance to antibiotics, such as daptomycin. In order to investigate potential mechanisms of daptomycin resistance the Steenkeste laboratory (44) created a fluorescent-tagged daptomycin analog and exploited dynamic imaging techniques to examine daptomycin transport within the biofilms. Using time-lapse fluorescence (to investigate daptomycin uptake) and fluorescence recovery after photobleaching (to investigate transport), the authors revealed that the biofilm did not significantly impede daptomycin uptake and diffusion, ruling out the biofilm as a barrier to drug penetration. The authors suggested alternative resistance mechanisms relating to changes in the membranes of the cells due to the altered environment of the biofilm. In another study, the same laboratory (45) investigated the dynamic interactions of vanamycin with planktonic cells and biofilms using fluorescence correlation spectroscopy, fluorescence lifetime imaging microscopy, and fluorescence recovery after photobleaching. The fluorescence correlation spectroscopy method enabled the laboratory to extend their transport/diffusion measurements to lower concentrations of antibiotic while the fluorescence lifetime imaging provided information on changes to molecular environment around the antibiotic. The authors were able to observe changes in the diffusion of vanamycin in the biofilm as compared planktonic cells. However, the authors suggested that the altered diffusion was not ultimately responsible for antibiotic resistance. The techniques developed in these papers could be potentially useful in assessing accessibility and transport of AMPs in biofilms as well.

CONCLUDING REMARKS

In this focused review, I have attempted to provide a flavor of the range of dynamics AMPs undergo when presented with membranes, cells and cell populations. Although these peptides are seemly simple, since they possess no tertiary structure, they are able to provide effective defenses against microbes encountered by many species in the animal and plant kingdoms. Optical spectroscopy and microscopy approaches combined with judicious labeling of peptides, membranes, and sub-cellular structures has enabled the determination of key events leading to cell killing activities. One of the broad results of these studies is that the dynamics detected in cells (by microscopy) appears to be orders of magnitude slower than processes studied in model membranes (by stopped flow fluorescence) and often exhibit lag-phases in behavior for minutes or hours. Peptide binding, secondary structure formation, orientation changes and peptide-peptide interactions in membranes, as studied by rapid mixing techniques occurs on the millisecond to second timescale, which likely reflect initial effects in one leaflet of a lipid bilayer. However, in cells, peptides need to transverse multiple barriers and can undergo a number of subsequent steps in addition to binding, conformation change and peptide-peptide interaction, including peptide nucleation/accumulation, membrane defect/pore creation and defect/pore re-sealing, peptide desorption, peptide translocation, membrane re-binding, peptide transport and interaction with non-membrane targets including (but not limited to) nucleic acids and DNA. The cellular landscape is heterogeneous in several respects (chemically, biologically, spatially, and temporally) and peptide concentrations within and between cells can be highly heterogeneous adding to the observed complexities in dynamics. Moreover, it needs to be remembered that cells are living, social entities, with feedback mechanisms and adaption, which have evolved over billions of years. What is needed are methods to track the physico-chemical states of the peptides in parallel with the relevant biological states of the microbe being targeted. In this way the relevant physical state of the peptide (structure, orientation, oligomeric state, cell location) which impedes microbial action can be better elucidated. It is emerging that membrane permeability may not be the only symptom of AMP action and a greater exploration of peptide-induced cell insults is needed. Improvements in imaging methods and probes will greatly assist in this endeavor.

AUTHOR CONTRIBUTIONS

AC wrote the paper.

FUNDING

AC acknowledges the Australian Research Council for previously funding research activities related to anti-microbial peptides.

ACKNOWLEDGMENTS

The author is grateful to Emeritus Professor William H. Sawyer who introduced the author to biophysics in general and peptide-membrane interactions in particular, and for his patience, guidance, and friendship.

REFERENCES

1. Hancock RE, Sahl HG. Antimicrobial and host-defense peptides as new anti-infective therapeutic strategies. *Nat Biotechnol*. (2006) 24:1551–7. doi: 10.1038/nbt1267
2. Bechinger B. The structure, dynamics and orientation of antimicrobial peptides in membranes by multidimensional solid-state NMR spectroscopy. *Biochim Biophys Acta.* (1999) 1462:157–83. doi: 10.1016/S0005-2736(99)00205-9
3. Cornell B, Separovic, F, Baldassi AJ, Smith R. Conformation and orientation of gramicidin-a in oriented phospholipid bilayers measured by solid-state C-13 NMR. *Biophys J.* (1988) 53:67–76. doi: 10.1016/S0006-3495(88)83066-2
4. Smith R, Separovic F, Milne TJ, Whittaker A, Bennett FM, Cornell BA, et al. Structure and orientation of the pore-forming peptide melittin,

in lipid bilayers. *J Mol Biol*. (1994) 241:456–66. doi: 10.1006/jmbi.1994.1520
5. He K, Ludtke SJ, Worcester DL, Huang HW. Neutron scattering in the plane of membranes: structure of alamethicin pores. *Biophys J*. (1996) 70:2659–66. doi: 10.1016/S0006-3495(96)79835-1
6. Qian S, Wang W, Yang L, Huang HW. Structure of the alamethicin pore reconstructed by x-ray diffraction analysis. *Biophys J*. (2008) 94:3512–22. doi: 10.1529/biophysj.107.126474
7. Lee MT, Sun T-L, Hung W-C, Huang HW. Process of inducing pores in membranes by melittin. *Proc Natl Acad Sci USA*. (2013) 110:14243–8. doi: 10.1073/pnas.1307010110
8. Lee C, Sun Y, Qian S, Huang HW. Transmembrane pores formed by human antimicrobial peptide LL-37. *Biophys J*. (2011) 100:1688–96. doi: 10.1016/j.bpj.2011.02.018
9. Shai Y. Mechanism of the binding, insertion and destabilization of phospholipid bilayer membranes by a-helical antimicrobial and cell non-selective membrane-lytic peptides. *Biochim Biophys Acta*. (1999) 1462:55–70. doi: 10.1016/S0005-2736(99)00200-X
10. Last NB, Miranker AD. Common mechanism unites membrane poration by amyloid and antimicrobial peptides. *Proc Natl Acad Sci USA*. (2013) 110:6382–7. doi: 10.1073/pnas.1219059110
11. Bechinger B, Lohner K. Detergent-like actions of linear amphipathic cationic antimicrobial peptides. *Biochim Biophys Acta*. (2006) 1758:1529–39. doi: 10.1016/j.bbamem.2006.07.001
12. Wimley WC, Hristova K. Antimicrobial peptides: successes, challenges and unanswered questions. *J Membr Biol*. (2011) 239:27–34. doi: 10.1007/s00232-011-9343-0
13. Melo MN, Ferre R, Castanho MA. Antimicrobial peptides: linking partition, activity and high membrane-bound concentrations. *Nat Rev Microbiol*. (2009) 7:245–50. doi: 10.1038/nrmicro2095
14. Constantinescu I, Lafleur M. Influence of the lipid composition on the kinetics of concerted insertion and folding of melittin in bilayers. *Biochim Biophys Acta*. (2004) 1667:26–37. doi: 10.1016/j.bbamem.2004.08.012
15. Tucker MJ, Tang J, Gai F. Probing the kinetics of membrane-mediated helix folding. *J Phys Chem B*. (2006) 110:8105–9. doi: 10.1021/jp060900n
16. Tang J, Signarvic RS, DeGrado WF, Gai F. Role of helix nucleation in the kinetics of binding of mastoparan X to phospholipid bilayers. *Biochemistry*. (2007) 46:13856–63. doi: 10.1021/bi7018404
17. Andreev OA, Engelman DM, Reshetnyak YK. Targeting diseased tissues by pHLIP insertion at low cell surface pH. *Front Physiol*. (2014) 5:97. doi: 10.3389/fphys.2014.00097
18. Ennaceur SM, Hicks MR, Pridmore CJ, Dafforn TR, Rodger A, Sanderson JM. Peptide adsorption to lipid bilayers: slow processes revealed by linear dichroism spectroscopy. *Biophys J*. (2009) 96:1399–407. doi: 10.1016/j.bpj.2008.10.039
19. Tang J, Yin H, Qiu J, Tucker MJ, DeGrado WF, Gai F. Using two fluorescent probes to dissect the binding, insertion, and dimerization kinetics of a model membrane peptide. *J Am Chem Soc*. (2009) 131:3816–7. doi: 10.1021/ja809007f
20. Rojko N, Kristan KC, Viero G, Žerovnik E, Maček P, Dalla Serra M, et al. Membrane damage by an α-helical pore-forming protein, Equinatoxin II, proceeds through a succession of ordered steps. *J Biol Chem*. 288:23704–15. doi: 10.1074/jbc.M113.481572
21. Kreutzberger MA, Pokorny A, Almeida PF. Daptomycin-phosphatidylglycerol domains in lipid membranes. *Langmuir*. (2017) 33:13669–79. doi: 10.1021/acs.langmuir.7b01841
22. Oreopoulos J, Epand RF, Epand RM, Yip CM. Peptide-induced domain formation in supported lipid bilayers: direct evidence by combined atomic force and polarized total internal reflection fluorescence microscopy. *Biophys J*. (2010) 98:815–23. doi: 10.1016/j.bpj.2009.12.4327
23. Wheaten SA, Ablan FDO, Logan Spaller B, Trieu JM, Almeida PF. Translocation of cationic amphipathic peptides across the membranes of pure phospholipid giant vesicles. *J Am Chem Soc*. (2013) 135:16517–25. doi: 10.1021/ja407451c
24. Paterson DJ, Tassieri M, Reboud J, Wilson R, Cooper JM. Lipid topology and electrostatic interactions underpin lytic activity of linear cationic antimicrobial peptides in membranes. *Proc Natl Acad Sci USA*. (2017) 114:E8324–32. doi: 10.1073/pnas.1704489114
25. Faust JE, Yang PY, Huang HW. Action of antimicrobial peptides on bacterial and lipid membranes: a direct comparison. *Biophys J*. (2017) 112:1663–72. doi: 10.1016/j.bpj.2017.03.003
26. He J, Krauson AJ, Wimley WC. Toward the de novo design of antimicrobial peptides: lack of correlation between peptide permeabilization of lipid vesicles and antimicrobial, cytolytic, or cytotoxic activity in living cells. *Biopolymers*. (2014) 102:1–6. doi: 10.1002/bip.22281
27. Starr CG, He J, Wimley WC. Host cell interactions are a significant barrier to the clinical utility of peptide antibiotics. *ACS Chem Biol*. (2016) 11:3391–9. doi: 10.1021/acschembio.6b00843
28. Munoz A, Read ND. Live-cell imaging and analysis shed light on the complexity and dynamics of antimicrobial peptide action. *Front Immunol*. (2012) 3:248. doi: 10.3389/fimmu.2012.00248
29. Leptihn S, Har JY, Chen J, Ho B, Wohland T, Ding JL. Single molecule resolution of the antimicrobial action of quantum dot-labeled sushi peptide on live bacteria. *BMC Biol*. (2009) 7:22. doi: 10.1186/1741-7007-7-22
30. Choi H, Rangarajan N, Weisshaar JC. Lights, camera, action! Antimicrobial peptide mechanisms imaged in space and time. *Trends Microbiol*. (2016) 24:111–22. doi: 10.1016/j.tim.2015.11.004
31. Sochacki KA, Barns KJ, Bucki R, Weisshaar JC. Real-time attack on single *Escherichia coli* cells by the human antimicrobial peptide LL-37. *Proc Natl Acad Sci USA*. (2011) 108:E77–81. doi: 10.1073/pnas.1101130108
32. Rangarajan N, Bakshi S, Weisshaar JC. Localized permeabilization of *E. coli* membranes by the antimicrobial peptide Cecropin A. *Biochemistry*. (2013) 52:6584–94. doi: 10.1021/bi400785j
33. Barns KJ, Weisshaar JC. Real-time attack of LL-37 on single *Bacillus subtilis* cells. *Biochim Biophys Acta*. (2013) 1828:1511–20. doi: 10.1016/j.bbamem.2013.02.011
34. Barns KJ, Weisshaar JC. Single-cell, time-resolved study of the effects of the antimicrobial peptide alamethicin on *Bacillus subtilis*. *Biochim Biophys Acta*. (2016) 1858:725–32. doi: 10.1016/j.bbamem.2016.01.003
35. Choi H, Yang Z, Weisshaar JC. Oxidative stress induced in *E. coli* by the human antimicrobial peptide LL-37. *PLoS Pathog*. (2017) 13:e1006481. doi: 10.1371/journal.ppat.1006481
36. Yang Z, Choi H, Weisshaar JC. Melittin-induced permeabilization, re-sealing, and re-permeabilization of *E. coli* membranes. *Biophys J*. (2018) 114:368–79. doi: 10.1016/j.bpj.2017.10.046
37. Gee ML, Burton M, Grevis-James A, Hossain MA, McArthur S, Palombo EA, et al. Imaging the action of antimicrobial peptides on living bacterial cells. *Sci Rep*. (2013) 3:1557. doi: 10.1038/srep01557
38. Burton MG, Huang QM, Hossain MA, Wade JD, Palombo EA, Gee ML, et al. Direct measurement of pore dynamics and leakage induced by a model antimicrobial peptide in single vesicles and cells. *Langmuir*. (2016) 32:6496–505. doi: 10.1021/acs.langmuir.6b00596
39. Park CB, Kim HS, Kim SC. Mechanism of action of the antimicrobial peptide buforin II: buforin II kills microorganisms by penetrating the cell membrane and inhibiting cellular functions. *Biochem Biophys Res Commun*. (1998) 244:253–7. doi: 10.1006/bbrc.1998.8159
40. Shagaghi N, Bhave M, Palombo EA, Clayton AH. Revealing the sequence of interactions of PuroA peptide with *Candida albicans* cells by live-cell imaging. *Sci Rep*. (2017) 7:43542. doi: 10.1038/srep43542
41. Zdybicka-Barabas A, Staczek S, Pawlikowska-Pawlega B, Mak P, Luchowski R, Skrzypiec K, et al. Studies on the interactions of neutral *Galleria mellonella* cecropin D with living bacterial cells. *Amino Acids*. (2019) 51:175–91. doi: 10.1007/s00726-018-2641-4
42. Wu F, Tan C. Dead bacterial absorption of antimicrobial peptides underlies collective tolerance. *J R Soc Interface*. (2019) 16:20180701. doi: 10.1098/rsif.2018.0701
43. Snoussi M, Talledo JP, Del Rosario NA, Mohammadi S, Ha BY, Košmrlj A, et al. Heterogeneous absorption of antimicrobial peptide LL37 in *Escherichia coli* cells enhances population survivability. *Elife*. (2018) 7:e38174. doi: 10.7554/eLife.38174

44. Boudjemaa R, Briandet R, Revest M, Jacqueline C, Caillon J, Fontaine-Aupart MP, et al. New insight into daptomycin bioavailability and localization in *Staphylococcus aureus* biofilms by dynamic fluorescence imaging. *Antimicrob Agents Chemother*. (2016) 60:4983–90. doi: 10.1128/AAC.00735-16
45. Daddi Oubekka S, Briandet R, Fontaine-Aupart MP, Steenkeste K. Correlative time-resolved fluorescence microscopy to assess antibiotic diffusion-reaction in biofilms. *Antimicrob Agents Chemother*. (2012) 56:3349–58. doi: 10.1128/AAC.00216-12

Conflict of Interest: The author declares that the research was conducted in the absence of any commercial or financial relationships that could be construed as a potential conflict of interest.

frontiers in Medical Technology

MINI REVIEW
published: 04 February 2021
doi: 10.3389/fmedt.2021.622096

Antibiotic Potential and Biophysical Characterization of Amphipathic β-Stranded $[XZ]_n$ Peptides With Alternating Cationic and Hydrophobic Residues

Erik Strandberg[1], *Parvesh Wadhwani*[1] *and Anne S. Ulrich*[1,2]*

[1] Karlsruhe Institute of Technology, Institute of Biological Interfaces (IBG-2), Karlsruhe, Germany, [2] Karlsruhe Institute of Technology, Institute of Organic Chemistry, Karlsruhe, Germany

OPEN ACCESS

Edited by:
Lorenzo Stella,
University of Rome Tor Vergata, Italy

Reviewed by:
Jayanta Haldar,
Jawaharlal Nehru Centre for Advanced Scientific Research, India
Charles Deber,
Hospital for Sick Children, Canada

***Correspondence:**
Anne S. Ulrich
anne.ulrich@kit.edu

Specialty section:
This article was submitted to Pharmaceutical Innovation, a section of the journal Frontiers in Medical Technology

Received: *27 October 2020*
Accepted: *12 January 2021*
Published: *04 February 2021*

Citation:
Strandberg E, Wadhwani P and Ulrich AS (2021) Antibiotic Potential and Biophysical Characterization of Amphipathic β-Stranded $[XZ]_n$ Peptides With Alternating Cationic and Hydrophobic Residues. Front. Med. Technol. 3:622096. doi: 10.3389/fmedt.2021.622096

Cationic membrane-active peptides are considered to be promising candidates for antibiotic treatment. Many natural and artificial sequences show an antimicrobial activity when they are able to take on an amphipathic fold upon membrane binding, which in turn perturbs the integrity of the lipid bilayer. Most known structures are α-helices and β-hairpins, but also cyclic knots and other irregular conformations are known. Linear β-stranded antimicrobial peptides are not so common in nature, but numerous model sequences have been designed. Interestingly, many of them tend to be highly membranolytic, but also have a significant tendency to self-assemble into β-sheets by hydrogen-bonding. In this minireview we examine the literature on such amphipathic peptides consisting of simple repetitive sequences of alternating cationic and hydrophobic residues, and discuss their advantages and disadvantages. Their interactions with lipids have been characterized with a number of biophysical techniques—especially circular dichroism, fluorescence, and infrared—in order to determine their secondary structure, membrane binding, aggregation tendency, and ability to permeabilize vesicles. Their activities against bacteria, biofilms, erythrocytes, and human cells have also been studied using biological assays. In line with the main scope of this Special Issue, we attempt to correlate the biophysical results with the biological data, and in particular we discuss which properties (length, charge, aggregation tendency, etc.) of these simple model peptides are most relevant for their biological function. The overview presented here offers ideas for future experiments, and also suggests a few design rules for promising β-stranded peptides to develop efficient antimicrobial agents.

Keywords: linear β-stranded antimicrobial peptides, cationic membrane-active peptides, peptides with alternating cationic and hydrophobic residues, biophysical studies of peptides in membranes, circular dichroism spectroscopy, fluorescence spectroscopy, peptide folding, peptide aggregation

INTRODUCTION

Cationic, amphipathic membrane-active peptides are considered to be promising new candidates for antibiotic treatment (1, 2). The simplest possible such peptides are made up from an alternate repeat sequence of cationic and hydrophobic amino acids, which can be expected to form amphipathic β-strands in a membrane (see **Figure 1**), with a fully extended backbone according to the Ramachandran plot (as in a β-sheet, but considering only a single strand here). All cationic residues will be aligned on one face and point toward the water, while the hydrophobic residues on the opposite side point into the hydrophobic interior of the membrane. Such amphipathic structures are usually membrane-active, and several peptides of this type have indeed shown antimicrobial activity.

A lot of interest has been shown in α-helical AMPs, but there is a lack of review articles covering amphipathic β-stranded peptides, and we therefore here try to summarize all relevant publications from 1981 to date about simple repetitive sequences able to form amphipathic β-strands (see **Table 1**).

The peptides covered here have repeating alternating sequences of cationic and hydrophobic amino acids, i.e., of the type $[XZ]_n$ or $[ZX]_n$, where X is a cationic and Z a hydrophobic amino acid. Using one-letter codes for natural amino acids, X can be K (lysine) or R (arginine), and Z can be V (valine), L (leucine), I (isoleucine), W (tryptophan) or F (phenylalanine). This gives ten XZ combinations, and most but not all of them have been studied (see **Table 1**). KL peptides have seen the largest interest, and also RL peptides have been examined. KI and RI peptides were studied as well, but only with a fixed length of eight amino acids. KW and RW peptides with different lengths have been investigated by several groups. We also found studies of KV but not of RV peptides. KF and RF peptides seem to have been ignored so far.

The main questions this minireview will try to answer are: (**Q1**) Do such repetitive sequences bind to membranes and form β-strands? (**Q2**) Do they show high antimicrobial activity? (**Q3**) Are the peptides selective, in terms of high antimicrobial activity vs. low hemolytic side effects? (**Q4**) Is there an optimal length of these peptides? (**Q5**) What is their mechanism of membrane permeabilization?

These questions are investigated using different methods. Binding, secondary structure and leakage are studied with biophysical methods in vesicles or monolayers, whereas

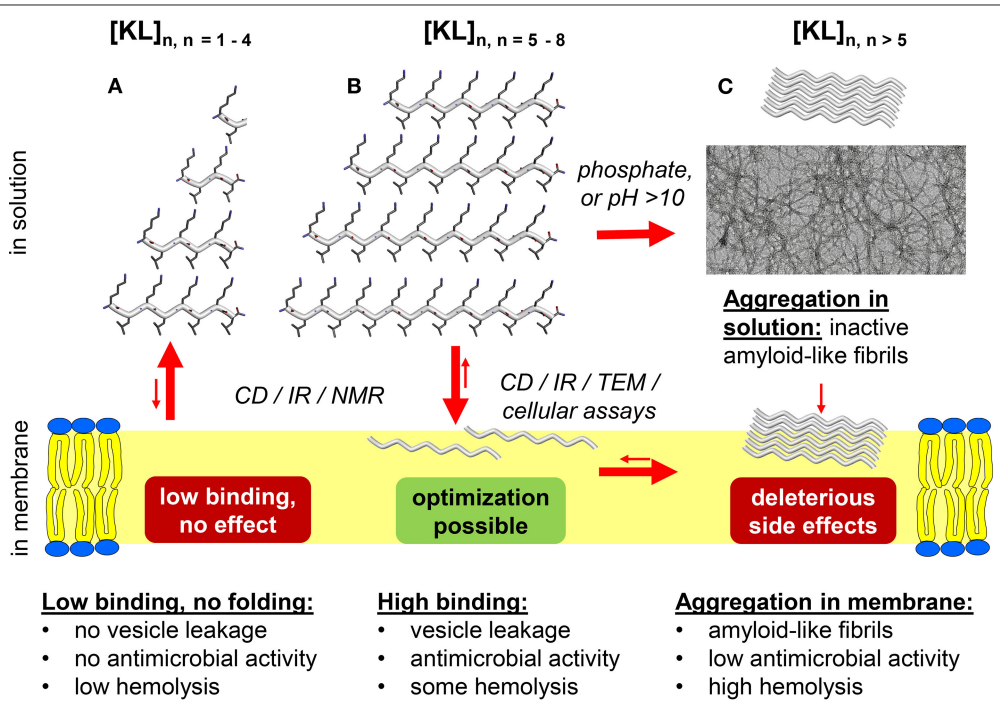

FIGURE 1 | Overview of the length-dependent membrane perturbing activity of peptides composed of alternating cationic and hydrophobic residues. General XZ sequences are here illustrated by $[KL]_n$, which have been studied extensively by biophysical and spectroscopic methods, as well as electron microscopy and microbiology. **(A)** Low binding, no effect: Very short KL peptides with up to 8 residues show a very low ability to bind or to fold in the membrane, and thus have essentially no antimicrobial activity. They do not self-assemble in the lipid bilayer, so they do not show much membrane toxicity in form of hemolysis either. **(B)** Optimization possibility: Medium-length KL peptides show higher binding and folding, hence they induce good membrane activity in the form of antimicrobial action and vesicle leakage. Based on length and kinetics of aggregation, they are able to self-assemble in the membrane into amyloid-like fibrils and therefore demonstrate moderate hemolytic side effects. **(C)** Side effects: KL peptides longer than 10 residues display a pronounced phosphate-dependent pre-aggregation already in solution, which causes extensive loss of the active molecules in form of toxic aggregates, before they can even bind to the membrane. This loss of material causes a lowering of the desired antimicrobial membrane activity, while at the same time the strong (pre-)aggregation correlates with increased hemolysis.

TABLE 1 | List of peptide sequences and which methods have been used to study them.

Peptides[a]	Sequences	Methods[b]	References
KI	$[IK]_4$-NH_2	BFA, CD, EM, FL, HA, MIC	(3)
KL	poly-[LK]	CD, IR	(4)
KL	$L[KL]_3$	CD, IR, ML	(5)
KL	Acetyl-$[KL]_9$-NH_2	HA, MIC, RT	(6)
KL	$[KL]_n$, $n = 8,10$	CD, IR, VCD	(7)
KL	Dansyl-$[KL]_4K$-NH_2, Dansyl-$[KL]_5K$-NH_2, Dansyl-$[KL]_6K$-NH_2, Dansyl-$[KL]_7K$-NH_2	BA, FL, HA, IR, LA, ML, RT	(8)
KL	Dansyl-$[KL]_4K$-NH_2, Dansyl-$[KL]_5K$-NH_2, Dansyl-$[KL]_7K$-NH_2	CA, MIC	(9)
KL	$[LK]_n$, $n = 2,5,7,8,9,10,11,12,18,24$	AF, HA, MIC	(10)
KL	$[KL]_4K$, $[KL]_7K$	CD, RS	(11)
KL	$[KL]_3$-NH_2, $[KL]_5$-NH_2, $[KL]_7$-NH_2, $[KL]_9$-NH_2	BA, CD, EM, HA, LA, MIC	(12)
KL	$[KL]_n$, $n = 3,4,5,6,7,8,9,10,11,12,13$; $[LK]_5$; $L[KL]_n$, $n = 4,5,6,7$; $[KL]_nK$, $n = 4,5,6,7$ (all $-NH_2$)	CD, HA, LA, MIC, NMR, OCD	(13)
KV	Ac-$[KV]_n$-$NHCH_3$, $n = 2,3,4$	CD, FL, LA, MIC	(14)
KV	C_{16}-$[VK]_4$	AF, CA, CD, EM, ITC, MIC	(15)
KW	$[KW]_3$, $[WK]_3$	AF, BA, CD, HA, MIC, LA	(16)
KW	$[KW]_2$-NH_2, $[KW]_3$-NH_2, $[KW]_4$-NH_2, $[KW]_5$-NH_2	AF, CV	(17)
RI	$[IR]_4$-NH_2	BFA, CD, EM, FL, HA, MIC	(3)
RL	$[LR]_n$, $n = 7,9,11$	AF, HA, MIC	(10)
RW	$[RW]_2R$-NH_2, $W[RW]_2$-NH_2, $[RW]_3$-NH_2	HA, MIC	(18)
RW	RWR-NH_2, WRW-NH_2, $[WR]_2$-NH_2, $R[WR]_2$-NH_2, $[WR]_2W$-NH_2, $[RW]_3$-NH_2, $[WR]_3$-NH_2	MIC	(19)
RW	RW-NH_2, $[RW]_2$-NH_2, $[RW]_3$-NH_2, $[RW]_4$-NH_2, $[RW]_5$-NH_2	BA, CD, FL, HA, MIC	(20)
RW	$[RW]_2$-NH_2, $[RW]_3$-NH_2, $[RW]_4$-NH_2, $[RW]_5$-NH_2	AF, CV	(17)
RW	$[RW]_3$-NH_2, lipidation	CV, HA, MIC, RT	(21)
$X_1Z_1X_2Z_2$	$[VRVK]_2$-NH_2, $[VRVK]_3$-NH_2, $[IRIK]_2$-NH_2, $[IRIK]_3$-NH_2, $[IRVK]_2$-NH_2, $[IRVK]_3$-NH_2, $[FRFK]_2$-NH_2, $[WRWK]_2$-NH_2	BFA, CD, EM, FL, HA, MIC	(3)

[a] *The repetitive sequence is given; charged residues are always stated first (i.e., $[KL]_n$ and $[LK]_n$ peptides are all listed under KL).*

[b] *Abbreviations: AF, antifungal assay; BA, binding assay; BFA, biofilm assay; CA, cell assays; CD, circular dichroism spectroscopy; CV, cell viability assay; EM, electron microscopy; FL, fluorescence spectroscopy; HA, hemolysis assay; IR, infrared spectroscopy; ITC, isothermal titration calorimetry; LA, leakage assay; MIC, minimum inhibitory concentration assay; ML, monolayer studies; NMR, nuclear magnetic resonance; OCD, oriented CD; RS, Raman spectroscopy; RT, HPLC retention time; VCD, vibrational CD.*

antimicrobial and hemolytic activities are determined using biological assays. A main theme in this review is therefore to combine results from vesicle and cell studies.

PEPTIDE BINDING TO MEMBRANES

Fluorescence methods have been used to study peptide binding to membranes. Trp fluorescence is sensitive to the environment and it is therefore a preferred method to use for peptides containing Trp. $[WK]_3$ and $[KW]_3$ were shown to bind to anionic lipid vesicles using this method (16). RW peptides with 2–10 amino acids bind to anionic phosphatidylglycerol (PG) vesicles (20). A series of KL peptides with different length were labeled at the N-termini with NBD, a fluorophore whose intensity is sensitive to the environment. Amongst these KL peptides, those with 6–18 amino acids had a high affinity for vesicles composed of neutral (zwitterionic) POPC and negatively charged POPG lipids (POPC/POPG, 1/1 mol/mol), and the longer ones were found to bind most strongly (12). In another study of dansyl-labeled KL peptides, peptides with 9–15 amino acids were binding to egg-PC/cholesterol (10/1) membranes with a higher lipid affinity for longer peptides (8).

These results are mostly quantitative, and only for KL peptides were binding constants calculated (8, 12). But it is obvious to conclude that the cationic XZ peptides experience a long-range electrostatic attraction to negatively charged membranes, and hydrophobic interactions can drive the binding further. In the case of RW, even very short dipeptides bind (20).

ASSUMING A β-STRANDED CONFORMATION IN MEMBRANES

We now consider question (**Q1**) above, whether the amphipathic XZ peptides indeed take on a β-stranded conformation when bound to membranes. Circular dichroism spectroscopy (CD) is the method of choice to study the secondary structure of peptides (22, 23), but cannot define the degree of assembly or oligomerization. Infrared spectroscopy (IR) can also be used to determine the local secondary structure (24), provided that the material is free from trifluoroacetic acid (25). It is not always possible with these methods to discriminate between monomeric β-strands, oligomeric β-sheets or long amyloid-like cross-β-sheet fibrils, so we will simply refer to a

β-stranded conformation. X-ray diffraction and/or transmission electron microscopy (TEM) would be needed to characterize any assembly on the supramolecular scale. The published results from CD and IR studies on XZ peptides are summarized in **Supplementary Table 1**, and are discussed below.

KL peptides with 6–26 amino acids were studied with CD in pure water and shown to bind to POPC/POPG vesicles. Peptides consisting of eight or more amino acids exhibited distinct β-stranded line shapes (13). $[IR]_4$ and $[IK]_4$ are unstructured in pure water, but show a β-stranded conformation in the presence of SDS micelles (no buffer was used) (3). $[KV]_4$–but not $[KV]_2$ and $[KV]_3$–binds to anionic vesicles in HEPES buffer and becomes β-stranded (14).

Most AMPs depend on a membrane environment to fold into their active amphipathic structure; in contrast, some XZ peptides have been found to do so in solution without a membrane, especially in the presence of phosphate.

CD spectra of $[KW]_3$ and $[WK]_3$ showed line shapes similar to α-helical conformations in 10 mM phosphate buffer and in the presence of neutral vesicles, but they bind to anionic vesicles and turn β-stranded (16). Monolayer studies were done for KL peptides at the water-air interface, with and without DMPC lipids. Peptides with 9–15 amino acids were found to give characteristic antiparallel β-sheet IR line shapes under all conditions, with peptides oriented flat on the membrane surface (8). Poly-LK ($[LK]_n$, where n is not exactly known, but is a large number) was shown with CD and IR to form antiparallel β-sheets *per se* in aqueous solution in absence of lipids (4). A later study using both electronic and vibrational CD, combined with IR, also showed that $[KL]_8$ and $[KL]_{10}$ form antiparallel β-sheets in D_2O at high peptide concentration (7). The aggregation of KL peptides into β-sheet amyloid-like fibrils (as was confirmed by TEM) in solution was found to be enhanced by buffers containing phosphate ions, and the speed of folding increases with phosphate concentration and peptide length (12). The short sequence of $[KL]_3$ did not fold, but aggregation was very fast for KL peptides with 14 or more amino acids (12). RW peptides with 4–10 amino acids showed signs of β-stranded CD signals in 20 mM phosphate buffer (20).

This means that in any studies using membranes—model bilayers as well as native cells—in phosphate buffer (like the RW and KL peptides above), it is not clear whether the observed folding occurs in the lipid bilayer or the peptide have pre-aggregated already in solution. As it was seen in the previous section that these cationic peptides tend to bind strongly to anionic lipids, it seems reasonable to assume that at least some of the peptides are located in the membrane in a β-stranded conformation.

Furthermore, a minimum length seems to be required for β-strand formation in the membrane (in absence of phosphate). KL peptides (13), and KV peptides (14) needed at least eight amino acids, as shorter peptides did not fold at all. For KI and RI peptides, a length of eight amino acids is also enough (shorter ones were not tested) (3). For RW peptides already tetrapeptides formed β-strands (20), though it is not clear if this would also be the case without any phosphate ions present in the medium.

MEMBRANE DAMAGE, VESICLE LEAKAGE

After establishing that the XZ peptides bind to anionic membranes in β-stranded conformations above a certain length, the question arises whether the peptides perturb the lipid bilayer and induce damage. This can be tested using fluorescence-based vesicle leakage assays. Several assays are available, and several types of XZ peptides have been tested:

- KL peptides were tested using an ANTS/DPX assay (12, 13). In POPC/POPG (1/2) vesicles, peptides with at least 10 amino acids showed >80% leakage, while shorter peptides were mostly inactive at a peptide-to-lipid molar ratio (P/L) of 1/20 (12).
- KV peptides were tested using a carboxyfluorescein assay in DPPC/DPPG (3/1) at P/L=1/10 (14). At 45°C, when the lipids were in a liquid crystalline phase, $[KV]_2$ gave no leakage, with $[KV]_3$ around 20% leakage was observed, and with $[KV]_4$ up to 50% leakage was found.
- $[KW]_3$ and $[WK]_3$ were tested using a calcein leakage assay (16). Leakage was strongly concentration dependent and also lipid-dependent. In anionic EYPC/EYPG (7/3) both peptides gave over 50% leakage at P/L = 1/10.

It is hard to compare these results on different peptides, since different lipids, buffers and dyes were used, and peptide concentrations varied. Only for the KL series, a wide range of peptide lengths has been systematically examined. It seems that KW and KV peptides are active already when they are at least six and eight amino acids long, respectively, whereas KL peptides needs to be at least 10 amino acids long to cause leakage. However, the minimum length required for the activity might vary and depend strongly on the experimental conditions.

At least for the KL and KV peptides, there is a correlation between folding into a β-stranded conformation and vesicle leakage activity. The short $[KL]_3$ binds to the membrane, but does not form β-strands and does not induce leakage (**Figure 1A**). $[KL]_5$ binds stronger than $[KL]_3$, forms β-strands (**Figure 1B**) and can also induce leakage (12). The longer KL peptides have a medium to high tendency to aggregate already in aqueous conditions as β-sheet fibrils (**Figure 1C**), especially in the presence of phosphate ions. KV peptides with eight amino acids formed β-strands and also induced leakage, whereas the shorter analogs did not fold into β-strands and gave no or low leakage (14).

ANTIMICROBIAL ACTIVITY

Comparing the results of antimicrobial assays between different studies in a quantitative manner is virtually impossible, because different experimental conditions and different bacteria have been used. Here we try to establish whether a peptide is active against any bacteria or not. MIC (minimum inhibitory concentration) values <10 μg/mL or μM, we will call "high activity"; MIC values of 10–100 μg/mL or μM, "medium activity"; and MIC values >100 μg/mL or μM, "low activity." If no activity was found at the highest tested concentration, we will call it "no activity." Results of studies of antimicrobial

activity of XZ peptides are discussed below. More details can be found in **Supplementary Table 2**, where also the microbes used are specified.

- KL peptides with 6–26 amino acids showed a length dependent activity in MIC tests against four different bacterial strains, with low activity for 6-mers, medium activity for peptides with eight amino acids, high activity for intermediate lengths (9–15 amino acids), and medium activity for longer peptides (13). The activity was slightly better against Gram-positive than Gram-negative bacteria, but usually not by more than a factor of two. The observed MIC values strongly depended on how the assay was performed, e.g., MIC values increased up to a factor 32 when peptides were exposed to phosphate buffer (12), illustrating how ambiguous it is to compare results from different studies.
- KL peptides (labeled with dansyl at the N-terminus) with nine amino acids showed high activity against some Gram-positive and Gram-negative strains, whereas peptides with 11 or 15 amino acids only showed medium activity (9).
- LK peptides with 14–24 amino acids all showed a similar, low to medium activity against Gram-positive and Gram-negative bacteria (10). LR peptides with 14 or 18 amino acids were compared in the same study. $[LR]_7$ had a similar activity as $[LK]_7$, but $[LR]_9$ and $[LR]_{11}$ had almost no activity. The LK and LR peptides were also tested for anti-fungal activity, and only the peptides with 14 amino acids showed a high activity; longer ones showed medium or low activity and shorter ones were not tested (10).
- $[IR]_4$ had a high activity against Gram-positive and Gram-negative bacteria and medium activity against *C. albicans*; $[IK]_4$ showed high activity against Gram-positive bacteria and *C. albicans*, and medium activity against Gram-negative bacteria (3). The difference in MIC between $[IR]_4$ and $[IK]_4$ could be as large as a factor of 8.
- KV peptides with 4–8 amino acids did not show any antimicrobial activity (up to 100 μg/ml peptide concentration) (14). $[KV]_4$ with a hexadecanoic acid chain attached to the N-terminus also did not show any activity (up to 32 μg/ml peptide) against 11 tested microbes (15). This indicates that membrane affinity (binding) and folding into an amphipathic β-stranded conformation is not sufficient for antimicrobial activity.
- $[KW]_3$ and $[WK]_3$ had medium or low activity against many bacteria, and somewhat higher activity against Gram-negative than Gram-positive bacteria. $[KW]_3$ usually had a lower MIC value than $[WK]_3$, by a factor of 2 (16).
- $[KW]_2$ and $[RW]_2$ showed no antifungal activity, but $[KW]_3$, $[RW]_3$, and $[RW]_4$ had a medium and $[KW]_4$, $[KW]_5$, and $[RW]_5$ had a high activity against *F. solani* and *F. oxysporum* (17).
- RW peptides have been examined in several studies. [RW] and $[RW]_2$ had no activity, $[RW]_3$ medium activity, $[RW]_4$ and $[RW]_5$ high activity against *E. coli* and *S. aureus* (20). Another study found that $[RW]_3$ had high activity while $W[RW]_2$ and $[RW]_2R$ showed medium activity against three tested bacteria (18). The same group later tested further peptides with 3–6 amino acids, and found that peptides with 2 or 3 amino acids had low or no activity, $W[RW]_2$ had medium activity and was more active than $[RW]_2R$, and $[RW]_3$ and $[WR]_3$ had a high activity (19). In another study, a Lys residue with an attached acyl chain was added to the N- or C-terminus of $[RW]_3$, and the effect of different acyl chain lengths was investigated (21). $[RW]_3$ itself had high activity against Gram-positive and medium activity against Gram-negative bacteria. In contrast to the KV peptide, here the activity improved when an acyl chain with 8–12 carbons was added (21).

From these results it can be concluded that (i) The activity of XZ peptides covers a broad spectrum; activity is similar against Gram-positive and Gram-negative bacteria, and some have also high activity against fungi. (ii) KV and RV peptides are much less active than the other combinations. (iii) XZ peptides need a minimum threshold length to be highly active, and from the studies mentioned 6–9 amino acids appear to be the threshold length. (iv) Activity depends on the sequence, e.g., Trp-containing peptides are active already with six amino acids, whereas Leu peptides needs at least nine amino acids. For IR and IK, only peptides with eight amino acids were tested and they had medium to high activity. For KW, peptides with six amino acids showed medium activity. Peptides containing Ile or Val have not been studied in sufficient detail to determine a threshold length. (v) For KL peptides, the minimum length needed for activity is similar to the minimum length needed for folding into a β-stranded conformation in membranes, and it is also similar to the threshold length needed for vesicle leakage (12, 13). (vi) KL peptides with more than 14 amino acids are less active (even when compared in a weight-by-weight manner) than the mid-length analogs. This intriguing observation was attributed to the enhanced tendency of the long peptides to pre-aggregate in solution, as illustrated in **Figure 1C** (12, 13). LK and LR peptides also seem to become less active when they get too long (10). The other XZ combinations have not been tested using long peptides with more than 10 amino acids, so it may be too early to conclude that they would also become less active when they get longer, but it seems very likely.

HEMOLYSIS

Comparing hemolysis values from different studies should be approached with caution, as human blood is not a standardized product, different protocols are used, and some studies present HC_{50} numbers (peptide concentration for 50% hemolysis) whereas others gives the percentage of hemolysis at a given peptide concentration. Nonetheless, this erythrocyte-based assay indicates whether a certain peptide show side-effects against human cells or not.

- In a study of KL peptides with 6–26 amino acids, hemolytic activity was low for peptides up to 10 amino acids (HC_{50} >40 μg/mL), but very high for 14 or more amino acids (HC_{50} ≤ 2 μg/mL) (13). In another study, acetyl-$[KL]_9$-NH_2 gave negligible hemolysis at 100 μg/ml (6).

- $[IR]_4$ and $[IK]_4$ gave only low hemolysis (HC_{10} >100 μg/mL) (3).
- $[KW]_3$ and $[WK]_3$ showed no hemolysis up to a concentration of 400 μM (16).
- RW with 2–10 amino acids showed overall low hemolysis (HC_{50} >75 μg/mL), with longer peptides being more active (20). $[RW]_3$, $W[RW]_2$, and $[RW]_2R$ showed no hemolysis up to 1,000 μg/ml (18). $[RW]_3$ showed low hemolysis also in another study (<10% at 250 μg/ml), but it increased upon lipidation (21). In the latter study, the effect of RW peptides on cell lines was also studied. $[RW]_3$ with a C_8 acyl chain connected to the N- or C-terminus was toxic to cancer cell lines ($IC_{50} \approx 4$ μM against MCF7 and HT29 cells), but less toxic to non-malignant fibroblast (GM5657) cells ($IC_{50} \approx 32$ μM) (21).

Even if it hard to compare the hemolytic effects found in different studies, is seems safe to state that short peptides with up to 10 amino acids give only low hemolysis, independent of the exact sequence. We believe that this is due to their slow kinetics to aggregate in the membrane into toxic fibrils. KL peptides with more than 14 amino acids, which have a high tendency to aggregate, are on the other hand highly hemolytic. Other sequences have not been tested using peptides with more than 10 amino acids, but there is a clear trend toward higher activity for longer peptides, so it seems reasonable to assume that any XZ peptide would also be highly hemolytic once it is long enough. Note that this continual upwards trend in hemolysis differs from the corresponding antimicrobial effects, which become reduced again for the very long peptides.

SELECTIVITY

The selectivity of peptides can be determined by comparing MIC values and hemolysis. Only a few studies have investigated both MIC and hemolysis. We here try to compare MIC with HC_{50} and define high selectivity when the therapeutic index ($TI = HC_{50}/MIC$) is at least 10.

For KL peptides, high selectivity was found for peptides with 8–10 amino acids, but for peptides with 14 or more amino acids, TI was below 1 (13). For RW peptides, one study found no hemolysis (18), which indicates high selectivity. Another study found TI > 10 for RW peptides with 4–10 amino acids (20). For $[RW]_3$, high selectivity was found, also when acyl chains were attached to the N- or C-terminus (21). From these results we conclude that for short XZ peptides with up to 10 amino acids, selectivity is high.

LONGER REPETITIVE SEQUENCES

Some longer repetitive sequences of the type $[X_1Z_1X_2Z_2]_n$ have been examined, but no systematic overview of all combinations has been made. In one study, seven peptides of the type $[Z_1KZ_2R]_n$ were compared to $[IR]_4$ and $[IK]_4$ (3). The results were similar as for the $[XZ]_n$ peptides discussed above. All peptides gave β-stranded CD line shapes in SDS micelles. For hemolysis, two trends were observed: (i) longer peptides with the same repetitive sequence produced more hemolysis, which may be due to self-assembly as discussed above; and (ii) peptides containing V or F were less hemolytic than peptides containing I or W, which fits with the observation that more hydrophobic peptides are usually more hemolytic (26–28). MIC tests against four bacterial strains showed that no peptide performed the best in all cases. Overall, the authors found that $[IRIK]_2$ and $[IRVK]_3$ were the most promising peptides (3).

MECHANISM OF ACTION

The basic assumption is that the antimicrobial activity of XZ peptides is due to membrane interactions. Many models have been proposed how AMPs can lead to membrane damage, and some indications to the mechanism of action can come from biophysical studies.

$[KL]_nK$ peptides were shown with IR to lie flat on the surface of an air-water interface, or a DMPC monolayer (8). $[KL]_5$ and $[KL]_7$ have been studied with solid-state ^{19}F-NMR in several lipid bilayer systems, and were found to lie flat on the membrane surface for all lipid compositions, independent of peptide concentration (13). A transmembrane orientation could indicate that peptides form pores through the membrane, but this was not observed. Leakage of KL peptides could be correlated with peptide length (even at constant weight-to-weight), but there was no dependence on membrane thickness. A certain dependence on bilayer thickness would have been expected if the peptides were to assemble into a transmembrane pore, such as a β-barrel. All in all, there was no sign of pore formation, and the most likely mechanism was proposed to be a carpet mechanism, with peptides on the membrane surface destabilizing the membrane by lateral crowding (13). Other XZ peptides have not been studied with these structural methods, so it is not clear if they all use the same mechanism of action. Apart from membrane permeabilization, it is likely that these cationic peptides can also disturb membrane integrity by clustering of anionic lipids, as found for other cationic AMPs (29). It is also possible that the peptides can pass through the membrane and be active against internal targets in the cell.

BALANCE BETWEEN CHARGED AND HYDROPHOBIC RESIDUES

XZ peptides have repeating alternating sequences of cationic and hydrophobic amino acids. If the number of residues is odd, then there will be more cationic or more hydrophobic residues, and the effects of this shift in the balance between charge and hydrophobicity can be observed in some studies.

In two studies, $[WR]_2W$ showed a higher antimicrobial activity than $R[WR]_2$ (18, 19). In another study, $[RW]_3$ was a bit more active than $K[RW]_3$ or $[RW]_3K$ (21). This seems to indicate that too much charge is reducing the antimicrobial activity, so that an overweight of hydrophobic residues may be advantageous. For KL peptides, it was found that $[KL]_4K$ had a slightly lower antimicrobial activity than $L[KL]_4$, and $[KL]_5K$ was less active than $L[KL]_5$. But on the other hand, $[KL]_6K$ was clearly

more active than $L[KL]_6$, and $[KL]_7K$ was much more active than $L[KL]_7$ (13). Thus, it seems that the balance shifts for longer peptides, so that higher hydrophobicity gives lower activity. This can be explained by the increased tendency of longer peptides to form aggregates, which reduces the antimicrobial activity. When peptides are more hydrophobic, this aggregation tendency is increased. For the short peptides, on the other hand, aggregation propensity is low so aggregation is not an issue, and it is likely that short peptides with less hydrophobicity have a lower affinity for membranes and are therefore less active.

For peptides with an even number of residues, there are as many cationic as hydrophobic residues. Here, the balance between hydrophobicity and charge mainly depends on the nature of the hydrophobic residues. Studies of these peptides show that the hydrophobicity has to be high enough: Val seems not to be sufficiently hydrophobic, and KV peptides are not active up to a length of eight residues (14). Leu is more hydrophobic than Val and KL peptides with eight residues have medium activity (13). Trp is probably the most hydrophobic and interfacially active residue, and this can be the reason KW and RW peptides show high activity even with six residues (17, 19, 20). Also in this case, the behavior changes with peptide length. $[VRVK]_2$ is much less active than $[IRIK]_2$, but $[VRVK]_3$ is more active than $[IRIK]_3$ (3).

Another way of shifting the balance between charge and hydrophobicity is to add an acyl chain to the peptide, which was done for $[RW]_3$ peptides (21). Adding a chain with 2 or 4 carbons did not improve the activity, but chains of 6–12 carbons improved MIC values. This fits with the observation above that for short peptides, additional hydrophobicity can improve activity.

Terminal groups can also modify the balance of charge and hydrophobicity. C-terminal amidation leads to a higher net positive charge and higher hydrophobicity. N-terminal acetylation leads to less positive charge and higher hydrophobicity. As can be seen in **Table 1**, some studies have used peptides with amidated or acetylated termini, but we have not found any studies where peptides with different terminal groups have been compared. From the results mentioned above, we predict that acetylation would be good for short but bad for long peptides. The effect of amidation is harder to predict, since both positive charge and hydrophobicity are increased.

More hydrophobic peptides are more hemolytic. For KL peptides, in all tested cases $L[KL]_n$ peptides showed more hemolysis than $[KL]_nK$ ($n = 4,5,6,7$) (13). For Z_1KZ_2R peptides, the amount of hemolysis of peptides increased according to $[VRVK]_2 < [IRVK]_2 < [IRIK]_2$ (3), which correlates with the hydrophobicity. For short peptides, where higher hydrophobicity led to higher antimicrobial effects, and hemolysis is low, increased hydrophobicity can be good for selectivity, but for long peptides lower hydrophobicity is preferable since this can both increase antimicrobial activity and reduce hemolysis.

THERAPEUTIC POTENTIAL

Before peptides can be used for therapy, many questions must be addressed. Are the peptides stable against proteases or will they be quickly degraded in the body? Will the pathogens develop resistance against the peptides? Will they be effective not only against bacteria *in vitro* but also *in vivo*? We have not found any studies of XZ peptides addressing these issues, so these are open questions where future studies would be needed.

CONCLUSIONS

We now return to the questions posed in the introduction about amphipathic $[XZ]_n$ sequences. (**Q1**) Do such repetitive sequences bind to membranes and form β-strands? **Answer**: Yes, if they are at least 6–10 amino acids long. (**Q2**) Do they show high antimicrobial activity? **Answer**: Yes, many of the tested sequences have shown a high activity (MIC < 10 μg/ml) against Gram-positive and Gram-negative bacteria, and against fungi. Peptides containing Val are less active. However, not all peptides are highly active against all bacteria, and different peptides showed the best activity against different bacteria, so testing is necessary to find the best candidate against a specific pathogen. (**Q3**) Are the peptides selective, in terms of high antimicrobial activity vs. low hemolytic side effects? **Answer**: Yes. All peptides with up to 10 amino acids show low or very low hemolysis, so if they are active against the relevant microbes then hemolysis seems not to be a problem. (**Q4**) Is there an optimal length of these peptides? **Answer**: Yes. Too short peptides do not bind and fold, and too long peptide aggregates and have reduced antimicrobial activity and increased their hemolytic activity, so there is an optimal length, which is different for different sequences, and seems to be related to the hydrophobicity of the Z residues. For KL peptides, the ideal length is 9–11 amino acids. For KW and RW peptides, 6–8 seems good. For the other sequences, not enough different lengths have been tested to answer this question. (**Q5**) What is their mechanism of membrane permeabilization? **Answer**: There have been few studies in this area, and only for KL peptides have a model been proposed (13), as illustrated in **Figure 1**. Binding of cationic XZ peptides to anionic membranes is clearly driven by long-range electrostatic attraction, but favorable hydrophobic interactions will also enable zwitterionic vesicles to be covered by peptides to a considerable extent. They then probably act via a "carpet mechanism," but have not been observed to form transient pores or well-defined β-barrels. Instead, lateral crowding in the outer monolayer of the plasma membrane seems to be responsible for imminent antimicrobial action. At this stage, both peptide length as well as concentration have to be high enough that the molecules assume a β-stranded conformation and become self-assembled. When pre-aggregation into amyloid-like fibrils is too vigorous and occurs already in solution, this material is lost and antimicrobial activity decreases. These pre-aggregated oligomers nonetheless seem to be membranolytic against red blood cells (but not bacteria), so hemolysis becomes more and more pronounced the longer and more aggregation-prone the peptides are.

Since the therapeutic potential of a peptide can be assessed by comparing MIC and HC_{50}, we can conclude that the simple XZ peptides with 6–11 amino acids bear quite some promise. Still, the interest in optimizing these kinds of peptides seems to be low. So far, no systematic effort has been made to compare

all suggested combinations of cationic and hydrophobic amino acids, and in most studies only a few discrete peptides lengths have been used. There is still much work needed to get a clear picture of these simple peptides, to determine which sequence and length has the most promising therapeutic potential, to resolve the remaining mechanistic details in each particular case. There is also a need of studies of peptide stability, and to determine if microbes develop resistance and if peptides are effective *in vivo*.

AUTHOR CONTRIBUTIONS

All authors listed have made a substantial, direct and intellectual contribution to the work, and approved it for publication.

FUNDING

This work was supported by the Helmholtz Association Program BIF-TM and by the German Research Foundation (DFG) by grants UL127/7-1 and INST 121384/58-1 FUGG. We acknowledge financial support from the KIT Publication Fund for open access publication fees.

SUPPLEMENTARY MATERIAL

The Supplementary Material for this article can be found online at: https://www.frontiersin.org/articles/10.3389/fmedt.2021.622096/full#supplementary-material

REFERENCES

1. Magana M, Pushpanathan M, Santos AL, Leanse L, Fernandez M, Ioannidis A, et al. The value of antimicrobial peptides in the age of resistance. *Lancet Infect Dis.* (2020) 20:e216–30. doi: 10.1016/S1473-3099(20)30327-3
2. Mahlapuu M, Bjorn C, Ekblom J. Antimicrobial peptides as therapeutic agents: opportunities and challenges. *Crit Rev Biotechnol.* (2020) 40:978–92. doi: 10.1080/07388551.2020.1796576
3. Ong ZY, Gao SJ, Yang YY. Short synthetic β-sheet forming peptide amphiphiles as broad spectrum antimicrobials with antibiofilm and endotoxin neutralizing capabilities. *Adv Funct Mater.* (2013) 23:3682–92. doi: 10.1002/adfm.201202850
4. Brack A, Spach G. Multiconformational synthetic polypeptides. *J Am Chem Soc.* (1981) 103:6319–23. doi: 10.1021/ja00411a009
5. DeGrado WF, Lear JD. Induction of peptide conformation at apolar/water interfaces. 1. A study with model peptides of defined hydrophobic periodicity. *J Am Chem Soc.* (1985) 107:7684–9. doi: 10.1021/ja00311a076
6. Blondelle SE, Houghten RA. Design of model amphipathic peptides having potent antimicrobial activities. *Biochemistry.* (1992) 31:12688–94. doi: 10.1021/bi00165a020
7. Baumruk V, Huo DF, Dukor RK, Keiderling TA, Lelievre D, Brack A. Conformational study of sequential Lys and Leu based polymers and oligomers using vibrational and electronic CD spectra. *Biopolymers.* (1994) 34:1115–21. doi: 10.1002/bip.360340815
8. Castano S, Desbat B, Dufourcq J. Ideally amphipathic β-sheeted peptides at interfaces: structure, orientation, affinities for lipids and hemolytic activity of $(KL)_mK$ peptides. *Biochim Biophys Acta.* (2000) 1463:65–80. doi: 10.1016/S0005-2736(99)00175-3
9. Beven L, Castano S, Dufourcq J, Wieslander A, Wroblewski H. The antibiotic activity of cationic linear amphipathic peptides: lessons from the action of leucine/lysine copolymers on bacteria of the class *Mollicutes*. *Eur J Biochem.* (2003) 270:2207–17. doi: 10.1046/j.1432-1033.2003.03587.x
10. Strom RM, Brondsema PJ. *Periodic Antimicrobial Peptides*. Washington, DC: U.S. Patent and Trademark Office (2006).
11. Hernández B, Boukhalfa-Heniche FZ, Seksek O, Coïc YM, Ghomi M. Secondary conformation of short lysine- and leucine-rich peptides assessed by optical spectroscopies: effect of chain length, concentration, solvent, and time. *Biopolymers.* 81, 8–19. doi: 10.1002/bip.20366
12. Strandberg E, Schweigardt F, Wadhwani P, Bürck J, Reichert J, Cravo HLP, et al. Phosphate-dependent aggregation of $[KL]_n$ peptides affects their membranolytic activity. *Sci Rep.* (2020) 10:12300. doi: 10.1038/s41598-020-69162-0
13. Schweigardt F. *$[KL]_n$ Peptide – Optimierung von β-Faltblatt-Modellpeptiden zur Generierung neuer antimikrobieller Peptide mit therapeutischem Potenzial* (Ph.D. thesis). Karlsruhe Institute of Technology, Karlsruhe, Germany (2020).
14. Ono S, Lee S, Mihara H, Aoyagi H, Kato T, Yamasaki N. Design and synthesis of basic peptides having amphipathic β-structure and their interaction with phospholipid membranes. *Biochim Biophys Acta.* (1990) 1022:237–44. doi: 10.1016/0005-2736(90)90119-9
15. de Almeida NR, Han YC, Perez J, Kirkpatrick S, Wang YL, Sheridan MC. Design, synthesis, and nanostructure-dependent antibacterial activity of cationic peptide amphiphiles. *ACS Appl Mater Inter.* (2019) 11:2790–801. doi: 10.1021/acsami.8b17808
16. Gopal R, Kim YJ, Seo CH, Hahm KS, Park Y. Reversed sequence enhances antimicrobial activity of a synthetic peptide. *J Pept Sci.* (2011) 17:329–34. doi: 10.1002/psc.1369
17. Gopal R, Na H, Seo CH, Park Y. Antifungal activity of $(KW)_n$ or $(RW)_n$ peptide against *Fusarium solani* and *Fusarium oxysporum*. *Int J Mol Sci.* (2012) 13:15042–53. doi: 10.3390/ijms131115042
18. Strom MB, Rekdal O, Svendsen JS. Antimicrobial activity of short arginine- and tryptophan-rich peptides. *J Pept Sci.* (2002) 8:431–7. doi: 10.1002/psc.398
19. Strom MB, Haug BE, Skar ML, Stensen W, Stiberg T, Svendsen JS. The pharmacophore of short cationic antibacterial peptides. *J Med Chem.* (2003) 46:1567–70. doi: 10.1021/jm0340039
20. Liu ZG, Brady A, Young A, Rasimick B, Chen K, Zhou CH, et al. Length effects in antimicrobial peptides of the $(RW)_n$ series. *Antimicrob Agents Chemother.* (2007) 51:597–603. doi: 10.1128/AAC.00828-06
21. Albada HB, Prochnow P, Bobersky S, Langklotz S, Schriek P, Bandow JE, et al. Tuning the activity of a short Arg-Trp antimicrobial peptide by lipidation of a C- or N-terminal lysine side-chain. *ACS Med Chem Lett.* (2012) 3:980–4. doi: 10.1021/ml300148v
22. Kelly SM, Jess TJ, Price NC. How to study proteins by circular dichroism. *Biochim Biophys Acta.* (2005) 1751:119–39. doi: 10.1016/j.bbapap.2005.06.005
23. Micsonai A, Wien F, Bulyaki E, Kun J, Moussong E, Lee YH, et al. BeStSel: a web server for accurate protein secondary structure prediction and fold recognition from the circular dichroism spectra. *Nucleic Acids Res.* (2018) 46:W315–22. doi: 10.1093/nar/gky497
24. Barth A. Infrared spectroscopy of proteins. *Biochim Biophys Acta.* (2007) 1767:1073–101. doi: 10.1016/j.bbabio.2007.06.004
25. Haris PI, Chapman D. The conformational analysis of peptides using Fourier transform IR spectroscopy. *Biopolymers.* (1995) 37:251–63. doi: 10.1002/bip.360370404
26. Wieprecht T, Dathe M, Beyermann M, Krause E, Maloy WL, MacDonald DL, et al. Peptide hydrophobicity controls the activity and selectivity of magainin 2 amide in interaction with membranes. *Biochemistry.* (1997) 36:6124–32. doi: 10.1021/bi9619987

27. Zelezetsky I, Pag U, Sahl HG, Tossi A. Tuning the biological properties of amphipathic alpha-helical antimicrobial peptides: rational use of minimal amino acid substitutions. *Peptides*. (2005) 26:2368–76. doi: 10.1016/j.peptides.2005.05.002
28. Strandberg E, Kanithasen N, Bürck J, Wadhwani P, Tiltak D, Zwernemann O, et al. Solid state NMR analysis comparing the designer-made antibiotic MSI-103 with its parent peptide PGLa in lipid bilayers. *Biochemistry*. (2008) 47:2601–16. doi: 10.1021/bi701944r
29. Wadhwani P, Epand RF, Heidenreich N, Bürck J, Ulrich AS, Epand RM. Membrane-active peptides and the clustering of anionic lipids. *Biophys J*. (2012) 103:265–74. doi: 10.1016/j.bpj.2012.06.004

Conflict of Interest: The authors declare that the research was conducted in the absence of any commercial or financial relationships that could be construed as a potential conflict of interest.

frontiers in Medical Technology

PERSPECTIVE
published: 16 February 2021
doi: 10.3389/fmedt.2021.640929

Precision Design of Antimicrobial Surfaces

Declan C. Mullen[1], *Xing Wan*[2], *Timo M. Takala*[2], *Per E. Saris*[2]* *and V. M. Moreira*[1,3,4]*

[1] *Strathclyde Institute of Pharmacy and Biomedical Sciences, University of Strathclyde, Glasgow, United Kingdom,* [2] *Department of Microbiology, Faculty of Agriculture and Forestry, University of Helsinki, Helsinki, Finland,* [3] *Laboratory of Pharmaceutical Chemistry, Faculty of Pharmacy, University of Coimbra, Coimbra, Portugal,* [4] *Centre for Neuroscience and Cell Biology, University of Coimbra, Coimbra, Portugal*

The overall expectation from an antimicrobial surface has been high considering the need for efficiency in preventing the attachment and growth of pathogenic microbes, durability, safety to both humans and environment as well as cost-effectiveness. To date, antimicrobial surface design has been mostly conducted liberally, without rigorous consideration of establishing robust structure-activity relationships for each design strategy or of the use intended for a specific antimicrobial material. However, the variability among the domain bacteria, which is the most diverse of all, alongside the highly dynamic nature of the bacteria-surface interface have taught us that the likelihood of finding universal antimicrobial surfaces is low. In this perspective we discuss some of the current hurdles faced by research in this promising field, emphasizing the relevance and complexity of probing the bacteria-surface interface, and explain why we feel it would greatly benefit from a more streamlined *ad-hoc* approach.

Keywords: surface, antimicrobial, biofilm, interface, bacteria

OPEN ACCESS

Edited by:
Miguel A. R. B. Castanho, University of Lisbon, Portugal

Reviewed by:
Pradeep Kumar, Institute of Genomics and Integrative Biology (CSIR), India
Cesar de la Fuente-Nunez, University of Pennsylvania, United States

***Correspondence:**
Per E. Saris
per.saris@helsinki.fi
V. M. Moreira
vmoreira@ff.uc.pt

Specialty section:
This article was submitted to Pharmaceutical Innovation, a section of the journal Frontiers in Medical Technology

Received: *12 December 2020*
Accepted: *28 January 2021*
Published: *16 February 2021*

Citation:
Mullen DC, Wan X, Takala TM, Saris PE and Moreira VM (2021) Precision Design of Antimicrobial Surfaces. Front. Med. Technol. 3:640929. doi: 10.3389/fmedt.2021.640929

ANTIMICROBIAL SURFACES—WHY ARE THEY SO IMPORTANT?

Interest in the development of antimicrobial surfaces has escalated in the last two decades. Literature searches on the Web of Science reveal impressive 3- and 6-fold increases in the number of original and review articles as well as in patents devoted to antimicrobial surfaces, from 2000 to 2010 and from 2000 to 2020, respectively. Patents alone account for 29% of the 42,691 publication universe under the keyword "antimicrobial surface."

This interest in antimicrobial surfaces goes hand-in-hand with the 2012–2022 explosion in the global market for nanoengineered surfaces (NES) where the building sector heads the expected million USD revenues, followed by electronics and the biomedical sector (1). Within the latter, the sub-sectors of anti-bacterial sterilization and anti-biofouling radically evolved from having a negligible value in 2012 to an expected value of 106.4 and 51.7 billion USD by 2022, respectively, with an estimated total Compound Annual Growth Rate (CAGR) of 127.5% in this period.

Antimicrobial surfaces are needed to prevent the growth and spread of infectious microbes on a plethora of materials that routinely serve humans. They have become ubiquitous and indispensable in extending the shelf-life of both consumer and industrial goods as well as in reducing health risks across a wide range of sectors including health, food packaging, furniture, textiles, and the building and shipping industries (2–5). The outstanding impact of antimicrobial surfaces on boosting future technologies is predicted in the design of self-driving cars, for instance, where they will help to reduce the maintenance and downtime of key parts (6).

The need to build physical barriers between humans and infectious agents to prevent their spread within our community by contact has very recently been evidenced by the global pandemic

caused by SARS-CoV-2. Although extensive efforts have been directed toward the design of surfaces to target bacteria, little has been done to find those that efficiently kill and/or repel viruses, with the first steps toward understanding the method and duration of their surface adherence currently taking place (5, 7). At present, the remarkable evolution of community-disseminated super-resistant bacteria, alongside the scarcity of new antibacterial drugs to have reached the market in the past decades (8), represents a latent menace that threatens to cause the next global health crisis.

Overall, the expectations from an antimicrobial surface have been high. They should efficiently prevent the attachment and growth of pathogenic microbes indiscriminately thus limiting their spread by contact, be durable, harmless to human health and to the environment and cost-effective. However, can one single surface meet such a highly demanding wish list? Is the surface development process conveniently streamlined to ensure that the upcoming years will witness significant advances in the biomedical field?

ANTIMICROBIAL SURFACES THAT LEACH

By far the most straightforward strategy to design surfaces that target bacteria remains the incorporation, by physical adsorption, of an antimicrobial agent onto a polymeric matrix (2–5). Such surfaces are deemed leaching, i.e., they kill bacteria upon release of the antimicrobial agent over time. Despite being effective, leaching surfaces will eventually become inactivated once the antimicrobial agent has been exhausted and cannot therefore be regarded as long-lasting solutions. In addition, they are only as good as the agent they release, i.e., there is a limited number of antimicrobial agents that can be used due to stringent regulations.

Although the mode of action of leaching surfaces is easily ascribed to the respective agent they release, the exact load of antimicrobial agent comprised by the surface can be hard to accurately quantify, and the environmental impact of the leaching process is of concern (9). Metals and metal salts including silver, copper, zinc, and titanium dioxide are the most commonly used. They are known to act by inducing bacterial membrane disruption and oxidative stress. Long-term toxicity associated with exposure to silver is not yet fully established in humans, but its ecotoxicity is well-documented (10). Quaternary ammonium compounds (QACs), bearing permanent positive charges that disrupt bacterial membranes, lack sufficient efficiency and are prone to development of bacterial resistance (11, 12). In a similar fashion, bacteriostatic triclosan was banned over toxicity to both humans and the environment (13).

Natural antimicrobial peptides (AMPs), both bacterial and human, have also been under investigation (14). Among the diverse mechanisms of action known for AMPs, their net charges may allow for interaction with cell membranes while hydrophobic regions can maneuver into the phospholipid bilayers and in some instances result in pore formation and leakage of cell components (15). However, as AMPs are part of the innate immune system of all multicellular organisms, the potential for resistance development cannot be overlooked, particularly if human AMPs are employed. AMPs can also be chemically grafted at the surface of polymers (14, 16–22) and in this case the leaching ability will depend upon the coupling method selected which will determine the stability of the chemical bond established. Amides are among the strongest chemical bonds whereas esterification and silanization will afford less stable bonds. A quick agar plate test is usually sufficient to rule out this leaching effect. AMPs are chemically complex molecules and therefore any translation of their outstanding antimicrobial properties will likely rely on the development of simplified synthetic counterparts.

Nonetheless, antimicrobial surfaces that leach have been successfully translated into very useful practical applications. For instance, despite the fact that roughly 1/3 of the silver present in conventional wound-dressings leaches out and becomes black due to oxidation hindering visualization of the healing process, silver-based dressings are a mainstay (23) among antimicrobial dressings, a market valued at 9.16 billion USD in 2014 and expected to exceed more than 23 billion by 2024 (24).

THE NEED TO EXPLORE THE INTERFACE WITH BACTERIA

The early 90's realization that bacteria exist in nature as biofilms as opposed to single entities and the extensive knowledge of bacterial behavior gathered thereafter (25, 26), have impacted the paradigm of antimicrobial surface design. Biofilms are very seldom eradicated by leaching antimicrobial agents alone due to the presence of the sheltering extracellular matrix. One of the best depictions of this behavior is provided by *B. subtilis* biofilms (27) which are more non-water-wetting than Teflon, presenting extreme impenetrability to liquid antimicrobials and gases.

Intensive research into the physico-chemical mechanisms specifically involved in bacterial adhesion onto surfaces has been underway (28–32) in the hope of finding key events that can be targeted for limiting early biofilm establishment. In this regard, a dissection of the interactions occurring at the interface of antimicrobial surfaces and the outermost external components of bacterial cells has become crucial in order to explain how surfaces can either kill or repel bacteria (or both) directly upon contact. Such explorations have often been complemented by computational models to predict bacterial attachment (33, 34). These surfaces are referred to as contact-active, and typically they are complex, either entailing a pattern at the surface or a random arrangement, yet their mode of action is independent of any leaching substance. They are usually perceived as potentially more ecofriendly if they are biodegradable, and more efficient if they can overcome clogging by dead bacteria and/or debris over time.

For instance, QACs and antibiofilm peptides have been immobilized at the surface of several polymers leading to contact-killing activity (35–39). The regular separation of both positive and negative charges along zwitterionic polymers successfully resulted in anti-fouling and bactericidal properties with self-cleaning capacity (40). Immobilized bacteriocins such as nisin

on various abiotic surfaces can prevent the formation of biofilms, and this approach has been explored by the food industry (41, 42). More recently, small tricyclic diterpenoids covalently bound onto nanocellulose through stable amide bonds (43, 44) rendered contact-active anionic antimicrobial surfaces capable of limiting biofilm formation.

Although hard to characterize both experimentally and theoretically, the tentative modes of action of contact-active surfaces are supported from studies regarding the activity of biosurfactants (45) and the interactions of nanoparticles with bacteria (32, 46, 47). It is likely that the surfaces are perceived by bacteria as complex polymeric matrices, unevenly branched with hydrophobic and hydrophilic regions or net charges that can intercalate into bacterial external structures, bind to surface proteins or modulate their activity through ion chelation, and/or have the ability to extract lipopolysaccharides, ultimately causing cell death. Other mechanisms may include enzymatic degradation of cellular membrane components or disruption of eDNA as well as limitation of the nutrient reservoir (48, 49). The presence of photoinduced compounds bound at the surface to kill bacteria by generation of oxidative radical species following activation has also been reported (35).

Regardless of the approach, the chemistry at the surface is a key determinant of the activity. Topographical manipulation of surfaces alone, i.e., devoid of any concomitant chemical modification, can compromise bacterial adhesion and in particular settings result in a contact-killing effect (50, 51). However, the number of materials that will entail the specific topographical features needed for the activity is limited and this strategy lacks sufficient efficiency to be regarded as a self-standing solution.

WHY ARE BACTERIA WINNING THE DAY?

The cumulative experience from the last two decades of research has taught us that bacteria-surface interfaces are outstandingly dynamic and that the likelihood of being successful with a simple approach, either leaching or non-leaching, is low. Therefore, the combination of leaching and non-leaching actions on the same surface, i.e., mixed action surfaces, has been investigated (2–5). One extreme example depicts the combination of topographical manipulation with chemical functionalization and the inclusion of a lubricating layer of liquid to build a slippery liquid-infused porous surface (SLIPS) that was able to prevent the attachment of both Gram-positive and Gram-negative bacteria for a whole week (52).

Indeed, the domain bacteria is the most diverse of all and this makes it virtually impossible to fine-tune a surface to meet the specific requirements of each bacterial strain in terms of hydrodynamics, topography-induced cell ordering, air-entrapment, chemical gradients, physicochemical force fields or cell membrane deformation, among other factors. In addition, even though bacteria use their surface structures, such as fimbriae, pili, flagella, and S-layer for adhesion to surfaces, these structures may also prevent bacteria or their membranes from coming into close contact with antimicrobial surfaces.

Bacteria have different preferences for hydrophilic and hydrophobic surfaces (53) which could relate to differences in charges and/or composition of their bacterial membranes and the extracellular polymeric matrix (EPS) they produce en route to establishing biofilms. In general, hydrophobic surfaces gain greater biofilm formation (54). As in antimicrobial drug discovery, the outer membrane of Gram-negative bacteria is a strikingly differentiating factor. The presence of lipopolysaccharide O-antigen is reported to hamper adhesion of surfaces onto bacteria by neutralizing the negative charge usually carried by the supporting cell envelope (32). Moreover, bacteria are well-prepared to adapt and evolve to survive in the presence of external stress. Finally, compared to research settings which work with primarily monoculture biofilms in controlled environments, natural biofilms also frequently host other microbes as symbionts to establish polymicrobial communities, thus challenging the performance of antimicrobial surfaces when used in real settings.

As exemplified by contact-active surfaces, a plethora of different surface chemistries will work against bacteria through manipulations of net charge, hydrophobicity, topography, or other factors, yet to date there is no clear cut structure-activity relationships that can be inferred to guide future design efforts. This is largely due to the diversity of polymer substrates, antimicrobial agents and functionalization strategies currently portrayed in the literature, which are extremely broad and essentially random, hampering what should be a systematic approach. At least one study has applied combinatorial chemistry and high-throughput screening to identify a group of structurally related polymers that limit pathogenic bacterial adhesion at their surface (55). With this approach, it is possible to focus on a single polymer class and determine, with a higher level of precision, exactly which variations in chemistry afforded the best antimicrobial properties. With this information at hand, predictive computational models can be built (29), yet their robustness is likely to be at present modest in light of the extreme complexity in accurately depicting bacteria-surface interactions.

On the other hand, while the majority of available reports focuses on finding broad-action antimicrobial surfaces, the translational value of selectively targeting one specific bacteria type remains to be determined. Clues on how to design surfaces that discriminate between Gram-positive and Gram-negative bacteria as well as fungi are available from literature on microbe detection systems (30). The fact that the activity of cationic polymers can be modulated by buffer concentration is notable.

TIME TO CONSOLIDATE TO STEP UP TO THE CHALLENGE

The intricacy of bacteria-surface interactions turns the idea of an universal antimicrobial surface into a chimera. We foresee that advancements in this field will come from focusing the design of antimicrobial surfaces on the very specific features required by its intended use. This precision design will entail a comprehensive knowledge of the microbes that need to be targeted as well as of the polymers that bear the most convenient properties for

good performance in a particular setting. These should include biopolymers such as (nano)cellulose, silk, collagen, or alginate for the sake of sustainability.

To support this endeavor, a very wide range of experimental, computational, and theoretical approaches will be mandatory where knowledge of chemistry including computational chemistry, microbiology, membrane biophysics and bioinformatics is key. In addition, the development of antimicrobial surfaces would greatly benefit from a "design of experiments approach" to streamline the process for building robust structure-activity relationships.

Our ability to continue to explore bacteria-surface interactions will dictate how much we can say of specific modes of action for each surface at the atomic level. For instance, despite significant advances in molecular dynamics to study the mode of action of small AMPs (56, 57), extending these studies to the scale and complexity of a surface is still way beyond the limits of this technique. Proteomics, transcriptomics, and mutagenesis studies will continue to be essential techniques in deciphering the interactions of antimicrobial surfaces with bacteria.

Regardless of addressing the main mode of action, the most important thing is functionality, i.e., to find surfaces that work. How broad-acting, durable, biodegradable, or cytocompatible they need to be should be dictated by their final use. Therefore, the selection of suitable control materials and bioassays that address the complexity of single-cell and multispecies biofilms is of utmost importance. Surfaces should also be screened in combination with other techniques to target biofilms including, for instance, cold plasmas (58). Finally, however specific these insights may be for bacteria, we believe the strategy for surface design outlined herein will apply for other microbes including fungi and viruses, conveniently adapted to their particular biology.

DATA AVAILABILITY STATEMENT

The original contributions generated for the study are included in the article/supplementary material, further inquiries can be directed to the corresponding author/s.

AUTHOR CONTRIBUTIONS

DM, XW, TT, and PS carried out literature searches. VM compiled the manuscript. All authors contributed to the views expressed in the article, and critically helped to write and revise the document.

FUNDING

VM acknowledges Tenovus Scotland (project S18-23) for funding. VM and DM thank the Engineering and Physical Sciences Research Council (EPSRC) for funding (Doctoral Training Partnership 2018–19, Grant No. EP/R513349/1).

REFERENCES

1. Oliver, J. *Bioinspired and Nanoengineered Surfaces: Technologies, Applications and Global Markets - AVM089A*. (2013). Available at: http://www.bccresearch.com/market-research/advanced-materials/bioinspired-nanoengineered-surfaces-avm089a.html?tid=eGMwdiov (accessed March 16, 2016).
2. Hasan J, Crawford J, Ivanova EP. Antibacterial surfaces: the quest for a new generation of biomaterials. *Trends Biotechnol.* (2013) 31:295–304. doi: 10.1016/j.tibtech.2013.01.017
3. Banerjee I, Pangule RC, Kane RS. Antifouling coatings: recent developments in the design of surface that prevent the fouling by proteins, bacteria, and marine organisms. *Adv Mater.* (2011) 23:690–718. doi: 10.1002/adma.201001215
4. Adlhart C, Verran J, Azevedo NF, Olmez MM, Gouveia I, Melo LF, et al. Surface modifications for antimicrobial effects in the healthcare setting: a critical overview. *J Hosp Infect.* (2018) 99:239–49. doi: 10.1016/j.jhin.2018.01.018
5. Cassidy SS, Sanders DJ, Wade J, Parkin IP, Carmalt CJ, Smith AM, et al. Antimicrobial surfaces: a need for stewardship? *PLoS Pathog.* (2020) 16:e1008880. doi: 10.1371/journal.ppat.1008880
6. Bettenhausen C. Self-driving cars are coming. Chemical makers are racing to keep up. *C&EN News.* (2020) 98:27–33. Available online at: https://cen.acs.org/business/consumer-products/Self-driving-cars-coming-Chemical/98/i41
7. van Doremalen N, Bushmaker AT, Morris DH, Holbrook MG, Gamble A, Williamson BN, et al. Aerosol and surface stability of SARS-CoV-2 as compared with SARS-CoV-1. *N Engl J Med.* (2020) 382:1564–67. doi: 10.1056/NEJMc2004973
8. Plackett B. Why big pharma has abandoned antibiotics. *Nature.* (2020) 586:S50–2. doi: 10.1038/d41586-020-02884-3
9. Bruenke J, Roschke I, Agarwal S, Riemann T, Greiner A. Quantitative comparison of the antimicrobial efficiency of leaching versus nonleaching polymer materials. *Macromol Biosci.* (2016) 16:647–654. doi: 10.1002/mabi.201500266
10. Seltenrich N. Nanosilver: weighing the risks and benefits. *Environ Health Perspect.* (2012) 121:A220–25. doi: 10.1289/ehp.121-a220
11. Gerba CP. Quaternary ammonium biocides: efficacy in application. *Appl Environ Microbiol.* (2015) 81:464–9. doi: 10.1128/AEM.02633-14
12. Jennings MC, Minbiole KPC, Wuest WM. Quaternary ammonium compounds: an antimicrobial mainstay and platform for innovation to address bacterial resistance. *ACS Infect Dis.* (2015) 1:288–303. doi: 10.1021/acsinfecdis.5b00047
13. Weatherley LM, Goose JA. Triclosan exposure, transformation, and human health effects. *J Toxicol Environ Health B Crit Rev.* (2017) 20:447–69. doi: 10.1080/10937404.2017.1399306
14. Riool M, de Breij A, Drijfhout JW, Nibbering PH, Zaat SAJ. Antimicrobial peptides in biomedical device manufacturing. *Front Chem.* (2017) 5:63. doi: 10.3389/fchem.2017.00063
15. Jenssen H, Hamill P, Hancock RE. Peptide antimicrobial agents. *Clin Microbiol Rev.* (2006) 19:491–511. doi: 10.1128/CMR.00056-05
16. Costa F, Carvalho IF, Montelaro RC, Gomes P, Martins MCL. Covalent immobilization of antimicrobial peptides (AMPs) onto biomaterial surfaces. *Acta Biomaterialia.* (2011) 7:1431–40. doi: 10.1016/j.actbio.2010.11.005
17. Yala J-F, Thebault P, Héquet A, Humblot V, Pradier C-M, Berjeau J-M. Elaboration of antibiofilm materials by chemical grafting of an antimicrobial peptide. *Appl Microbiol Biotechnol.* (2011) 89:623–34. doi: 10.1007/s00253-010-2930-7
18. Etayash H, Norman L, Thundat T, Kaur K. Peptide-bacteria interactions using engineered surface-immobilized peptides from class IIa bacteriocins. *Langmuir.* (2013) 12:4048–56. doi: 10.1021/la3041743
19. Song DW, Kim SH, Kim HH, Lee KH, Ki CS, Park YH. Multi-biofunction of antimicrobial peptide-immobilized silk fibroin nanofiber membrane: implications for wound healing. *Acta Biomater.* (2016) 39:146–55. doi: 10.1016/j.actbio.2016.05.008
20. Homaeigohar S, Boccaccini AR. Antibacterial biohybrid nanofibers for wound dressings. *Acta Biomater.* (2020) 107:25–49. doi: 10.1016/j.actbio.2020.02.022
21. Yang X, Liu W, Xi G, Wang M, Liang B, Shi Y, et al. Fabricating antimicrobial peptide-immobilized starch sponges for hemorrhage

control and antibacterial treatment. *Carbohyd Polym.* (2019) 222:115012. doi: 10.1016/j.carbpol.2019.115012
22. Wang X, Mao J, Chen Y, Song D, Gao Z, Zhang G, et al. Design of antibacterial biointerfaces by surface modification of poly (ε-caprolactone) with fusion protein containing hydrophobin and PA-1. *Colloids Surf B Biointerfaces.* (2017) 151:255–63. doi: 10.1016/j.colsurfb.2016.12.019
23. Leaper D. An overview of the evidence on the efficacy of silver dressings. The silver debate. *J Wound Care.* (2011) 20(Suppl. 2):8–14. doi: 10.12968/jowc.2011.20.Sup2.8
24. *Data from: Wound Dressing Market Size, Share & Trends Analysis Report by Product [Traditional, Advanced (Moist, Antimicrobial, Interactive)], by Region, and Segment Forecasts, 2012-2022.* Grand View Research (2018) Available online at: https://www.grandviewresearch.com/industry-analysis/wound-dressing-market (access December 1, 2020).
25. Flemming H-C, Wingender J, Szewzyk U, Steinberg P, Rice SR, Kjelleberg S. Biofilms: an emergent form of bacterial life. *Nat Rev Microbiol.* (2016) 14:563–75. doi: 10.1038/nrmicro.2016.94
26. Koo H, Allan RN, Howlin RP, Stoodley P, Hall-Stoodley L. Targeting microbial biofilms: current and prospective therapeutic strategies. *Nat Rev Microbiol.* (2017) 15:740–55. doi: 10.1038/nrmicro.2017.99
27. Epstein AK, Pokroy B, Seminara A, Aizenberg J. Bacterial biofilm shows persistent resistance to liquid wetting and gas penetration. *Proc Natl Acad Sci USA.* (2011) 108:995–1000. doi: 10.1073/pnas.1011033108
28. Tuson HH, Weibel DB. Bacteria-surface interactions. *Soft Matter.* (2013) 9:4368–80. doi: 10.1039/C3SM27705D
29. Mkulskis P, Hook A, Dundas AA, Irvine D, Sanni O, Anderson D, et al. Prediction of broad-spectrum pathogen attachment to coating materials for biomedical devices. *ACS Appl Mater Interfaces.* (2018) 10:139–49. doi: 10.1021/acsami.7b14197
30. Yuan H, Liu Z, Liu L, Lv F, Wang Y, Wang S. Cationic conjugated polymers for discrimination of microbial pathogens. *Adv Mater.* (2014) 26:4333–8. doi: 10.1002/adma.201400636
31. Feng ZV, Gunsolus IL, Qiu TA, Hurley KR, Nyberg LH, Frew H, et al. Impacts of gold nanoparticle charge and ligand type on surface binding and toxicity to Gram-negative and Gram-positive bacteria. *Chem Sci.* (2015) 6:5186–96. doi: 10.1039/C5SC00792E
32. Beaussart A, Beloin C, Ghigo J-M, Chapot-Chartier M-P, Kulakauskas S, Duval JFL. Probing the influence of cell surface polysaccharides on nanodendrimer binding to Gram-negative and Gram-positive bacteria using single-nanoparticle force spectroscopy. *Nanoscale.* (2018) 10:12743–53. doi: 10.1039/C8NR01766B
33. Chinnaraj SB, Jayathilake PG, Dawson J, Ammar J, Portoles J, Jakubovics N, et al. Modelling the combined effect of surface roughness and topography on bacterial attachment. *J Materials Sci Technol.* (2021) 81:151–61. doi: 10.1016/j.jmst.2021.01.011
34. Acemel, RC, Govantes, F, Cuetos A. Computer simulation study of early bacterial biofilm development. *Sci Rep.* (2018) 8:5340. doi: 10.1038/s41598-018-23524-x
35. Kaur R, Liu S. Antibacterial surface design – contact kill. *Progress Surf Sci.* (2016) 91:136–53. doi: 10.1016/j.progsurf.2016.09.001
36. Siedenbiedel F, Tiller JC. Antimicrobial polymers in solution and on surfaces: overview and functional principles. *Polymers.* (2012) 4:46–71. doi: 10.3390/polym4010046
37. Alfei S, Schito AM. Positively charged polymers as promising devices against multidrug resistant Gram-negative bacteria: a review. *Polymers.* (2020) 12:1195. doi: 10.3390/polym12051195
38. Poverenov E, Klein M. Formation of contact active antimicrobial surfaces by covalent grafting of quaternary ammonium compounds. *Colloids Surf B Biointerfaces.* (2018) 169:195–205. doi: 10.1016/j.colsurfb.2018.04.065
39. Wang D, Haapasalo M, Gao Y., Ma J, Shen Y. Antibiofilm peptides against biofilms on titanium and hydroxyapatite surfaces. *Bioactive Mater.* (2018) 3:418–25. doi: 10.1016/j.bioactmat.2018.06.002
40. Mi L, Jiang S. Integrated antimicrobial and nonfouling zwitterionic polymers. *Angew Chem Int Ed.* (2014) 53:1746–54. doi: 10.1002/anie.201304060
41. Qi X, Poernomo G, Wang K, Chen Y, Chan-Park M-B, Xu R, et al. Covalent immobilization of nisin on multi-walled carbon nanotubes: superior antimicrobial and anti-biofilm properties. *Nanoscale.* (2011) 3:1874–80. doi: 10.1039/c1nr10024f
42. Mauriello G, Ercolini D, La Storia A, Casaburi A, Villani F. Development of polythene films for food packaging activated with an antilisterial bacteriocin from *Lactobacillus curvatus* 32Y. *J Appl Microbiol.* (2004) 97:314–22. doi: 10.1111/j.1365-2672.2004.02299.x
43. Hassan G, Forsman N, Wan X, Keurulainen L, Bimbo LM, Johansson L-S, et al. Dehydroabietylamine-based cellulose nanofibril films: a new class of sustainable biomaterials for highly efficient, broad-spectrum antimicrobial effects. *ACS Sustainable Chem Eng.* (2019) 7:5002–9. doi: 10.1021/acssuschemeng.8b05658
44. Hassan G, Forsman N, Wan X, Keurulainen L, Bimbo LM, Stehl S, et al. Non-leaching, highly biocompatible nanocellulose surfaces that efficiently resist fouling by bacteria in an artificial dermis model, *ACS Appl Bio Mater.* (2020) 3:4095–108. doi: 10.1021/acsabm.0c00203
45. Otzen D E. Biosurfactants and surfactants interacting with membranes and proteins: same but different? *Biochim Biophys Acta Biomembr.* (2017) 1859:639–49. doi: 10.1016/j.bbamem.2016.09.024
46. Richards S-J, Isufi K, Wilkins LE, Lipecki J, Fullam E, Gibson MI. Multivalent antimicrobial polymer nanoparticles target mycobacteria and Gram-negative bacteria by distinct mechanisms. *Biomacromolecules.* (2018) 19:256–64. doi: 10.1021/acs.biomac.7b01561
47. Pillai PP, Kowalczyk B, Kandere-Grzybowska K, Borkowska M, Grzybowski BA. Engineering Gram selectivity of mixed-charge gold nanoparticles by tuning the balance of surface charges. *Angew Chem Int Ed.* (2016) 55:8610–4. doi: 10.1002/anie.201602965
48. Das T, Sharma PK, Busscher HJ, van der Mei HC, Krom BP. Role of extracellular DNA in initial bacterial adhesion and surface aggregation. *Appl Environ Microbiol.* (2010) 76:3405–3408. doi: 10.1128/AEM.03119-09
49. Saggu SK, Jha G, Mishra PC. Enzymatic degradation of biofilm by metalloprotease from *Microbacterium* sp. SKS10. *Front Bioeng Biotechnol.* (2019) 7:192. doi: 10.3389/fbioe.2019.00192
50. Cheng Y, Feng G, Moraru CI. Micro- and nanotopography sensitive bacterial attachment mechanisms: A review. *Front Microbiol.* (2019) 10:191. doi: 10.3389/fmicb.2019.00191
51. Hasan J, Chatterjee K. Recent advances in engineering topography mediated antibacterial surfaces. *Nanoscale.* (2015) 7:15568–75. doi: 10.1039/C5NR04156B
52. Epstein AK, Wong T-S, Belisle RA, Boggs EM, Aizenberg J. Liquid-infused structured surfaces with exceptional antibiofouling performance. *Proc Natl Acad Sci USA.* (2012) 109:13182–7. doi: 10.1073/pnas.1201973109
53. Krasowska A, Sigler K. How microorganisms use hydrophobicity and what does this mean for human needs? *Front Cell Infect Microbiol.* (2014) 4:112. doi: 10.3389/fcimb.2014.00112
54. De-la-Pinta I, Cobos M, Ibarretxe J, Montoya E, Eraso E, Guraya T, et al. Effect of biomaterials hydrophobicity and roughness on biofilm development. *J Mater Sci Mater Med.* (2019) 30:77. doi: 10.1007/s10856-019-6281-3
55. Hook AL, Chang C-Y, Yang J, Luckett J, Cockayne A, Atkinson S, et al. Combinatorial discovery of polymers resistant to bacterial attachment. *Nat Biotechnol.* (2012) 30:868–75. doi: 10.1038/nbt.2316
56. Im W, Khalid S. Molecular simulations of Gram-negative bacterial membranes come of age. *Annual Rev Phys Chem.* (2020) 71:171–88. doi: 10.1146/annurev-physchem-103019-033434
57. Gumbart JC, Beeby M, Jensen GJ, Roux B. *Escherichia coli* peptidoglycan structure and mechanics as predicted by atomic-scale simulations. *PLoS Comput Biol.* (2014) 10:e1003475. doi: 10.1371/journal.pcbi.1003475
58. Gilmore BF, Flynn PB, O'Brien S, Hickok N, Freeman T, Bourke P. Cold plasmas for biofilm control: opportunities and challenges. *Trends Biotechnol.* (2018) 36:627–38. doi: 10.1016/j.tibtech.2018.03.007

Conflict of Interest: The authors declare that the research was conducted in the absence of any commercial or financial relationships that could be construed as a potential conflict of interest.

frontiers in Medical Technology

ORIGINAL RESEARCH
published: 22 February 2021
doi: 10.3389/fmedt.2021.626481

Modeling Cell Selectivity of Antimicrobial Peptides: How Is the Selectivity Influenced by Intracellular Peptide Uptake and Cell Density

Bethany R. Schefter[1], *Shokoofeh Nourbakhsh*[1], *Sattar Taheri-Araghi*[2] *and Bae-Yeun Ha*[1]*

[1] Department of Physics and Astronomy, University of Waterloo, Waterloo, ON, Canada, [2] Department of Physics and Astronomy, California State University, Northridge, CA, United States

Antimicrobial peptides (AMPs) are known to attack bacteria selectively over their host cells. Many attempts have been made to use them as a template for designing peptide antibiotics for fighting drug-resistant bacteria. A central concept in this endeavor is "peptide selectivity," which measures the "quality" of peptides. However, the relevance of selectivity measurements has often been obscured by the cell-density dependence of the selectivity. For instance, the selectivity can be overestimated if the cell density is larger for the host cell. Furthermore, recent experimental studies suggest that peptide trapping in target bacteria magnifies the cell-density dependence of peptide activity. Here, we propose a biophysical model for peptide activity and selectivity, which assists with the correct interpretation of selectivity measurements. The resulting model shows how cell density and peptide trapping in cells influence peptide activity and selectivity: while these effects can alter the selectivity by more than an order of magnitude, peptide trapping works in favor of host cells at high host-cell densities. It can be used to correct selectivity overestimates.

Keywords: antimicrobial peptides, peptide activity and selectivity, biophysical modeling, Langmuir binding model, minimal inhibition concentration, minimal hemolytic concentration

OPEN ACCESS

Edited by:
Maria A. Deli,
Institute of Biophysics, Hungary

Reviewed by:
Manuel N. Melo,
New University of Lisbon, Portugal
Jens Rolff,
Freie Universität Berlin, Germany

***Correspondence:**
Bae-Yeun Ha
byha@uwaterloo.ca

Specialty section:
This article was submitted to Pharmaceutical Innovation, a section of the journal Frontiers in Medical Technology

Received: *06 November 2020*
Accepted: *20 January 2021*
Published: *22 February 2021*

Citation:
Schefter BR, Nourbakhsh S, Taheri-Araghi S and Ha B-Y (2021) Modeling Cell Selectivity of Antimicrobial Peptides: How Is the Selectivity Influenced by Intracellular Peptide Uptake and Cell Density. Front. Med. Technol. 3:626481. doi: 10.3389/fmedt.2021.626481

INTRODUCTION

Antimicrobial peptides (AMPs) are naturally-occurring peptide antibiotics and attack bacteria selectively over host cells (1–3). AMPs are mostly cationic and have stronger binding affinity for bacterial membranes, which carry a large fraction of anionic lipids (1–4). Their amphiphilic structure enables them to attach to and perturb membranes (1–5). While membrane perturbation is not the sole mechanism of action, it is the first decisive event they induce (1, 2, 5). Indeed, AMPs are multitasking molecules: they are pore formers, metabolic inhibitors (1, 2), and/or immunomodulators (6–8). Their membrane-perturbing ability has, however, spurred many attempts to use them as a template for designing potent peptide antibiotics, especially for fighting conventional drug-resistant bacteria (1, 2, 4, 9). Developing bacterial resistance against membrane-perturbing peptides would involve "costly" redesigning of their membranes (1). Nevertheless, pathogens can evolve antimicrobial resistance (10, 11). Consequences of this need to be considered in our endeavor in searching for potent peptide antibiotics. Despite this challenge, the therapeutic potential of these multitasking molecules has generated interest in designing optimized peptides [see a recent review (7) and references therein].

A central concept in assessing peptide potency is "peptide selectivity." For a given peptide, it is quantified by the ratio of a minimum hemolytic concentration (MHC) to a minimum inhibitory concentration (MIC) [see for instance; (9)]. For large MHC/MIC, there is a range of peptide concentration at which a given peptide is active against bacteria only. The requirement of a minimum peptide concentration (either MIC or MHC) for membrane rupture suggests that cell density is a control parameter for peptide activity and selectivity, as recently discussed (12, 13). Increasing the cell density is equivalent to reducing the amount of peptides available to each cell. As a result, MICs and MHCs increase as the cell density increases; the ratio MHC/MIC is cell-density dependent.

A related quantity is a threshold coverage of peptides on membranes (3, 14–17). Let P/L be the molar ratio of bound peptides to lipids. At the MIC or MHC, P/L reaches the threshold value, P/L^*, beyond which bound peptides permeabilize the membrane. The value of P/L^* depends on the type of peptide and lipid (3, 14–17). It is typically larger for lipid membranes mimicking bacterial membranes.

The correct interpretation of selectivity measurements has often been obscured by the cell-density dependence of the selectivity (12, 13, 18). For instance, the selectivity can be overestimated if the cell density is larger for the host cell. Furthermore, a number of recent studies highlight the effect of peptide trapping inside (dead) cells on peptide activity and selectivity (19–21). It was shown that each cell can absorb $\sim 10^7$ peptides (19–21). Often referred to as an *inoculum* effect [see (19–22) and references therein], this enhances population survivability (21), since it lowers the peptide concentration in the solution. As a result, the MIC obtained for a bacterial culture increases more rapidly with the cell density (21), compared to what corresponding model membranes would suggest (12, 13).

Here we offer a biophysical model of peptide activity and selectivity that assists with the correct interpretation of selectivity measurements. Our primary goal is to present a theoretical model, which can be used to predict peptide activity and selectivity under a variety of conditions, once their biophysical parameters are characterized. Indeed, an experimental approach to the relationship between peptide selectivity and cell densities is complex in a multi-species cultures, despite its relevance in biological and medical contexts. Our model will be beneficial for clarifying the relevance of selectivity measurements under controlled conditions.

Here we consider two approaches to quantifying cell selectivity (MHC/MIC). Imagine measuring MICs and MHCs in separate cell cultures (each containing a single species) and combining them into MHC/MIC. In this work, the resulting selectivity is referred to as "noncompetitive selectivity." Alternatively, one can measure MICs and MHCs in a multi-species cell culture containing both bacteria and host cells and then calculate MHC/MIC. The resulting (competitive) selectivity is generally different from the corresponding noncompetitive one (12). If the competitive selectivity reflects adequately the competition between host cells and bacteria in binding peptides, the noncompetitive one can be exaggerated, when the host cell density is high, as correctly referred to as an experimental "illusion" by Matsuzaki (18).

Consistent with earlier studies (12, 13, 19–21), our results suggest that both MICs and MHCs increase with cell densities C_{cell}; in a low cell-density limit, they become C_{cell}-independent, i.e., intrinsic to a given peptide. Our results also show that peptide trapping increases both MICs and MHCs, magnifying their cell-density dependence, since the competition for peptides between cells is now stronger. This is a key feature highlighted in recent experiments (19–21) but left out in earlier theoretical studies (12, 13). The net effect of peptide trapping on peptide selectivity is that it tends to enhance the selectivity in the large host-cell density limit. With the parameter choices used, noncompetitive selectivity can be exaggerated by an order of magnitude. Our model also offers a systematic approach to correcting the selectivity for exaggeration; a noncompetitive selectivity can be corrected into a corresponding competitive one.

THEORETICAL MODEL

In this section, we discuss how peptide selectivity depends on cell density. We first introduce a few key parameters relevant in this work. Let C_{p} be the total concentration of peptides. Recall that P/L is the molar ratio of membrane-bound peptides to lipids; $(P/L)_{\text{B}}$ for bacterial membranes and $(P/L)_{\text{H}}$ for host cell membranes. At a certain value of C_{p}, denoted as C_{p}^*, P/L reaches a threshold value required for membrane rupture, $(P/L)^*$; C_{p}^* is either MIC or MHC. Also, the cell density, C_{cell}, is a key parameter for peptide activity and selectivity (12, 13, 19–21); $C_{\text{cell}} = C_{\text{B}}$ for bacteria and $C_{\text{cell}} = C_{\text{H}}$ for host cells. A related quantity is the surface area of each cell, A_{cell} (12): $A_{\text{cell}} = A_{\text{B}}$ or $A_{\text{cell}} = A_{\text{H}}$ for bacteria and host cells, respectively. Doubling A_{cell} for given C_{cell} is equivalent to doubling C_{cell} for given A_{cell}. Similarly, a_{B} and a_{H} are the lipid headgroup area for bacterial and host-cell membranes, respectively. Finally, N_{p} is the number of trapped peptides per cell: N_{pB} and N_{pH} for bacteria and host cells, respectively.

The cell-density dependence of peptide activity, especially for a mixture of bacterial and host cells, is illustrated in **Figure 1** [see (13) for a homogeneous case]. Here, the concentric circles in blue represent bacterial cells and the pink ones stand for host cells. **Figure 1(i)** shows a single-cell limit at an MIC. The introduction of a host cell will reduce the amount of peptides for the existing bacterial cell as shown in (ii). The extra number of peptides to maintain at the MIC is equal to $(P/L)_{\text{H}} \times A_{\text{H}}/a_{\text{H}}$; similarly, in (iii), the number of peptides that should be added is $(P/L)_{\text{B}}^* \times A_{\text{B}}/a_{\text{B}} + 2\,(P/L)_{\text{H}} \times A_{\text{H}}/a_{\text{H}}$.

A number of studies have unambiguously shown that (dead) cells can absorb a large number of peptides ($\sim 10^7$-10^8) (19–21). This enhances the so-called "inoculum" effect: it amplifies the cell-density dependence of MICs and MHCs, since it increases the number of peptides consumed by each cell. Along the line of what was done recently (13), this effect can be taken into account. Recall that N_{pB} and N_{pH} are the number of absorbed peptides per cell in bacterial and host cells, respectively. Our consideration replies on the following justifiable simplification: $N_{\text{pB}} = 0$ below

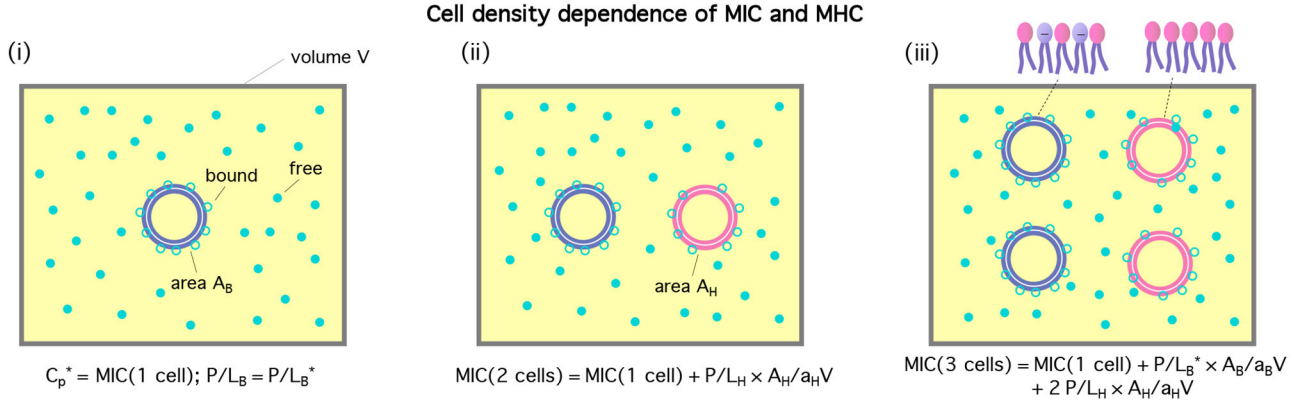

FIGURE 1 | Cell-density dependence of C_p^*, i.e., either MIC or MHC. Cells are represented by two concentric circles and peptides by filled (free) or unfilled circles (bound) circles; if the blue circles represent bacterial cells, the pink ones stand for host cells. Let $A_{cell} = A_B$ or A_H be the bacterial or host cell surface area, respectively. The progression from **(i)–(iii)** suggests that $MIC(C_{cell}) = MIC_0 + A_B/a_B \times (P/L)_B^* C_B + A_H/a_H \times (P/L)_H C_H$. If we exchange the role between bacterial and host cells, we arrive at $MHC(C_{cell}) = MHC_0 + A_H/a_H \times (P/L)_H^* C_H + A_B/a_B \times (P/L)_B C_B$. The figure was adapted with permission from (12), Copyright (2015) American Chemical Society, and from (13) with permission from The Royal Society of Chemistry.

MIC and similarly $N_{pH} = 0$ below MHC. Prior to membrane rupture, penetration of peptides into a cell is expected to be a rare event, since it involves overcoming a large free energy barrier for crossing an otherwise intact cell membrane.

Following the reasoning in **Figure 1** and taking into account peptide trapping, one can arrive at

$$MIC(C_B, C_H) = MIC_0 + \left[\left(\frac{P}{L}\right)_B^* \frac{A_B}{a_B} + N_{pB}^*\right] C_B + \left(\frac{P}{L}\right)_H \frac{A_H}{a_H} C_H \quad (1a)$$

$$MHC(C_B, C_H) = MHC_0 + \left[\left(\frac{P}{L}\right)_H^* \frac{A_H}{a_H} + N_{pH}^*\right] C_H + \left[\left(\frac{P}{L}\right)_B \frac{A_B}{a_B} + N_{pB}\right] C_B. \quad (1b)$$

Here MIC_0 and MHC_0 are, respectively, MIC and MHC in the low-cell density (or single-cell) limit: $C_{cell} \to 0$ (C_{cell} is either C_B or C_H). The term inside [. . .] can be interpreted as the total number of peptides consumed per cell; recall N_p^* is the value of N_p at C_p^* (e.g., either MIC or MHC). It is assumed that MHC > MIC: peptides are selective, i.e., at the MIC, host cells remain intact. This has to be understood with caution. If MICs and MHCs are measured separately in a noncompetitive way, MICs can be larger than MHCs. This is, however, irrelevant for our discussion here. As a result of this inequality, the relations in Equation (1) are not fully symmetric with respect to the exchange between the subscripts "B" and "H."

It is worth noting that the values of $(P/L)_B$ and $(P/L)_H$ depend on the total concentration of peptides and cell densities. They are determined by chemical equilibrium between free and bound peptides [see the **Appendix**]. In contrast, $(P/L)_B^*$ and $(P/L)_H^*$ are constants, which are set by the membrane-peptide parameters (3, 14–16).

Finally, note that the term $\left[(P/L)_B\,(A_B/a_B) + N_{pB}\right]$ in Equation (1b) is larger than [. . .] in Equation (1a), since the former is evaluated at a larger value of C_p above the MIC. In this case, however, pore formation in bacterial membranes will alter the energetics of peptide binding. In the limit $C_H \gg C_B$, as is often the case, this will not limit the applicability of Equation (1b), since this term has a minimal impact on the MHC.

For a noncompetitive or homogeneous case, the last term in Equations (1a,b) will disappear. It is worth noting that the values of MIC_0, MHC_0, N_{pB}^*, and N_{pH}^* can be obtained from noncompetitive measurements. If $(P/L)^*$ is not known, the number of peptides consumed per cell, i.e., the term inside [. . .] in Equation (1), can be viewed as a fitting parameter. See below for a competitive case.

It will be instructive to compare the two terms inside [. . .] in Equation (1): the number of membrane-bound peptides and the number of adsorbed peptides per cell. For this consideration, we invoke some simplification: a cell viewed as a sack of molecules enclosed by a bilayer. For *E. coli* as a representative bacterium, $A_B \approx 12\,\mu m^2$, twice the area of each lipid layer (either inner or outer) in the cytoplasmic membrane. Since $a_B \approx a_H \approx 70\,Å^2$, $A_B/a_B \approx 1.7 \times 10^7$. For the peptide melittin, $(P/L)_B^* \approx 0.02$ and $(P/L)_H^* \approx 0.01$ (14–16). We thus find $(P/L)_B^*\,(A_B/a_B) \approx 3.4 \times 10^5$. This number is much smaller than $N_{pB} \approx 10^7$-10^8 (21). The presence of outer membranes will not change this inequality. For human red blood cells as representative host cells, $A_H \approx 17 A_B$ and $A_H/a_H \approx 2.9 \times 10^8$. As a result, we obtain $(P/L)_H^*\,(A_H/a_H) \approx 2.9 \times 10^6$, which is smaller than $N_{pH} \approx 10^7$ (19, 20). The main source of inoculum effects is the trapping of peptides inside dead cells (i.e., for $P/L > (P/L)^*$).

A full analysis of Equation (1) is involved, since it requires the determination of four unknowns: $(P/L)_B$, $(P/L)_H$, N_{pB}, and N_{pH}, as a function of C_p [see (12, 13) for earlier efforts]; also the energetics of peptide trapping including peptide binding

to intracellular components has yet to be understood in a quantitative manner.

In some relevant limits, we can use Equation (1) to map out a few scenarios regarding peptide selectivity. In the competitive case, if $C_H \gg C_B$ as in whole blood, Equation (1) can be approximated as

$$\mathrm{MIC}(C_B, C_H) \approx \mathrm{MIC}_0 + \left(\frac{P}{L}\right)_H \frac{A_H}{a_H} C_H, \quad (2a)$$

$$\mathrm{MHC}(C_B, C_H) \approx \mathrm{MHC}_0 + \left[\left(\frac{P}{L}\right)^*_H \frac{A_H}{a_H} + N^*_{pH}\right] C_H. \quad (2b)$$

Here $(P/L)_H$ in Equation (2a) is to be evaluated at $C_p = \mathrm{MIC}$.

In Equation (2), MIC_0 and MHC_0 can be viewed as fitting parameters. In a more systematic approach, they can be related to binding energy, w, which characterizes the interaction of a peptide with a membrane (see the **Appendix**); in this work, w_B and w_H are the binding energy for bacterial and host-cell membranes, respectively.

Chemical equilibrium between free and bound peptides [see Equation A3 in the Appendix and the SI of (12)] leads to[1]

$$\mathrm{MIC}(C_B, C_H) \approx \frac{1}{\nu_p} \cdot \frac{\frac{A_p}{a_H}\left(\frac{P}{L}\right)_H}{1 - \frac{A_p}{a_H}\left(\frac{P}{L}\right)_H} e^{w_H/k_B T} + \left(\frac{P}{L}\right)_H \frac{A_H}{a_H} C_H. \quad (3)$$

Here, ν_p is the volume occupied by each peptide in the bulk and A_p is the peptide area on the membrane surface.

We can use Equation (3) to eliminate $(P/L)_H$ in Equation (2a) by equating the first terms in these two equation[2]; similarly, $(P/L)^*_H$ in Equation (2b) can be eliminated in favor of $(\mathrm{MHC})_0$:

$$\mathrm{MIC}(C_B, C_H) \approx \mathrm{MIC}_0 + \left(\frac{\mathrm{MIC}_0 \nu_p}{\mathrm{MIC}_0 \nu_p + e^{w_H/k_B T}} \frac{A_H}{A_p}\right) C_H, \quad (4a)$$

$$\mathrm{MHC}(C_B, C_H) \approx \mathrm{MHC}_0 + \left(\frac{\mathrm{MHC}_0 \nu_p}{\mathrm{MHC}_0 \nu_p + e^{w_H/k_B T}} \frac{A_H}{A_p} + N^*_{pH}\right) C_H. \quad (4b)$$

The MIC in Equation (4a) increases linearly with C_H. It can be strikingly different from the corresponding noncompetitive MIC in the limit $C_B \to 0$: MIC_0. For sufficiently large C_H, the former can be much larger than the latter.

The ratio MHC/MIC becomes

$$\frac{\mathrm{MHC}}{\mathrm{MIC}} \approx \frac{\mathrm{MHC}_0 + \left[\left(\frac{P}{L}\right)^*_H \frac{A_H}{a_H} + N^*_{pH}\right] C_H}{\mathrm{MIC}_0 + \left[\frac{\mathrm{MIC}_0 \nu_p}{\mathrm{MIC}_0 \nu_p + e^{w_H/k_B T}} \frac{A_H}{A_p}\right] C_H} = \frac{\mathrm{MHC}_0 + \left(\frac{\mathrm{MHC}_0 \nu_p}{\mathrm{MHC}_0 \nu_p + e^{w_H/k_B T}} \frac{A_H}{A_p} + N^*_{pH}\right) C_H}{\mathrm{MIC}_0 + \left(\frac{\mathrm{MIC}_0 \nu_p}{\mathrm{MIC}_0 \nu_p + e^{w_H/k_B T}} \frac{A_H}{A_p}\right) C_H}. \quad (5)$$

This implies that peptide trapping in host cells enhances peptide selectivity. Compared to the case $N^*_{pH} \approx 0$, more peptides will be needed in order for $(P/L)_H$ to reach $(P/L)^*_H$ for $N^*_{pH} \gg 1$. Since the second term inside [. . .] in the numerator of Equation (5) is larger than the first term roughly by an order of magnitude, the effect of peptide trapping on the selectivity is up to about 10-fold.

Note that the MHC in Equation (4b) holds for a host-cell only case as well. In contrast, the MIC for a bacterial-cell only case becomes

$$\mathrm{MIC}(C_B) = \mathrm{MIC}_0 + \left(\frac{\mathrm{MIC}_0 \nu_p}{\mathrm{MIC}_0 \nu_p + e^{w_B/k_B T}} \frac{A_B}{A_p} + N^*_{pB}\right) C_B. \quad (6)$$

This can be obtained from Equation (4b) by exchanging the role of host cells with that of bacteria.

The main advantage of Equations (4), (5), and (6) is that P/L^* is not shown explicitly. It is absorbed into MIC_0 or MHC_0, which are experimentally more accessible. Also it is worth noting that the use of Equation (4) or Equation (5) would not necessarily require measurements of such biophysical parameters as ν_p, w_H, w_B, N^*_{pH}, and N^*_{pB}. The term inside (. . .) on the right-hand side of Equations (4) and (6) as a whole can be viewed as a fitting parameter. It is a slope of either MIC or MHC curve as a function of the cell density and can be obtained from the corresponding homogeneous case. See the last section for relevant points.

RESULTS

We have analyzed Equations (4) and (5) to clarify inoculum effects on peptide activity and selectivity. For lipid bilayers mimicking cell membranes, the parameters in these equations have been characterized (12–16). They are, however, not known

[1]Here $(P/L)_H$ is to be evaluated at the peptide concentration $C_p = \mathrm{MIC}$. As a result, w_H in this expression corresponds to $(P/L)_H$ smaller than $(P/L)^*_H$. Here we ignore the possible dependence of w_H on $(P/L)_H$. For pure-lipid membranes, this dependence can, in principle, be mapped out (13). If we use the final expression in Equation (4a) as a fitting model, this issue becomes irrelevant.

[2]The origin of the cell-density dependent term in Equation (3) is obvious from the illustration in **Figure 1**. At the low-cell density limit, Equation (3) is equivalent to saying that

$$\mathrm{MIC}_0 = \frac{1}{\nu_p} \cdot \frac{\frac{A_p}{a_H}\left(\frac{P}{L}\right)_H}{1 - \frac{A_p}{a_H}\left(\frac{P}{L}\right)_H} e^{w_H/k_B T}. \quad (7)$$

This can be obtained from Equation (A3) in the Appendix. More directly, chemical equilibrium at $C_p = \mathrm{MIC}_0$ in the low-cell density limit requires

$$\ln\left(\nu_p \mathrm{MIC}_0\right) = \frac{w_B}{k_B T} + \ln \frac{\frac{A_p}{a_B}\left(\frac{P}{L}\right)^*_B}{1 - \frac{A_p}{a_B}\left(\frac{P}{L}\right)^*_B} = \frac{w_H}{k_B T} + \ln \frac{\frac{A_p}{a_H}\left(\frac{P}{L}\right)_H}{1 - \frac{A_p}{a_H}\left(\frac{P}{L}\right)_H}. \quad (8)$$

The second term in each line is the entropic chemical potential of bound peptides in units of $k_B T$ (23). The second equality leads to Equation (7), which shows the relationship between the total peptide concentration, i.e., MIC_0, and $(P/L)_H$. Equation (7) can readily be solved for $(P/L)_H$:

$$\left(\frac{P}{L}\right)_H = \frac{\mathrm{MHC}_0 \nu_p}{\mathrm{MHC}_0 \nu_p + e^{w_H/k_B T}}. \quad (9)$$

This is used in the transition from Equations (2A) to (4A).

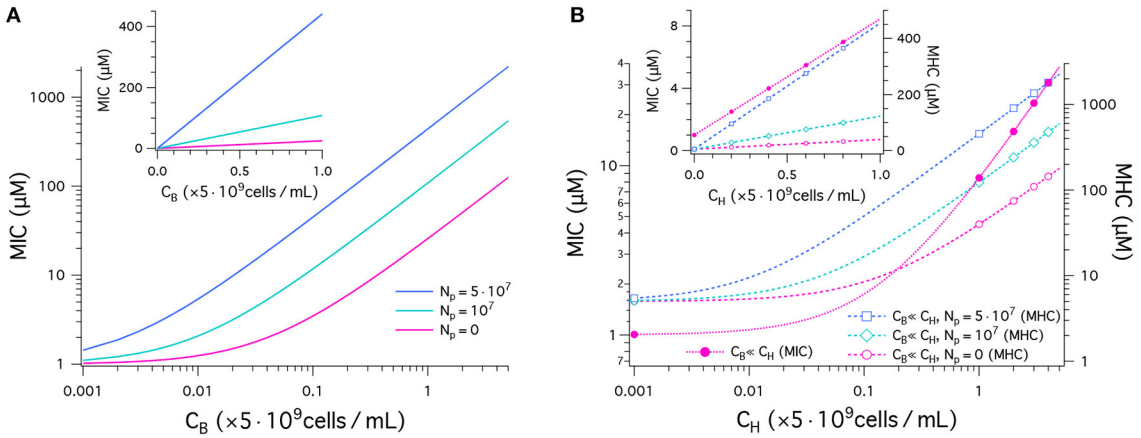

FIGURE 2 | Peptide activity, i.e., MICs and MHCs. We have chosen the parameters as follows: $(\text{MIC})_0 = 1\,\mu$M and $(\text{MHC})_0 = 5\,\mu$M; $w_B = -16.6\,k_BT$ and $w_H = -6.72\,k_BT$; $A_p = 400^2$; $v_p = 33^3$ [3]; $A_B = 1.2 \times 10^{92}$ and $A_H = 17 \times A_B$. The number of trapped peptides N_p is chosen to be the same for bacteria and host cells: $N_p = 0, 10^7, 5 \times 10^7$. **(A)** This graph shows the results for MICs as a function of C_B in units of 5×10^9cells/mL obtained in a noncompetitive way. In all cases, the MIC increases from $\text{MIC}_0 = 1$, as C_B increases (Equation 1). The MIC is higher for a larger value of N_p. The sensitivity of the MIC to N_p is better captured in the linear plot in the inset; all the curves indicate a linear relationship between the MIC and C_B. **(B)** MICs (left axis) and MHCs (right axis) are shown as a function of C_H given in units of 5×10^9 cells/mL obtained in a competitive way. Various symbols are used to distinguish between different choices of N_p. If $C_H \gg C_B$, MICs are roughly independent of N_p; in this case, MHCs are approximately the same for the competitive and noncompetitive cases. As C_H increases, the MIC increases up to 40-fold from MIC_0 at $C_H = 0$ (Equation 4a). Similarly MHCs increase as a function of C_H, more rapidly for larger N_p (Equation 4b); for $N_p = 10^7$, the MHC increases by up to two orders of magnitude. The inset graph recaptures the data in a linear plot.

for real cells. In particular, the interdependence between w, P/L^*, and C_p^* is elusive because of the complexities of cell structures. For instance, w_B for Gram-negative bacteria should take into account the peptide interaction with their outer membrane (OM), among others. Recall that this is an effective parameter, in which microscopic details (e.g., peptide charge, peptide interaction with the OM, and the presence of cholesterol in the host-cell membrane) are subsumed. This has only recently been mapped out theoretically for lipid bilayers (13). Here we do not attempt to calculate the effective binding energy w (either w_B or w_H) for real cells and to use it in the computation of MIC_0 and MHC_0. Instead, we start with conveniently-chosen but biophysically-relevant values of MIC_0 and MHC_0. The resulting analysis will not involve $(P/L)^*$ explicitly. For simplicity, the number of trapped peptides N_p is chosen to be the same for bacteria and host cells: $N_p = 0, 10^7, 5 \times 10^7$.

Otherwise, we have used peptide parameters relevant for the peptide melittin (12–16): peptide charge $Q = 5$, $A_p = 400\text{Å}^2$, and $v_p = 33^3\text{Å}^3$. For this peptide, w was mapped out for model membranes, mimicking bacterial and host-cell membranes: $w_B = -16.6\,k_BT$ and $w_H = -6.72k_BT$ (13). They are used as representative binding energy. Also, $a_B = 74\,\text{Å}^2$, $a_H = 71\,\text{Å}^2$, $A_B = 1.2 \times 10^9\,\text{Å}^2 = 12\,\mu\text{m}^2$ as for *E. coli*, and $A_H = A_B$ or $A_H = 17A_B$ as for human red blood cells (12).

We have plotted our results for MICs and MHCs in **Figure 2**. For this, we have chosen the parameters as follows: $\text{MIC}_0 = 1\,\mu$M and $\text{MHC}_0 = 5\,\mu$M. **Figure 2A** shows the MIC as a function of C_B in units of 5×10^9cells/mL obtained in a noncompetitive way. In all cases, the MIC increases linearly from $\text{MIC}_0 = 1\,\mu$M, as C_B increases, as expected from Equation (1). The inset recaptures the MIC data in linear plot. It indicates a linear relationship between the MIC and C_B. The MIC curve is steeper for a larger value of N_p. This is well aligned with recent experiments (21). The inoculum effect increases the slope of the MIC curves, not the "y"-intercept, which coincides with cell-density independent MIC_0.

In **Figure 2B**, MICs (left axis) and MHCs (right axis) are shown as a function of C_H given in units of 5×10^9 cells/mL obtained in a competitive way. They are represent by dashed lines with symbols. First, note that MHCs are approximately the same for the competitive and noncompetitive cases as long as $C_H \gg C_B$; also MICs are insensitive to C_B and N_p, if $C_H \gg C_B$ and $\text{MHC}_0 > \text{MIC}_0$ (see Equation 4). This is distinct from larger MICs for larger N_p in the noncompetitive case in **Figure 2A**. As C_H increases, the MIC increases up to 40-fold from MIC_0 at $C_H = 0$ (Equation 4A). This is consistent with the observation that peptide interactions with host cells diminish peptide activity *in vivo* (24). Similarly, MHCs increase as a function of C_H, more rapidly for larger N_p (Equation 4B and the inset graph). For $N_p = 10^7$, the MHC increases by up to two orders of magnitude.

Figure 3 displays our results for peptide selectivity, which combines the graphs in **Figures 2A** and **B**. The graph in **Figure 3A** shows our results for MHC/MIC as a function of C_B obtained in a noncompetitive way. In all cases presented by various colors, the ratio MHC/MIC or the selectivity decreases, as C_B increases. The selectivity is higher for larger values of C_H. Also, it is higher for larger N_p if $C_B \lesssim 0.07 \times 10 \times 10^9$ cells/mL but is smaller if $C_B \gtrsim 0.07 \times 10 \times 10^9$ cells/mL. Peptide trapping increases both MHC and MIC. At low C_B, the net effect is to

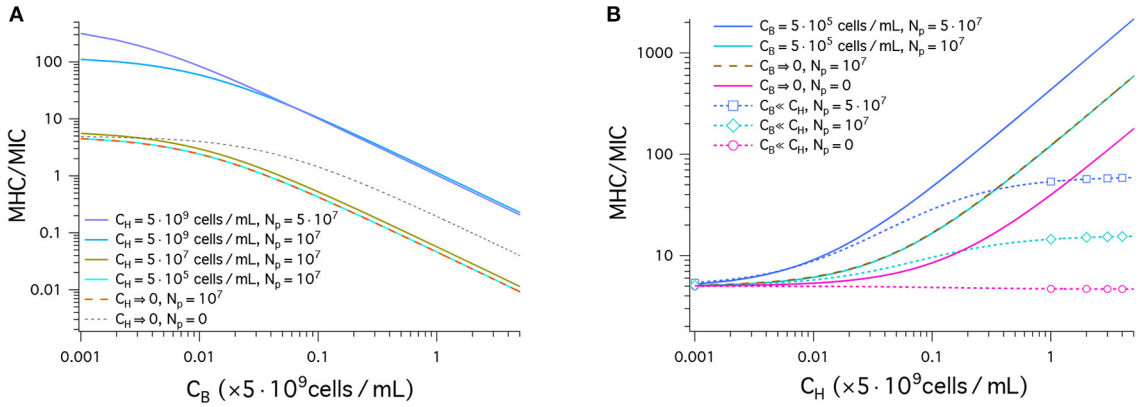

FIGURE 3 | Cell selectivity of antimicrobial peptides, i.e., MHC/MIC. We have used the same parameters as in **Figure 2**: $(\mathrm{MIC})_0 = 1\,\mu$M, and $(\mathrm{MHC})_0 = 5\,\mu$M; $w_B = -16.6\,k_BT$, and $w_H = -6.72\,k_BT$; $A_p = 400^2$; $v_p = 33^3\,^3$; $A_B = 1.2 \times 10^{92}$ and $A_H = 17 \times A_B$; $N_p = 0, 10^7, 5 \times 10^7$ (the same for bacteria and host cells). **(A)** This graph shows MHC/MIC as a function of C_B in units of 5×10^9cells/mL obtained in a noncompetitive way. In all cases, the selectivity decreases, as C_B increases. The selectivity is higher for larger values of C_H. It is also larger for larger N_p unless $C_H = 0$ (black dashed) or $C_B \gtrsim 0.07 \times 5 \times 10^9$ (compare the top two curves). Also note that there is no essential difference between the two cases: $C_H = 0, N_p = 10^7$ (tangerine) and $C_H = 5 \times 10^5$ cells/mL, $N_p = 10^7$ (cyan). This means that the latter case falls in the single-cell limit. **(B)** MHC/MIC are shown as a function of C_H given in units of 5×10^9 cells/mL. Competitive (dashed lines with various symbols) and noncompetitive (solid lines) cases are compared. For the competitive case, Equation (4) was used, which holds for $C_H \gg C_B$. The competitive selectivity increases as C_H increases, except for $N_p = 0$ (magenta). In all noncompetitive cases shown, the selectivity increases as C_H increases. In all cases, the selectivity is higher for larger N_p. In the noncompetitive case, the presence of 5×10^5cells/mL does not change the selectivity with reference to the corresponding limiting case $C_B \to 0$; at this density of bacterial cells, $\mathrm{MIC} \approx \mathrm{MIC}_0$. Compared to the corresponding competitive selectivity, the noncompetitive selectivity is overestimated, more so for larger C_H; for $C_H = 5 \times 10^9$ cells/mL, the latter is exaggerated by an order of magnitude.

enhance the selectivity; at high C_B, it reduces the selectivity, since lots of peptides are trapped in bacteria and "wasted."

Also note that there is no essential difference between the two cases: $C_H = 0, N_p = 10^7$ (tangerine) and $C_H = 5 \times 10^5$ cells/mL, $N_p = 10^7$ (cyan). This means that the latter case falls in the single-cell limit.

In **Figure 3B**, the results for MHC/MIC are shown as a function of C_H. Competitive (dashed line with various symbols) and noncompetitive (solid lines) cases are compared. For the competitive case, Equation (4) was used, which holds for $C_H \gg C_B$. The competitive selectivity increases as C_H increases, except for $N_p = 0$ (magenta). In all noncompetitive cases, the selectivity increases as C_H increases; the presence of $C_B = 5 \times 10^5$ cells/mL does not change the selectivity with reference to the corresponding limiting case $C_B \to 0$, since at this density of bacterial cells, $\mathrm{MIC} \approx \mathrm{MIC}_0$. In both the competitive and noncompetitive cases shown, the selectivity is higher for larger N_p: peptide trapping enhances the selectivity.

Similarly to what earlier studies suggest (12, 18), the results in **Figure 3B** show how peptide selectivity can be mistakenly estimated. Compared to the corresponding competitive selectivity, the noncompetitive selectivity is overestimated, more so for larger C_H; for $C_H = 5 \times 10^9$ cells/mL, the latter is exaggerated by an order of magnitude.

These results also clear up possible confusions. Even in the presence of a large amount of host cells, the selectivity measured in a competitive environment is not an experimental artifact. It just reflects correctly the cell-density dependence of the selectivity, as discussed in the section 2.

DISCUSSIONS AND CONCLUSIONS

We have discussed the cell-density dependence of peptide activity and selectivity. For this, we have combined physical arguments, which relate peptide activity and selectivity to cell density, and a Langmuir-type model, in which the amount peptide binding (or trapping) is dictated by an effective binding energy. This combined effort produced a predictive model for peptide activity and selectivity. It can be used to calculate MICs, MHCs, and MHC/MIC, once a few key biophysical parameters are characterized, which include the number of trapped peptides per cell (19–21) and peptide-membrane interactions.

Alternatively, our model can be used as a fitting model for analyzing data. For instance, the "y"-intercept and the "slope" can be extracted from noncompetitive measurements of MICs or MHCs vs. cell density. This will determine $(\mathrm{MIC})_0$ or $(\mathrm{MHC})_0$ as well as the terms inside $(\ldots)$ on the right-hand side of Equations (4b) and (6). This information can be used in Equation (4) (or more generally Equation 1), which represents a heterogeneous mixture of bacteria and host cells.

This consideration, however, would necessitate prior knowledge about one of N^*_{pB} and $(P/L)^*_B$ (or equivalently w_B). To see this, notice that homogeneous measurements lead to the value of the sum of the two terms inside $(\ldots)$ in Equation (6). If $(P/L)^*_B$ is known, as is most obvious for pure-lipid membranes (3, 17), N^*_{pB} can be extracted from noncompetitive measurements.

An alternative but possibly less practical approach is to measure several MICs in a competitive setting. By fitting the

data to Equation (4a) will produce the coefficient of C_H. One can then obtain MIC, MHC, and MHC/MIC as a function of C_B or C_H, the density of bacteria or host cells, respectively. For instance, in whole blood, $C_H \approx 5 \times 10^9$cells/mL. The density of bacteria depends on the degree and location of infection. It ranges from 1 colony-forming unit (CFU/mL) (in blood stream) to 10^9 CFU/mL (in soft tissue or peritonea) [see a recent review (20) and relevant references therein]. Graphs similar to those in **Figure 2** or **Figure 3** will be beneficial for understanding the activity and selectivity of antimicrobial peptides in varying biological environments.

As pointed out in a number of earlier studies (12, 18–20), the selectivity measured noncompetitively is often much larger than the corresponding competitive one, if the host cell density is much larger than the bacterial cell density. The results in **Figure 3** offer a quantitative picture of how the selectivity can be excessively overestimated. It can, however, be corrected, since noncompetitive measurements can be converted into competitive ones. For instance, suppose that noncompetitive measurements led to $w_B = -16.6\,k_BT$, $w_H = -6.72\,k_BT$, $N_p = 10^7$, $MIC_0 = 1\,\mu$M, and $MHC_0 = 5\,\mu$M, as in **Figure 3**. In the presence of $C_B = 5 \times 10^5$ cells/mL and $C_H = 5 \times 10^9$ cells/mL ($C_B \ll C_H$), these parameters choices would lead to the following noncompetitive selectivity: MHC/MIC $\approx$ 100 (Equation 1 and **Figure 3**). It can be corrected graphically (**Figure 3**) or mathematically (Equation 4) into the corresponding competitive selectivity MHC/MIC $\approx$ 10.

As a final remark, we wish to mention that peptide activity against live cells is time-dependent, as observed in recent experiments (21). Accordingly, the density of bacterial cells, is a dynamic quantity. Furthermore, heterogeneous absorption of peptides in cells was shown to have a nontrivial consequence on population survivability. Because of the stochastic nature of molecular interactions occurring on the cell surface and inside, some cells absorb a large number of peptides ($\sim 10^7$-10^8) (19–21), thus reducing the availability of peptides to the rest and contributing favorably to population survivability (21). Also, the density of peptides can change with time, depending on how fast the host cells produce them (21). It is also influenced by peptide degradation by protease (20, 24). Its effect on peptide activity is similar to what we expect from peptide trapping. Taking into all these known and unknown details goes beyond the scope of what can be done at present. Future considerations are warranted.

DATA AVAILABILITY STATEMENT

The raw data supporting the conclusions of this article will be made available by the authors, without undue reservation.

AUTHOR CONTRIBUTIONS

B-YH and BRS conducted the research. B-YH wrote the manuscript. BRS, SN, and ST-A commented on the manuscript. SN helped solve the peptide binding equations. All authors contributed to the article and approved the submitted version.

FUNDING

This work was supported by NSERC (Canada) (B-YH) and the National Institute of Health (R15-GM124640) (ST-A).

ACKNOWLEDGMENTS

We acknowledge the reviewers for their useful comments on the relevance of our work to selectivity measurements in multi-species cultures and on bacterial resistance against antimicrobial peptides, and for bringing relevant work to our attention (22).

REFERENCES

1. Zasloff M. Antimicrobial peptides of multicellular organisms. *Nature.* (2002) 415:389–95. doi: 10.1038/415389a
2. Brogden KA. Antimicrobial peptides: pore formers or metabolic inhibitors in bacteria? *Nat Rev Microbiol.* (2005) 3:238–50. doi: 10.1038/nrmicro1098
3. Melo MN, Ferre R, Castanho MARB. Antimicrobial peptides: linking partition, activity and high membrane-bound concentrations. *Nat Rev Microbiol.* (2009) 7:245–50. doi: 10.1038/nrmicro2095
4. Epand RM Epand RF. Biophysical analysis of membrane-targeting antimicrobial peptides: membrane properties and the design of peptides specifically targeting gram-negative bacteria. In: Wang G, editor. *Antimicrobial Peptides Discovery, Design and Novel Therapeutic Strategies.* Wallingford: CABI (2010).
5. Matsuzaki K. Why and how are peptide-lipid interactions utilized for self-defense? Magainins and tachyplesins as archetypes. *Biochim Biophys Acta.* (1999) 1462:1–10. doi: 10.1016/s0005-2736(99)00197-2
6. Hancock RE, Haney EF, Gill EE. The immunology of host defence peptides: beyond antimicrobial activity. *Nat Rev Immunol.* (2016) 16:321–34. doi: 10.1038/nri.2016.29
7. Mookherjee N, Anderson MA, Haagsman HP, Davidson DJ. Antimicrobial host defence peptides: functions and clinical potential. *Nat Rev Drug Discov.* (2020) 19:311–32. doi: 10.1038/s41573-019-0058-8
8. Hancock REW, Sahl HG. Antimicrobial and host-defense peptides as new anti-infective therapeutic strategies. *Nat Biotechnol.* (2006) 24:1551–7. doi: 10.1038/nbt1267
9. Jiang Z, Vasil AI, Hale JD, Hancock REW, Vasil ML, Hodges RS. Effects of net charge and the number of positively charged residues effects on the biological activity of amphipathic α-helical cationic antimicrobial peptides. *Biopolymers.* (2007) 90:369–83. doi: 10.1002/bip.20911
10. Perron GG, Zasloff M, Bell G. Experimental evolution of resistance to an antimicrobial peptide. *Proc R Soc B.* (2006) 273:251–6. doi: 10.1098/rspb.2005.3301
11. Peschel A, Sahl HG. The co-evolution of host cationic antimicrobial peptides and microbial resistance. *Nat Rev Microbiol.* (2006) 4:529–36. doi: 10.1038/nrmicro1441
12. Bagheri A, Taheri-Araghi A, Ha BY. How cell concentrations are implicated in cell selectivity of antimicrobial peptides. *Langmuir.* (2015) 31:8052–62. doi: 10.1021/acs.langmuir.5b01533
13. Nourbakhsh S, Taheri-Araghi S, Ha BY. Toward building a physical model for membrane selectivity of antimicrobial peptides: making a quantitative sense of the selectivity. *Soft Matter.* (2019) 15:7509–26. doi: 10.1039/c9sm00930b
14. Lee MT, Chen FY, Huang HW. Energetics of pore formation induced by membrane active peptides. *Biochemistry.* (2004) 43:3590–9. doi: 10.1021/bi036153r

15. Lee M, Hung W, Chen F, Huang HW. Many-body effect of antimicrobial peptides: on the correlation between Lipid's spontaneous curvature and pore formation. *Biophys J.* (2005) 89:4006–16. doi: 10.1529/biophysj.105.068080
16. Huang HW. Molecular mechanism of antimicrobial peptides: the origin of cooperativity. *Biochim Biophys Acta Biomembr.* (2006) 1758:1292–302. doi: 10.1016/j.bbamem.2006.02.001
17. Melo MN, Ferre R, Feliu L, Bardají E, Planas M, Castanho MARB. Prediction of antibacterial activity from physicochemical properties of antimicrobial peptides. *PLoS ONE.* (2011) 6:e28549. doi: 10.1371/journal.pone.0028549
18. Matsuzaki K. Control of cell selectivity of antimicrobial peptides. *Biochim Biophys Acta Biomembr.* (2009) 1788:1687–92. doi: 10.1016/j.bbamem.2008.09.013
19. Savini F, Luca V, Bocedi A, Massoud R, Park Y, Mangoni ML, et al. Cell-density dependence of host-defense peptide activity and selectivity in the presence of host cells. *ACS Chem Biol.* (2017) 12:52–6. doi: 10.1021/acschembio.6b00910
20. Savini F, Bobone S, Roversi D, Mangoni ML, Stella W. From liposomes to cells: filling the gap between physicochemical and microbiological studies of the activity and selectivity of host-defense peptides. *Peptide Sci.* (2018) 110:e24041–1-14. doi: 10.1002/pep2.24041
21. Snoussi M, Talledo JP, Rosario NAD, Mohammadi S, Ha BY, Košmrlj A, Taheri-Araghi S. Heterogeneous absorption of antimicrobial peptide LL37 in *Escherichia coli* cells enhances population survivability. *eLife.* (2018) 7:e38174. doi: 10.7554/eLife.38174
22. Loffredo MR, et al. Inoculum effect of antimicrobial peptides. (2020) Available online at: https://www.biorxiv.org/content/10.1101/2020.08.21.260620v1.full
23. Dill K, Bromberg S. *Molecular Driving Forces: Statistical Thermodynamics in Biology, Chemistry, Physics, and Nanoscience*. 2nd Edition. New York, NY: Garland Science.
24. Starr CG, He J, Wimley WC. Host cell interactions are a significant barrier to the clinical utility of peptide antibiotics. *ACS Chem Biol.* (2016) 11:3391–9. doi: 10.1021/acschembio.6b00843

Conflict of Interest: The authors declare that the research was conducted in the absence of any commercial or financial relationships that could be construed as a potential conflict of interest.

APPENDIX

Here we present a Langmuir model of peptide binding [see (23) and the SI of (12)]. Let μ_B and μ_H be the chemical potential of bound peptides, and σ_B and σ_H their planar density, on the bacterial and host-cell surface, respectively. The planar density is related to P/L through $\sigma_B a_B = (P/L)_B$ and $\sigma_H a_H = (P/L)_H$. Recall that w_B and w_H are the peptide binding energy for bacterial and host-cell membranes, respectively. In general, the binding energy depends on the value of P/L mainly through the interaction between bound peptides. In recent studies (13), it was estimated at $P/L = (P/L)^*$. The resulting binding energy can be used to find $(P/L)^*$, i.e., either MIC or MHC.

Let v_p be the volume occupied by each peptide in the bulk and A_p the area occupied by each bound peptide on the membrane surface. In the presence of two types of cells, we find

$$\begin{aligned}\mu_B &= w_B + k_B T \ln\left(\frac{\sigma_B A_p}{1-\sigma_B A_p}\right)\\ \mu_H &= w_H + k_B T \ln\left(\frac{\sigma_H A_p}{1-\sigma_H A_p}\right)\end{aligned} \tag{A1}$$

as well as

$$\mu_{free} = k_B T \ln\left\{\left[C_p - (C_B\sigma_B A_B + C_H\sigma_H A_H)\right] v_p\right\}. \tag{A2}$$

In equilibrium, $\mu_B = \mu_H = \mu_{free}$. We thus arrive at

$$C_p = \left(\frac{P}{L}\right)_B \frac{A_B}{a_B} C_B + \left(\frac{P}{L}\right)_H \frac{A_H}{a_H} C_H + \frac{1}{v_p} \frac{\frac{A_p}{a_B}\left(\frac{P}{L}\right)_B}{1-\frac{A_p}{a_B}\left(\frac{P}{L}\right)_B} e^{w_B/k_B T} \tag{A3a}$$

$$C_p = \left(\frac{P}{L}\right)_B \frac{A_B}{a_B} C_B + \left(\frac{P}{L}\right)_H \frac{A_H}{a_H} C_H + \frac{1}{v_p} \frac{\frac{A_p}{a_H}\left(\frac{P}{L}\right)_H}{1-\frac{A_p}{a_H}\left(\frac{P}{L}\right)_H} e^{w_H/k_B T}. \tag{A3b}$$

In this expression, we eliminated the planar density in favor of P/L. These equations can be solved simultaneously for the two unknowns: $(P/L)_H$ and $(P/L)_B$ for a given value of C_p. The value of C_p at which $(P/L)_H = (P/L)_H^*$ ($(P/L)_B = (P/L)_B^*$) is an MHC (MIC). If evaluated at P/L^*, the last term in Equations A3(a) and (b) is the C_p^* in the low-cell density limit: either MHC_0 or MIC_0.

frontiers in Medical Technology

ORIGINAL RESEARCH
published: 24 February 2021
doi: 10.3389/fmedt.2021.625975

Bridging the Antimicrobial Activity of Two Lactoferricin Derivatives in *E. coli* and Lipid-Only Membranes

Lisa Marx[1,2,3†], *Enrico F. Semeraro*[1,2,3†], *Johannes Mandl*[1,2,3†], *Johannes Kremser*[1,2,3], *Moritz P. Frewein*[1,2,3,4], *Nermina Malanovic*[1,2,3], *Karl Lohner*[1,2,3] *and Georg Pabst*[1,2,3*]

[1] Department of Biophysics, Institute of Molecular Biosciences, University of Graz, Graz, Austria, [2] BioTechMed Graz, Graz, Austria, [3] Field of Excellence BioHealth—University of Graz, Graz, Austria, [4] Soft Matter Science and Support Group, Institut Laue-Langevin, Grenoble, France

OPEN ACCESS

Edited by:
Sattar Taheri-Araghi,
California State University, Northridge,
United States

Reviewed by:
Iolanda Cuccovia,
University of São Paulo, Brazil
Miguel A. R. B. Castanho,
University of Lisbon, Portugal

***Correspondence:**
Georg Pabst
georg.pabst@uni-graz.at

[†]These authors have contributed equally to this work

Specialty section:
This article was submitted to Pharmaceutical Innovation, a section of the journal Frontiers in Medical Technology

Received: 04 November 2020
Accepted: 19 January 2021
Published: 24 February 2021

Citation:
Marx L, Semeraro EF, Mandl J, Kremser J, Frewein MP, Malanovic N, Lohner K and Pabst G (2021) Bridging the Antimicrobial Activity of Two Lactoferricin Derivatives in E. coli and Lipid-Only Membranes. Front. Med. Technol. 3:625975. doi: 10.3389/fmedt.2021.625975

We coupled the antimicrobial activity of two well-studied lactoferricin derivatives, LF11-215 and LF11-324, in *Escherichia coli* and different lipid-only mimics of its cytoplasmic membrane using a common thermodynamic framework for peptide partitioning. In particular, we combined an improved analysis of microdilution assays with ζ-potential measurements, which allowed us to discriminate between the maximum number of surface-adsorbed peptides and peptides fully partitioned into the bacteria. At the same time, we measured the partitioning of the peptides into vesicles composed of phosphatidylethanolamine (PE), phosphatidylglycerol (PG), and cardiolipin (CL) mixtures using tryptophan fluorescence and determined their membrane activity using a dye leakage assay and small-angle X-ray scattering. We found that the vast majority of LF11-215 and LF11-324 readily enter inner bacterial compartments, whereas only 1–5% remain surface bound. We observed comparable membrane binding of both peptides in membrane mimics containing PE and different molar ratios of PG and CL. The peptides' activity caused a concentration-dependent dye leakage in all studied membrane mimics; however, it also led to the formation of large aggregates, part of which contained collapsed multibilayers with sandwiched peptides in the interstitial space between membranes. This effect was least pronounced in pure PG vesicles, requiring also the highest peptide concentration to induce membrane permeabilization. In PE-containing systems, we additionally observed an effective shielding of the fluorescent dyes from leakage even at highest peptide concentrations, suggesting a coupling of the peptide activity to vesicle fusion, being mediated by the intrinsic lipid curvatures of PE and CL. Our results thus show that LF11-215 and LF11-324 effectively target inner bacterial components, while the stored elastic stress makes membranes more vulnerable to peptide translocation.

Keywords: antimicrobial peptides, lactoferricin, minimum inhibitory concentration, partitioning, zeta-potential, dye-leakage assay, tryptophan fluorescence, small-angle X-ray scattering

1. INTRODUCTION

The history of research on antimicrobial peptides (AMPs) as promising agents to combat infectious diseases is long and rich in diverse aspects. Studied for about four decades (1), AMPs continue to spur significant research efforts by their ability to discriminate the lipid architecture of cell envelopes, and evade classical resistance mechanisms based on direct molecular (key-lock) interactions, which increasingly limits medical treatments by conventional antibiotics [for review, see e.g., (2, 3)].

AMPs are typically composed of cationic and hydrophobic amino acids making them highly membrane active. Responses of their target membranes depend on the AMPs' physicochemical properties (primary structure, hydrophobic moment, length, etc.) and concentration (partitioning), as revealed from studies on membrane model systems, and include membrane thinning (4), or thickening (5), lipid flip/flop (6) or changes in membrane elasticity (7) at relatively low concentrations. Pore-formation (barrel-stave, toroidal/worm-hole) (8) or changes in membrane topology (9, 10) have been reported at elevated AMP concentrations, eventually leading to complete micellization (11) of the membrane, also known as the carpet model (12). It is increasingly becoming clear, however, that the observed effects strongly depend on the lipid composition of the used membrane mimics and the resulting collective membrane properties (13–15). At the same time, several studies also indicate that AMPs may have intracellular targets (16, 17), which might be coupled to highly specific interactions with cytosolic components and lead to the inhibition of different metabolic or biosynthesis pathways. Such multiple inhibitory processes, however, do not exclude any AMP activity within the bacterial membranes (17).

In order to shed some light on this issue, it would be highly instructive to compare AMP partitioning studies in microbes and artificial lipid-only membranes. However, and to the best of our knowledge, such data are currently not available. Instead, the peptide-to-lipid molar ratio commonly used in lipid-only systems, for example, dye leakage experiments, is about five orders of magnitude lower than in microbial killing assays (2, 18, 19). Estimates based on the surface/volume ratio of bacteria consequently indicate a large number of non-membrane bound peptides per cell (18). This may, however, be strongly biased by not considering cell-surface deformation, vesiculation processes, or extracellular peptide aggregation (16, 20). Reflecting on such controversies, Wimley and Hristova (2) formulated almost 10 years ago several unanswered questions relating to AMP activity studies in model membrane systems and microbes. Answering these questions is often challenged by the different experimental windows and sensitivities of the applied techniques (21). Here, focusing on the lactoferricin derivatives LF11-215 (H-FWRIRIRR-NH_2) and LF11-324 (H-PFFWRIRIRR-NH_2), we set out to address three of these questions: *(i) How are vesicle leakage and microbial killing correlated? (ii) Is membrane binding the sole basis for selectivity?* and *(iii) Is membrane translocation required for activity?*

Derived from human lactoferrin, the peptide lactoferricin and its 11 amino acids fragment LF11 are well-known for their affinity to lipid A and antimicrobial activity (22), with LF11-215 and LF11-324 being among the most promising LF11 derivatives with significantly improved activities against a broad range of Gram-positive and Gram-negative strains (20, 23–25). LF11-215 leads, for example, to a damage of the cell wall of Gram-negative bacteria, including an increased distance between cytoplasmic and outer membranes, membrane ruffling and formation of external blebs (20, 25). The somewhat increased hydrophobicity of LF11-324 was linked to a stronger efficacy in planktonic cultures, but at the same time led to a lower cell specificity (25). Interestingly, LF11-215 was instead reported to be more effective against bacterial biofilms (26), which is probably related to its lower hydrophobicity, facilitating the peptide diffusion within the matrix of microorganisms. Model membrane studies, using selected bacterial lipid species, suggest that both peptides interact preferentially with the negatively charged cardiolipin (CL), inducing a segregation into peptide-enriched and peptide-poor lipid domains (25). Further, LF11-215 and LF11-324 were shown to efficiently kill *Escherichia coli*, but exhibited at the same time only moderate membrane permeabilization in lipid vesicles consisting of *E. coli* total lipid extracts even at high peptide-to-lipid ratios, while N-acylated LF11 derivatives showed high activity both against bacteria and lipid-only membranes (20). Further, also effects of LF11-215 and LF11-324 on membranes, such as thinning or stored curvature stress, were rather modest (20). This suggests that the activity of both peptides in cytoplasmic membranes might not be the primary cause for their high efficiency in killing Gram-negative bacteria.

In order to gain some deeper insight in view of the three questions quoted above, we therefore correlated the partitioning of peptides in both bacterial cells and lipid-only systems with their effects on bacterial growth inhibition, membrane permeabilization, and structure, focusing on *E. coli* as representative strain of Gram-negative bacteria to demonstrate the feasibility of our approach. In particular, we exploited a thermodynamic framework that allowed us to relate the total number of AMPs located within bacteria at the minimum inhibitory concentration (MIC) to the membrane-bound fraction, combining a standard microbiological assay with ζ-potential measurements. The same theoretical framework was also applied to different lipid-only mimics of bacterial cytoplasmic membranes to determine the partitioning of the peptides and their membrane associated effects as a function of lipid composition, combining Trp fluorescence and dye leakage assays with small-angle X-ray scattering (SAXS). In agreement with previous studies, we find that LF11-324 is more active against *E. coli* than LF11-215 (20, 25). Performing our studies as a function of cell density, it has been further demonstrated that this difference in activity is enhanced at elevated cell concentrations, but also that the number of cell-associated AMPs at the MIC is about 4 times lower for LF11-324, while the number of surface-bound AMPs is about equal within the error of our experiments. At the same time, however, our results provide evidence that the vast majority of both peptides (up to 95—99%) are located in intracellular compartments. A slightly ($\sim$ 1.3 times) higher membrane partitioning of LF11-215 was observed in lipid mixtures of palmityol-oleoyl-phosphatidylethanolamine

(POPE), palmitoyl-oleoyl-phosphatidylglycerol (POPG), and tetra-oleoyl-cardiolipid (TOCL), which most closely mimic *E. coli* cytoplasmic membrane, while differences in peptide partitioning into POPE/POPG membrane mimics were negligible. The overall partition process of AMPs into these systems plateaued after 10−20 min. Pure POPG bilayers instead showed instantaneous uptake of the peptides, but disparate partitioning for LF11-215 and LF11-324. Dye leakage experiments in turn showed intriguing effects. While pure POPG membranes followed typical permeabilization behavior [see, e.g., (27)] and showed the highest peptide partitioning coefficient, POPE/POPG and POPE/POPG/TOCL vesicles exhibited a maximum leakage at low peptide concentration, followed by a decrease of permeabilization upon further addition of peptide. Using dynamic light scattering (DLS) and SAXS, we were able to attribute this effect to the formation of large aggregate structures containing collapsed lipid membranes, sandwiching the peptides, and capable of encapsulating the dyes. No aggregates with collapsed lipid bilayers were formed for POPG. While the initial formation of the collapsed bilayers was most rapid for TOCL-containing membranes (within 30 s), the overall process including a relaxation was slower and occurred over the course of $\sim$ 2 h.

2. MATERIALS AND METHODS

2.1. Samples

2.1.1. Lipids, Peptides, and Chemicals

POPE, POPG, and TOCL were purchased from Avanti Polar Lipids (Alabaster, AL) as powder (purity >99%), and freeze-dried LF11-215 and LF11-324 (purity >95%) were obtained from PolyPeptide Laboratories (San Diego, CA). ANTS (8-aminonaphthalene-1,3,6-trisulfonic acid, disodium salt) and DPX (*p*-xylene-bis-pyridinium bromide) were purchased from Molecular Probes (Eugene, OR) and dimethyl sulfoxide (DMSO) from Sigma-Aldrich (Vienna, Austria). HEPES (purity >99.5%) and LB-agar and LB-medium (Luria/Miller) powders were purchased from Carl Roth (Karlsruhe, Germany). All other chemicals were obtained from Sigma-Aldrich (Vienna, Austria) in *pro analysis* quality.

2.1.2. Bacterial Suspensions

Colonies of *E. coli* K12 5K (courtesy of Günther Koraimann, University of Graz) were grown in LB-agar plates at 37°C. Overnight cultures (ONCs) were prepared by inoculating a single colony in 3 ml LB-medium in sterile polypropylene conical tubes (15 ml), enabling bacterial growth under aerobic conditions for 12−16 h in a shaking incubator at 37°C. Main cultures were prepared by suspending an aliquot of the ONCs in 10 ml LB-medium in sterile polypropylene conical tubes (50 ml) and harvested in the middle of the exponential growth phase. Bacteria were then immediately washed twice and re-suspended in nutrient-free and isotonic phosphate-buffered saline (PBS) solution (phosphate buffer 20 mM, NaCl 130 mM) at pH 7.4. Bacterial concentration was measured via turbidity measurements. The optical density at $\lambda = 600$ nm (OD_{600}) was acquired with the spectrophotometer Thermo Spectronic Genesys 20 (Thermo Fisher Scientific, Waltham, MA), where $OD_{600} = 1$ corresponds approximately to 8×10^8 CFU/ml (where CFU is colony forming units).

2.1.3. Lipid Vesicles

Lipid stock solutions for sample preparation were prepared in organic solvent chloroform/methanol (9:1, vol/vol) and phosphate assayed for quantification of lipid content (28). Lipid thin films for SAXS measurements were prepared by mixing appropriate amounts of lipid stock solutions to obtain samples composed of POPE/POPG (3:1, mol/mol) and POPE/POPG/TOCL (82:6:12, mol/mol) followed by solvent evaporation under a nitrogen stream at 35°C and overnight storage in a vacuum chamber. Dry lipid films were hydrated in HEPES-buffered saline (HBS) solution (10 mM HEPES, 140 mM NaCl, pH 7.4).

All hydrated samples were equilibrated for 1 h at 40°C followed by 5 freeze-and-thaw cycles using liquid N_2 and intermittent vortex-mixing. Large unilamellar vesicles (LUVs) were obtained by 31 extrusions with a handheld mini extruder (Avanti Polar Lipids, Alabaster, AL) using a 100 nm pore diameter polycarbonate filter. Vesicle size and polydispersity were determined via DLS using a Zetasizer NANO ZSP (Malvern Panalytical, Malvern, UK). ANTS/DPX-containing vesicles were separated from free ANTS/DPX by exclusion chromatography using a column filled with SephadexTM G-75 (Amersham Biosciences, Little Chalfont, UK) fine gel swollen in iso-osmotic HBS. Phospholipid concentrations for all samples were determined by phosphate analysis.

2.1.4. Peptides

Peptide stock solutions of LF11-215 and LF11-324 were prepared in PBS solution for bacteria and HBS solution for lipid vesicles. Due to the weak solubility of LF11-324 in buffer, AMP stock solutions were prepared by adding acetic acid and DMSO, up to 0.3% and 3% vol/vol, respectively. Prior to each measurement, the concentrations of such compounds were systematically lowered down to 0.01% acetic acid and 0.1% vol/vol DMSO (final pH 7.2), in order to minimize, or even remove, any effect on the membrane structure (29). AMP concentrations of the stock solutions were determined by comparing against the absorption band of the aromatic amino acids with the spectrophotometer NanoDrop ND-1000 (Thermo Fisher Scientific, Waltham, MA). Peptide stock solutions were stored in silanized glass tubes until use.

2.2. Methods

2.2.1. Microdilution Assay

The antimicrobial activity of the AMPs on *E. coli* was tested using a modified susceptibility microdilution assay (30) in the bacterial concentration range of 5×10^5 to 10^9 CFU/ml. Bacterial suspensions were incubated at a given AMP concentration for 2 h at 37°C (control samples were incubated in buffer only). Then, cell growth was monitored upon addition of double concentrated LB-medium for about 20 h using a Bioscreen C MBR (Oy Growth Curves Ab, Helsinki, Finland).

Data were analyzed assuming that the AMP-induced delayed bacterial growth is entirely due to a lower number density of survived cells, which is supported by the observation that the growth rate in the exponential phase does not depend on peptide concentration (**Supplementary Figure 1A**), i.e., the growth of the viable fraction of cells is similar to bacterial growth in absence of AMPs. This allowed us to quantify the number density of surviving bacteria from the onset of the exponential growth via the relation $\Delta t_{\mathrm{exp}} = a + b\log(n_{\mathrm{cell}})$, where a and b were obtained from a calibration curve in absence of AMPs (**Supplementary Figure 1B**). Then, the inhibited bacterial fraction $\mathrm{IF} = 1 - n_{\mathrm{cell}}([P])/n^0_{\mathrm{cell}}$ was calculated for different values of peptide concentration, $[P]$, and of bacterial number density of the control sample, n^0_{cell}. Following the so-called "equi-activity" analysis (27, 31), we further interpolated IF using a Gompertz function, which enabled us to derive inhibitory peptide concentrations IC_x, where x is the corresponding inhibited bacterial fraction (**Supplementary Figure 1C**). By convention, the standard MIC is defined at inhibition levels of 99.9%, i.e., $\mathrm{IC}_{99.9} \equiv \mathrm{MIC}$. Additional control experiments were performed in order to test whether DMSO and acetic acid, used in buffer solutions of both peptides (see above), affect bacterial growth. In particular, the microdilution assays were repeated with LF11-215 dissolved in pure PBS, yielding equivalently delayed onsets of bacterial growth. This suggests that DMSO and acetic acid at low concentrations used in this study do not significantly affect our derived MIC and IC_x-values.

2.2.2. Size and ζ-Potential Measurements

DLS and ζ-potential measurements were carried out with a Zetasizer Nano ZSP (Malvern Panalytical, Malvern, UK). *E. coli* suspensions were incubated with a given AMP concentration at 37°C for 1 h prior to each measurement. The used AMP concentrations were centered at the MIC values, and ranged from about 0.2× to 2.5×MIC. Control samples (no AMPs) were suspended and incubated in buffer alone. A concentration of 10^7 CFU/ml was found to provide the optimal compromise between high signal-to-noise ratio and low multiple-scattering bias. Because of the high conductivity of PBS, the electrode voltage was set to 4 V for ζ-potential measurements to keep currents below 1 mA. Further, measurements were paused for 180 s between individual runs. This prevented Joule heating leading to sample denaturation and electrode blackening. Experiments were repeated three times on different preparations, each consisting of at least six measurements. Reported ζ-potential values are given by the median of the corresponding measurements (i.e., from at least 18 values) and errors were derived using the median absolute deviations.

2.2.3. Leakage

Dye leakage experiments were performed combining previously reported protocols (20, 27). In brief, the dependencies of ANTS/DPX leakage on lipid and peptide concentration were determined by first incubating lipid vesicles ($[L] = 1$, 4, 10, and 20 mM) with peptides [$[P] = (0.025 - 2)$ mM] at 37°C for 1 h using a gently rocking shaker (Eppendorf Thermomixer C, Hamburg, Germany). Similar time protocols were applied previously (27) and are justified here based on separate time-resolved leakage experiments (**Supplementary Figure 3**) and Trp-fluorescence measurements (**Figure 3**), showing that a quasi steady state has been reached after 1 h. Before measurements, lipid/peptide solutions were diluted with HBS to a lipid concentration of 50 μM, and every measurement was repeated at least twice. Vesicle size was checked after each incubation period using DLS. Samples were excited at $\lambda = 360$ nm, and the intensity of the fluorescence emission peak at $\lambda = 530$ nm, I_p, was recorded with a slit width of 10 nm for both excitation and emission monochromators. Measurements were performed in quartz cuvettes in 2 ml of the iso-osmotic buffer on a Cary Eclipse Fluorescence Spectrophotometer (Varian/Agilent Technologies, Palo Alto, CA). The percentage of leakage, $E_{\%}$, was calculated according to the relation

$$E_{\%} = \frac{I_p - I_{min}}{I_{max} - I_{min}}, \tag{1}$$

where I_{min} is the initial fluorescence without peptide, and I_{max} is the fluorescence corresponding to 100% leakage determined through the addition of a 1 vol% solution of Triton X-100. The initial, monotonic increase of $E_{\%}$ values with increasing [P] was interpolated with a sigmoidal function. This enabled us to obtain peptide and lipid concentrations leading to a specific $E_{\%}$ value, which can in turn be used to calculate the partitioning parameters (see section 2.3.1).

2.2.4. Tryptophan Fluorescence

Fluorescence emission from Trp, present in both peptides, was measured with the Cary Eclipse Fluorescence Spectrophotometer, setting the excitation wavelength to $\lambda = 280$ nm, which corresponds to the maximum intensity of the Trp absorption/excitation band. Intensities of exciting and emitting light were adjusted by setting the slit widths of both incident and outgoing beam to 5 or 10 nm, depending on the emission intensity, in order to optimize the signal-to-noise ratio. Emission spectra were background-subtracted to remove contributions originating from the instrument's baseline and scattered light from vesicles. All samples were measured in HBS at 37°C using a quartz cuvette, with a magnetic stirrer to prevent sample sedimentation in the case of aggregation. LUVs ($[L] = 100$ μM) were mixed with peptides ($[P] = 2$ and 4 μM), recording fluorescence spectra at various post-mixing time intervals ranging from 0.5 to 60 min. Peptide solutions were measured at concentrations of 2, 3, and 4 μM in order to calibrate their intensity dependence in buffer.

The fluorescence emission band was fitted with the log-normal-like function (32, 33)

$$I(I_0, \lambda, \Gamma) = \begin{cases} I_0 \exp\left[-\frac{\ln 2}{\ln^2 \alpha} \ln^2\left(1 + \frac{(\lambda - \lambda_{\max})}{y\Gamma}\right)\right], & \lambda > \left(\lambda_{\max} - y\Gamma\right) \\ 0, & \lambda \leq \left(\lambda_{\max} - y\Gamma\right) \end{cases} \tag{2}$$

where $\lambda_{\max}$ and I_0 are, respectively, wavelength and intensity of the emission peak; Γ is the full-width-at-half-maximum

(FWHM) of the band; α is a skewness parameter (fixed at an optimum values 1.36 after testing); and $y = \alpha/(\alpha^2 - 1)$. Spectra from mixtures of LUVs and peptides were analyzed with a linear combination of two independent bands I^W and I^B, referring to AMPs in bulk (W) and partitioned into the lipid bilayer (B). λ^W and Γ^W were fixed to the reference values obtained by analyzing spectra from pure AMPs. Instead, I_0^W, I_0^B, λ^B, and Γ^B were adjustable parameters. The so obtained set of I_0^W values was converted to the concentration of dissociated peptides $[P]_W$ and further analyzed for peptide partitioning as detailed in section 2.3.1.

2.2.5. Small-Angle X-ray Scattering (SAXS)

SAXS experiments were performed at the highflux Austrian beamline at Elettra Synchrotron in Trieste, Italy (34) using a photon energy of 8 keV. SAXS patterns were recorded using a Pilatus 1 M detector (Dectris, Baden-Daettwil, Switzerland) in the q-range from 0.1 to 5 nm^{-1}, and further processed with FIT2D (35). A custom-build cell, termed "nanodrop," was used, allowing for precise measurements of very small volumes (10 μl) (36). Measurements were performed at a lipid concentration of 20 mg/ml (24.5−27.9 mM depending on the used membrane mimic) at 37°C. Lipids and peptides were mixed using an automatic sample changer and automatically injected into the nanodrop cell immediately after mixing. Peptide kinetics were measured starting 30 s after lipid-peptide mixing with an acquisition time of 1 s and a rest time of 10 s.

For the end-states, lipids mixed with peptides were incubated at 37°C for at least 4 h. These samples were measured using 12 frames of 10 s exposure each and a rest time of 12 s. Data were analyzed based on Bragg peak positions only. Using Bragg's law, the reported d-spacing values are simply given by $d = 2\pi/q_h$, where q_h is the peak position.

2.3. Data Analysis

2.3.1. Partitioning Equations for Lipid and Bacterial Systems

Following a previously reported thermodynamic formalism for the partitioning of peptides into lipid bilayers (37), based on the free energy of transfer of molecules from water into octanol (38), we define the mole fraction partitioning coefficient, K, as

$$K = \frac{[P]_B/([P]_B + [L])}{[P]_W/([P]_W + [W])} \simeq \frac{[P]_B[W]}{[P]_W[L]}, \tag{3}$$

where $[P]_B$ is the molar concentration of peptides partitioned into the lipid phase; $[P]_W$ is the peptide concentration in the water phase; and $[L]$ and $[W]$ are, respectively, the molar concentrations of lipids and bulk water (55.5 M at 25°C and 55.3 M at 37°C). The approximation for K (Equation 3) is obtained applying $[W] \gg [P_W]$ and $[L] \gg [P_B]$ (similarly, the concentration of ions in water, i.e., buffer solutions, is negligible compared to $[W]$). By definition, the total concentration of peptides is $[P] = [P]_W + [P]_B$, thus leading to

$$[P] = \underbrace{\frac{R_B[W]}{K}}_{[P]_W} + \underbrace{R_B[L]}_{[P]_B} = R_B\left(\frac{[W]}{K} + [L]\right), \tag{4}$$

where $R_B = [P]_B/[L]$.

An analogous approach can be applied to cells (39), replacing the lipid membrane with a so-called "cell phase," i.e., treating bacteria as a homogeneous medium consisting of all cell compartments accessible to the peptides. Then, similarly to Equation (3), the mole fraction partitioning coefficient, K_C, of peptides in bacterial cells is defined as

$$K_C \simeq \frac{[P]_B[W]}{[P]_W[X]}, \tag{5}$$

where $[X]$ is the total molar concentrations of all molecular species within the cell phase, including cytoplasmic water. This leads to

$$[P] = [P]_B\left(1 + \frac{[W]}{K_C[X]}\right). \tag{6}$$

Furthermore, $[P]_B$ and $[X]$ can be expressed as a function of the cell number density n_{cell}:

$$[P]_B = \frac{N_B\, n_{\text{cell}}}{N_A} \quad \text{and} \quad [X] = \frac{N_X\, n_{\text{cell}}}{N_A}, \tag{7}$$

where N_B is the absolute number of partitioned peptides per single cell, N_A is Avogadro's constant, and N_X, in analogy to $[X]$, represents the *number of molecules that constitute the accessible compartments of a single cell*. The combination of Equations (6) and (7) gives:

$$[P](n_{\text{cell}}) = \underbrace{\frac{N_B[W]}{N_X K_C}}_{[P]_W} + \underbrace{\frac{N_B}{N_A} n_{\text{cell}}}_{[P]_B} = \frac{N_B}{N_A}\left(\frac{N_A[W]}{N_X K_C} + n_{\text{cell}}\right) \tag{8}$$

Since N_X is inaccessible, we thus define the *effective partitioning coefficient* $K^{eff} = N_X K_C$ as measurable quantity.

2.3.2. Estimating the Maximum Number of AMPs Adsorbed to the Bacterial Surface

Remembering that ζ-potential values are sensitive only to the charges exposed to the outside of any particle, including bacteria, we can obtain upper boundaries for the number of surface adsorbed peptides. Given the high abundance of lipopolysaccharides (LPS) in the outer leaflet (about 70–90 vol%) of Gram-negative bacteria, as compared to other charged lipid species such as PG and CL (<2 vol%) and membrane proteins (7–20 vol%) (40), it is justified to assume that LPS dominates the surface potential of *E. coli*. Then, following considerations put forth for peptides partitioning in liposomes (31, 41), the ratio of ζ-potential values in the presence and absence of AMPs is

$$\frac{\zeta}{\zeta_0} \approx \frac{\sigma}{\sigma_0} \simeq \left(\frac{S_0}{S}\right)\frac{\sum_i N_i z_i + N_P z_P}{N_{\text{LPS}}^0 z_{\text{LPS}}}, \tag{9}$$

where (σ, σ_0) and (S, S_0) are the corresponding surface charge densities and cell surface areas, respectively. Further, N_{LPS}^0 is the initial number of LPS molecules in the outer leaflet, with a nominal charge $z_{\text{LPS}} \simeq -6$ (42); N_P is the number of surface adsorbed AMPs of nominal charge $z_P \simeq +5$ (20); and $\sum_i N_i z_i =$

$N_{\mathrm{LPS}}z_{\mathrm{LPS}} + N_{\mathrm{PG}}z_{\mathrm{PG}} + N_{\mathrm{CL}}z_{\mathrm{CL}}$ considers anionic lipids that translocate into the outer leaflet due to AMP activity (3, 6, 18). This term also accounts for a possible loss of LPS molecules in the outer leaflet due to vesiculation processes (25). Note that Equation (9) is only valid for $|\zeta| \leq 25$ mV, in which range $\zeta \propto \sigma$ (43). Equation (9) also assumes that the position of the slipping plane is not significantly altered upon the addition of peptides. Rearranging Equation (9) leads to

$$\frac{N_P}{N^0_{\mathrm{LPS}}} \simeq \left(\frac{z_{\mathrm{LPS}}}{z_P}\right)\left(\frac{\zeta}{\zeta_0}\frac{S}{S_0} - \frac{\sum_i N_i z_i}{N^0_{\mathrm{LPS}} z_{\mathrm{LPS}}}\right), \tag{10}$$

which is physically meaningful only if

$$\frac{\zeta}{\zeta_0}\frac{S}{S_0} \leq \frac{\sum_i N_i z_i}{N^0_{\mathrm{LPS}} z_{\mathrm{LPS}}} \leq 1. \tag{11}$$

This leads to two extreme cases, the first one being the maximum "charge scrambling"

$$\frac{\zeta}{\zeta_0}\frac{S}{S_0} = \frac{\sum_i N_i z_i}{N^0_{\mathrm{LPS}} z_{\mathrm{LPS}}}, \tag{12}$$

leading to $N_P/N^0_{\mathrm{LPS}} = 0$, i.e., complete dissociation of peptides from the bacteria, which is physically not realistic. The second limiting scenario is given by $\sum_i N_i z_i = N^0_{\mathrm{LPS}} z_{\mathrm{LPS}}$, i.e., bacteria retain their original surface exposure of LPS, which yields, upon insertion into Equation (10),

$$\frac{N^{\max}_P}{N^0_{\mathrm{LPS}}} \approx \left(\frac{z_{\mathrm{LPS}}}{z_P}\right)\left(\frac{\zeta}{\zeta_0} - 1\right), \tag{13}$$

where $N^{\max}_P$ is the upper boundary of surface adsorbed peptides. Moreover, this assumes $S/S_0 \sim 1$, which may be contradictory to previously observed bacterial cell shrinking in the presence of AMPs [see, e.g., (44)]. However, it can be justified in view of our goal to obtain an estimate the upper boundary values for N^{max}_P. N^0_{LPS} can be estimated using $N^0_{\mathrm{LPS}} \approx 0.9S_0/A_{\mathrm{LPS}}$, where $A_{\mathrm{LPS}} \simeq 1.6$ nm^2 (45, 46) is the lateral area per LPS molecule and S_0 is supplied by size measurements. The prefactor originates from considering a maximum surface coverage of 90% by LPS molecules (40). For example, using DLS, we measured a hydrodynamic diameter of *E. coli* K12 $2R_H = 980\pm30$ nm, from which we calculate $S_0 \simeq 4.5 \times 10^6$ nm^2, approximating the bacteria's shape with a cylinder of radius r and length l using $R^2_H \simeq r^2/2 + l^2/12$ and $r \sim 400$ nm (47). This yields $N^0_{\mathrm{LPS}} \approx 3 \times 10^6$.

3. RESULTS

3.1. Antimicrobial Activity and Partitioning in Bacterial Systems

3.1.1. Efficacy and Partitioning

We started our analysis of peptide activity in *E. coli* with measuring a range of inhibitory concentrations, including the MIC, by means of a slightly modified susceptibility assay, and for different bacterial concentrations. An example using LF11-324 is reported in **Figure 1A**, showing different IC_x values as a function of n_{cell} (note that in these bacterial suspensions 1 CFU corresponds to one single cell).

The partitioning formalism, described in section 2.3.1, was used to fit the linear increase of IC_x with cell concentration (**Figure 1A**) (LF11-215 data not shown). Also the MIC values increased linearly with cell concentration (**Figure 1B**), but more rapidly for LF11-215; results at $n \simeq 5 \times 10^5$ CFU/ml are consistent with previous reports (20, 25). At low concentrations, $n_{\mathrm{cell}} \ll N_A[W]/K^{eff} \sim 2 \times 10^8$ ml^{-1}, $[P] \approx [P]_W$, explaining the apparent plateau in the semi-log plot at low bacterial densities (see inset in **Figure 1B**). In this regime, the number of peptides dispersed in buffer dominates the total AMP amount. At high concentrations, instead, i.e., $n_{\mathrm{cell}} \gg N_A[W]/K^{eff}$, most of AMPs partition into the cell volume; thus $[P] \approx [P]_B$.

Finally, results for N_B and K^{eff} from our thermodynamic analysis are shown in **Figures 2A,B**. About four times less LF11-324 is needed to bind to the cells compared to LF11-215 in order to induce full growth inhibition (**Figure 2A**). Interestingly, this is not related to the affinity of the AMPs to the cell (see **Figure 2B**), as LF11-215 exhibits ∼2-fold higher K^{eff} values over the whole range of inhibited fractions. Further, K^{eff} slightly decreases as a function of inhibited fraction for both AMPs, suggesting that the likelihood of interactions with cells becomes lower the more AMPs are added to the system.

3.1.2. Outer Leaflet Distribution of AMPs

The distribution of charged AMPs on the outer leaflet of the outer cell membrane was interrogated by analyzing ζ-potential data. Unfortunately, the "equi-activity" approach (31) was not applicable, because ζ-potential differences from the control systems were weak in magnitude and constant over a wide range of $[P]$ around the MIC values (**Figure 2C**). Nevertheless, the maximum number of peptides partitioned in the outer bacterial surface, $N^{\max}_P$, can be estimated to be in the order of 10^6 AMPs for both LF11 molecules. $N^{\max}_P$ (corresponding to about one peptide over 2–3 LPS molecules) is rather constant in the concentration range of 0.3× to 2.5×[MIC], suggesting that the cellular surface is already saturated with peptides in the sub-MIC range. In addition, $N^{\max}_P$ can be compared with the total number of peptides per cell, N_B. The ratio $N^{\max}_P/N_B$ as a function of the inhibited fraction, and hence of the peptide concentration, is displayed in **Figure 2D**. We found $N^{\max}_P/N_B \leq 25\%$ at the lowest measured inhibited fraction, followed by a decrease of about 1 and 5% at the MIC of LF11-215 and LF11-324, respectively.

3.2. Effects in Cytoplasmic Membrane Mimics

In order to compare the growth inhibition of *E. coli* by LF11-215 and LF11-324 with their membrane activity, we prepared 100 nm sized LUVs of three different cytoplasmic membrane mimics, pure POPG, POPE/POPG (3:1 mol/mol), and POPE/POPG/TOCL/ (82:6:12 mol/mol/mol), all of which are frequently used in biophysical studies on the mode of action of AMPs [see e.g., (15, 48–50)]. Out of these

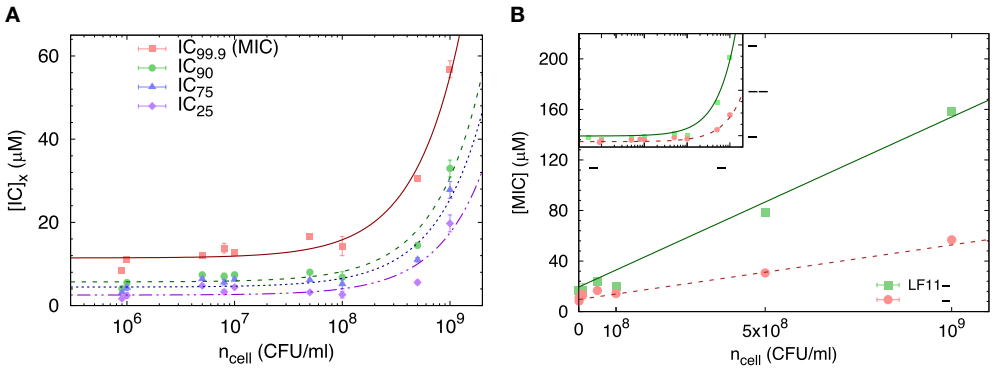

FIGURE 1 | (A) Selected IC_x-values of LF11-324 related to different inhibited fractions (see legend) as a function of n_{cell}. Lines represent best fits using Equation (8). **(B)** Dependence of minimum inhibitory concentration (MIC) on the cell number density for LF11-215 and LF11-324, including best fits using Equation (8) (straight lines). The inset displays the same data on logarithmic scale.

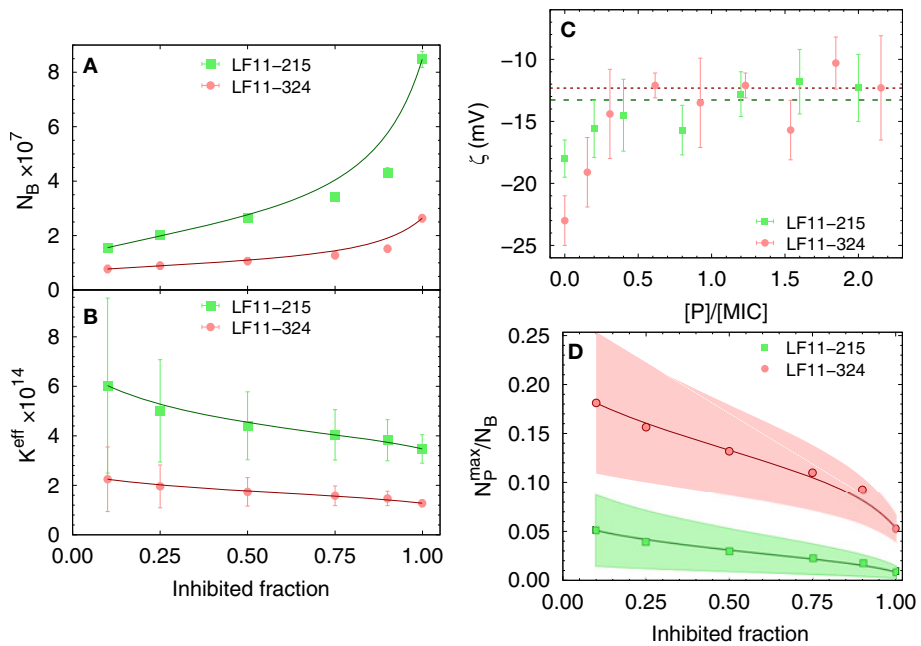

FIGURE 2 | Dependence of the total number of antimicrobial peptides (AMPs) partitioned into *E. coli* **(A)**, as well as the effective partitioning coefficient **(B)** on the inhibited bacterial fraction; lines are a guide to the eyes. **(C)** Variation of ζ-potential with peptide concentration [normalized by the respective minimum inhibitory concentrations (MICs)]. The lines mark the average, constant ζ-values from $[P] = 0.3 \times$ MIC to $2.5 \times$ MIC for LF11-215 (green dashed line) and LF11-324 (red dotted line). **(D)** Upper boundaries of the ratio of surface-adsorbed to cell-partitioned AMPs as a function of inhibited fraction. Color-shaded areas represent confidence intervals; lines are guides to the eyes.

systems, POPE/POPG/TOCL/ (82:6:12 mol/mol/mol) most closely resembles the natural lipid composition of *E. coli* inner membranes (51).

3.2.1. Tryptophan Fluorescence

We first measured the partitioning of the two peptides using Trp fluorescence. The emission spectra of the single Trp residue of LF11-215 and LF11-324 exhibited in buffer a band with $\lambda^W \simeq 354$ nm and $\Gamma^W \simeq 65$ nm [see e.g., **Figure 3A**]. This is in agreement with the emission maximum of Trp exposed to a polar environment (52). When peptides were added to the LUVs, the Trp emission bands exhibited a blue-shift regardless of lipid composition and peptide type (example in **Figure 3A**). The analysis of the spectra (see example in **Figure 3B** and details in section 2.2.4) enabled us to derive the kinetics of AMPs partitioning into the different bilayers. For all membranes, the fluorescence signal from the partitioned AMPs exhibited values of $\lambda^B \simeq (331 - 335)$ nm and $\Gamma^B \simeq (49 - 54)$ nm, indicating an average location of the Trp residues within the hydrophobic region of the lipid bilayer (52).

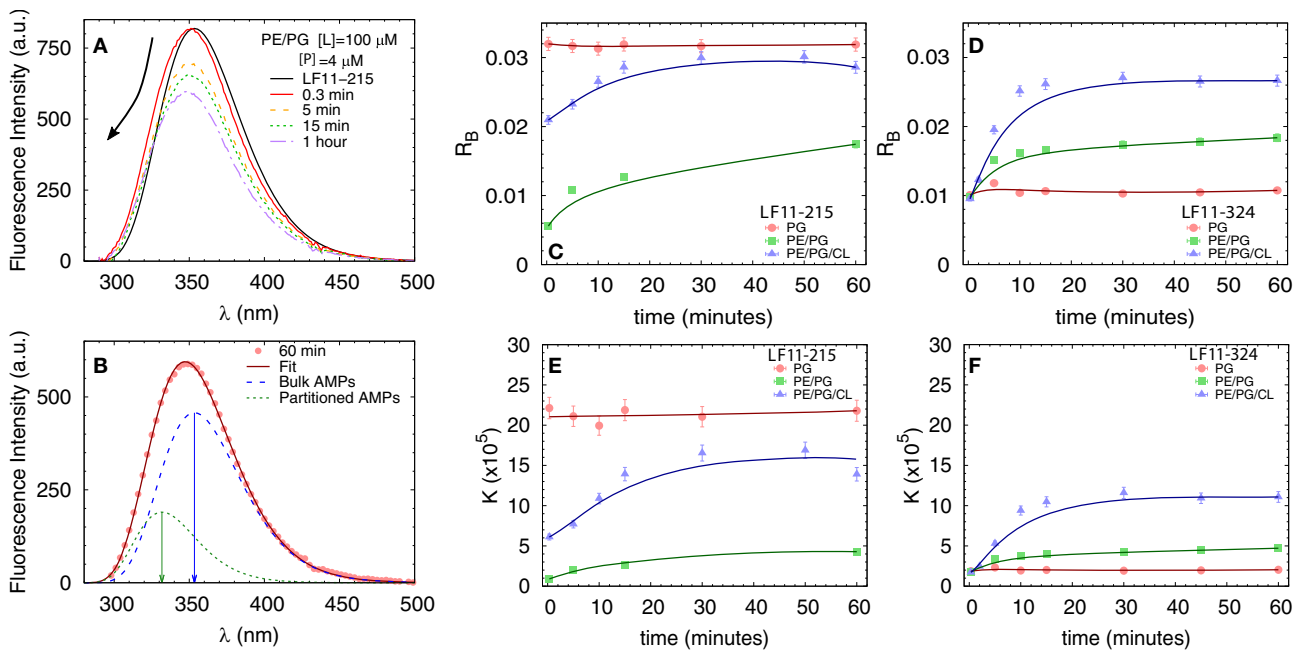

FIGURE 3 | Peptide partitioning from Trp fluorescence experiments. **(A)** Example of Trp emission-band kinetics. The arrow indicates the decrease in intensity and blue-shift as a function of time. **(B)** Example of spectral analysis (POPE/POPG [*L*] = 100 μM, LF11-215 [*P*] = 4 μM); red line: best fit; blue dashed line: emission from antimicrobial peptides (AMPs) in suspension; green dotted line: emission from AMPs partitioned into the membrane. The arrows mark the different λ_{max} values. **(C,D)** Adsorption kinetics for LF11-215 and LF11-324, respectively, for three different membrane mimics. **(E,F)** Kinetics of the partitioning coefficient *K* for LF11-215 and LF11-324, respectively, for three different membrane mimics.

CL-containing systems displayed broader bands, $\Gamma^B \approx 65$ nm, after 20−30 min of incubation, probably due to a heterogeneous distribution of Trp locations within the bilayers (33). Speculating that this might be related to supramolecular structural changes, we performed DLS after 60 min of incubation. Indeed, we observed large aggregate structures, for POPE/POPG/TOCL samples, but also for POPE/POPG in presence of 4 μM LF11-324 (see **Supplementary Figure 2A** and **Table 1**). We note, however, that the derived AMP partitioning data are not directly linked to such morphological changes. Overall, CL and LF11-324-containing samples showed the highest propensity to form aggregates, whereas POPG LUVs remained intact under present conditions.

Table 1 reports results of the AMP partitioning analysis (see section 2.1) after 60 min of incubation with the peptides, and the temporal evolution of these parameters for $[P] = 4$ μM is shown in **Figures 3C–F**. Both peptides quickly achieve stationary R_B and K values in POPG LUVs (within 30 s), but the amount of adsorbed LF11-215 is three times higher than for LF11-324. In PE-containing bilayers both peptides instead exhibited similar adsorption and partitioning kinetics, with an increase over the first 10-20 min before reaching stable values. Both peptides showed, however, a higher affinity to POPE/POPG/TOCL membranes than to POPE/POPG. In contrast, at lower peptide concentration (2 μM), this effect was not observed (**Table 1**). In this case, the parameters derived from the partitioning analysis including POPG did not depend on whether LF11-215 or LF11-324 was added.

3.2.2. Leakage

To test the permeability of the three membrane mimics, we investigated the dye efflux from LUVs after incubation with LF11-215 at various lipid-to-peptide ratios. This allowed us to pursue the effect of peptides at a physiological temperature, where all lipid systems are in the fluid phase, up to very high lipid concentrations typically used in small angle scattering experiments ($[L] \sim 20$ mM). **Figures 4A–C** display leakage percentages as a function of $[P]$ for different concentrations of POPG, POPE/POPG, and POPE/POPG/TOCL systems. In all three systems, substantial leakage seemed to coincide with the formation of larger structures, as corroborated with DLS measurements (see example in **Supplementary Figure 2B**). Indeed, the transformation from unilamellar vesicles to larger aggregates (marked as a gray, shaded areas in **Figures 4A–C**) depends on the overall lipid and peptide concentrations, and coincides with a leakage of 15−20%, and $[P] \leq 1$ mM for POPG and $[P] \leq 0.25$ mM for PE-containing systems. Interestingly, while POPG LUVs showed a sharp, sigmoidal increase of leakage up to 100%, PE-containing systems exhibited a maximum at a certain peptide-to-lipid ratio, followed by a leakage decrease and, most likely, a stabilization at higher $[P]$ values. POPE/POPG vesicles, in particular, resulted in a relatively low total efflux $\leq$ 40%. In analogy with the equi-activity analysis used for the susceptibility assay, leakage curves where exploited to calculate the partitioning parameters (27). The peptide concentrations needed to induce leakage $E_{\%}$ at a given $[L]$ were all fitted with Equation (4), demonstrating that

TABLE 1 | Partitioning parameters calculated from the spectral analysis of the Trp emission band for LF11-215 and LF11-324.

LF11-215 (2 μM / 4 μM)	R_B **$\times 10^{-3}$**	K **$\times 10^4$**	$[P]_W$ **(μM)**
POPG	14.9 ± 0.3 / 31.9 ± 0.4	161 ± 6 / 217 ± 8	0.513 ± 0.015 / 0.81 ± 0.04
POPE/POPG	11.2 ± 0.3 / 17.5 ± 0.7	70 ± 4 / 43 ± 3	0.88 ± 0.03 / 2.25 ± 0.07
POPE/POPG/TOCL*	11.9 ± 0.2 / 28.6 ± 0.3	82 ± 4 / 139 ± 6	0.81 ± 0.02 / 1.14 ± 0.03
LF11-324 (2 μM / 4 μM)	R_B **$\times 10^{-3}$**	K **$\times 10^4$**	$[P]_W$ **(μM)**
POPG	10.5 ± 0.3 / 10.7 ± 0.9	61 ± 4 / 20 ± 20	0.95 ± 0.03 / 2.93 ± 0.09
POPE/POPG*	11.0 ± 0.3 / 18.4 ± 0.6	67 ± 4 / 47 ± 3	0.90 ± 0.02 / 2.16 ± 0.06
POPE/POPG/TOCL**	10.6 ± 0.3 / 26.7 ± 0.4	63 ± 4 / 111 ± 5	0.95 ± 0.03 / 1.33 ± 0.04

Data refer to systems after 1 h of incubation with peptides (see ***Figure 3****), and [L] = 100 μM. *Samples showing aggregation at [P] = 4 μM; **Samples showing aggregation at [P] = 2 and 4 μM.*

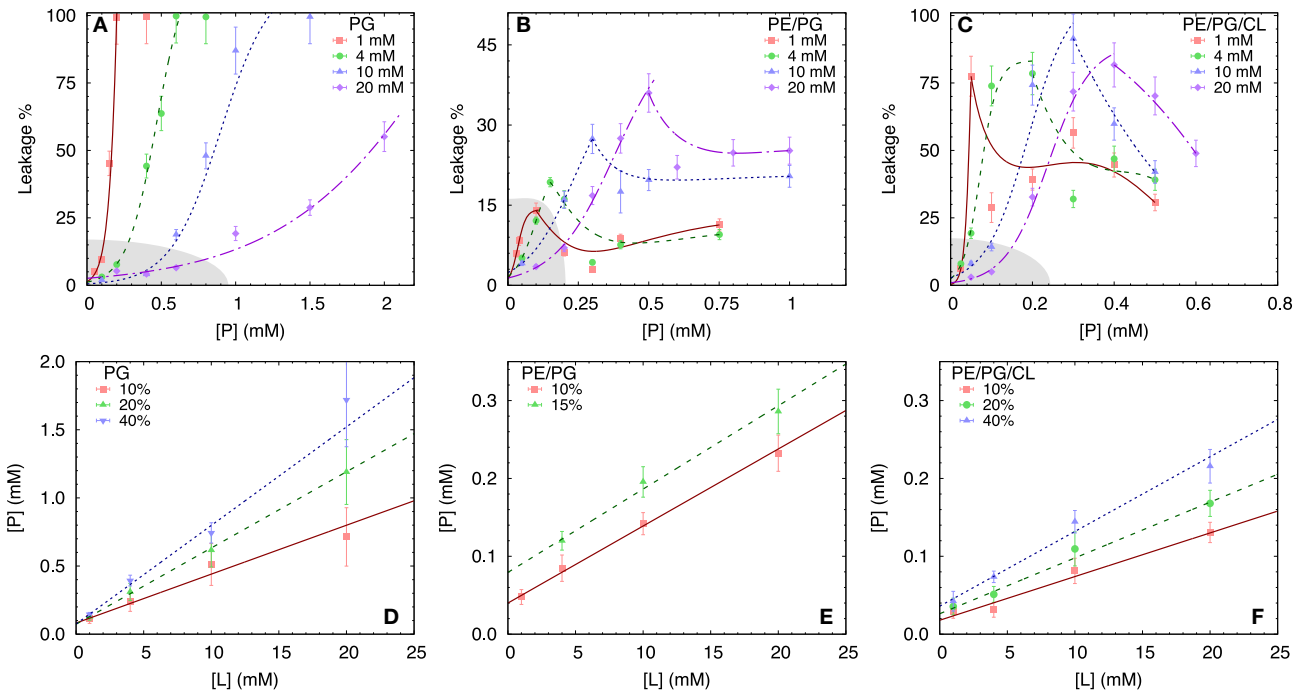

FIGURE 4 | LF11-215 induced permeabilization of LUVs composed of POPG **(A)**, POPE/POPG **(B)**, and POPE/POPG/TOCL **(C)** at different lipid concentrations (see legend). A sigmoidal function was used to interpolate the initial leakage increase, whereas lines describing the following decrease **(B,C)** are just guides to the eyes. Gray-shaded areas indicate regimes where the formation of large aggregates was not detected. **(D–F)** Analysis of peptide induced ANTS/DPX leakage (see legend) in terms of Equation (4) (straight lines) for the different membrane mimics. For result, see **Table 2**.

in these ranges of $[P]$ and $[L]$, the partitioning characteristic are alike, regardless of transitions from a unilamellar system to more complex lipid aggregates. Fitting results are shown in **Table 2**. POPG samples seem to require a high number of LF11-215 per lipid in order to achieve leakage, showing the highest R_B and K values, which increase along with higher leakage, and with a rather constant $[P]_W$. This means that at $[L] \simeq 20$ mM, $>$ 90% of peptides are partitioned into the lipid phase. Leakage from PE-containing systems instead needs less AMPs per lipid (see **Table 2**), with a maximum amount of partitioned AMPs of $<$ 80% for $[L] \simeq 20$ mM.

3.2.3. SAXS

We performed SAXS experiments to investigate structural changes in membrane mimics induced by the peptides. Vesicles composed of POPG, POPE/POPG, and POPE/POPG/TOCL without AMPs (reference systems) as well as end-states at a lipid-to-peptide ratio of 1:25 measured 4 h after lipid-peptide mixing are shown in **Figures 5A,B** for LF11-215 and LF11-324, respectively. All reference systems showed purely diffuse scattering patterns originating from positionally uncorrelated lipid bilayers, as expected for LUVs. In the case of POPG liposomes, after addition of either peptide, a shift of the first

TABLE 2 | Partitioning parameters for LF11-215, resulting from the leakage assay analysis of three differently composed LUVs (see also **Figure 4**).

Leakage	R_B ×10^{-3}	K ×10^4	$[P]_W$ (mM)
POPG 10%	36 ± 4	2.4 ± 0.7	0.08 ± 0.03
POPG 20%	55.9 ± 1.6	4.2 ± 0.4	0.073 ± 0.009
POPG 40%	72 ± 6	5.4 ± 1.4	0.08 ± 0.03
POPE/POPG 10%	9.8 ± 0.4	1.37 ± 0.16	0.040 ± 0.006
POPE/POPG 15%	10.7 ± 1.0	0.75 ± 0.15	0.08 ± 0.02
POPE/POPG/TOCL 10%	5.6 ± 0.7	1.7 ± 0.8	0.018 ± 0.010
POPE/POPG/TOCL 20%	7.2 ± 0.5	1.5 ± 0.3	0.026 ± 0.007
POPE/POPG/TOCL 40%	9.6 ± 0.9	1.5 ± 0.4	0.036 ± 0.012

Concentration ranges: $[L] = (1 - 20)$ *mM,* $[P] = (0.05 - 2)$ *mM.*

minimum at $q \sim 2.8$ nm^{-1} can be observed, which could originate from a thinning of the membrane. Most pronounced for PE-containing mimics, the measurements after peptide mixing showed a small, but clearly discernible positional correlation peak at $q \sim 1.1 - 1.3$ nm^{-1} in addition to a significant diffuse scattering pattern; a similar feature—but much less expressed—was also observed for POPG in the presence of LF11-215. The diffuse scattering of POPE/POPG and POPE/POPG/TOCL mixtures in the presence of both peptides showed an additional modulation at $q \sim 2$ nm^{-1}. This feature might originate from a preferential enrichment of AMPs in one leaflet or the formation of thin peptide-enriched domains. Clarification of the underlying structures would require dedicated experiments using neutron scattering combined with contrast variation and computational modeling [see e.g., (49)]. This is, however, beyond the scope of the present study. Instead, we focused on the evolution of the correlation peak in case of LF11-215 using time-resolved SAXS (**Figure 6**). For the PE-containing samples, especially in the case of POPE/POPG/TOCL, addition of peptides led to a rapid precipitation of the sample, which reduced the amount of sample being hit by the X-ray beam. This explains the increased noise of scattering data at longer times. For liposomes consisting of pure POPG, only the final pattern contained a weak feature of a positional correlation peak. In turn, TOCL-containing membrane mimics showed the onset of peak formation already 30 s after mixing, while this was slightly delayed to about 5 min in POPE/POPG. The d-value, derived directly from the peak position, exhibited a non-monotonic behavior over time in both POPE/POPG and POPE/POPG/TOCL mimics (**Figure 6D**), showing first a decrease and subsequent increase over several minutes after peptide addition. During this equilibration process, the d-values of POPE/POPG were always larger than those of POPE/POPG/TOCL mixtures, with a difference of $\sim$ 0.1 nm in the end-states. Interestingly, final d-values of both PE-containing mixtures were even lower in the presence of LF11-324 (POPE/POPG: $d = 5.12$ nm and POPE/POPG/TOCL: $d = 5.07$ nm). This could stem either from a pronounced membrane thinning or/and different penetration depths of the peptides within the bilayer (see section 4). Notably, the time scale of the related equilibration process is much longer (hours) than peptide adsorption (minutes) (see **Figure 3**).

4. DISCUSSION

We exploited a common thermodynamic framework for the partitioning of antimicrobial peptides to bridge the activities of LF11-215 and LF11-324 in *E. coli* and different lipid-only mimics of their cytoplasmic membranes. In the case of bacteria, this was achieved by evolving a susceptibility microdilution assay for the antimicrobial activity of the two AMPs. This yielded more accurate results (confidence $< 3\%$) than standard MIC evaluations over a broad range of cell concentrations. In particular, we found $\text{MIC}_{\text{LF11-215}} = (13.7 \pm 0.4)\ \mu$M and $\text{MIC}_{\text{LF11-324}} = (11.1 \pm 0.6)\ \mu$M at $n_{\text{cell}} = 10^6$ CFU/ml [in agreement with (20, 25)] increasing linearly up to $\text{MIC}_{\text{LF11-215}} = (158 \pm 2)\ \mu$M and $\text{MIC}_{\text{LF11-324}} = (57 \pm 2)\ \mu$M at $n_{\text{cell}} = 10^9$ CFU/ml. The higher antimicrobial efficacy of LF11-324 was conserved for all measured cell concentrations and extended also to lower growth-inhibited fractions at decreased AMP concentrations. Intriguingly, LF11-324 showed a lower partitioning coefficient than LF11-215, suggesting energetically less-favored interaction with cells, despite its higher efficacy. Combing these data with ζ-potential measurements further allowed us to obtain an upper boundary for the surface adsorbed AMP fraction. Strikingly, we found that both lactoferricin derivatives bind about equally to the microbial envelope, but constitute only a minor fraction of the total number of AMPs interacting with the bacteria. That is, at the MIC only 1−5% of AMPs are surface bound, and even at bacteria inhibition levels of 10% only $\sim$ 5% (LF11-215) to $\sim$ 18% (LF11-324) of the cell associated peptides do not enter inner compartments (**Figure 2**). Consequently, both peptides target mainly inner bacterial components.

Partitioning of LF11-215 and LF11-324 in lipid membrane mimics was instead investigated using Trp fluorescence and ANTS/DPX leakage. While the first technique quantifies the actual number of partitioned peptides per lipid, the second provides the number of adsorbed AMPs leading to a specific dye-efflux. Trp fluorescence revealed a faster and stronger partitioning into POPG membranes than into PE systems in the case of LF11-215, whereas LF11-324 showed the lowest adsorption and partitioning into POPG. Based on pure electrostatic interactions of anionic POPG and cationic residues, which are identical for both peptides, this appears counterintuitive. It can be understood, however, considering that the amphipathic moment of both LF11 peptides is normal to the membrane plane, with the aromatic amino acids of the N-terminal inserted into the hydrophobic core of the membrane, and the Arg-rich section of the amidated C-terminal interacting with the lipid head-groups and exposed to the solvent as reported from previous studies on this family of peptides (25, 53). Indeed, our fluorescence data show that the Trp side chain is segregated into the apolar environment of the bilayer, hence suggesting that the protonated amino group of the N-terminal lies in the same region. Consequently, the positively charged N-terminus of

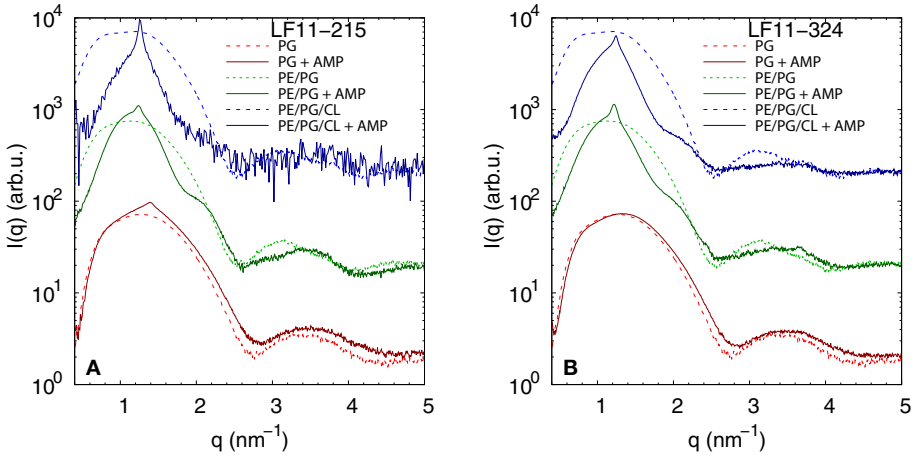

FIGURE 5 | SAXS patterns of POPG, POPE/POPG, and POPE/POPG/TOCL before and after 4 h after incubation with **(A)** LF11-215 and **(B)** LF11-324 (end-states) at $[P]/[L] = 1:25$, corresponding to $[L] = (24.5–27.9$ mM) and $[P] \sim 1.1$ mM.

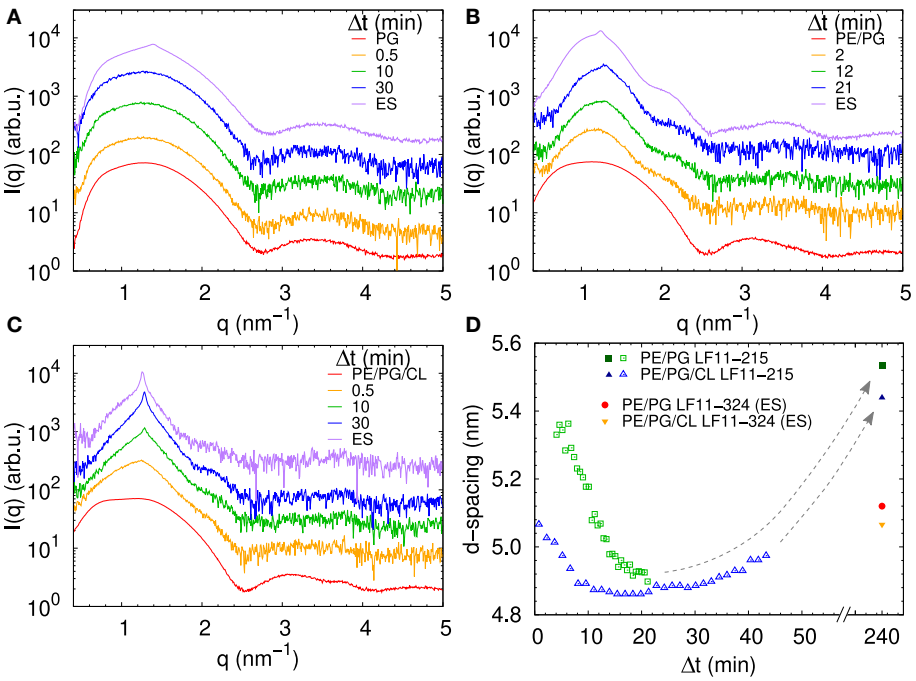

FIGURE 6 | LF11-215-induced structural kinetics as observed in the evolution of SAXS patterns of **(A)** POPG, **(B)** POPE/POPG, and **(C)** POPE/POPG/TOCL; $[P]/[L] = 1:25$, corresponding to $[L] = (24.5–27.9$ mM) and $[P] \sim 1.1$ mM. Panel **(D)** shows the changes in *d*-spacing over time for POPE/POPG and POPE/POPG/TOCL with LF11-215, as well as end-states (ES) for LF11-215 and LF11-324 measured after 4 h of system equilibration.

LF11-324 needs, because of the additional Phe and Pro residues, to insert deeper into the hydrophobic core of the bilayer and thus further away from the anionic PG than in the case of LF11-215, leading to an unfavorable configuration. In the case of PE-containing mixtures, such electrostatic interactions are less pronounced; moreover, peptide-induced domain formation, as previously observed for CL-containing mixtures in the presence of LF11 derivatives (20, 25), may facilitate peptide insertion due to packing defects at domain boundaries [see e.g., (54)]. Hence, POPE/POPG and POPE/POPG/TOCL mixtures are thus more reliable mimics of *E. coli* inner membranes than pure POPG. Moreover, the approximate similar adsorption of both peptides (**Figures 3C,D**) resembles roughly the findings in *E. coli* (**Figure 2D**), thus suggesting that these mimics are also first-order proxies to peptide partitioning into outer membranes, despite the lack of LPS.

Dye leakage experiments for PE-containing mimics showed an effect that, to the best of our knowledge, has not been reported before. Upon raising peptide concentration, we observed an initial increase of dye-efflux, peaking at relatively low peptide concentrations, followed by a subsequent decrease of permeabilization upon further addition of peptide (**Figures 4A–C**). POPG vesicles in contrast showed a typical pure sigmoidal increase of permeabilization [see e.g., (27)], but required significantly higher peptide concentrations than in other mixtures, which aligns with our above discussion on competing electrostatic interactions of the charged N-terminus with PG headgroups. Moreover, DLS experiments revealed that significant leakage was always associated with the formation of large aggregates, independent of the lipid membrane mimic (i.e., also for pure POPG). The intricate entrapment of dyes in POPE/POPG and POPE/POPG/TOCL membranes at increased levels of AMP concentration can be rationalized considering our SAXS data. Here all three lipid mixtures, with the exception of POPG in the presence of LF11-324, showed the formation of a weak Bragg peak (**Figure 5**), signifying the presence of a minor fraction of positionally well-correlated aggregates.

While a sole correlation peak does not enable a conclusion about the specific supramolecular structure, it is still possible to derive *d*-spacing values from the peak positions, which can be connected to previous studies on peptide-induced multibilayer systems with collapsed interbilayer distance (10). Consider first POPE/POPG (3:1 mol/mol) and its steric bilayer thickness, which has been previously determined with high accuracy to be $\sim$ 4.7 nm (49). The final *d*-values for this system after addition of LF11-215 and LF11-324 were 5.53 and 5.12 nm. This suggests that the Bragg peaks originate from lamellar aggregates with almost completely collapsed bilayers, most likely only separated by the steric size of peptides partially inserted into the membranes. Thus, the lower *d*-value observed for LF11-324 suggests pronounced membrane thinning as a result of a stronger perturbation of the membrane, which could be due to the bigger size of the peptides' hydrophobic patch, leading to stronger disordering effects within the hydrocarbon chain region.

For TOCL containing mixtures, we found slightly lower final *d*-values for both peptides, but again more pronounced for LF11-324 (**Figure 6D**). Since we do not have any reference data on the steric thickness of POPE/POPG/TOCL (82:6:12 mol/mol/mol) bilayers, this might be due to either differences in membrane thickness in the absence of peptide or peptide-induced membrane perturbation. However, given that the hydrocarbon thickness of TOCL is expected to be about equal to POPG and POPE, we speculate that the smaller *d*-values for POPE/POPG/TOCL are due to an increased membrane perturbation by the peptides. Indeed, a more pronounced effect of peptides for TOCL containing mixtures, as compared to POPE/POPG, was also observed in Trp fluorescence experiments, where these mixtures exhibited the higher partitioning coefficients, as well as faster kinetics (**Figure 3**). Faster kinetics were also observed for the formation of the collapsed lamellar phase in the presence of LF11-215, where the weak Bragg peak was present in POPE/POPG/TOCL 30 s after the addition of peptides, but needed about 5 min to form in POPE/POPG (**Figure 6D**). The initial decrease in *d*-spacing observed for the first 10−20 min interestingly correlates with the Trp fluorescence kinetics. This suggests that the shift of the peak position over time is related to an initial accumulation of peptides on the membranes during approximately 20 min, followed by a slow equilibration over the course of the next few hours, where peptides diffuse into the newly formed aggregates, most of which are not forming collapsed multibilayers.

Interestingly, the lowest *d*-values of both membranes are $\sim$ 4.9 nm (**Figure 6D**), which is about equal to the steric membrane thickness of POPE/POPG (49). This provides evidence that the membranes come in close contact. The negative intrinsic curvatures of POPE (55) and TOCL (56) and their well-known propensity to form non-lamellar structures [see e.g., (57)] make them highly prone to induce membrane fusion (58, 59). We thus propose that the *d* value minima indicate time points of membrane fusion. Note that peptide-induced fusion of membranes was reported previously (10). Membrane fusion would also explain why some of the dyes are not released by the peptides activity, but remain trapped within some aggregates (**Figure 4**). Interestingly, however, also POPG showed in the presence of LF11-215 a weak signature of collapsed bilayers after extended equilibration times (**Figure 5A**), with a $d \sim 4.5$ nm that is even lower than the smallest values observed for POPE/POPG and POPE/POPG/TOCL (**Figure 5D**). Note that POPG has an intrinsic curvature close to zero (15), and is well-known as a lamellar-phase forming lipid. The collapsed lamellar structure formed in POPG is thus unlikely to be related to membrane fusion, but merely the result of possibly disintegrated membrane patches, forming a stack of bilayers. This notion is supported by the high permeability of POPG vesicles and the absence of a drop of dye leakage at increased peptide concentrations (**Figure 4A**).

The overall higher peptide activity in PE and PE/CL-containing mixtures (as observed, for example, by the lower amounts of peptide needed to induce dye leakage) further suggests that the intrinsic lipid curvatures of these lipids and the resulting stored elastic energy stress (60) makes the bilayers more vulnerable to the peptides. A similar view has been previously proposed as the "balanced spring model for membrane interactions" (61), where membrane active compounds can relief the stored elastic stress in bilayers upon insertion. Finally, we note that also LPS is known for their propensity to form non-lamellar structures (62, 63). We thus expect analogous driving forces occurring in the bacterial outer membrane, although details of membrane composition and in particular asymmetry certainly cannot be neglected. *Nota bene*, we do not necessarily expect that both peptides induce membrane fusion in live bacterial systems, as the complex architecture of the cell envelope or the presence of a densely packed cytosol provides additional constrains. The occurrence of fusion events in lipid-only systems is a mere indication for elastic curvature stress stored within the membranes, which upon relaxation in the presence of peptides will assist their translocation into the cytosol.

In conclusion, our results show that bridging peptide activities in live bacteria and lipid membrane mimics is intricate and that a simple delineation of common leakage experiments can be

highly misleading. In particular, for the here studied LF11-215 and LF11-324, one might have concluded based on leakage data that pure POPG would be sufficient to explain the membrane permeabilizing potential of both peptides. Yet, detailing the partitioning of the peptides in different membrane mimics and microbes allowed us to arrive at a completely different picture. Instead, LF11-215 and LF11-324 both target mainly intracellular components, presumably DNA due to its highly negative charge, reaching local concentrations of up to ∼ 100 mM at the MIC. Moreover, the elastic curvature stress stored in POPE/POPG, and to an even greater extent in the more realistic POPE/POPG/TOCL mixture, bestows the membranes with an increased potential for peptide translocation, which might in general be exploited by surface adsorbed wedge-like AMPs. Thus, at least for the presently studied peptides we may answer the initially posed questions as follows: *(ad i)* Vesicle leakage and microbial killing are not directly correlated, but some valuable insight can be obtained upon coupling leakage data to peptide partitioning and studies of membrane structural changes. *(ad ii)* Both peptides bind about equally well to membranes, so for this part, their selectivity indeed seems determined by membrane binding. The difference in their efficacy, however, is due to specific interactions with cytosolic components, and most likely DNA. *(ad iii)* Our partitioning studies provide strong evidence that membrane translocation is definitely required for LF11-215 and LF11-324. Additional studies using different bacteria and AMPs need to be performed to verify whether it is possible to generalize these findings. In general, and although we restricted our study to two AMPs and a single bacterial strain, the developed framework provides a path and guidelines for future studies intending to get deep insight on AMP activity by coupling *in vitro* cell studies with lipid membrane mimics.

DATA AVAILABILITY STATEMENT

The original contributions presented in the study are included in the article/**Supplementary Materials**, further inquiries can be directed to the corresponding author/s.

AUTHOR CONTRIBUTIONS

LM, ES, NM, GP, and KL conceptualized and designed the study. LM, ES, JM, JK, MF, and NM carried out the experiments. LM, ES, JM, and GP carried out the data analysis and interpretation. LM, ES, and GP wrote the manuscript. All authors provided critical feedback and helped to shape the research, analysis, and manuscript.

FUNDING

This project was supported by the Austrian Science Funds (FWF), project no. P 30921 (to KL).

ACKNOWLEDGMENTS

We thank Heinz Amenitsch for technical assistance at the SAXS beamline.

SUPPLEMENTARY MATERIAL

The Supplementary Material for this article can be found online at: https://www.frontiersin.org/articles/10.3389/fmedt.2021.625975/full#supplementary-material

REFERENCES

1. Steiner H, Hultmark D, Engström Å, Bennich H, Boman HG. Sequence and specificity of two antibacterial proteins involved in insect immunity. *Nature*. (1981) 292:246–48. doi: 10.1038/292246a0
2. Wimley WC, Hristova K. Antimicrobial peptides: Successes, challenges and unanswered questions. *J Membr Biol*. (2011) 239:27–34. doi: 10.1007/s00232-011-9343-0
3. Lohner K. Membrane-active antimicrobial peptides as template structures for novel antibiotic agents. *Curr Top Med Chem*. (2017) 17:508–19. doi: 10.2174/1568026616666160713122404
4. Heller WT, Waring AJ, Lehrer RI, Harroun TA, Weiss TM, Yang L, et al. Membrane thinning effect of the beta-sheet antimicrobial protegrin. *Biochemistry*. (2000) 39:139–45. doi: 10.1021/bi991892m
5. Pabst G, Grage SL, Danner-Pongratz S, Jing W, Ulrich AS, Watts A, et al. Membrane thickening by the antimicrobial peptide PGLa. *Biophys J*. (2008) 95:5779–88. doi: 10.1529/biophysj.108.141630
6. Nguyen MHL, DiPasquale M, Rickeard BW, Doktorova M, Heberle FA, Scott HL, et al. Peptide-induced lipid flip-flop in asymmetric liposomes measured by small angle neutron scattering. *Langmuir*. (2019) 35:11735–44. doi: 10.1021/acs.langmuir.9b01625
7. Kumagai A, Dupuy FG, Arsov Z, Elhady Y, Moody D, Ernst RK, et al. Elastic behavior of model membranes with antimicrobial peptides depends on lipid specificity and d-enantiomers. *Soft Matter*. (2019) 15:1860–8. doi: 10.1039/C8SM02180E
8. Salditt T, Li C, Spaar A. Structure of antimicrobial peptides and lipid membranes probed by interface-sensitive X-ray scattering. *Biochim Biophys Acta*. (2006) 1758:1483–98. doi: 10.1016/j.bbamem.2006.08.002
9. Hickel A, Danner-Pongratz S, Amenitsch H, Degovics G, Rappolt M, Lohner K, et al. Influence of antimicrobial peptides on the formation of nonlamellar lipid mesophases. *Biochim Biophys Acta*. (2008) 1778:2325–33. doi: 10.1016/j.bbamem.2008.05.014
10. Kabelka I, Pachler M, Prévost S, Letofsky-Papst I, Lohner K, Pabst G, et al. Magainin 2 and PGLa in bacterial membrane mimics II: membrane fusion and sponge phase formation. *Biophys J*. (2020) 118:612–23. doi: 10.1016/j.bpj.2019.12.019
11. Bechinger B, Lohner K. Detergent-like actions of linear amphipathic cationic antimicrobial peptides. *Biochim Biophys Acta*. (2006) 1758:1529–39. doi: 10.1016/j.bbamem.2006.07.001
12. Shai Y. Mechanism of the binding, insertion and destabilization of phospholipid bilayer membranes by alpha-helical antimicrobial and cell non-selective membrane-lytic peptides. *Biochim Biophys Acta*. (1999) 1462:55–70. doi: 10.1016/S0005-2736(99)00200-X
13. Sevcsik E, Pabst G, Jilek A, Lohner K. How lipids influence the mode of action of membrane-active peptides. *Biochim Biophys Acta*. (2007) 1768:2568–95. doi: 10.1016/j.bbamem.2007.06.015
14. Lohner K, Sevcsik E, Pabst G. Liposome-based biomembrane mimetic systems: implications for lipid-peptide interactions. In: Leitmannova-Liu A, editor. *Advances in Planar Lipid Bilayers and Liposomes*. Vol. 6. Amsterdam: Elsevier (2008). p. 103–37. doi: 10.1016/S1554-4516(07)06005-X

15. Leber R, Pachler M, Kabelka I, Svoboda I, Enkoller D, Vácha R, et al. Synergism of antimicrobial frog peptides couples to membrane intrinsic curvature strain. *Biophys J*. (2018) 114:1945–54. doi: 10.1016/j.bpj.2018.03.006
16. Brogden KA. Antimicrobial peptides: pore formers or metabolic inhibitors in bacteria? *Nat Rev Microbiol*. (2005) 3:238–50. doi: 10.1038/nrmicro1098
17. Le CF, Fang CM, Sekaran SD. Intracellular targeting mechanisms by antimicrobial peptides. *Antimicrob Agents Chemother*. (2017) 61:1–16. doi: 10.1128/AAC.02340-16
18. Wimley WC. Describing the mechanism of antimicrobial peptide action with the interfacial activity model. *ACS Chem Biol*. (2010) 5:905–17. doi: 10.1021/cb1001558
19. Snoussi M, Talledo JP, Del Rosario NA, Mohammadi S, Ha BY, Košmrlj A, et al. Heterogeneous absorption of antimicrobial peptide LL37 in *Escherichia coli* cells enhances population survivability. *eLife*. (2018) 7:1–21. doi: 10.7554/eLife.38174
20. Zweytick D, Deutsch G, Andrä J, Blondelle SE, Vollmer E, Jerala R, et al. Studies on Lactoferricin-derived *Escherichia coli* membrane-active peptides reveal differences in the mechanism of N-acylated versus nonacylated peptides. *J Biol Chem*. (2011) 286:21266–76. doi: 10.1074/jbc.M110.195412
21. Malanovic N, Marx L, Blondelle SE, Pabst G, Semeraro EF. Experimental concepts for linking the biological activities of antimicrobial peptides to their molecular modes of action. *Biochim Biophys Acta*. (2020) 1862:183275. doi: 10.1016/j.bbamem.2020.183275
22. Zweytick D, Pabst G, Abuja PM, Jilek A, Blondelle SE, Andra J, et al. Influence of N-acylation of a peptide derived from human lactoferricin on membrane selectivity. *Biochim Biophys Acta*. (2006) 1758:1426–35. doi: 10.1016/j.bbamem.2006.02.032
23. Sánchez-Gómez S, Lamata M, Leiva J, Blondelle SE, Jerala R, Andrä J, et al. Comparative analysis of selected methods for the assessment of antimicrobial and membrane-permeabilizing activity: a case study for lactoferricin derived peptides. *BMC Microbiol*. (2008) 8:196. doi: 10.1186/1471-2180-8-196
24. Blondelle SE, Jerala R, Pristovšek P, Majerle A, Zorko M, Japelj B, et al. *Antimicrobial Peptides: International Patent Publication WO 2008/006125 A1*. (2008). Available online at: https://books.google.at/books?id=-dHcOAAACAAJ
25. Zweytick D, Japelj B, Mileykovskaya E, Zorko M, Dowhan W, Blondelle SE, et al. N-acylated peptides derived from human lactoferricin perturb organization of cardiolipin and phosphatidylethanolamine in cell membranes and induce defects in *Escherichia coli* cell division. *PLos ONE*. (2014) 9:e90228. doi: 10.1371/journal.pone.0090228
26. Sánchez-Gómez S, Ferrer-Espada R, Stewart PS, Pitts B, Lohner K, Martínez de Tejada G. Antimicrobial activity of synthetic cationic peptides and lipopeptides derived from human lactoferricin against *Pseudomonas aeruginosa* planktonic cultures and biofilms. *BMC Microbiol*. (2015) 15:137. doi: 10.1186/s12866-015-0473-x
27. Heerklotz H, Seelig J. Leakage and lysis of lipid membranes induced by the lipopeptide surfactin. *Eur Biophys J*. (2007) 36:305–14. doi: 10.1007/s00249-006-0091-5
28. Bartlett GR. Colorimetric assay in methods for free and phosphorylated glyceric acids. *J Biol Chem*. (1959) 234:469–71. doi: 10.1016/S0021-9258(18)70227-5
29. Gironi B, Kahveci Z, McGill B, Lechner BD, Pagliara S, Metz J, et al. Effect of DMSO on the mechanical and structural properties of model and biological membranes. *Biophys J*. (2020) 119:274–86. doi: 10.1016/j.bpj.2020.05.037
30. Jorgensen JH, Ferraro MJ. Antimicrobial susceptibility testing: a review of general principles and contemporary practices. *Clin Infect Dis*. (2009) 49:1749–55. doi: 10.1086/647952
31. Fan HY, Nazari M, Raval G, Khan Z, Patel H, Heerklotz H. Utilizing zeta potential measurements to study the effective charge, membrane partitioning, and membrane permeation of the lipopeptide surfactin. *Biochim Biophys Acta*. (2014) 1838:2306–12. doi: 10.1016/j.bbamem.2014.02.018
32. Burstein EA, Emelyanenko VI. Log-normal description of fluorescence spectra of organic fluorophores. *Photochem Photobiol*. (1996) 64:316–20. doi: 10.1111/j.1751-1097.1996.tb02464.x
33. Ladokhin AS, Jayasinghe S, White SH. How to measure and analyze tryptophan fluorescence in membranes properly, and why bother? *Anal Biochem*. (2000) 285:235–45. doi: 10.1006/abio.2000.4773
34. Amenitsch H, Rappolt M, Kriechbaum M, Mio H, Laggner P, Bernstorff S. First performance assessment of the small-angle X-ray scattering beamline at ELETTRA. *J Synchrotron Rad*. (1998) 5:506–8. doi: 10.1107/S090904959800137X
35. Hammersley AP, Svensson SO, Hanfland M, Fitch AN, Hausermann D. Two-dimensional detector software: from real detector to idealised image or two-theta scan. *High Press Res*. (1996) 14:235–48. doi: 10.1080/08957959608201408
36. Haider R, Marmiroli B, Sartori B, Radeticchio A, Wolf M, Dal Zilio S, et al. *Nanodrop Cell for X-Ray and Nanoanalytic Applications*. (2019). Available online at: https://www.nffa.eu/media/225894/d69_nanodrop-cell-for-x-ray-and-nanoanalytic-applications.pdf
37. White SH, Wimley WC, Ladokhin AS, Hristova K. Protein folding in membranes: determining energetics of peptide-bilayer interactions. In: Ackers GK, Johnson ML, editors. *Energetics of Biological Macromolecules, Part B. Vol. 295 of Methods in Enzymology*. San Diego, CA; London: Academic Press (1998). p. 62–87. doi: 10.1016/S0076-6879(98)95035-2
38. Wimley WC, Creamer TP, White SH. Solvation energies of amino acid side chains and backbone in a family of host−guest pentapeptides. *Biochemistry*. (1996) 35:5109–24. doi: 10.1021/bi9600153
39. Savini F, Luca V, Bocedi A, Massoud R, Park Y, Mangoni ML, et al. Cell-density dependence of host-defense peptide activity and selectivity in the presence of host cells. *ACS Chem Biol*. (2017) 12:52–6. doi: 10.1021/acschembio.6b00910
40. Seltmann G, Holst O. *The Bacterial Cell Wall*. Berlin; Heidelberg: Springer (2002). doi: 10.1007/978-3-662-04878-8
41. Freire JM, Domingues MM, Matos J, Melo MN, Veiga AS, Santos NC, et al. Using zeta-potential measurements to quantify peptide partition to lipid membranes. *Eur Biophys J*. (2011) 40:481–7. doi: 10.1007/s00249-010-0661-4
42. Wiese A, Münstermann M, Gutsmann T, Lindner B, Kawahara K, Zähringer U, et al. Molecular mechanisms of polymyxin B-membrane interactions: direct correlation between surface charge density and self-promoted transport. *J Membr Biol*. (1998) 162:127–38. doi: 10.1007/s002329900350
43. Adamson AW, Gast AP. *Physical Chemistry of Surfaces*. 6th ed. New York, NY; Chichester: Wiley (1997).
44. Sochacki KA, Barns KJ, Bucki R, Weisshaar JC. Real-time attack on single *Escherichia coli* cells by the human antimicrobial peptide LL-37. *Proc Natl Acad Sci USA*. (2011) 108:E77–81. doi: 10.1073/pnas.1101130108
45. Kim S, Patel DS, Park S, Slusky J, Klauda JB, Widmalm G, et al. Bilayer properties of lipid A from various gram-negative bacteria. *Biophys J*. (2016) 111:1750–60. doi: 10.1016/j.bpj.2016.09.001
46. Micciulla S, Gerelli Y, Schneck E. Structure and conformation of wild-type bacterial lipopolysaccharide layers at air-water interfaces. *Biophys J*. (2019) 116:1259–69. doi: 10.1016/j.bpj.2019.02.020
47. Semeraro EF, Marx L, Mandl J, Frewein MPK, Scott HL, Prévost S, et al. Evolution of the analytical scattering model of live *Escherichia coli*. *J. Appl. Cryst*. (2020) 54. doi: 10.1107/S1600576721000169
48. Malanovic N, Leber R, Schmuck M, Kriechbaum M, Cordfunke RA, Drijfhout JW, et al. Phospholipid-driven differences determine the action of the synthetic antimicrobial peptide OP-145 on gram-positive bacterial and mammalian membrane model systems. *Biochim Biophys Acta*. (2015) 1848(10 Pt A):2437–47. doi: 10.1016/j.bbamem.2015.07.010
49. Pachler M, Kabelka I, Appavou MS, Lohner K, Vácha R, Pabst G. Magainin 2 and PGLa in bacterial membrane mimics I: peptide-peptide and lipid-peptide interactions. *Biophys J*. (2019) 117:1858–69. doi: 10.1016/j.bpj.2019.10.022
50. Swain J, El Khoury M, Kempf J, Briée F, van der Smissen P, Décout JL, et al. Effect of cardiolipin on the antimicrobial activity of a new amphiphilic aminoglycoside derivative on *Pseudomonas aeruginosa. PLos ONE*. (2018) 13:e0201752. doi: 10.1371/journal.pone.0201752
51. Wilkinson SG. Gram-negative bacteria. In: Ratledge C, Wilkinson SG, editors. *Microbial Lipids*. London: Academic Press (1988). p. 299–488.
52. Burstein EA, Vedenkina NS, Ivkova MN. Fluorescence and the location of tryptophan residues in protein molecules. *Photochem Photobiol*. (1973) 18:263–79. doi: 10.1111/j.1751-1097.1973.tb06422.x
53. Zorko M, Japelj B, Hafner-Bratkovic I, Jerala R. Expression, purification and structural studies of a short antimicrobial peptide. *Biochim Biophys Acta*. (2009) 1788:314–23. doi: 10.1016/j.bbamem.2008.10.015

54. Epand RM, Epand RF. Domains in bacterial membranes and the action of antimicrobial agents. *Mol Biosyst*. (2009) 5:580–7. doi: 10.1039/b900278m
55. Kollmitzer B, Heftberger P, Rappolt M, Pabst G. Monolayer spontaneous curvature of raft-forming membrane lipids. *Soft Matter*. (2013) 9:10877–84. doi: 10.1039/c3sm51829a
56. Chen YF, Tsang KY, Chang WF, Fan ZA. Differential dependencies on Ca2+ and temperature of the monolayer spontaneous curvatures of DOPE, DOPA and cardiolipin: effects of modulating the strength of the inter-headgroup repulsion. *Soft Matter*. (2015) 11:4041–53. doi: 10.1039/C5SM00577A
57. Koller D, Lohner K. The role of spontaneous lipid curvature in the interaction of interfacially active peptides with membranes. *Biochim Biophys Acta*. (2014) 1838:2250–9. doi: 10.1016/j.bbamem.2014.05.013
58. Ellens H, Siegel DP, Alford D, Yeagle PL, Boni L, Lis LJ, et al. Membrane fusion and inverted phases. *Biochemistry*. (1989) 28:3692–703. doi: 10.1021/bi00435a011
59. Siegel DP. The Gaussian curvature elastic energy of intermediates in membrane fusion. *Biophys J*. (2008) 95:5200–15. doi: 10.1529/biophysj.108.140152
60. Marsh D. Lateral pressure profile, spontaneous curvature frustration, and the incorporation and conformation of proteins in membranes. *Biophys J*. (2007) 93:3884–99. doi: 10.1529/biophysj.107.107938
61. Laggner P, Lohner K. Liposome phase systems as membrane activity sensors for peptides. In: Katsaras J, Gutberlet T, editors. *Lipid Bilayers. Structure and Interactions*. Berlin: Springer (2000). p. 233–64. doi: 10.1007/978-3-662-04496-4_11
62. Seydel U, Koch MHJ, Brandenburg K. Structural polymorphisms of rough mutant lipopolysaccharides Rd to Ra from *Salmonella minnesota*. (1993). 110:232–43. doi: 10.1006/jsbi.1993.1026
63. Rappolt M, Rössle M, Kaconis Y, Howe J, Andrä J, Gutsmann T, et al. X-ray scattering of bacterial cell wall compounds and their neutralization. In: Bauwens CM, editor. *X-Ray Scattering. Materials Science and Technologies*. Hauppauge, NY: Nova Science Publishers (2011) p. 133–48.

Conflict of Interest: The authors declare that the research was conducted in the absence of any commercial or financial relationships that could be construed as a potential conflict of interest.

frontiers in Medical Technology

MINI REVIEW
published: 12 March 2021
doi: 10.3389/fmedt.2021.640981

Developing Antimicrobial Synergy With AMPs

Leora Duong[1], *Steven P. Gross*[2,3]* *and Albert Siryaporn*[1,3]*

[1] Department of Molecular Biology & Biochemistry, University of California, Irvine, Irvine, CA, United States, [2] Department of Developmental and Cell Biology, University of California, Irvine, Irvine, CA, United States, [3] Department of Physics & Astronomy, University of California, Irvine, Irvine, CA, United States

Antimicrobial peptides (AMPs) have been extensively studied due to their vast natural abundance and ability to kill microbes. In an era critically lacking in new antibiotics, manipulating AMPs for therapeutic application is a promising option. However, bacterial pathogens resistant to AMPs remain problematic. To improve AMPs antimicrobial efficacy, their use in conjunction with other antimicrobials has been proposed. How might this work? AMPs kill bacteria by forming pores in bacterial membranes or by inhibiting bacterial macromolecular functions. What remains unknown is the duration for which AMPs keep bacterial pores open, and the extent to which bacteria can recover by repairing these pores. In this mini-review, we discuss various antimicrobial synergies with AMPs. Such synergies might arise if the antimicrobial agents helped to keep bacterial pores open for longer periods of time, prevented pore repair, perturbed bacterial intracellular functions at greater levels, or performed other independent bacterial killing mechanisms. We first discuss combinations of AMPs, and then focus on histones, which have antimicrobial activity and co-localize with AMPs on lipid droplets and in neutrophil extracellular traps (NETs). Recent work has demonstrated that histones can enhance AMP-induced membrane permeation. It is possible that histones, histone fragments, and histone-like peptides could amplify the antimicrobial effects of AMPs, giving rise to antimicrobial synergy. If so, clarifying these mechanisms will thus improve our overall understanding of the antimicrobial processes and potentially contribute to improved drug design.

Keywords: antimicrobial peptides, histones, antimicrobial synergism, antibiotic resistance, intracellular targeting

OPEN ACCESS

Edited by:
Sattar Taheri-Araghi, California State University, Northridge, United States

Reviewed by:
Laura Orian, University of Padua, Italy
Dario Spelzini, Consejo Nacional de Investigaciones Científicas y Técnicas (CONICET), Argentina

***Correspondence:**
Steven P. Gross
sgross@uci.edu
Albert Siryaporn
asirya@uci.edu

Specialty section:
This article was submitted to Pharmaceutical Innovation, a section of the journal Frontiers in Medical Technology

Received: *12 December 2020*
Accepted: *12 February 2021*
Published: *12 March 2021*

Citation:
Duong L, Gross SP and Siryaporn A (2021) Developing Antimicrobial Synergy With AMPs. Front. Med. Technol. 3:640981. doi: 10.3389/fmedt.2021.640981

INTRODUCTION

Bacterial infections are an increasing threat to global health, due to both an increase in bacterial resistance to current therapeutics and also a decline in new antibiotic development. This results in rising numbers of untreatable health complications and deaths worldwide (1). There is thus an urgent need to identify new antibacterial strategies to effectively treat drug-resistant pathogens. The demand for such new strategies has encouraged scientists to investigate biologically-abundant antimicrobial tools that can be manipulated to kill bacteria. Repurposing and modifying known natural antimicrobial proteins may contribute to successful development of new therapeutic strategies.

Antimicrobial peptides (AMPs) have broad spectrum antimicrobial activity and are found ubiquitously in nature. They have been extensively studied as a promising option to combat multidrug-resistant bacteria. However, the rapid ability of bacteria to evolve requires new

approaches to limit potential bacterial resistance to AMPs (2–4). Here, we discuss the use of AMPs in conjunction with other antimicrobials to form antimicrobial synergy, in which the combined antimicrobial effect is greater than the sum of either treatment alone. Antimicrobial synergy could potentially reduce the rise of bacterial resistance. A number of synergistic approaches using AMPs have been sought, with 300 reports made during the last 5 years as determined by PubMed. We examine and propose potential mechanisms that give rise to antimicrobial synergy with AMPs.

PHYSIOLOGICAL ROLES

AMPs are ubiquitously observed in nature and are known for their physiological antimicrobial roles. They are produced by both prokaryotic and eukaryotic organisms, ranging from bacteria (5, 6), insects (7–9), amphibians (10–12), and humans (13–16). AMPs protect organisms from microbial harm and thus play vital roles in innate immunity (17) by directly or indirectly killing microbes. AMPs directly kill microbes by acting at the bacterial membrane (18, 19) or eliciting bacterial cell death via inhibition of macromolecular functions (20). AMPs indirectly kill microbes by directing cytokines to sites of infection for increased immunological responses in hosts (21). Neutrophils, the first line of innate immune defense, have dense granules that are packed with AMPs that are used to defend against microbial infections (22). When stimulated, neutrophils can also release their intracellular contents to form neutrophil extracellular traps (NETs). These web-like structures, consisting of DNA, AMPs, and other antimicrobial agents, can entrap and kill bacteria (23, 24). Similar to neutrophil elastases, AMPs have vital roles in NETs in controlling microbial threats (25). A recent report indicates that AMPs also localize to cellular lipid droplets with histones (26) and contribute to lipid-droplet based cellular immunity.

STRUCTURE AND FUNCTION

AMPs are typically small peptides, ranging from about 5 to 50 amino acids, but can be as large as over 100 amino acids (27). Most AMPs are positively charged (+2 to +9) due to their high proportions of arginine and lysine residues (28), though negatively charged AMPs do also exist (21, 29, 30). Structures of AMPs include α-helix, β-sheet, extended, and loop (31), with α-helix and β-sheet structures being the most common. More complex structures also exist, including cyclic and lasso peptides (32). AMPs are known for their amphipathic nature, typically consisting 50% of hydrophobic residues including alanine, glycine, and leucine (28, 33). The biophysical properties of AMPs contribute to their potent antimicrobial activity. Cationic (positively charged) AMPs can bind to anionic (negatively charged) lipopolysaccharide (LPS) and lipoteichoic acid (LTA), which are major components of bacterial membranes (34). The amphipathic nature of AMPs also enables them to interact with and insert into bacterial cell membranes.

Many reports attribute the antimicrobial activity of AMPs to the formation of pores within bacterial membranes, which can elicit cell damage and death. Several different classes of AMP-induced membrane pores have been proposed, including barrel-stave, toroidal, and carpet (20). In a barrel-stave model, peptide monomers form a transmembrane channel that is parallel to bacterial membrane phospholipids. A toroidal model proposes that AMPs insert into bacterial cell membranes and force membrane lipid structures to change in conformation, as opposed to pore insertion through an intact membrane like that of the barrel-stave model. The carpet model suggests that AMPs do not form transmembrane pores but instead localize to the bacterial membrane surface, where they disrupt membrane organization and integrity (35). These membrane disruptions can cause loss of bacterial membrane proton gradient, cell leakage, and eventually cell death (19). Alternative models to pore formation in membranes have also been proposed, with pore formation and cell leakage being attributed to the high concentrations of AMPs that are typically used in membrane pore formation studies (35). In particular, the entry of AMPs into bacterial cells may induce intracellular damage, including disruption of bacterial nucleic acid synthesis, protein synthesis, cell wall synthesis, and cell division (20).

BACTERIAL RESISTANCE TO AMPs

LPS in Gram-negative bacterial membranes and LTA in Gram-positive cell walls contribute to overall negative charges of bacterial cell exteriors. Negatively charged membranes, which are conserved among bacteria, provide cytoplasmic rigidity and proper cationic gradients that are necessary for bacterial survival (36). However, cationic AMPs can easily bind to anionic components of bacterial membranes via electrostatic interactions to elicit cell damage. Complete bacterial resistance to AMPs is unlikely because evolving a bacterial membrane that possesses an outer neutral or positive charge simply for the purpose of avoiding AMPs would be too evolutionarily costly (37, 38). Still, many studies have shown that bacteria can have intrinsic resistance or evolve resistance to AMPs (2–4, 39, 40).

A vast array of bacterial resistance and defense mechanisms against AMPs exist, including the utilization of efflux pumps (41–43), modifications to cell membrane charge (38), expression of protective barriers around bacterial membranes (44), inhibition of antimicrobials via peptide cleavage (45, 46), and potential membrane healing and recovery post-damage (47). Both multidrug-resistant Gram-negative and Gram-positive bacteria utilize efflux pump mechanisms to actively pump AMPs back out into the extracellular environment to prevent cell damage (41, 42). In Gram-negative *S.* Typhimurium and *P. aeruginosa*, the lipid A portion of LPS is modified with the addition of 4-amino-4-deoxy-L-arabinose, which reduces the overall negative charge and thus reduces the binding affinity of positively charged AMPs, including azurocidin, polymyxin B (PMB), indolicidin, and LL-37 (48–50). In Gram-positive *S. aureus*, lysine is added to membrane phospholipids, reducing the overall

anionic charge and affinity to defensin-like cationic AMPs (51). Colanic acid is a polysaccharide which functions as a protective capsule around many *Enterobacteriaceae* (52) and may prevent AMP-mediated activity. It has been suggested that these capsular polysaccharides play a role in bacterial resistance (40, 53) and virulence (54, 55). For example, capsular polysaccharides increase resistance of *K. pneumoniae*, *S. pneumoniae*, and *P. aeruginosa* to both PMB and human neutrophil alpha-defensin 1 (53). Additionally, increased slime production by *S. epidermidis* in medical catheters has been reported when bacterial capsular polysaccharides are expressed (54, 55). Bacterial species like *E. coli* and *S.* Typhimurium also release proteases to cleave and inhibit antimicrobials that threaten their survival, particularly protamine and alpha helical cationic AMPs, respectively (45, 46).

Recent work suggests that bacteria can recover from pores formed by LL-37 (47). However, the duration in which AMPs can keep bacterial pores open and the extent to which bacteria can repair these pores is unknown. It is possible that efflux pumps are used to eject AMPs out of the membrane to allow for bacterial lipid bilayers to reform. Additionally, bacterial cell wall biosynthesis may be upregulated for the purpose of membrane repair.

ANTIMICROBIAL SYNERGIES WITH AMPs

To optimize the use of antibiotics, it is important to mitigate potential bacterial resistance mechanisms. Many AMPs have been tested in clinical trials due their potent antimicrobial activity (56, 57). However, as with any antibiotic, using AMPs is associated with the risk of ever-evolving bacterial resistance that could negate their effects. A potential way to reduce the risk of drug-resistance to AMPs in clinical settings is to use AMPs in conjunction with other antimicrobials, focusing on combinations that lead to effective antimicrobial synergies. Synergistic combinations that have multiple targets in independent pathways could require two independent and simultaneous sets of mutations to address both challenges. Synergy could also be more lethal, decreasing the likelihood that bacteria can escape and develop resistance.

It has been suggested that bacteria are less likely to evolve resistance to antibiotic cocktails than to a single antimicrobial (58, 59). Consistent with this is the fact that multiple AMPs are released during immune responses *in vivo*, making it difficult for bacteria to develop resistance (60). Therefore, using AMP cocktails, especially ones that convey antimicrobial synergy, could be an effective strategy. Synergistic antibacterial combinations with AMPs could enable bacterial pores to stay open for longer durations, prevent pore repair, increase perturbation of bacterial intracellular functions, or convey other independent but complementary bacterial killing mechanisms. These mechanisms may potentially increase antimicrobial efficacy, decrease resistance, and reduce host toxicity if only low concentrations of each antimicrobial component are needed to carry out a large antimicrobial effect (61). The abundance of antimicrobial synergies discovered with AMPs presents exciting possibilities for the potential use of synergistic AMP combinations in clinical settings.

Synergy With Other AMPs

Numerous reports indicate that AMPs synergize with other AMPs. We discuss antimicrobial synergies of AMPs from organisms like insects, amphibians, and mammals, suggesting that synergistic interactions are common between AMPs within the animal kingdom.

The insect AMPs, diptericins and attacins, show synergistic killing against *P. burhodogranariea* in flies (62). A combination of the synthetic AMP pexiganan and bumblebee AMP melittin show *S. aureus* killing effects comparable to that of Vancomycin, a last line of defense antibiotic (39). Additionally, the antimicrobial activity of a bumblebee AMP, abaecin, is synergistically enhanced by the presence of a pore forming AMP, hymenoptaecin (63). In this example, hymenoptaecin forms membrane pores, potentially causing cell leakage or lytic cell death and enabling the entry of abaecin into bacterial cells. The hymenoptaecin-induced pores may increase the ability for abaecin to access and bind to DnaK, a molecular chaperone, to inhibit bacterial replication (63). Thus, the two AMPs work together to kill bacteria on both a membrane and intracellular level.

AMPs can potentially bind to other AMPs to form more potent antibacterial agents. For example, the amphibian AMPs magainin-2 and peptidyl-glycylleucine-carboxyamide (PGLa) work synergistically to inhibit *E. coli* growth (11). When magainin-2 and PGLa are added together, they form a "supramolecule" to quickly induce bacterial membrane pores and mediate pore stabilization (64). Moreover, it has been reported that PGLa forms an antiparallel dimer that spans the cell membrane where it binds to magainin-2 at the C-terminus (65), forming toroidal pore structures (66). These results are consistent with an additional report in which fused AMPs induce greater killing activities in *S. mutans* than on their own (67). These findings suggest that AMPs can bind other AMPs or other types of antimicrobials to give rise to antimicrobial synergy.

The mammalian AMP protegrin 1 has been reported to exhibit synergistic killing activity with indolicidin, LL-37, and bactenecin against *P. aeruginosa* and *E. coli* (68). Additionally, the combination of indolicidin and bactenecin gives rise to antimicrobial synergy against *E. coli* (68). The combinations of protegrin 1 with LL-37, bactenecin with LL-37, and protegrin 1 with bactenecin are also synergistic against *E. faecalis* (68). Lastly, human platelet-derived synthetic AMP combinations of PD1 through PD4 and Arg-Trp repeats RW1 through RW5 are synergistically antimicrobial in platelets (69).

AMPs can be effective when their mechanisms are complementary, such as in the case of the AMPs coleoptericin and defensin. Coleoptericin contributes to the survival of the mealworm beetle, *Tenebrio molitor*, but does not reduce bacterial load. In contrast, defensin does not improve host survival but reduces bacterial load (70). Their combined use both significantly increases host survival and reduces bacterial load (70). Using multiple AMPs together can thus maintain the independent functions of each AMP, resulting in a more effective treatment strategy.

While many studies demonstrate robust antimicrobial synergies with just two AMPs, synergies with three AMPs reveal even greater effects. For example, while apidaecin functions antagonistically with either pexiganan or LL 19-27 (an analog of LL-37), the triple combination of apidaecin, pexiganan, and LL 19-27 demonstrate strong synergism (58). Synergy was also observed from the combination of human β-defensin, LL-37, and lysozyme, which are produced on the skin, against *S. aureus* and *E. coli* (13). The observation of synergy between these antimicrobials is an example in which natural defense molecules have greater activity in combination rather than individually. Thus, combining natural antimicrobials could yield further discoveries of synergy.

Synergy With Antibiotics

AMPs can also synergize with antibiotics, and in some cases, overcome antibiotic resistance. The use of AMPs to increase the efficacy of already approved antibiotics appears to be a promising option to combat commonly drug-resistant pathogens. The human AMPs, LL-37 and human β-defensin 3 (HBD3), have antimicrobial synergy with the antibiotics tigecycline, moxifloxacin, piperacillin-tazobactam, and meropenem. Specifically, antibiotic killing against *C. difficile* is improved when both LL-37 and HBD3 are present (71). Lastly, LL 17-29 establishes antimicrobial synergy with the antibiotic chloramphenicol against highly virulent bacterial strains, including methicillin-resistant *S. aureus* and multidrug-resistant *P. aeruginosa* (59).

Combining the AMPs nisin Z, pediocin, or colistin with various antibiotics, including penicillin, ampicillin, or rifampicin, is effective in overcoming antibiotic-resistance in *P. fluorescens* (72). Also, the AMP melamine has synergistic killing activities when paired with ciprofloxacin, a fluoroquinolone antibiotic, against antibiotic-resistant strains of *P. aeruginosa*. This combination may aid in overcoming *P. aeruginosa* resistance to fluoroquinolone antibiotics (73). Synergistic combinations of AMPs with PMB (originally discovered as an AMP), erythromycin, and tetracycline have also been shown. In particular, variants of the AMP indolicidin synergize with the antibiotics PMB, tobramycin, gentamycin, and amikacin (74).

One of the mechanisms by which AMPs improve antibiotic function is by disrupting bacterial membranes to aid in the delivery of antibiotics into the bacterial cytoplasm, where antibiotics can act on intracellular targets. For example, the AMP arenicin-1 synergistically functions with antibiotics including ampicillin, erythromycin, and chloramphenicol to kill *S. aureus*, *S. epidermis*, *P. aeruginosa*, and *E. coli* (75). Arenicin-1 assists in the uptake of antibiotics into cells and inhibits bacterial growth via hydroxyl radical formation (75), which suggests complementary mechanisms are at play.

Synergy With Histones

Histones, more commonly known for their roles in condensing eukaryotic DNA, have antibacterial properties (76, 77). However, the mechanisms by which histones kill bacteria have not previously been understood (78). Since histones are positively charged and have similar structures to that of AMPs, it has been suggested that histones and AMPs have redundant antibacterial roles (79, 80). Histones and AMPs colocalize in innate immunity components, including on cellular lipid droplets and in NETs, suggesting that they could work together to kill microbes (26, 81–83). For fish in particular, fractions of salmon histone H1 have reported antimicrobial synergy with lysozyme and a flounder AMP, pleurocidin (84). Recent work demonstrates that histones H2A and H3 can function with the pore-forming AMPs LL-37 and magainin-2 to produce antibacterial synergy against Gram-positive and Gram-negative bacteria (47). Additionally, H2A and the pore-forming antimicrobial PMB synergistically work together to completely inhibit *E. coli* growth over 24 hours (47). It is important to note that histones must be paired with pore forming AMPs in order for this synergistic model to be effective; histones alone have minimal antimicrobial effects at physiological conditions (47). It is possible that other histones, histone fragments, and histone-like peptides also amplify the antimicrobial effects of AMPs and give rise to antimicrobial synergy.

The mechanism of synergy between AMPs and histones is due the ability of AMPs to form pores in bacterial membranes, enabling histones to enter the bacterial cytoplasm (47, 85). Here, histones inhibit global transcription and reorganize bacterial chromosomes. Furthermore, histones enhance AMP-mediated pores that bacteria otherwise would be able to recover from, leading to reduced cell sizes and increased cytoplasmic leakage (47). The uptake of AMPs and histones into bacterial cells elicits an effective antimicrobial response consistent with a positive feedback loop (47). Importantly, if bacterial intracellular functions, like transcription and translation, are inhibited, this could reduce bacterial cell membrane integrity and repair.

Another potential effect of histones is that they may induce stress on bacterial membranes. This membrane stress could aid AMPs to more effectively form bacterial membrane pores. Altered membrane physiology, revealed through scanning

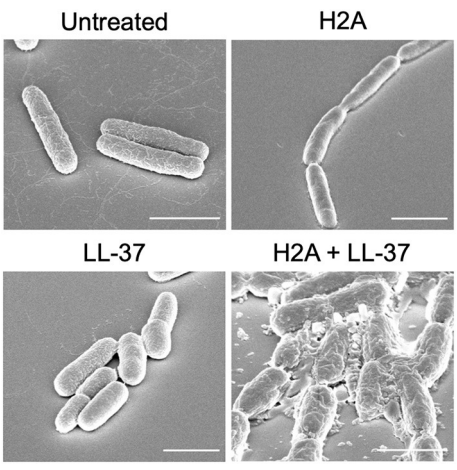

FIGURE 1 | SEM images *E. coli* that are untreated or treated with H2A, LL-37, or both. *E. coli* that are treated with both H2A and LL-37 demonstrate extensive cellular damage. Scale bars indicate 2 μm.

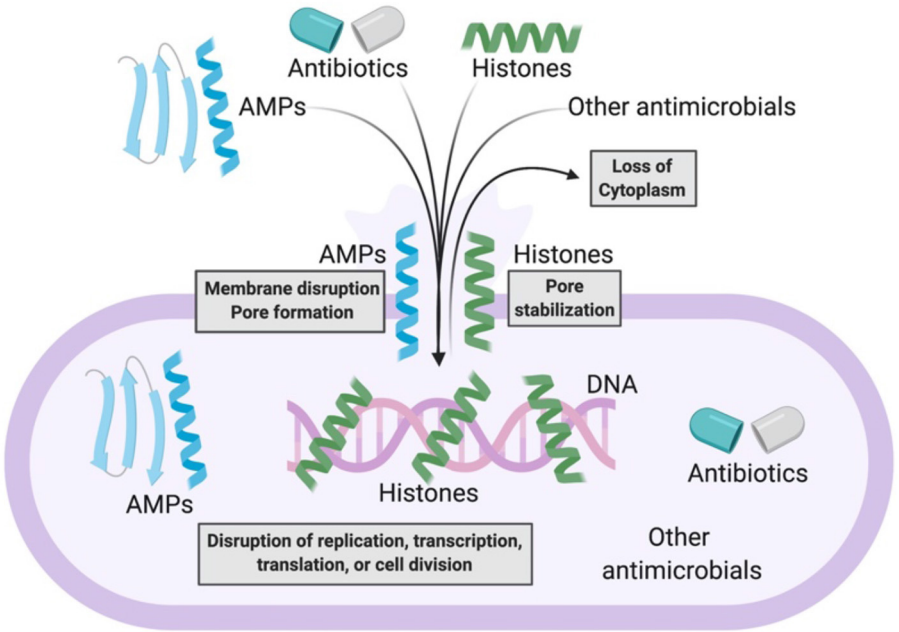

FIGURE 2 | Model of antimicrobial synergy between AMPs and other AMPs, antibiotics, histones, and other antimicrobials. AMPs form bacterial membrane pores or disrupt bacterial membranes. This enables the entry of more AMPs, antibiotics, histones, or other antimicrobials into bacteria. As a result, there is loss of bacterial cytoplasm and disruption of bacterial macromolecular functions. Histones potentially stabilize AMP-induced pores that enable further synergistic antimicrobial activity.

electron microscopy (SEM), suggests that when bacteria are treated with only an individual AMP or histone, the membrane largely remains intact (**Figure 1**). However, the treatment with both AMPs and histones induces gross cell deformation and leakage of cytoplasmic contents (**Figure 1**). The reduced membrane integrity from the AMP and histone treatment also inhibits *E. coli* from maintaining their proton gradient, which is necessary for ATP production (47). Thus, membrane damage caused by synergistic combinations with AMPs may lead to lack of recovery from AMP-mediated pores, rapid loss of cytoplasmic content, failure to produce ATP, and ultimately bacterial cell death. In response to histone exposure, the *rcs* gene responsible for colanic acid expression is upregulated in *E. coli* (47). The bacterial upregulation of colanic acid, which functions as a bacterial membrane protective capsule, suggests that there is an active microbial attempt to mitigate potential membrane stress effects due to histones.

Synergy With Other Antimicrobial Agents

AMPs also synergize with other antimicrobial agents. For example, silver nitrate and silver nanoparticles can synergize with PMB and Gramicidin S, enhancing their intracellular antimicrobial effects in Gram-negative bacteria (86). Additionally, peptoid analogs of AMPs are known to have effective and specific antimicrobial activity (87). AMPs can synergize with peptoids against Gram-negative bacteria (88). The AMP *Galleria mellonella* anionic peptide 2 and antimicrobial enzyme lysozyme are also synergistic against Gram-negative bacteria (89).

CONCLUSION

The combination of AMPs with current antimicrobial strategies can produce synergy through a number of distinct mechanisms (**Figure 2**). The introduction of antibiotics inside bacteria has often been a challenge. However, AMPs can address this challenge by forming membrane pores, thus facilitating entry of antibiotics into the cytoplasm, where the antibiotics can bind to their intracellular targets. The combination of AMPs with antibiotics could thus be an effective antibacterial strategy. This strategy could limit bacterial resistance because defense from the multifaceted attack could be significantly more difficult to achieve.

If the ability for AMPs to synergize with other AMPs or antimicrobials is a conserved characteristic, then relatively low doses of each antimicrobial can be used as antibiotic treatments to exhibit large antimicrobial effects. Lower drug concentrations might also limit harmful side effects. For example, PMB is now an FDA-approved and potent last-resort antibiotic; however, PMB is also highly toxic to the nephrotic and nervous systems (90, 91). Using PMB in a synergistic antimicrobial combination, like with indolicidin or histones, would potentially require lower doses of each antimicrobial agent, potentially reducing host toxicity, while maintaining effective antimicrobial activity. Since the production of peptides can be costly, taking advantage of lower antimicrobial doses needed for synergistic treatments may also reduce production expenses. If toxicity remains an issue even with the low doses required in synergistic antimicrobial combinations, changing amino acids on AMPs has been shown

to have strong effects on synergy (74). Moreover, AMPs that can synergize with preexisting AMPs in hosts could be especially potent *in vivo*, due to the activation of natural AMP release by the immune system. In innate immunity, humans express LL-37; therefore, synergies that arise with LL-37, like histones and protegrin 1, would be especially critical to consider for antibiotic applications.

Synergistic antimicrobial combinations are promising candidates that reduce potential bacterial resistance, overcome preexisting resistance to current antibiotics, prevent host toxicity, and increase antimicrobial efficacy. Thus, an improved understanding of mechanisms by which AMPs synergize with other antimicrobials is necessary. Moving forward, the synergistic interactions between AMPs and other antimicrobials will provide promising options to be explored in the development of new antibiotics.

AUTHOR CONTRIBUTIONS

LD wrote the initial draft of the manuscript. LD, SG, and AS edited the manuscript. All authors discussed the vision, direction, and scope of the manuscript.

FUNDING

AS was supported by NIH R21 Grant R21AI139968.

ACKNOWLEDGMENTS

We thank Tory Doolin for providing the SEM images. **Figure 2** was created using BioRender.com.

REFERENCES

1. Ventola CL. The antibiotic resistance crisis. *Pharm Ther.* (2015) 40:277–283.
2. El Shazely B, Yu G, Johnston PR, Rolff J. Resistance evolution against antimicrobial peptides in staphylococcus aureus alters pharmacodynamics beyond the MIC. *Front Microbiol.* (2020) 11:103. doi: 10.3389/fmicb.2020.00103
3. Bauer ME, Shafer WM. On the in vivo significance of bacterial resistance to antimicrobial peptides. *Biochim Biophys Acta.* (2015) 1848:3101–11. doi: 10.1016/j.bbamem.2015.02.012
4. Anaya-López JL, López-Meza JE, Ochoa-Zarzosa A. Bacterial resistance to cationic antimicrobial peptides. *Crit Rev Microbiol.* (2013) 39:180–95. doi: 10.3109/1040841X.2012.699025
5. McCafferty DG, Cudic P, Yu MK, Behenna DC, Kruger R. Synergy and duality in peptide antibiotic mechanisms. *Curr Opin Chem Biol.* (1999) 3:672–80. doi: 10.1016/s1367-5931(99)00025-3
6. Nes IF, Diep DB, Holo H. Bacteriocin diversity in streptococcus and enterococcus. *J Bacteriol.* (2007) 189:1189–98. doi: 10.1128/JB.01254-06
7. Choi JH, Jang AY, Lin S, Lim S, Kim D, Park K, et al. Melittin, a honeybee venom-derived antimicrobial peptide, may target methicillin-resistant *Staphylococcus aureus. Mol Med Rep.* (2015) 12:6483–90. doi: 10.3892/mmr.2015.4275
8. Romanelli A, Moggio L, Montella RC, Campiglia P, Iannaccone M, Capuano F, et al. Peptides from royal jelly: studies on the antimicrobial activity of jelleins, jelleins analogs and synergy with temporins. *J Pept Sci.* (2011) 17:348–52. doi: 10.1002/psc.1316
9. Wu Q, Patočka J, Kuča K. Insect antimicrobial peptides, a mini review. *Toxins.* (2018) 10:461. doi: 10.3390/toxins10110461
10. Mor A, Hani K, Nicolas P. The vertebrate peptide antibiotics dermaseptins have overlapping structural features but target specific microorganisms. *J Biol Chem.* (1994) 269:31635–41.
11. Westerhoff HV, Zasloff M, Rosner JL, Hendler RW, Waal AD, Gomes AV, et al. Functional synergism of the magainins PGLa and Magainin-2 in *Escherichia coli*, tumor cells and liposomes. *Eur J Biochem.* (1995) 228:257–64. doi: 10.1111/j.1432-1033.1995.0257n.x
12. Patocka J, Nepovimova E, Klimova B, Wu Q, Kuca K. Antimicrobial peptides: amphibian host defense peptides. *Curr Med Chem.* (2019) 26:5924–46. doi: 10.2174/0929867325666180713125314
13. Chen X, Niyonsaba F, Ushio H, Okuda D, Nagaoka I, Ikeda S, et al. Synergistic effect of antibacterial agents human beta-defensins, cathelicidin LL-37 and lysozyme against *Staphylococcus aureus* and *Escherichia coli. J Dermatol Sci.* (2005) 40:123–32. doi: 10.1016/j.jdermsci.2005.03.014
14. Singh PK, Tack BF, McCray PB, Welsh MJ. Synergistic and additive killing by antimicrobial factors found in human airway surface liquid. *Am J Physiol Lung Cell Mol Physiol.* (2000) 279:L799–805. doi: 10.1152/ajplung.2000.279.5.L799
15. Tollin M, Bergman P, Svenberg T, Jörnvall H, Gudmundsson GH, Agerberth B. Antimicrobial peptides in the first line defence of human colon mucosa. *Peptides.* (2003) 24:523–30. doi: 10.1016/s0196-9781(03)00114-1
16. Wang G. Human antimicrobial peptides and proteins. *Pharmaceuticals.* (2014) 7:545–94. doi: 10.3390/ph7050545
17. Diamond G, Beckloff N, Weinberg A, Kisich KO. The roles of antimicrobial peptides in innate host defense. *Curr Pharm Des.* (2009) 15:2377–92. doi: 10.2174/138161209788682325
18. Lehrer RI, Barton A, Daher KA, Harwig SS, Ganz T, Selsted ME. Interaction of human defensins with *Escherichia coli*. Mechanism of bactericidal activity. *J Clin Invest.* (1989) 84:553–61.
19. Shai Y. Mode of action of membrane active antimicrobial peptides. *Biopolymers.* (2002) 66:236–48. doi: 10.1002/bip.10260
20. Le CF, Fang CM, Sekaran SD. Intracellular targeting mechanisms by antimicrobial peptides. *Antimicrob Agents Chemother.* (2017) 61:e02340–16. doi: 10.1128/AAC.02340-16
21. Lai Y, Gallo RL. AMPed Up immunity: how antimicrobial peptides have multiple roles in immune defense. *Trends Immunol.* (2009) 30:131–41. doi: 10.1016/j.it.2008.12.003
22. Wetering S van, Tjabringa GS, Hiemstra PS. Interactions between neutrophil-derived antimicrobial peptides and airway epithelial cells. *J Leukoc Biol.* (2005) 77:444–50. doi: 10.1189/jlb.0604367
23. Fuchs TA, Abed U, Goosmann C, Hurwitz R, Schulze I, Wahn V, et al. Novel cell death program leads to neutrophil extracellular traps. *J Cell Biol.* (2007) 176:231–41. doi: 10.1083/jcb.200606027
24. Brinkmann V, Reichard U, Goosmann C, Fauler B, Uhlemann Y, Weiss DS, et al. Neutrophil extracellular traps kill bacteria. *Science.* (2004) 303:1532–5. doi: 10.1126/science.1092385
25. Rocha JDB, Nascimento MTC, Decote-Ricardo D, Côrte-Real S, Morrot A, Heise N, et al. Capsular polysaccharides from *Cryptococcus neoformans* modulate production of neutrophil extracellular traps (NETs) by human neutrophils. *Sci Rep.* (2015) 5:8008. doi: 10.1038/srep08008
26. Bosch M, Sánchez-Álvarez M, Fajardo A, Kapetanovic R, Steiner B, Dutra F, et al. Mammalian lipid droplets are innate immune hubs integrating cell metabolism and host defense. *Science.* (2020) 370:eaay8085. doi: 10.1126/science.aay8085
27. Bahar AA, Ren D. Antimicrobial peptides. *Pharmaceuticals.* (2013) 6:1543–75. doi: 10.3390/ph6121543
28. Yeaman MR, Yount NY. Mechanisms of antimicrobial peptide action and resistance. *Pharmacol Rev.* (2003) 55:27–55. doi: 10.1124/pr.55.1.2
29. Brogden KA. Antimicrobial peptides: pore formers or metabolic inhibitors in bacteria? *Nat Rev Microbiol.* (2005) 3:238–50. doi: 10.1038/nrmicro1098
30. Steffen H, Rieg S, Wiedemann I, Kalbacher H, Deeg M, Sahl H-G, et al. Naturally processed dermcidin-derived peptides do not permeabilize bacterial membranes and kill microorganisms irrespective of their charge. *Antimicrob Agents Chemother.* (2006) 50:2608–20. doi: 10.1128/AAC.00181-06

31. Powers J-PS, Hancock REW. The relationship between peptide structure and antibacterial activity. *Peptides.* (2003) 24:1681–91. doi: 10.1016/j.peptides.2003.08.023
32. Koehbach J, Craik DJ. The vast structural diversity of antimicrobial peptides. *Trends Pharmacol Sci.* (2019) 40:517–28. doi: 10.1016/j.tips.2019.04.012
33. Wang G, Li X, Wang Z. APD2: the updated antimicrobial peptide database and its application in peptide design. *Nucleic Acids Res.* (2009) 37:D933–7. doi: 10.1093/nar/gkn823
34. Sitaram N, Nagaraj R. Interaction of antimicrobial peptides with biological and model membranes: structural and charge requirements for activity. *Biochim Biophys Acta BBA.* (1999) 1462:29–54. doi: 10.1016/S0005-2736(99)00199-6
35. Wimley WC. Describing the mechanism of antimicrobial peptide action with the interfacial activity model. *ACS Chem Biol.* (2010) 5:905–17. doi: 10.1021/cb1001558
36. Farha MA, Verschoor CP, Bowdish D, Brown ED. Collapsing the proton motive force to identify synergistic combinations against *Staphylococcus aureus*. *Chem Biol.* (2013) 20:1168–78. doi: 10.1016/j.chembiol.2013.07.006
37. Yu G, Baeder DY, Regoes RR, Rolff J. Predicting drug resistance evolution: insights from antimicrobial peptides and antibiotics. *Proc R Soc B Biol Sci.* (2018) 285:20172687. doi: 10.1098/rspb.2017.2687
38. Andersson DI, Hughes D, Kubicek-Sutherland JZ. Mechanisms and consequences of bacterial resistance to antimicrobial peptides. *Drug Resist Updat.* (2016) 26:43–57. doi: 10.1016/j.drup.2016.04.002
39. Dobson AJ, Purves J, Kamysz W, Rolff J. Comparing Selection on *S. aureus* between antimicrobial peptides and common antibiotics. *PLoS ONE.* (2013) 8:e76521. doi: 10.1371/journal.pone.0076521
40. Campos MA, Vargas MA, Regueiro V, Llompart CM, Albertí S, Bengoechea JA. Capsule polysaccharide mediates bacterial resistance to antimicrobial peptides. *Infect Immun.* (2004) 72:7107–14. doi: 10.1128/IAI.72.12.7107-7114.2004
41. Schindler BD, Kaatz GW. Multidrug efflux pumps of Gram-positive bacteria. *Drug Resist Updat Rev Comment Antimicrob Anticancer Chemother.* (2016) 27:1–13. doi: 10.1016/j.drup.2016.04.003
42. Otreebska-Machaj E, Chevalier J, Handzlik J, Szymańska E, Schabikowski J, Boyer G, et al. Efflux pump blockers in gram-negative bacteria: the new generation of hydantoin based-modulators to improve antibiotic activity. *Front Microbiol.* (2016) 7:622. doi: 10.3389/fmicb.2016.00622
43. Nikaido H. Multidrug efflux pumps of gram-negative bacteria. *J Bacteriol.* (1996) 178:5853–9.
44. Pando JM, Karlinsey JE, Lara JC, Libby SJ, Fang FC. The Rcs-regulated colanic acid capsule maintains membrane potential in *Salmonella enterica Serovar typhimurium*. *mBio.* (2017) 8:e00808–17. doi: 10.1128/mBio.00808-17
45. Stumpe S, Schmid R, Stephens DL, Georgiou G, Bakker EP. Identification of OmpT as the protease that hydrolyzes the antimicrobial peptide protamine before it enters growing cells of *Escherichia coli*. *J Bacteriol.* (1998) 180:4002–6. doi: 10.1128/JB.180.15.4002-4006.1998
46. Guina T, Yi EC, Wang H, Hackett M, Miller SI. A PhoP-regulated outer membrane protease of *Salmonella enterica Serovar typhimurium* promotes resistance to alpha-helical antimicrobial peptides. *J Bacteriol.* (2000) 182:4077–86. doi: 10.1128/JB.182.14.4077-4086.2000
47. Doolin T, Amir HM, Duong L, Rosenzweig R, Urban LA, Bosch M, et al. Mammalian histones facilitate antimicrobial synergy by disrupting the bacterial proton gradient and chromosome organization. *Nat Commun.* (2020) 11:3888. doi: 10.1038/s41467-020-17699-z
48. Gunn JS, Lim KB, Krueger J, Kim K, Guo L, Hackett M, et al. PmrA-PmrB-regulated genes necessary for 4-aminoarabinose lipid A modification and polymyxin resistance. *Mol Microbiol.* (1998) 27:1171–82. doi: 10.1046/j.1365-2958.1998.00757.x
49. Gunn JS, Ryan SS, Van Velkinburgh JC, Ernst RK, Miller SI. Genetic and functional analysis of a PmrA-PmrB-regulated locus necessary for lipopolysaccharide modification, antimicrobial peptide resistance, and oral virulence of *Salmonella enterica Serovar typhimurium*. *Infect Immun.* (2000) 68:6139–46. doi: 10.1128/iai.68.11.6139-6146.2000
50. McPhee JB, Lewenza S, Hancock REW. Cationic antimicrobial peptides activate a two-component regulatory system, PmrA-PmrB, that regulates resistance to polymyxin B and cationic antimicrobial peptides in *Pseudomonas aeruginosa*. *Mol Microbiol.* (2003) 50:205–17. doi: 10.1046/j.1365-2958.2003.03673.x
51. Ernst CM, Staubitz P, Mishra NN, Yang S-J, Hornig G, Kalbacher H, et al. The Bacterial defensin resistance protein MprF consists of separable domains for lipid lysinylation and antimicrobial peptide repulsion. *PLOS Pathog.* (2009) 5:e1000660. doi: 10.1371/journal.ppat.1000660
52. Grant WD, Sutherland IW, Wilkinson JF. Exopolysaccharide colanic acid and its occurrence in the *Enterobacteriaceae*. *J Bacteriol.* (1969) 100:1187–93. doi: 10.1128/JB.100.3.1187-1193.1969
53. Llobet E, Tomás JM, Bengoechea JA. Capsule polysaccharide is a bacterial decoy for antimicrobial peptides. *Microbiol Read Engl.* (2008) 154:3877–86. doi: 10.1099/mic.0.2008/022301-0
54. Christensen GD, Simpson WA, Bisno AL, Beachey EH. Adherence of slime-producing strains of *Staphylococcus epidermidis* to smooth surfaces. *Infect Immun.* (1982) 37:318–26.
55. Davenport DS, Massanari RM, Pfaller MA, Bale MJ, Streed SA, Hierholzer WJ. Usefulness of a test for slime production as a marker for clinically significant infections with coagulase-negative staphylococci. *J Infect Dis.* (1986) 153:332–9. doi: 10.1093/infdis/153.2.332
56. Koo HB, Seo J. Antimicrobial peptides under clinical investigation. *Pept Sci.* (2019) 111:e24122. doi: 10.1002/pep2.24122
57. Greber KE, Dawgul M. Antimicrobial peptides under clinical trials. *Curr Top Med Chem.* (2017) 17:620–8. doi: 10.2174/1568026616666160713143331
58. Yu G, Baeder DY, Regoes RR, Rolff J. Combination effects of antimicrobial peptides. *Antimicrob Agents Chemother.* (2016) 60:1717–24. doi: 10.1128/AAC.02434-15
59. Rajasekaran G, Kim EY, Shin SY. LL-37-derived membrane-active FK-13 analogs possessing cell selectivity, anti-biofilm activity and synergy with chloramphenicol and anti-inflammatory activity. *Biochim Biophys Acta Biomembr.* (2017) 1859:722–33. doi: 10.1016/j.bbamem.2017.01.037
60. Pasupuleti M, Schmidtchen A, Malmsten M. Antimicrobial peptides: key components of the innate immune system. *Crit Rev Biotechnol.* (2012) 32:143–71. doi: 10.3109/07388551.2011.594423
61. Xu X, Xu L, Yuan G, Wang Y, Qu Y, Zhou M. Synergistic combination of two antimicrobial agents closing each other's mutant selection windows to prevent antimicrobial resistance. *Sci Rep.* (2018) 8:7237. doi: 10.1038/s41598-018-25714-z
62. Hanson MA, Dostálová A, Ceroni C, Poidevin M, Kondo S, Lemaitre B. Synergy and remarkable specificity of antimicrobial peptides in vivo using a systematic knockout approach. *eLife.* (2019) 8:e44341. doi: 10.7554/eLife.44341
63. Rahnamaeian M, Cytryńska M, Zdybicka-Barabas A, Dobslaff K, Wiesner J, Twyman RM, et al. Insect antimicrobial peptides show potentiating functional interactions against Gram-negative bacteria. *Proc R Soc B Biol Sci.* (2015) 282:20150293. doi: 10.1098/rspb.2015.0293
64. Matsuzaki K, Mitani Y, Akada KY, Murase O, Yoneyama S, Zasloff M, et al. Mechanism of synergism between antimicrobial peptides magainin 2 and PGLa. *Biochemistry.* (1998) 37:15144–53. doi: 10.1021/bi9811617
65. Zerweck J, Strandberg E, Kukharenko O, Reichert J, Bürck J, Wadhwani P, et al. Molecular mechanism of synergy between the antimicrobial peptides PGLa and magainin 2. *Sci Rep.* (2017) 7:13153. doi: 10.1038/s41598-017-12599-7
66. Tremouilhac P, Strandberg E, Wadhwani P, Ulrich AS. Synergistic transmembrane alignment of the antimicrobial heterodimer PGLa/magainin. *J Biol Chem.* (2006) 281:32089–94. doi: 10.1074/jbc.M604759200
67. He J, Eckert R, Pharm T, Simanian MD, Hu C, Yarbrough DK, et al. Novel synthetic antimicrobial peptides against *Streptococcus mutans*. *Antimicrob Agents Chemother.* (2007) 51:1351–8. doi: 10.1128/AAC.01270-06
68. Yan H, Hancock REW. Synergistic interactions between mammalian antimicrobial defense peptides. *Antimicrob Agents Chemother.* (2001) 45:1558–60. doi: 10.1128/AAC.45.5.1558-1560.2001
69. Mohan KVK, Rao SS, Gao Y, Atreya CD. Enhanced antimicrobial activity of peptide-cocktails against common bacterial contaminants of ex vivo stored platelets. *Clin Microbiol Infect Off Publ Eur Soc Clin Microbiol Infect Dis.* (2014) 20:O39–46. doi: 10.1111/1469-0691.12326
70. Zanchi C, Johnston PR, Rolff J. Evolution of defence cocktails: antimicrobial peptide combinations reduce mortality and persistent infection. *Mol Ecol.* (2017) 26:5334–43. doi: 10.1111/mec.14267

71. Nuding S, Frasch T, Schaller M, Stange EF, Zabel LT. Synergistic effects of antimicrobial peptides and antibiotics against clostridium difficile. *Antimicrob Agents Chemother.* (2014) 58:5719–25. doi: 10.1128/AAC.02542-14
72. Naghmouchi K, Le Lay C, Baah J, Drider D. Antibiotic and antimicrobial peptide combinations: synergistic inhibition of *Pseudomonas fluorescens* and antibiotic-resistant variants. *Res Microbiol.* (2012) 163:101–8. doi: 10.1016/j.resmic.2011.11.002
73. Kampshoff F, Willcox MDP, Dutta D. A pilot study of the synergy between two antimicrobial peptides and two common antibiotics. *Antibiotics.* (2019) 8:60. doi: 10.3390/antibiotics8020060
74. Ruden S, Rieder A, Chis Ster I, Schwartz T, Mikut R, Hilpert K. Synergy pattern of short cationic antimicrobial peptides against multidrug-resistant *Pseudomonas aeruginosa*. *Front Microbiol.* (2019) 10:2740. doi: 10.3389/fmicb.2019.02740
75. Choi H, Lee DG. Synergistic effect of antimicrobial peptide arenicin-1 in combination with antibiotics against pathogenic bacteria. *Res Microbiol.* (2012) 163:479–86. doi: 10.1016/j.resmic.2012.06.001
76. Miller BF, Abrams R, Dorfman A, Klein M. Antibacterial properties of protamine and histone. *Science.* (1942) 96:428–30. doi: 10.1126/science.96.2497.428
77. Hirsch JG. Bactericidal action of histone. *J Exp Med.* (1958) 108:925–44. doi: 10.1084/jem.108.6.925
78. Doolin T, Gross S, Siryaporn A. Physical mechanisms of bacterial killing by histones. In: Duménil S, van Teeffelen S, editors. *Physical Microbiology Advances in Experimental Medicine Biology* (Cham: Springer International Publishing). p. 117–33. doi: 10.1007/978-3-030-46886-6_7
79. Kawasaki H, Isaacson T, Iwamuro S, Conlon JM. A protein with antimicrobial activity in the skin of schlegel's green tree frog *Rhacophorus schlegelii* (*Rhacophoridae*) identified as histone H2B. *Biochem Biophys Res Commun.* (2003) 312:1082–6. doi: 10.1016/j.bbrc.2003.11.052
80. Pavia KE, Spinella SA, Elmore DE. Novel histone-derived antimicrobial peptides use different antimicrobial mechanisms. *Biochim Biophys Acta.* (2012) 1818:869–76. doi: 10.1016/j.bbamem.2011.12.023
81. Cermelli S, Guo Y, Gross SP, Welte MA. The lipid-droplet proteome reveals that droplets are a protein-storage depot. *Curr Biol.* (2006) 16:1783–95. doi: 10.1016/j.cub.2006.07.062
82. Anand P, Cermelli S, Li Z, Kassan A, Bosch M, Sigua R, et al. A novel role for lipid droplets in the organismal antibacterial response. *eLife.* (2012) 1:e00003. doi: 10.7554/eLife.00003
83. Brinkmann V, Zychlinsky A. Neutrophil extracellular traps: is immunity the second function of chromatin? *J Cell Biol.* (2012) 198:773–83. doi: 10.1083/jcb.201203170
84. Patrzykat A, Zhang L, Mendoza V, Iwama GK, Hancock REW. Synergy of histone-derived peptides of coho salmon with lysozyme and flounder pleurocidin. *Antimicrob Agents Chemother.* (2001) 45:1337–42. doi: 10.1128/AAC.45.5.1337-1342.2001
85. Duong L, Gross SP, Siryaporn A. A novel antibacterial strategy: histone and antimicrobial peptide synergy. *Microb Cell.* (2020) 7:309–11. doi: 10.15698/mic2020.11.736
86. Ruden S, Hilpert K, Berditsch M, Wadhwani P, Ulrich AS. Synergistic interaction between silver nanoparticles and membrane-permeabilizing antimicrobial peptides. *Antimicrob Agents Chemother.* (2009) 53:3538–40. doi: 10.1128/AAC.01106-08
87. Chongsiriwatana NP, Patch JA, Czyzewski AM, Dohm MT, Ivankin A, Gidalevitz D, et al. Peptoids that mimic the structure, function, and mechanism of helical antimicrobial peptides. *Proc Natl Acad Sci USA.* (2008) 105:2794–9. doi: 10.1073/pnas.0708254105
88. Chongsiriwatana NP, Wetzler M, Barron AE. Functional synergy between antimicrobial peptoids and peptides against gram-negative bacteria. *Antimicrob Agents Chemother.* (2011) 55:5399–402. doi: 10.1128/AAC.00578-11
89. Zdybicka-Barabas A, Mak P, Klys A, Skrzypiec K, Mendyk E, Fiołka MJ, et al. Synergistic action of *Galleria mellonella* anionic peptide 2 and lysozyme against Gram-negative bacteria. *Biochim Biophys Acta BBA - Biomembr.* (2012) 1818:2623–35. doi: 10.1016/j.bbamem.2012.06.008
90. Falagas ME, Kasiakou SK. Toxicity of polymyxins: a systematic review of the evidence from old and recent studies. *Crit Care.* (2006) 10:R27. doi: 10.1186/cc3995
91. Zavascki AP, Nation RL. Nephrotoxicity of polymyxins: is there any difference between colistimethate and polymyxin B? *Antimicrob Agents Chemother.* (2017) 61:e02319–16. doi: 10.1128/AAC.02319-16

Conflict of Interest: The authors declare that the research was conducted in the absence of any commercial or financial relationships that could be construed as a potential conflict of interest.

Advantages of publishing in Frontiers

OPEN ACCESS
Articles are free to read for greatest visibility and readership

FAST PUBLICATION
Around 90 days from submission to decision

HIGH QUALITY PEER-REVIEW
Rigorous, collaborative, and constructive peer-review

TRANSPARENT PEER-REVIEW
Editors and reviewers acknowledged by name on published articles

Frontiers
Avenue du Tribunal-Fédéral 34
1005 Lausanne | Switzerland

Visit us: www.frontiersin.org
Contact us: frontiersin.org/about/contact

REPRODUCIBILITY OF RESEARCH
Support open data and methods to enhance research reproducibility

DIGITAL PUBLISHING
Articles designed for optimal readership across devices

FOLLOW US
@frontiersin

IMPACT METRICS
Advanced article metrics track visibility across digital media

EXTENSIVE PROMOTION
Marketing and promotion of impactful research

LOOP RESEARCH NETWORK
Our network increases your article's readership